

VILI LAMPINEN

Engineering of Norovirus-like Particles for Vaccine Applications

VILI LAMPINEN

Engineering of Norovirus-like Particles for Vaccine Applications

ACADEMIC DISSERTATION

To be presented, with the permission of
the Faculty of Medicine and Health Technology
of Tampere University,
for public discussion in the F115 auditorium
of the Arvo building, Arvo Ylpön katu 34, Tampere,
on 8th of March 2024, at 13 o'clock.

ACADEMIC DISSERTATION

Tampere University, Faculty of Medicine and Health technology
Finland

<i>Responsible supervisor and Custos</i>	Professor Vesa Hytönen Tampere University Finland	
<i>Supervisors</i>	Docent Minna Hankaniemi Tampere University Finland	Docent Marko Pesu Tampere University Finland
<i>Pre-examiners</i>	APL Professor Carlos Guzmán Hannover Medical School Helmholtz Centre for Infection Research Germany	Professor Lloyd Ruddock University of Oulu Finland
<i>Opponent</i>	Professor Adam Sander University of Copenhagen Denmark	

The originality of this thesis has been checked using the Turnitin OriginalityCheck service.

Copyright ©2024 author

Cover design: Roihu Inc.

ISBN 978-952-03-3320-1 (print)

ISBN 978-952-03-3321-8 (pdf)

ISSN 2489-9860 (print)

ISSN 2490-0028 (pdf)

<http://urn.fi/URN:ISBN:978-952-03-3321-8>



Carbon dioxide emissions from printing Tampere University dissertations have been compensated.

PunaMusta Oy – Yliopistopaino
Joensuu 2024

ACKNOWLEDGEMENTS

This PhD thesis project was done in the Protein Dynamics, Virology and Vaccine Immunology, and Immunoregulation research groups under the Faculty of Medicine and Health Technology of Tampere University between 2018 and 2024. Science is collaboration, and therefore I'm happy to have been able to utilize this large group of experts with a wide total range of expertise. The output of all current and former members of all collaborating research groups has been imperative in directing and aiding my thesis project to its final destination. Out of all the collaborators, our wonderful lab technicians Ulla, Merja, Niklas, Janne and Ninni have had the most direct effect on my work by helping me find stuff in lab and teaching me most methods that I used during the project, among other things. During this project, I have taken every opportunity to share the gospel of ELISA, SpyCatcher, and noro-VLP to new people. For all the memorable moments in lab (and a bunch of data and proteins), I thank all lab interns and students who have participated in this project: Alvaro, Nasir, Fernanda, Clara, Amna, Jalmari, both Lenas, Susanna, and Essi. I am especially excited about MSc Jonna Alkula for carrying on the noro-VLP and vaccine work in her own PhD thesis project.

Special thanks belong to my three supervisors for giving me the chance to begin this whole research project and for guiding me through it according to all their unique styles of doing research. In addition to three supervisors, I was assisted by a steering group with Docent Olli Laitinen, PhD Sampo Tuukkanen, and Docent Ilkka Junntila. The yearly meetings of the whole steering group gave me new insights and motivation to go on. I would also like to express my gratitude to the pre-examiners of the thesis, Professors Carlos Guzmán and Lloyd Ruddock. Your encouraging comments and sharp eyes for things to enhance in my thesis manuscript made it significantly better. Thank you!

Like everything in life, research is much more pleasant to do with a full stomach and with gas in the convertible. This thesis project was mostly funded by research grants, small and large. Therefore, I wish to thank Scandinavian Society of Immunology, Tampere City Science Fund, the foundations of Finnish Virus Research, Aarne Koskelo, and Onni and Hilja Tuovinen, University of Tampere

Foundation, Orion Research Foundation, Tampere Tuberculosis Foundation, Finnish Foundation for Technology Promotion, Finnish Cultural Foundation and Tampere University Doctoral School. Sigrid Juselius Foundation, the Research Council Finland, and Finlab Laboratories also deserve credit for making this study possible.

Finally, I wish to thank my friends and family for the support they have shown during the long thesis project. Thank you for having confidence in me while I've worked on my science hobby at the university. Maybe just a little bit of more science after this, and I promise to at least consider getting a real job.

Tampere, January 2024

Vili Lampinen

ABSTRACT

Vaccination is an old but increasingly important tool for controlling infectious diseases that spread at an ever-increasing pace in the globalized world. One of the most interesting modern vaccine technologies are virus-like particle vaccines, where the composition of the product can be precisely tailored and rationally modified. Virus-like particles are noninfectious, but physically resemble the related native virus, and can thus be used as safe, stable vaccines. More recently, virus-like particles have been decorated with parts of antigens related to other diseases, so in the resulting vaccine the virus-like particle acts as an immune activator that can direct the immune response against the target. The target does not need to be immunogenic by itself, so vaccination can be used to target select, small parts of antigens or even self-antigens. The norovirus-like particle is well-studied and known to be particularly stable and easy to handle, but its use as a vaccine carrier molecule has not been comprehensively studied. During this thesis, we developed various versions of modified norovirus-like particles that we decorated with antigens of different kinds using split-protein conjugation. The experiments yielded the SpyTag-norovirus-like particle vaccine platform that can be covalently decorated to a high density with SpyCatcher-fused antigens by simple mixing in solution. We used the platform to generate novel vaccine candidates against influenza virus and against proprotein convertase self-proteins. The most promising vaccine candidates could be developed into universal influenza vaccines that inhibit several strains of influenza for a longer time span. We also showed in mice that the norovirus-like particle platform can be used to elicit an immune response against their own proteins, facilitating new treatments for diseases such as hypercholesterolemia and cancer.

TIIVISTELMÄ

Rokottaminen on lääketieteelliseksi keksinnöksi jo vanha, mutta sen merkitys on vain kasvanut vuosien saatossa. Tiiviissä ja globaalissa nyky-yhteiskunnassa leviämiskykyisimmät tartuntataudit pääsevät hetkessä jokaiseen maailmankolkkaan. Näitä uusia tauteja vastaan tarvitaan uusia rokoteteknologioita, joiden kehittäminen olisi nopeampaa ja varastointi ja kuljettaminen helpompaa kuin nykyisissä jo aikaa sitten kehitetyissä ratkaisuissa. Eräs kiinnostavimmista moderneista rokoteteknologioista on viruksen kaltaisiin partikkeleihin perustuvat rokotteet. Niiden koostumusta voidaan säädellä tarkasti ja sitä voidaan myös muokata tarpeen mukaan. Viruksen kaltaiset partikkelit eivät voi aiheuttaa tartuntaa, mutta ne muistuttavat fyysisiltä ominaisuuksiltaan alkuperäistä virusta, ja ne ovatkin siis jo itsessään turvallisia mutta tehokkaita rokotteita. Viime aikoina viruksen kaltaisia partikkeleita on päällystetty muihin tauteihin liittyvien antigeenien osilla, jolloin viruksen kaltainen partikkeli toimii rokotteessa immuunijärjestelmän aktivaattorina, joka ohjaa järjestelmän kohdeantigeeniä vastaan. Tällöin kohdeantigeenin ei tarvitse itse olla erityisen immunogeeninen, jolloin kohteeksi voidaan valikoida pieniä osia antigeeneistä tai jopa osia kehon omista proteiineista. Noroviruksen kaltaisen partikkelin tiedetään olevan erityisen stabiili ja helposti käsiteltävissä, mutta sen käyttöä rokotealustana ei ole kattavasti tutkittu. Tämän tutkimuksen aikana muokkasimme noroviruksen kaltaista partikkelia geneettisesti ja päällystimme sen erikokoisilla antigeeneillä jaettuuihin proteiinipareihin perustuvan SpyCatcher-konjugaation avulla. Tutkimukset johtivat rokotealustaan, jossa SpyTag-peptidillä päällystetty noroviruksen kaltainen partikkeli voidaan pinnoittaa SpyCatcher-fuusioideilla antigeeneillä sekoittamalla komponentit yhteen liuoksessa. Käytimme rokotealustaa uusien influenssarokotekandidaattien ja kehon omia proproteiinikonvertaasientsyymejä vastaan toimivien rokotekandidaattien valmistamiseen. Lupaavimpia kandidaatteja voitaisiin tulevaisuudessa käyttää ”universaalien”, eli laaja- ja pitkävaikutteisten influenssarokotteiden kehittämisessä. Näytimme hiirissä, että noroviruksen kaltaiseen partikkeliin perustuvaa rokotealustaa voidaan käyttää kehon omien proteiinien inhiboimiseen, mistä voisi olla hyötyä esimerkiksi uusien syöpähoitojen ja veren kolesterolin alentamisen yhteydessä.

CONTENTS

1	Introduction	17
2	Literature review.....	19
2.1	Vaccines.....	19
2.1.1	Vaccine types	19
2.1.2	The mechanism of action of vaccination	22
2.1.3	Immune reactions against antigen carriers in vaccines	28
2.1.4	Vaccine decoration with SpyCatcher/SpyTag.....	30
2.2	Norovirus	31
2.3	Influenza virus.....	35
2.3.1	Overview and life cycle	35
2.3.2	Hemagglutinin as an antigen	37
2.3.3	Matrix-2 protein as an antigen	38
2.4	Protein convertases	39
3	Aims of The Study	42
4	Materials and methods.....	43
4.1	Carrier and antigen design and modeling	43
4.2	Norovirus-like particle production	45
4.2.1	Baculovirus-dependent norovirus-like particle expression	46
4.2.2	Baculo-free norovirus-like particle expression	46
4.2.3	Purification of norovirus-like particles	47
4.3	Antigen production	48
4.3.1	Antigen expression.....	48
4.3.2	Antigen purification.....	48
4.4	SpyCatcher/SpyTag conjugation.....	49
4.5	Characterization and quality control of vaccine candidates.....	49
4.5.1	SDS-PAGE and Western blotting.....	49
4.5.2	Mass spectrometry	50
4.5.3	Particle size and morphology	51
4.5.4	Thermal stability measurements	51
4.5.5	Concentration measurements.....	52
4.6	Preclinical experiments	53
4.7	Immunological studies	54
4.7.1	Antibody levels by ELISA	54

4.7.2	Cytokine levels after splenocyte activation by FluoroSpot.....	55
4.7.3	Cytokine levels after splenocyte activation by ELISA	55
4.7.4	Flow cytometry	55
4.7.5	Cytokine levels in mouse serum.....	56
4.7.6	Statistical analyses.....	56
4.7.7	Noro-VLP histo-blood group antigen binding	57
4.7.8	Influenza neutralization assay.....	57
4.7.9	Diphtheria proteolysis assay	57
5	Summary of the results	59
5.1	Norovirus-like particle can self-assemble with C-terminal modifications	59
5.2	SpyCatcher fused antigens	63
5.3	SpyTag-noro-VLP tolerates conjugation of SpyCatcher-antigens	65
5.4	Potential candidates for universal influenza vaccines	69
5.5	Potential candidates for furin vaccines (IV)	74
5.6	Tagged and decorated noro-VLPs work as potential norovirus vaccines	77
5.7	SpyCatcher fusion enhances immune responses	79
6	Discussion.....	80
6.1	VLP based vaccines offer many benefits over conventional technologies	80
6.2	The norovirus-like particle as a vaccine platform.....	82
6.3	Novel influenza vaccine candidates developed during the project.....	84
6.4	Endogenous proprotein convertase vaccine candidates.....	86
6.5	The immunogenicity of SpyCatcher	88
7	Conclusions	90
8	References.....	93

List of Figures

Figure 1.	The innate and adaptive immune systems	23
Figure 2.	Environmental stability of norovirus-like particles	32
Figure 3.	Influenza and the hemagglutinin (HA) ministem.....	36
Figure 4.	Norovirus-like particle stability studies	63
Figure 5.	Conjugation of SpyCatcher-antigens on noro-VLP.....	66
Figure 6.	Size and morphology of norovirus-like particles.....	68
Figure 7.	Antibodies generated by influenza vaccine candidates.....	71
Figure 8.	Unadjuvanted PPC-coated noro-VLPs induce the production of PCSK9 and furin-specific IgGs.....	76
Figure 9.	Norovirus-specific antibody responses	78

List of Tables

Table 1.	Noro-VLP versions produced during the project.....	44
Table 2.	SpyCatcher-fused antigens produced during the project	44
Table 3.	M2e-based influenza vaccines and their doses used in the experiments.....	73

ABBREVIATIONS

APC	antigen-presenting cell
BCA	bicinchoninic acid (assay)
BCR	B-cell receptor
BSA	bovine serum albumin
CDR	complementarity-determining region
CnaB2	collagen adhesin domain (of FbaB)
DD	dimerization domain of nucleoprotein (of SARS-CoV-2)
DIIG	peptide based on PCSK9 LDLR binding site
DLS	dynamic light scattering
DSC	differential scanning calorimetry
DSF	differential scanning fluorimetry
ELISA	enzyme-linked immunosorbent assay
FbaB	(<i>S. pyogenes</i>) fibronectin binding protein
FBS	fetal bovine serum
GMT	geometric mean titer
HA	(influenza) hemagglutinin
HBGA	histo-blood group antigen
Hi5	“High Five” insect cells from <i>Trichoplusia ni</i> ovarian tissue
HRP	horseradish peroxidase
IC50	half-maximal inhibitory concentration
IFN- γ	interferon gamma
IL	interleukin
IPTG	isopropyl β -D-1-thiogalactopyranoside
LB	lysogeny broth
LDL	low-density lipoprotein
LDLR	low-density lipoprotein receptor
M1	(influenza) matrix 1 capsid protein
M2	(influenza) matrix 2 ion channel
M2e	ectodomain of influenza M2
MAMP	microbe associated molecular pattern

MDCK cells	Madin-Darby canine kidney cells
MHC	major histocompatibility complex
MOI	multiplicity of infection
MWCO	molecular weight cut-off
NA	(influenza) neuraminidase
NK cell	natural killer cell
OD _{600 nm}	optical density at 600 nm
OPD	o-phenylenediamine dihydrochloride
PAMP	pathogen associated molecular pattern
PBS	phosphate-buffered saline
PCSK	proprotein convertase subtilisin/kexin
PEED	peptide based on PCSK9 LDLR binding site
PEG	polyethylene glycol
PEI	polyethyleneimine
PPC	proprotein convertase
RBD	receptor binding domain (of SARS-CoV-2 Spike)
RT	room temperature
SARS-CoV-2	severe acute respiratory syndrome coronavirus 2
SDS-PAGE	sodium dodecyl sulfate polyacrylamide gel electrophoresis
SEC	size-exclusion chromatography
Sf9	insect cells from <i>Spodoptera frugiperda</i> ovarian tissue
SWG	peptide based on furin active site
TBS	Tris-buffered saline
TCR	T-cell receptor
TFF	tangential flow filtration
TEM	transmission electron microscopy
VLP	virus-like particle
WT	wild type

LIST OF ORIGINAL COMMUNICATIONS

This thesis work is based on the following original publications and unpublished data.

- I **Lampinen V**, Heinimäki S, Laitinen OH, Pesu M, Hankaniemi MM*, Blazevic V*, Hytönen VP*. Modular vaccine platform based on the norovirus-like particle. *Journal of Nanobiotechnology* 19 (2021). <https://doi.org/10.1186/s12951-021-00772-0>

- II Heinimäki S, **Lampinen V**, Tamminen K, Hankaniemi MM, Malm M, Hytönen VP, Blazevic V. Antigenicity and immunogenicity of HA2 and M2e influenza virus antigens conjugated to norovirus-like, VP1 capsid-based particles by the SpyTag/SpyCatcher technology. *Virology* 566 (2022). <https://doi.org/10.1016/j.virol.2021.12.001>

- III **Lampinen V**, Gröhn S, Soppela S, Hytönen VP, Hankaniemi MM. SpyTag/Catcher display of influenza M2e peptide on norovirus-like particle provides stronger immunization than direct genetic fusion. *Frontiers in Cellular and Infection Microbiology* 13 (2023). <https://doi.org/10.3389/fcimb.2023.1216364>

- IV **Lampinen V**, Ojanen MJT, Muñoz Caro F, Gröhn S, Hankaniemi MM, Pesu M, Hytönen VP. Experimental VLP vaccine displaying a furin antigen elicits autoantibodies and is well tolerated in mice. Submitted manuscript.

* Equal contribution

AUTHOR'S CONTRIBUTIONS

- I Hytönen, Blazevic and Laitinen conceptualized the use of noro-VLP as vaccine platform. Hankaniemi, Hytönen, Laitinen and Lampinen designed the experiments. Immunization regime and immunological analyses were designed together with Hankaniemi, Hytönen, Lampinen, Heinimäki and Blazevic. Lampinen produced the experimental vaccines and performed most experiments under the supervision of Hankaniemi, Hytönen and Pesu. Lampinen, Hankaniemi, Hytönen and Laitinen analyzed and interpreted the results. Lampinen drafted the manuscript and figures. All authors discussed the results and commented on the manuscript to help shape its final version. All authors read and approved the final manuscript.

- II Heinimäki, Lampinen, Tamminen and Hankaniemi contributed to the development of methods for the study. Lampinen produced and purified the SpyTag-noro-VLPs and SpyCatcher-fused influenza antigens that Heinimäki and Tamminen utilized in animal studies and immunological assays. Heinimäki, Lampinen, Tamminen and Blazevic contributed to the visualization of the results. Heinimäki prepared the first manuscript draft and figures. All authors reviewed and edited the manuscript to help write the final version. All authors read and approved the final manuscript.

III Lampinen, Hankaniemi, Hytönen and Blazevic contributed to conception and design of the study. Lampinen produced the experimental vaccines and performed most experiments. Gröhn and Soppela took part in the immunizations and completed the cell response studies and their data analysis independently. Lampinen prepared the first manuscript draft and figures, while Gröhn wrote sections of the manuscript. All authors discussed the results and commented on the manuscript to help shape its final version. All authors read and approved the final manuscript.

IV Pesu and Hytönen conceived the original idea for the project and developed the idea into the final research plan together with Lampinen, Ojanen and Hankaniemi. Lampinen produced the vaccines and performed the immunizations and experiments with Ojanen in the supervision of Hankaniemi, Hytönen and Pesu. Muñoz Caro performed the splenocyte stimulation experiments. Gröhn helped with the animal experiments. Lampinen and Ojanen analyzed and interpreted the results with contributions from Hytönen, Pesu and Hankaniemi. Lampinen and Ojanen drafted the manuscript and figures. All authors discussed the results and commented on the manuscript to help shape its final version. All authors read and approved the final manuscript.

1 INTRODUCTION

Vaccination is a centuries-old medical intervention that has had an enormous effect on the collective health of human civilization. In the past, it has been an equally important remedy against bacterial and viral diseases, and it still remains the most important aid against viral sickness. Virus pandemics have long emerged at regular intervals, but globalization and the increased proximity of humanity and wildlife territories are increasing the chances for pandemic spread of zoonotic pathogens (Clifford Astbury et al. 2023). The most recent one of these, severe acute respiratory syndrome coronavirus 2 (SARS-CoV-2), caused such panic in societies that it caused a dramatic increase in public interest and funding in the field of vaccination globally, leading to rapid finalization and implementation of mRNA vaccine technology. The current mRNA vaccine technology will likely expand the implementations of vaccination further, but still needs to be supplemented with other technologies to face the challenges from viruses emerging in the future and to move into new types of disease prevented or treated by vaccination.

Virus-like particles (VLPs) work as safe and effective modern vaccines. Unlike vaccines made of live viruses, they contain no viral genomic material, which frees them from the risk of causing disease related to the parental virus. VLPs are made by recombinant expression of virus capsid proteins followed by their subsequent self-assembly into capsids that are very similar in size and shape to the respective native virions. Like viruses themselves, VLPs are stable and resilient, and thus easy to store, transfer and administer as vaccines. The repetitive surface structure and suitable size of VLPs facilitate efficient formation of immune responses. This immune-activating ability can be utilized in making vaccines against the parental virus of the VLP or in using the VLP as an immunogenic carrier for presenting heterologous antigens. Both types of VLP vaccines are already in commercial use. The human papilloma virus vaccine Gardasil is an example of the prior case, while the recently approved Mosquirix H W 2300 consists of a malaria antigen presented on the surface of hepatitis B VLP. Mosquirix is the first and only clinically approved vaccine against malaria and is currently used to protect people at risk in countries in

Africa (Syed 2022). The malaria vaccine was decades in the making and the breakthrough obtained through VLP technology is proof of its power.

Heterologous display of antigens on VLPs or other immunogenic carriers makes it possible to use vaccines in new contexts. Small molecule weight fragments of pathogens, like peptides, are often weakly immunogenic by themselves and need a carrier or at least a strong adjuvant to be useful as vaccines. On the other hand, the patient's own proteins (self-proteins or endogenous proteins) can be harmful in certain cancers or metabolic disorders. Experimental vaccines against cancer direct the immune system to destroy the body's own malfunctioning cancer cells or reduce the levels of proteins that help tumor survival or growth (Palladini et al. 2018). For example, overexpression of HER2 is observed in many cancer types and is associated with poor prognosis (Slamon et al. 1987). Another example of a self-vaccine is a vaccine against the patient's own angiotensin II, which has shown promise in decreasing blood pressure by inhibiting the activity of this protein in phase II trials (Tissot et al. 2008). New vaccines have the potential to make long-term treatment of these chronic diseases easier and cheaper. Gain-of-function mutations in PCSK9 cause high blood cholesterol (Leren 2004), while loss-of-function in the same gene reduces cholesterol levels and the risk of cardiovascular disease (Cohen et al. 2005). Self-proteins and even peptides can be linked to VLPs and used as vaccines to inhibit cancer progression or to lower the effective concentration of proteins associated with the onset of diseases, following the concept of therapeutic antibodies. Notably, therapeutic antibodies are the fastest growing group of new drugs and currently there are more than 190 therapeutic antibodies approved for clinical use (www.antibodysociety.org/antibody-therapeutics-product-data; 9.11.2023).

In this project, we modified the C-terminus of the noro-VP1 protein to facilitate easy decoration of norovirus-like particles (noro-VLP) with heterologous antigens via SpyCatcher/SpyTag linkage and via direct fusion of the influenza M2e peptide. We used the SpyTag-noro-VLP to generate and test universal influenza vaccines against conserved parts of the influenza virus. Targeting conserved parts of the virus could enable a single vaccine to work against multiple influenza strains over a longer time span, as compared to current, annually renewed vaccines. We also immunized mice against their own PCSK9 and furin proteins, proving that the SpyTag-noro-VLP can be used as a basis for self-vaccines. PCSK9 inhibition is helpful in treatment of high cholesterol, while furin inhibition is already used to treat certain cancers and is considered for treating some dangerous infectious diseases.

2 LITERATURE REVIEW

2.1 Vaccines

2.1.1 Vaccine types

According to the Oxford English Dictionary, a vaccine is a “material prepared from the causative agent of a disease, or a product of such an agent, for use in immunization”. This definition and its further explanations in the entry cover all historical and current forms of vaccines. The earliest and simplest form of vaccination as per the definition was called variolation, in which healthy people were introduced to smallpox-containing material from a patient. Inoculation of the disease-causing virus was done via the skin of healthy people, causing the respiratory virus to inflict less damage than by typical infection through the lungs, but still providing resistance to future smallpox encounters. Some sources claim that this method had been in use for more than 2000 years throughout the Old World. In the late 1700s, Edward Jenner successfully used material obtained from a cow suffering from a related virus called cowpox in a human patient for prevention of smallpox. This method contained a significantly smaller risk of severe side effects as compared to variolation, where death was not uncommon. From 1796 onwards, Jenner’s smallpox vaccine was widely distributed as the first commercial vaccine and its derivations eventually eradicated smallpox from the world by 1977. (A Brief History of Vaccination (who.int); 28.7.2023)

Variolation and Jenner’s first smallpox vaccine were both examples of live virus vaccines. In most cases of both treatments, the immunization caused symptoms like the disease it is supposed to prevent. Some live vaccines are still in use today, but they are all attenuated (i.e., weakened), which significantly reduces unwanted symptoms from vaccination. The first attenuated vaccine against chicken cholera was invented by Louis Pasteur already in 1879 (<https://www.vbivaccines.com/evlp-platform/louis-pasteur-attenuated-vaccine/>; 28.7.2023). He attenuated the cholera bacteria simply by exposing them to oxygen for a prolonged time in the lab, reducing their ability to cause disease. Pasteur also made the first attenuated anti-virus vaccine

by repeatedly passaging rabies virus in rabbits before giving the virus to human patients. After multiple passages in another host, or later, temperature, the virus becomes more adapted to the artificial conditions, and at the same time, less adapted to infecting humans, and thus the virus is attenuated. During the 20th century, similarly attenuated live pathogens were used to prevent several formerly deadly diseases, and many vaccines in use now, e.g. the rotavirus vaccine (Rotateq, Merck, USA) in the Finnish vaccination program, are still of this type.

With the advent of the modern techniques of recombinant biology, vaccine components became more defined. Subunit vaccines only contain certain structural fragments of the pathogen, produced recombinantly in an expression organism (most often cultured bacteria, fungus, mammalian, or insect cells), and purified of other components in the expression system. The fragments may be polysaccharides from bacterial cell walls (e.g. Pneumovax pneumococcus vaccine, Merck, USA), soluble proteins from the surface of a virion (Flublok influenza vaccine, Protein Sciences, USA), or polysaccharides conjugated on immunogenic carrier proteins. Subunit vaccines are not in contact with the genome of the pathogen at any point of their preparation, which removes the risks of failed inactivation (inactivated vaccines) or reversal of attenuation of a live vaccine through mutation.

Soluble protein vaccines are safer and more defined than their predecessors, but compared to whole virions, soluble proteins are small and usually less immunogenic. Therefore, subunit vaccines often require added adjuvants to provide long-lasting protection. A vaccine adjuvant is a substance mixed into the vaccine formulation that aims to enhance or modulate the immune response. Many general mechanisms of action for adjuvants are known, but often all the mechanisms utilized by a specific adjuvant to produce its effect are unclear. For example, cyclic di-adenosine monophosphate provides pathogen associated molecular patterns (PAMPs) to the injection site, recruiting immune cells, activating the innate immunity, and inducing strong interferon gamma responses (Lirussi et al. 2021). Some common vaccine adjuvants, like alum ($\text{Al}(\text{OH})_3$), can activate humoral immune responses at the expense of the cellular response (Brewer et al. 1996). Its more modern derivative called AS04 mixes $\text{Al}(\text{OH})_3$ with monophosphoryl lipid A and gives a more balanced immune boosting effect, also activating cellular immunity (Casella and Mitchell 2008; Didierlaurent et al. 2009). Better vaccine adjuvants are under constant research, but there are still quite few licensed adjuvants of different types (Li et al. 2021).

In subunit protein vaccines, the gene encoding the protein is translated in an expression host cell and then purified before being given to the patient. Modern mRNA and viral vector vaccines transport the protein antigen into the cells of the

patient in a more direct way. Messenger RNA vaccines contain stabilized mRNA that encodes a pathogen protein (Verbeke et al. 2019). Because mRNA in the body is under constant degradation by nucleases, the biochemical structure of therapeutic mRNA has been modified for faster translation and slower degradation rates. The main innovations here are the addition of a 5' cap, a polyA tail, 5' and 3' untranslated regions, and modified nucleosides (Sahin et al. 2014; Verbeke et al. 2019). The mRNA is packaged in liposomes that protect it and allow passage into the cytosol of the patient's cell, where it is translated into protein, activating the immune response. The most successful SARS-CoV-2 vaccine (Comirnaty, Pfizer, USA and BioNTech, Germany) was the first clinically approved example of an mRNA vaccine. Viral vector vaccines, on the other hand, utilize modified non-pathogenic viruses (adenoviruses being the most used) as vectors that infect cells, and make the host cell produce the desired antigen from a pathogen (Draper and Heeney 2010).

The protein shell, or capsid, which protects the nucleic acid genome of a virion, is self-assembling in the case of most viruses, often even in the absence of the genome or other virus proteins. This means that recombinant expression of capsid proteins causes them to self-assemble into empty capsid structures that closely resemble the virions they are derived from. These structures are called virus-like particles (VLPs). Unlike soluble subunit vaccines, VLPs are of an optimal size (20–200 nm) to be taken up by antigen-presenting cells (APCs) and for direct entry into the lymphatic system (Bachmann and Jennings 2010). VLPs, like virions and the flagella of bacteria, have repetitive surface structures that are close to each other. The immune system has evolved to recognize structures like this as foreign, which leads to stronger immunogenicity of VLPs as compared to small, soluble subunit vaccines. A hepatitis B VLP vaccine against hepatitis B has been in clinical use already since 1986 (Recombivax HB, Merck, USA).

The vaccine type used in my PhD project could be called a chimeric VLP vaccine. In addition to providing immunity against the virus the VLP is derived from, these vaccine preparations have the VLP decorated with antigens from another pathogen. Here, the VLP acts as an antigen carrier and immune activator, presenting the heterologous antigen in a molecule in the optimal size range and in repetitive units spatially near each other. Presenting antigens on the surface of an immunogenic, virus-like particle makes it possible to immunize against antigens that are nonimmunogenic themselves, like very small antigens or antigens that the patient has tolerance for. Conjugation of a heterologous antigen onto the VLP can be executed by genetic fusion, chemical conjugation or through click chemistry linkers.

The world's first licensed malaria vaccine is a chimeric vaccine made of hepatitis B VLP that is genetically fused to a malaria antigen (Mosquirix, GSK, UK).

Before the widespread success of antibiotics starting from the 1930s (Hutchings et al. 2019), vaccines were the most important tool to fight both bacterial and viral diseases. Now, a set of vaccines is given to all citizens during their early life according to a national vaccination program in most countries. Against viruses, they remain the most important tool in humanity's dispersal. Out of the vaccine types outlined in this chapter, the most common vaccines in use are simple attenuated live vaccines and inactivated vaccines made by weakening or killing live pathogens. The pathogens are now grown more often in laboratory cell cultures and bioreactors than in live animals, but otherwise the process is similar. The past decade has seen the approval of the first human mRNA vaccines and the first chimeric VLP vaccine, so further expansion of the technology array is to be expected in the near future. More than 100 clinical trials involving VLP vaccines have been completed in the 21st century, and currently, there are 32 of such clinical trials ongoing (<https://clinicaltrials.gov/>; 9.11.2023).

2.1.2 The mechanism of action of vaccination

All multicellular organisms are under constant pressure from microbes that try to claim the nutrients stored in the body. Without an immune system to keep these opportunists at bay, they would take over in mere days. The immune systems of mammals can be roughly divided into innate and adaptive compartments, even though they also have some inter-activating properties (Figure 1). The innate system detects structures that are common to many pathogens, like cell wall components and conserved flagellin protein sequences of bacteria, or double-stranded RNA of viruses (Janeway and Medzhitov 2002). Additionally, the repetitive surface patterns found on the surface of virions or virus-like particles activate the innate complement system directly and through multivalent binding of natural IgM antibodies that in turn recruit complement components (Bachmann and Jennings 2010). These structures are collectively called pathogen or microbe associated molecular patterns (PAMPs or MAMPs). The innate immune system is enough to kill commensal bacteria that venture out from their tolerated locations within the body and to stop most mild infections in the first few days after onset, but if an infection is strong enough to persist after that, participation of adaptive immunity is needed in destroying the pathogen.

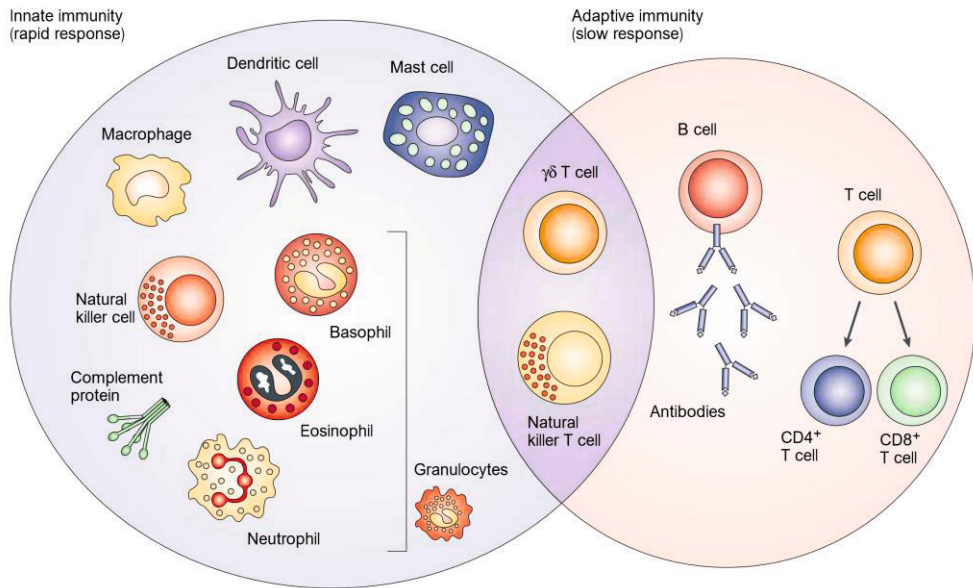


Figure 1. The innate and adaptive immune systems. The innate immunity is faster to respond when an infection begins, but it cannot eradicate the most serious infections and does not develop in pathogen encounters, like the adaptive system does. Dendritic cells are the main antigen-presenting cells of the innate immunity, macrophages, and natural killer (NK) cells take in pathogens and destroy them and mast cells and granulocytes secrete anti-pathogenic and immune activating molecules to their environment. The complement system is not made of immune cells but proteins that directly bind pathogens in a cascade reaction. Antibody-secreting B cells and cytotoxic (CD8⁺) and helper (CD4⁺) T cells are the main components of the adaptive immune system. The two immune systems intertwine, and natural killer T cells and $\delta\gamma$ T cells are examples of cells that have features from both arms of the immune system. Adapted with permission from (Dranoff 2004).

Instead of patterns common for many pathogens, adaptive immunity depends on specific surface shapes, and its effect is based on clonal expansion of immune cells. When encountering a pathogen for the first time, there are only a few immune cells specific for that pathogen, but after that, through clonal expansion of these cells, the animal prepares for the next insult by the same pathogen with up to a million faster-reacting memory cells that even maintain a base level of pathogen-inhibiting antibodies in the body (Tangye and Tarlinton 2009). All this reduces the time needed for the activation of adaptive immunity, but in any case, adaptive immunity takes at least a few days to reach its full effect, instead of hours or minutes for the innate immunity. Adaptive immunity is activated upon all pathogen encounters, priming the system to react faster and stronger upon the next contact with the same or closely related pathogen. The basic principle of vaccination is to achieve this priming against the pathogen as strongly as possible to prepare the immune system without causing strong symptoms of disease. Simultaneously, the response must be specific to the pathogen to avoid autoimmune disease.

The priming of the adaptive immune system is achieved by forming memory cells – long-lasting copies of the activated cells of the adaptive immune system. The main cells of the adaptive immunity are called B cells and T cells, which mature in the bone marrow (B) or the thymus (T). On their surface, both cell types express a receptor that is very specific to a certain ligand, called an epitope. All B or T cells express only a single type of their receptor with a single specificity. As pathogens come in almost all possible shapes, a huge number of immune cells with different receptor specificities needs to be generated. During the maturation of B and T cells, the genes of the B-cell receptor (BCR) or T-cell receptor (TCR) are shuffled in somatic V(D)J recombination (Hozumi and Tonegawa 1976). In this process, the part of the gene encoding the hypervariable complementarity-determining region (CDR) is constructed from dozens of different V, J and D segments in the genome. Different combinations of the segments can yield more than 1×10^{12} different receptor structures. Billions of B and T cells with different specificities patrol the mammalian body at all times, allowing a specific reaction to all imaginable pathogens and mutated self-cells. After a B or T cell has bound its specific antigen and activated, it starts proliferating, and thus preparedness for that type of pathogen is increased through increased numbers of specific defenders.

Although activated B cells mainly boost their effect through making copies of themselves, the progeny cells are also improved over their naive ancestors. The main effector function of B cells is to secrete antibodies that destroy or inhibit pathogens, infected cells, and mutated cells. Antibodies specifically bind their target with high

affinity, which may lead to its marking for phagocytosis (i.e., opsonization), neutralization or agglutination (Lu et al. 2018). Before encountering their epitopes, B cells can only secrete IgM and IgD antibodies, but after activation, B cells can go through class switching to express IgA, IgE or IgG (Cory and Adams 1980). The antibody class they switch to depends on the type of pathogen they face and the circumstances where they find the pathogen in. Class switching only changes the constant domains of the antibody, so the specificity does not change during the process. However, activation of a B cell also activates another process called somatic hypermutation, or affinity maturation, which introduces point mutations to the antigen-specific part of the generated antibodies (Odegard and Schatz 2006). Some of these mutations increase the affinity to the pathogen and some of them decrease it. Regulatory signals induce B cells that produce receptors with increased affinity to target antigen to survive and continue proliferating, while lowered affinity or affinity towards self-targets leads to apoptosis signals. Thus, total affinity of the pathogen-specific B cell population increases over multiplication rounds. Overall, the B cell response is enhanced by forming more copies of reactive B cells that secrete matured, high affinity antibodies suited for inhibition of the pathogen in question. After eradication of the pathogen, some of the class-switched and affinity matured B cells remain as memory cells, causing an immediate, dedicated response against the pathogen upon re-encountering it.

B cells recognize antigens directly through their B cell receptors, but T cell receptors, instead, recognize antigen fragments presented on the major histocompatibility complexes (MHCs) of other cells. As a result, B cell epitopes represent a segment on the surface of a larger antigen and encompass 5–30 amino acid residues, while the linear peptides that T cell receptors recognize can be 9–22 amino acids long (Sanchez-Trincado et al. 2017). All cells digest samples of the proteins they produce and present them on class I MHCs. This way cytotoxic, i.e., CD8⁺ T cells can recognize virus-infected cells expressing viral proteins or cancer cells expressing mutated self-proteins and destroy them. Antigen-presenting cells, mainly dendritic cells, macrophages, and also B cells take up extracellular pathogens, digest them and present their fragments on class II MHCs to activate helper (CD4⁺) T cells or regulatory T cells. Helper T cells are important in activating antigen-bound B cells to proceed to affinity maturation and antibody class switching, in activation of cytotoxic T cells to induce apoptosis, and in secreting the signaling molecules of the immune system, cytokines, to recruit and activate components of the innate immunity. Cytokines have varying effects on different immune cells depending on the combinations and circumstances they find the signals in. For example,

interleukin-12 (IL-12) and interferon gamma (IFN- γ) are important cytokines for vaccines as they mostly act as general signs of inflammation and activate and recruit T helper cells. Activated T helpers then secrete more of IFN- γ and tumor necrosis factor (TNF), activating themselves along with dendritic cells macrophages and cytotoxic T cells (Kopf et al. 2010). Professional antigen-presenting cells sometimes present also extracellular pathogens, especially viruses and virus-like particles, on their class I MHCs. This so-called cross-presentation helps activate cytotoxic response against the pathogen (Bachmann and Jennings 2010). Regulatory T cells, on the other hand, suppress all types of immune responses when activated. They have an important role in creating tolerance to self-proteins and harmless molecules in food and in keeping the immune system from over-reacting to microbes and potentially causing more damage than the invading microbe itself (Andersson et al. 2008).

As described above, the antigen-recognizing domains of B and T cell receptors and antibodies form their specificity through a random gene shuffling process. Unlike MAMPs that activate the innate immune response, B and T cells can develop to recognize almost any combination of shape, charge, and hydrophobicity, including in components of the own body. To avoid chronic inflammation and tissue destruction by the immune system, collectively called autoimmune disease, self-reactive B and T cells are under strict regulation. During maturation, these immune cells are actively tested for autoimmunity by presenting them with an antigen collection that includes tissue-specific protein fragments from around the whole body. Most self-reactive T cells and some B cells are removed through apoptosis through this mechanism already during their maturation in bone marrow or thymus (Chackerian et al. 2008). Some self-reactive cells undergo receptor editing (Chen et al. 1995a). These mechanisms eliminate self-reactive T cells almost completely, but a significant fraction of B cells evade these systems (Chackerian and Fritze 2016). Usually though, autoreactive B cells alone are not enough to cause autoimmune disease, because specific antigen recognition of most antigens does not activate a B cell without T helper coactivation (Bretscher and Cohn 1970). Instead, the B cell becomes anergic (Fulcher and Basten 1994). However, with multivalent antigens, like viruses or virus-like particles, where the epitopes are spatially close to each other, multiple B cell receptors on a single cell can bind the same antigen. This BCR crosslinking strongly activates B cells even without T cell help and can reduce the demand for T cell help, too (Dintzis et al. 1983, 1989).

To get a picture of the vertebrate immune system as a whole, let's imagine an influenza virus infecting a naive human. Virions enter via the lungs and a small part of them is able to pass the mucus layer protecting the epithelial cells below. As an enveloped virus produced in a human cell, the influenza virion resembles human cells by its lipid structure and the glycosylation pattern of its surface proteins, so in contrast to e.g., an invading bacterium, there are few MAMPs on the outside that the innate system could recognize. The virions attach to sialic acid on the cells via their hemagglutinin (HA) protein, get internalized and start multiplying with the use of the cell's machinery (Couceiro et al. 1993). At this point, the intracellular MAMP receptors of infected cells recognize the viral RNA due to its differences to mammalian RNA molecules and they start to recruit immune cells to the infected site. The infected cells start presenting freshly translated viral proteins on their surface and their fragments in class I MHCs, activating B cells and cytotoxic T cells, respectively. As this human has not encountered this strain of influenza before, naive B and T cells start multiplying slowly, but still the first IgM molecules and cytotoxic T cells have their role in subduing infection. IgM binds viral proteins on infected cells and virions and activates complement against them but penetrates poorly into tissue. Infected cells generally present less MHC on their surface than healthy cells do, which activates natural killer (NK) cells to induce apoptosis on them (Belizário et al. 2018). Provided that the human is strong enough to survive the first few days after the first infection, cells of the adaptive immunity have multiplied and matured enough to destroy all released virions and infected cells. A fraction of the cloned influenza-specific cells remains in the body for years to protect from infections by the same strain.

In summary, the goal of vaccination is to multiply B and T cells with the desired antigen specificities. Before vaccination, a few copies of the cells have already been produced in the body through a random genome shuffling process. After facing the antigen in the vaccine, these cells become activated, multiply, and maintain up to a million-fold higher clone number for a long time after the immunization (Hodgkin et al. 2007). The B cells also refine their secreted antibodies by increasing their affinity and changing the antibody class to increase the strength of response to the antigen and to tailor the immune response type to better suit the faced antigen. Class-switching is directed by the context and location the antigen is faced in vaccination, and carriers and adjuvants can have a role in adjusting this. In addition to increased clone numbers of relevant B and T cells, the concentration of antigen-specific antibodies circulating in the blood and tissues increases, sometimes remaining

elevated for decades. All these modifications to the immune system make the patient decisively better prepared for the next encounter with the antigen.

2.1.3 Immune reactions against antigen carriers in vaccines

When transporting vaccine antigens to the patient on immunogenic carriers or inside bacterial or viral vectors as nucleic acids, immune responses form against the carrier. The vaccine carrier or vector is often related to a human pathogen, meaning that in many cases, the adaptive immunity is already primed against the carrier or vector. Pre-immunity against the carrier or vector exists at the very least during the second immunization with the same carrier or vector, for example when administered as a booster shot with the same antigen load or if used as vaccine against a completely different vaccine target. This pre-immunity may affect the formation of immune responses against the transported antigen in different ways in various applications.

If pre-immunity against a pathogen-based vector vaccine exists, the vector's entry into other than immune cells may be restricted, and the time the vector spends in the patient's body is reduced due to actions of the immune system. This is particularly problematic for viral vectors that need to reach and infect their host cells to work. Especially a high titer of neutralizing antibodies against the viral vector would, by definition, stop most of the vector viruses from ever creating the vaccine antigen whose gene they are carrying. Saxena et al. reviewed 8 studies on viral vectors and reported that cell-mediated immune response was lowered by pre-immunity in 7 of them, while reduction of humoral responses was reported in 3/8 studies (Saxena et al. 2013). In the same review, it is noted that most vaccine vectors based on the intracellular Salmonella bacterium worked better in pre-immunized groups where the effect was determined, and humoral responses were increased in half of the studies.

The difference in the achieved results may be due to Salmonella vectoring ability benefitting from opsonization-dependent macrophage phagocytosis. Phagocytosis of Salmonella vectors lead to their cargo antigens being presented on macrophage surfaces (Saxena et al. 2009), while the same immune response destroys adenovirus vectors without any antigen expression (Carey et al. 2007). The main difference is that Salmonella is able to translate the antigen gene it carries, while the virus acts merely as a carrier and translation can take place in an infected cell only. However, knowledge on this topic is still limited, as most comparable studies have been conducted in mice and human studies are still limited. The most extensive human

studies on adenovirus vectors have been on SARS-CoV-2, where negative effects of pre-immunity have been shown (Zhu et al. 2020). For this reason, vaccinations based on virus vectors may utilize different strains of virus as carriers (like the Sputnik V SARS-CoV-2 vaccine by Gamaleya National Centre of Epidemiology and Microbiology, Russia). This strategy, however, could be challenging when considering vaccinations with antigens where multiple booster doses are required.

When target antigen proteins are presented on top of a VLP or another type of carrier molecule, the situation is probably very similar to the Salmonella-carried vaccines described above. The antigens are already translated, so the goal of vaccination is to simply transport the antigens into macrophages or dendritic cells for digestion and presentation to B and T cells. In this scenario, pre-immunity against the carrier may even be beneficial in increasing intake into antigen-presenting cells. In a mouse model, it was found that pre-immunized mice took a VLP-presented antigen more promptly into B cells, while uptake in naive mice was mostly into dendritic cells (Renjifo et al. 1998). This did not suppress the immune reaction, only directed it more towards a humoral direction. Also in mice, it was shown that immune responses against the presented antigen were suppressed with carrier pre-immunity, but the effect disappeared with repeated immunizations and increased vaccine dosage (Chuan et al. 2013; Jegerlehner et al. 2010). Jegerlehner et al. reported that increased antigen surface density also raised the number of antigen-specific antibodies, but Chuan et al. noticed no change. Jegerlehner et al. also showed that the inhibitory effect of pre-immunity was dependent on antibodies against carrier sterically blocking antibody binding on the peptides displayed on VLP surface, but not on regulatory T cells, as previously suggested. In VLP systems using chimeric hepatitis B and murine polyomavirus VLPs, pre-immunity against the carrier had no negative effect on antigen-specific antibodies (Marini et al. 2019). The critical difference here may lie in the antigen size, as the previous studies used peptide-like antigens (haptens), whereas Marini et al. decorated VLPs with a whole protein domain with several epitopes that are less likely to be blocked by competing anti-carrier antibodies. As with viral vectors, the effect of pre-immunity has mostly been studied in mice, and few human studies exist yet.

In summary, at least viral vectors greatly benefit from strategies limiting pre-immunity against the carrier. These include for example using non-human viruses, rare serotypes, and removal of key epitopes by mutating the vectors. These approaches do work in controlled experiments, but if all vaccines in current human use would be replaced by viral vector-based vaccines, the sheer number of viral vectors that would need to be invented and approved continuously raises some

questions on technical feasibility and cost-effectiveness. In VLP carrier vaccines, there is no obvious downside in having pre-immunity against the carrier itself, and indeed, negative effects of pre-immunity seem easily avoided through proper antigen design, dose, and boost regime selection.

2.1.4 Vaccine decoration with SpyCatcher/SpyTag

In protein biotechnology and especially vaccinology, it is often beneficial to be able to link two proteins together only after they have been translated and properly folded to make a fusion protein. The two proteins may require different expression systems to fold correctly, their folding may be disrupted by the fusion, their oligomeric status may be incompatible, or they might simply be too large to be produced in a single, genetically fused package. In any case, genetic fusion of protein domains usually requires a deal of optimization to work properly. Post-translational fusion can be achieved for example noncovalently through avidin-biotin linkage or HisTag-Ni²⁺ affinity or covalently through chemical crosslinking or Catcher/Tag peptide bond coupling (methods reviewed in (Brune and Howarth 2018)). The rest of this chapter will discuss SpyCatcher/SpyTag which was the main method used to decorate norovirus-like particles (noro-VLPs) in this project. The first example of using SpyCatcher/SpyTag to conjugate heterologous antigens on a VLP had SpyCatchers presented on an AP205 bacteriophage VLP to decorate them with malaria antigens (Brune et al. 2016).

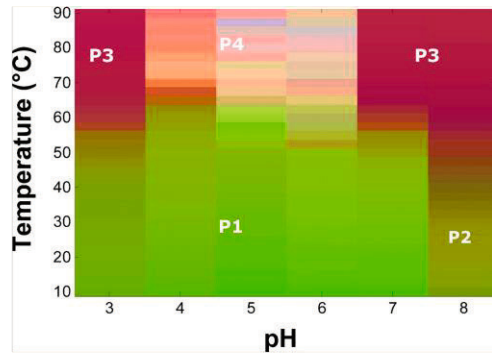
The original SpyCatcher/SpyTag is based on the immunoglobulin-like collagen adhesin domain (CnaB2) of the fibronectin binding protein (FbaB) of the pathogenic bacterium *Streptococcus pyogenes* (Zakeri et al. 2012). FbaB shows remarkable stability due to its internal isopeptide bond in the CnaB2 domain – a peptide bond crosslinking two amino acids in the same polypeptide by their side chains. By separating the beta strand containing the reactive Asp residue from the rest of the beta sheet domain, Zakeri et al. created a protein-peptide pair that folds together to complete the beta sheet structure and forms a covalent isopeptide bond between the two protein parts to lock them together. The beta sheet domain part of the pair contains the reactive Lys and a catalytic Glu which is needed in proximity of the reactive amino acids in the final fold for conjugation. After sequence optimization, the first versions of the peptide SpyTag and its protein partner, SpyCatcher, were able to form the isopeptide bond within minutes in various buffer conditions and temperatures. Further optimization of the proteins yielded a smaller SpyCatcher (Li

et al. 2014) and versions of the Catcher and Tag with faster reaction times (Keeble et al. 2017, 2019). This thesis work utilized the truncated SpyCatcher, and both the original (referred to as 001), and the 003 version of SpyTag. These protein linking tools have been widely applied in biotechnology, and currently, the Catcher/Tag toolbox contains a new, non-cross-reactive pair based on a different natural protein (Veggiani et al. 2016), a thermo-switchable non-covalent version (Vester et al. 2022), light-activatable versions (Rahikainen et al. 2023; Ruskowitz et al. 2023), and 3-part systems including two beta strands that are covalently conjugated in proximity with a catalytic beta-sheet protein domain (Buldun et al. 2018; Fierer et al. 2014).

2.2 Norovirus

After the widespread vaccination programs against rotaviruses in the 2000s, norovirus replaced rotavirus as the most common viral cause of gastroenteritis, or “stomach flu” (Atmar and Estes 2006). Noroviruses are members of the non-enveloped, positive-sense RNA virus family Caliciviridae. Norovirus mainly transmits via contaminated food or drinking water (Donaldson et al. 2010) and via the digestive system, which means that the virus needs to remain stable for long periods of time in harsh conditions. Indeed, it has been shown that noro-VLPs readily reassemble when returned to favorable conditions after disassembly by pH, but not after disassembly by high temperature (Ausar et al. 2006), and they tolerate a large range of pH values and ionic concentrations (Figure 2) (Shoemaker et al. 2010). Studies with infective virions showed that most genotypes of norovirus can remain infectious after 5 minutes of suspension in 70 % ethanol (Costantini et al. 2018; Sato et al. 2020) or after two weeks in seawater (Desdouts et al. 2022). The simple single protein capsid structure, efficient production in various protein expression systems (Mason et al. 1996; Prasad et al. 1999; Xia et al. 2007) and its resiliency make the noro-VLP an attractive platform for biotechnological development.

A



B

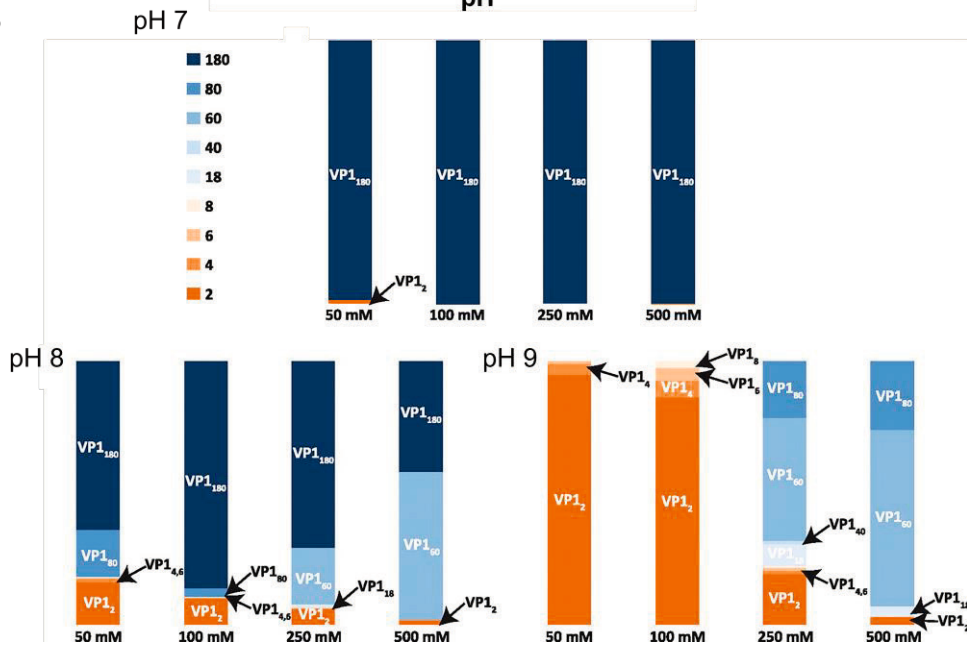


Figure 2. Environmental stability of norovirus-like particles. A) An empirical phase diagram for norovirus-like particles. P1: native, intact form; P2: disassembled; P3: soluble VP1 oligomers; P4: aggregated. Blocks of continuous color represent single empirically defined phases. B) Oligomeric state of norovirus-like particles at neutral and basic pH values and different ionic concentrations of ammonium acetate. Adapted from (Ausar et al. 2006; Shoemaker et al. 2010), used under CC BY 4.0 (<https://creativecommons.org/licenses/by/4.0/>).

Although norovirus (then, named Norwalk virus after the extraction site in Ohio, USA) was first described already in 1972 (Kapikian et al. 1972), cultivation of human norovirus was not possible until 2014 in B cells (Jones et al. 2014), and even then only to “modest levels of viral replication”. Since noroviruses can infect B cell deficient humans (Brown et al. 2016), B cells cannot be the only infectable cell type. Noroviruses bind histo-blood group antigens (HBGAs), whose type affects the susceptibility of a patient to different norovirus genotypes (Ruvoën-Clouet et al. 2013). These antigens are present on the surface of erythrocytes, certain epithelial cells, B cells and even in saliva and intestinal mucus of most people. Still, very few of these cell types work as a host for norovirus *in vitro*, meaning that other elements are needed for infection. A more sophisticated *in vitro* culture system based on human intestinal enteroids was able to replicate all tested genotypes of norovirus to a high degree (Ettayebi et al. 2016). While some genotypes of norovirus infected the enteroids under common culture conditions, others required an unknown modification of the host cells by some non-protein component in bile. For a long time, tissue tropism of norovirus has eluded researchers in the field, but taking together the advancements of the previous decade, it can be hypothesized that norovirus first enters and infects epithelial cells of the intestine, then spreads to underlying B cells or other immune cells. Norovirus needs HBGA for binding to cells, but entry is facilitated by some other, unknown receptor. Absence of secreted HBGA in the intestinal mucus of some individuals greatly reduces infectivity of many norovirus genotypes, but sometimes viruses can reach the underlying HBGA on epithelial cells through the mucus by some other means (e.g., damaged mucus layer).

As cell culture systems for the human norovirus were found only recently, most studies on norovirus so far are based on the norovirus-like particle (noro-VLP) that consists of the structural proteins only. The norovirus capsid is mostly made of a single protein, VP1. The first norovirus to be crystallized, of the genotype GI.1 showed a T=3 organization with 180 VP1 proteins making up the protein capsid (Prasad et al. 1999) and 1–2 basic VP2 proteins on the inside surface (Glass et al. 2000). The structure was obtained after recombinant expression of both structural proteins in *Spodoptera frugiperda* insect cells (Sf9). Later, noro-VLPs have been successfully produced in plants (Mason et al. 1996), yeast (Xia et al. 2007), in a cell-free protein synthesis system (Sheng et al. 2017), and in live silkworm larvae (Boonyakida et al. 2022) and pupae (Masuda et al. 2023). In later works, most labs have excluded VP2 from the expression cassette when producing noro-VLP, even

though slight increases in VLP yield (Bertolotti-Ciarlet et al. 2003) and stability (Lin et al. 2014) have been reported by including VP2 in the construct.

The crystal structure of noro-VLP solved for GI.1 noro-VLP remained the only available structure for a long time, which led to the assumption that all noro-VLPs exhibit mainly in T=3 symmetry. A population of smaller, assumably 60-mer particles with T=1 was recognized (White et al. 1997). GI.1 noro-VLP seems to assume this symmetry interchangeably with T=3 depending on assembly conditions, and both particle sizes could be disassembled and reassembled to the other size class. Only recently it was found that GII.4 noro-VLPs are predominantly in 240-mer, T=4 symmetry (Devant et al. 2019; Jung et al. 2019). GII.4 noro-VLP, which currently represents the most prevalent genotype of norovirus (Sharif et al. 2023), was also found in T=3 and T=1 symmetries in lower quantities (Devant and Hansman 2021). While T=1 (23 nm) is easily distinguished from the other forms by transmission electron microscopy (TEM), T=3 (41–43 nm) and T=4 (49 nm) particles are very similar in size and morphology.

Because norovirus is a harmful and extremely prevalent virus, immense efforts have been taken to develop efficient vaccines against the disease. The most advanced vaccine candidates are based on noro-VLPs, which are very protective against homotypic challenge, but rarely generate cross-reactive responses against other strains and genotypes in monovalent form (LoBue et al. 2006). The mutation rate of norovirus is high and escape mutants evolve quickly (Lindesmith et al. 2011), maybe due to the vast receptor range that the virus can utilize. Until the recent discovery of an effective culture system for the virus, *in vitro* studies of vaccine protectivity have been based on analysis of immune responses and an HBGA receptor blocking assay only. A comparison showed good correlation between a novel true virus neutralization assay and the HBGA assay, albeit the neutralization assay showed slightly better sensitivity (Ettayebi et al. 2016), meaning that results from HBGA blocking assays are underestimates of protection efficiency. Currently, there are 6 clinical norovirus vaccine studies ongoing, 5 of them focusing on multivalent vaccines (<https://clinicaltrials.gov/>; 9.11.2023). A recently patented bivalent norovirus vaccine called GelVac is based on insect cell expressed noro-VLPs and formulated into a dry powder (Ball et al. 2017). In this powdered form, they were able to store the vaccine at room temperature until use.

2.3 Influenza virus

2.3.1 Overview and life cycle

Influenza is an enveloped virus of the Orthomyxoviridae family. The viruses from both genera A and B are very common human pathogens, but only influenza A has caused serious pandemics. Influenza A viruses are further divided into subtypes based on the main antigenic glycoproteins they express on their surface — hemagglutinin (HA) and neuraminidase (NA). HA subtypes 1, 2, and 3 and NA subtypes 1 and 2 are involved in human epidemics. The RNA genome of influenza is segmented, so when two different viruses infect the same cell, RNA segments can mix to form new hybrid viruses in an event called antigenic shift. HA and NA are encoded in separate segments and can come in any combination, which is referred to in the name of the virus, e.g. H3N2 for HA subtype 3 and NA subtype 2 influenza. (Bouvier and Palese 2008)

In most strains of influenza, the infective virions form into a spherical shape with diameters between 100 and 200 nm. The virion capsid is surrounded by a lipid envelope taken from the previous host cell. On average, some 400 HA, 100 NA and a few matrix 2 (M2) proteins protrude the envelope of each virion, but the nonstructural proteins and the RNA segments are packed safely inside the envelope and the matrix 1 (M1) polyprotein capsid right beneath it (Figure 3A). (Szewczyk et al. 2014) When infecting a new host cell, the head domain of HA first binds to a sialic acid on the cell surface (Rossman and Lamb 2011). Sialic acid is a common post-translational modification in many cell surface proteins especially in the endothelial cells of the respiratory system, which directs the tissue tropism of influenza there (Kumlin et al. 2008). The chemical bond that attaches sialic acid to these cell surface proteins differs from one animal species to another, and influenza HA has to be optimized for the specific bond for efficient binding (Kimble et al. 2010). This makes e.g., avian influenza ineffective in infecting humans.

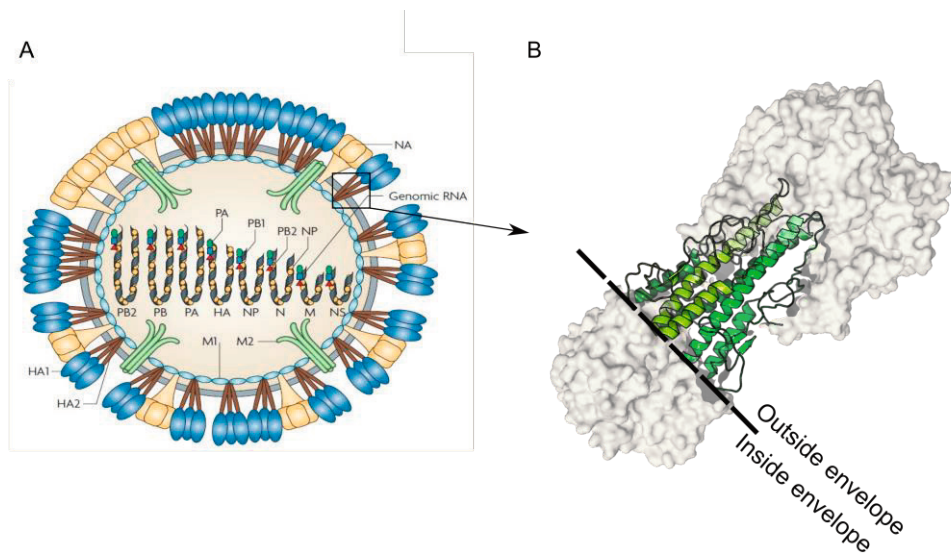


Figure 3. Influenza and the hemagglutinin (HA) ministem. A) RNA is shown here as the eight segments that each encode only one or two proteins, as described under the segment. Matrix 1 and 2 (M1 and M2) are both encoded in the same segment. The lipid envelope is shown here as a grey circle, pierced by the transmembrane proteins HA, NA and M2. B) A zoom in on the HA transmembrane protein. The HA ministem used in this work consists of the parts of HA highlighted in green. The head and transmembrane domains of the protein were left out and the protein was made trimeric by adding a Foldon trimerization domain to the construct (not shown here) in a design adapted to this work from (Mallajosyula et al. 2014). Panel A modified with permission from (Karlsson Hedestam et al. 2008). Panel B was prepared with the PyMol software based on the RCSB PDB structure 4M4Y (Hong et al. 2013).

After binding a cell, the influenza virion enters in an endosome, mainly through a clathrin-dependent endocytosis event (Rossman and Lamb 2011). The endosome separates the virion from the transcription and translation machinery in the cytosol. After endocytosis, the virion is still attached to the endosome membrane via HA. As the endosome matures, its pH is lowered, and influenza M2 starts pumping protons into the virion, balancing it by the outflux of K^+ (Leiding et al. 2010). The acidic environment in the virion loosens up the bonds between RNA and the virion capsid (Martin and Helenius 1991). Outside the virion envelope, the lowered pH of the maturing endosome triggers a drastic conformational change in influenza HA, almost doubling it in length (White et al. 1982). The enlengthened HA pierces the endosomal membrane, fusing it with the viral membrane. By then, the RNA genome

is loosened from the capsid and is free to escape into the host cell cytosol and further into the nucleus to be replicated and translated into new viral proteins.

After translation, HA is first formed as HA0, which needs to be cleaved proteolytically to form the pH-activatable heterohexamer of HA1 and HA2 (Bouvier and Palese 2008). Depending on influenza strain, the proteolysis event can happen both inside and outside of cells, but the intracellular processing in the Golgi apparatus is much more efficient and is mediated by furin or its relatives in the proprotein convertase (PPC) family (Stieneke-Gröber et al. 1992). To prevent premature conformational changes in strains utilizing intracellular processing, M2 pumps protons out of the normally acidic Golgi apparatus (Ciampor et al. 1992). From the Golgi apparatus, the transmembrane proteins M2, HA and NA are transferred in large quantities to the membrane of the host cell. The capsid package the RNA and the rest of the viral proteins beneath the transmembrane proteins to form new virions. M2 bends the cell membrane with its amphipathic helices, which allows new virions to bud off from the membrane (Chen et al. 2008; Cheung et al. 2005). At this point, NA cleaves bonds between HA and sialic acid on the cell membrane (Rossman and Lamb 2011), finally releasing the virions to infect new cells.

2.3.2 Hemagglutinin as an antigen

HA covers most of the surface of influenza virions and it is the most immunogenic antigen in natural influenza infections and in conventional influenza vaccines based on inactivated or attenuated whole virus. Most antibodies formed in these instances are directed against the head domain of HA, or NA to a smaller extent (Krammer 2019). Anti-HA antibodies neutralize the virus by preventing receptor binding, and therefore, cell entry (Rossman and Lamb 2011). The receptor binding motif of HA is smaller than most antibody epitopes, which allows efficient formation of escape mutants with no hindrance in sialic acid binding (Karlsson Hedestam et al. 2008). The head domains of both HA and NA are also heavily glycosylated to block antibody recognition. As an RNA virus, influenza mutates rapidly, and it is this antigenic drift into viable new strains and mutants that necessitates annual renewal of infections or conventional influenza vaccinations to maintain protective immunity.

Influenza has developed a number of ways mutate its HA head domain constantly to escape immune responses and to maintain effective infection cycles at the same

time. In contrast, the stem of HA has a conservation rate of more than 90 % in the surface areas of the most hazardous H1 and H3 influenza strains (Bommakanti et al. 2010). A prefusion stem-directed antibody able to bind all tested influenza A strains was found from a pool of human plasma (Corti et al. 2011). The antibody also neutralized all the most prevalent HA types (1, 3, 5, and 7). A vaccine that would produce an immune response with a similar efficiency could potentially work against all relevant influenza strains and provide immunity for decades. This kind of broadly reactive anti-virus vaccine is called a universal vaccine. However, adaptive immune responses are very rarely directed against the stem part of influenza HA in natural infections or conventional vaccines (Corti et al. 2011), perhaps due to the stem being poorly accessible under the immunogenic head domain.

A universal HA vaccine would need to consist of the conserved stem part of HA but keep in the prefusion conformation. HA first folds into an inactive, trimeric HA0 and becomes primed for membrane fusion only after cleavage into HA1 and HA2. The immunodominant head domain is mainly made of HA1, while the stem is mainly made of HA2. The stem is responsible for the conformational change needed for membrane fusion when infecting a new cell, and it needs parts of the head domain to keep it in the prefusion state (Chen et al. 1995b). Several versions of “headless” HA have been produced recently. The main idea in them is to include stabilizing fragments of HA1 that interact with the stalk domain and genetically fuse them into loops in HA2 to place them in the correct spatial positions (e.g. Bommakanti et al. 2010, Figure 3B). This was evolved further by removing parts not known to work as broadly neutralizing epitopes (Mallajosyula et al. 2014). The authors made the headless “ministem” trimeric (like HA in nature) by adding a Foldon trimerization domain in the C-terminus. The first versions were based on H1, but they later designed a ministem protein based on H5 (Valkenburg et al. 2016). The resulting ministem proteins expressed well in *Escherichia coli* and produced neutralizing and protecting responses in mice but were found ineffective in ferrets (Sutton et al. 2017).

2.3.3 Matrix-2 protein as an antigen

Besides the HA stem domain, the ectodomain of Matrix-2 (M2e) is also known to be well conserved and thus studied as a universal vaccine candidate. The capsid protein M1 and the transmembrane ion channel M2 are both encoded by the same RNA segment in the virion through alternate splicing (Bouvier and Palese 2008), so amino acid changes in M2 often would change M1, too. This partly explains the high

conservation rate of M2. The N-terminal 24-amino-acid ectodomain (M2e) that extends to the outside of the virion envelope or an infected cell is more than 94 % conserved between all influenza strains (Ebrahimi and Tebianian 2011), with the first 9 amino acids identical in all human infecting strains (Deng et al. 2015). The whole M2 protein is not conserved, however. The antivirals amantadine and rimantadine bind the variable trans-membrane domain of M2 and disturb proton flow through it, but were rapidly made obsolete by escape mutants after launch (Qin et al. 2010). The high conservation of M2e makes it an attractive target for vaccine development.

Some M2e-directed, broadly immunizing vaccine candidates have been tested in clinical trials. A common feature of them all is that M2e is displayed on a larger, immunogenic carrier to induce immune responses against this small peptide. For example, M2e displayed on bacterial flagellin was immunogenic in phase I (Turley et al. 2011). Hepatitis B VLPs decorated with M2e performed well in ferret challenge trials and were tested in phase I, but in humans the formed antibodies declined quickly (<https://clinicaltrials.gov/study/NCT00819013>; 9.11.2023). No universal influenza vaccines have been licensed yet.

2.4 Proprotein convertases

Proprotein convertases (here, PPCs, a.k.a. proprotein convertase subtilisin/kexins or PCSKs) are a ubiquitous family of serine proteases that work in almost all vertebrate cells and have homologs in bacteria (subtilisin) and yeast (kexin). Currently, 9 members of the family are known. The 7 PPCs that were described first all share a polybasic cleavage motif and have some overlap in their function (Turpeinen et al. 2013). However, their expression levels vary considerably by tissue type and they occupy different compartments in cells, while some are even secreted out of cells (Scamuffa et al. 2008; Seidah and Prat 2012; Shakya and Lindberg 2021). Therefore, some of them are indispensable and some can be completely replaced by other family members with the same substrate specificity, as shown by the lethal germ-line deletion of Furin in mice (Roebroek et al. 1998) and the healthy phenotype of Pcsk2 knock-out mice (Furuta et al. 1997). PCSK8 has a different, hydrophobic cleavage motif and PCSK9 has no enzymatic activity at all after it activates itself via autoproteolysis (Seidah and Prat 2012). The PCSK gene family works as a crucial regulator of hundreds of different targets and cell functions but has been found to be especially important in regulation of immunity and cellular metabolism.

Furin was the first PPC enzyme discovered in mammals and has served as a prototype of the protease family. It is well-conserved and expressed in almost all cell types in vertebrates (Thomas 2002). Furin has more than 100 substrates among mammalian proteins (Tian et al. 2011), but also many proteins of pathogens depend on it for their activation, for example diphtheria (Tsuneoka et al. 1993) and anthrax toxins (Klimpel et al. 1992), SARS-CoV-2 Spike (Essalmani et al. 2022) and influenza HA (Stieneke-Gröber et al. 1992). Many cancers are also associated with nonsense mutations or differential expression in furin (Braun and Sauter 2019; Siegfried et al. 2020). Anti-furin antibodies and small molecule inhibitors have shown protective effects in animal trials by preventing activation and maturation of viral proteins (Shiryaev et al. 2007) and by blocking toxin use by bacteria (Sarac et al. 2004). These anti-pathogen treatments are in preclinical phase, but an RNA interference cancer treatment based on an anti-furin short hairpin RNA (Vigil) has proceeded to clinical trials (Rocconi et al. 2021).

PCSK9 is a nonenzymatic member of the PPC family. After activation, it functions mainly by binding low-density lipoprotein receptor (LDLR) on the cell surface, which activates signals for the internalization and degradation of LDLR (Zhang et al. 2007). Without PCSK9 activity, LDLR is present on the cell membrane until it encounters LDL. LDL is a molecule complex that mammals use to transport cholesterol and other hydrophobic lipids in blood. After binding LDL, the LDLR takes it inside the cell and LDLR is recycled back onto the membrane. LDLR activity is necessary for the normal uptake of cholesterol by cells, where it is used for constructing membranes, signal molecule synthesis, and in specialized cell types in the liver for synthesis of bile acids and for excretion from the body (Ikonen 2008). All uptake of cholesterol from the blood into cells reduces blood cholesterol levels, and thus, PCSK9 activity increases blood cholesterol by reducing LDLR. Indeed, heterozygous loss-of-function of PCSK9, known especially in people from African descent, leads to significant reductions in blood cholesterol and cardiovascular disease (Cohen et al. 2005; Kotowski et al. 2006). Owing to this, therapeutic antibodies that inhibit PCSK9 are already in commercial use in human patients (evolocumab, Amgen, USA and alirocumab, Regeneron, USA). They are most often used in combination with statins when the maximal tolerated statin dose fails to reduce blood cholesterol enough.

Therapeutic antibodies are a very specific way to treat disease and their market is growing fast. However, they are very expensive drugs to manufacture and their half-life in the body is months at best. In chronic diseases like elevated blood cholesterol, anti-PCSK9 antibody treatment usually means treatment costs of more than 10 000

€/month (Arrieta et al. 2017) and monthly doctor's appointments for venous injection of the drug (Kaddoura et al. 2020). Small-molecule inhibitors are cheaper and can usually be formulated for oral intake, but often suffer from side effects caused by lower specificity. In the case of furin, all known inhibitors bind the active site, which is more than 85 % conserved in all 7 conventional PPCs (Zhu et al. 2012). In contrast, a well-designed self-vaccine could potentially activate the patient's own immune system to produce highly specific antibodies continuously, up to years after immunization.

3 AIMS OF THE STUDY

Despite being one of the oldest biological interventions, recent developments show that vaccine technologies still have room for improvement. Testing the vaccine carrier use of the prototypical VLPs of bacteriophage AP205 and hepatitis B virus has been extensively reported, but norovirus based VLPs remain largely unexplored in this application. Among VLPs, the noro-VLP is particularly robust and easy to produce, and it is also one of the most common viruses infecting humans globally. The aim of this PhD thesis project was to advance the field of VLP vaccines by examining the applicability of noro-VLP as a vaccine carrier.

The specific aims of this study were:

1. To develop a version of the noro-VLP that can be easily, flexibly, and efficiently decorated with different types of peptides and protein domains.
2. To analyze the biophysical and immunological properties of the modified noro-VLPs.
3. To use the noro-VLP-based vaccine platform to produce universal influenza vaccine candidates.
4. To use the noro-VLP-based vaccine platform to produce self-vaccines against furin and PCSK9 for cancer or hypercholesterolemia treatment and/or prevention.

4 MATERIALS AND METHODS

4.1 Carrier and antigen design and modeling

The norovirus *VP1* gene, which encodes the capsid protein that forms the carrier nanoparticle in this project, is from strain Hu/GII.4/Sydney/NSW0514/2012/AU (GenBank ID: AFV08795). We modified the noro-VLP to present different peptides on its surface by adding them as genetic fusions at the C-terminus of VP1 (Table 1). These were separated from the original noro-VP1 C-terminus by either a short TSGG linker (SpyTag-noro-VLP 1.0) or later by a long, disordered PAS peptide (TSASPAAPASPAPAPSAPAA; 23 amino acid residues) in SpyTag-noro-VLP 2.0 (Schlupschy et al. 2013). The plasmid encoding SpyTag-noro-VLP 1.0 was codon-optimized for insect cell expression, synthesized and subcloned into pFastBac Dual plasmid at GeneArt (now part of Thermo Fisher Scientific, USA). This gene was later modified at GenScript (USA) and subcloned into pOET5 plasmid (Oxford Expression Technologies, UK) and later into pOpIE2 (kindly provided by Joop van den Heuvel, Helmholtz Centre for Infection Research, Germany). All noro-VP1 gene versions but SpyTag-noro-VLP 2.0 in pOpIE2 were subcloned under the polyhedrin late baculovirus promoter. SpyTag-noro-VLP 2.0 uses the early IE2 promoter for transient expression.

All SpyCatcher fusion proteins produced during this project are based on a similar construct design (Table 2). We used the N- and C-terminally truncated form (109 amino acid residues) of SpyCatcher (Li et al. 2014) with an N-terminal (6x)HisTag for purification. The HisTag was separated from SpyCatcher by a TEV cleavage site. Antigens were all genetically fused to the C-terminus of SpyCatcher and separated only by a small LE linker. Even though SpyCatcher has been reported to work both as C and N-terminal fusions (Thrane et al. 2016), the 3D structure of the protein (PDB ID: 4MLS (Li et al. 2014)) suggests that the C-terminus would be more reachable in fusion proteins when SpyTag is fused to the C-terminus of a large virus-like particle. We used the SynLinker web application (discontinued since) (Liu et al. 2015), PyMOL (Schrödinger and DeLano 2020) and Swiss-PdbViewer (Guex and Peitsch 1997) to model and illustrate the fusion proteins. All SpyCatcher-antigen genes were produced synthetically and subcloned into the ampicillin-selectable pET-

11b(+)
11b(+) plasmid by GenScript. In the plasmid, the genes were subcloned between XbaI and BlnI under the T7 promoter, which is controlled by a *lac* operon.

Table 1. Noro-VLP versions produced during the project. The reported yields are for >90 % pure protein.

Name	Original publication	Total size (kDa)	Residues in tag	Yield (mg/L)	Plasmids	Addgene ID
SpyTag001-noro-VLP	I, II, III, IV	60.9	17	40–80	pFastBac Dual, pOET5	165989
M2e-noro-VLP	III	62.1	28	25	pOET5	201192
WT-noro-VLP	III	59.1	0	40–80	pOET5	—
SpyTag003-noro-VLP	Unpublished	61.3	20	40–80	pOET5	201199
SpyTag003-noro-VLP 2.0	Unpublished	62.9	39	40–80	pOET5, pOpIE2	201200

Table 2. SpyCatcher-fused antigens produced during the project. Total sizes refer to the whole antigen product monomer with SpyCatcher and HisTag. The reported yields are for >90 % pure protein. All antigens are fused from their N-terminus with the shortened version of SpyCatcher001 (Li et al. 2014) and a TEV-cleavable HisTag. HA2 was produced also without SpyCatcher fusion to be used in ELISA coating.

Name	Original publication	Type	Total size (kDa)	Antigen size (kDa)	Yield (mg/L)	Original protein	Addgene ID
HA2	I, II	Protein domain	31.0 (subunit in trimer)	19.0	>10	Influenza hemagglutinin	165991, 165992
M2e	I, II, III	Peptide	14.8	2.76	>30	Influenza matrix 2	165990
PEED	IV	Peptide	13.7	1.66	>50	PCSK9	201195
DIIG	IV	Peptide	13.2	1.16	>50	PCSK9	201196
SWG	IV	Peptide	13.5	1.46	>50	Furin	201194
P domain	IV	Protein domain	27.0	15.0	~1	Furin	201193

4.2 Norovirus-like particle production

Insect cells were used throughout the project for baculovirus vector amplification and noro-VLP expression. The *Trichoplusia ni* High Five (Hi5) cell line was used for the latter purpose, while Sf9 was used for baculovirus amplification. Sf9 and Hi5 were both cultured without antibiotics or serum in Insect-XPRESS Protein-free Insect Cell Medium with L-glutamine (Lonza, Switzerland) or HyClone SFM4 Insect cell culture media (Cytiva, USA). Hi5 cultures were at least weekly supplemented with 10 units/mL heparin to avoid aggregation of cells. Both cell lines were grown in suspension cultures and passaged 2–4 times per week to maintain them in the log phase of growth. Before baculovirus infection, the cells were passaged the previous day, counted to ensure viability of more than 95 % and diluted to 2×10^6 cells/mL.

The different versions of noro-VLP were all produced in insect cells during the project, but with three different strategies. The most complicated approach, called Bac-to-Bac (Thermo Fisher Scientific), introduced noro-VP1 gene first in DH10Bac *E. coli* into the pFastBac Dual plasmid. These bacteria contain a baculovirus genome called bMON14272, into which the noro-VP1 gene is transposed inside the bacterium. The resulting baculovirus genome (i.e., bacmid) was extracted and transfected into Sf9 insect cells. In insect cells, the modified baculovirus genome is translated into baculovirus proteins that assemble into infective virions. These were collected and amplified in Sf9 cells in sequential infections and finally used to transduce the noro-VP1 gene within into Hi5 insect cells for noro-VLP expression. Each baculovirus stock collected from the medium of each infection round was sterile-filtered and supplemented with 1–2 % fetal bovine serum (FBS) to prolong storage times. Baculovirus stocks remain stable for 6–18 months when stored at +4 °C.

The second approach we used was to subclone the norovirus VP1 gene into the pOET5 plasmid and transfect Sf9 cells directly with the VP1-containing pOET5 and the baculovirus genome FlashBAC PRIME or FlashBAC ULTRA (Oxford Expression Technologies). BaculoFectin II from the same supplier was used as a transfection agent that helps transfer the plasmids inside the cells where VP1 is transposed into the baculovirus genome, activating it to produce infective virions. The following steps of collecting and amplifying the resulting baculovirus and using it in Hi5 noro-VLP expressions were identical to the Bac-to-Bac method.

During the PhD project, we also adopted a baculovirus-free method of producing VLPs, as described first by (Korn et al. 2020). Here, we subcloned the noro-VP1 gene into a plasmid called pOpIE2 and directly transfected Hi5 insect cells with the

plasmid by aid of linear polyethylenimine (MW 40 000, #24765, Polysciences, USA). With this method, we could proceed directly into production of VLPs, without first forming, amplifying, titrating, and storing baculoviruses.

4.2.1 Baculovirus-dependent norovirus-like particle expression

After noro-VP1-encoding baculoviruses had been amplified to large quantities as described above, we usually measured the concentration of infective baculovirus in stock solution before using it for noro-VLP expression. The concentration was measured using the BacPAK Baculovirus Rapid Titer Kit (Takara Bio, Japan). Briefly, different dilutions of the baculovirus stock are used to infect Sf9 cells in a 96-well plate under a layer of methylcellulose to limit diffusion. Due to methylcellulose, initial infection by a single baculovirus is restricted to a small colony of surrounding cells that express the baculovirus gp64 protein on their surface. Individual infected cell colonies can then be detected by an anti-gp64 antibody and counted when starting concentrations become low enough. With the obtained concentration information, it is possible to optimize protein expression by multiplicity of infection (MOI, in simple terms, baculoviruses per cell). Optimization can of course be also done in relation to baculoviral stock volume, but MOI values are lot independent.

After establishing baculovirus stocks for each noro-VLP, the stocks were used to infect Hi5 cells at optimal MOI or volume as described above. By 4–6 days of noro-VP1 expression, most cells have been lysed by baculovirus infection and the self-assembled noro-VLPs have been released into the culture medium. Residual cells and cell fragments were separated from the culture medium either by centrifugation (2000 g, 30 min) or by filtering through an 0.2 μm filter by aid of Sartoclear Dynamics filter aid (Sartorius, Germany).

4.2.2 Baculo-free norovirus-like particle expression

We also produced noro-VLP by baculovirus-independent transient gene expression in insect cells as described earlier for other proteins (Korn et al. 2020) and SARS-CoV-2 VLPs (Jaron et al. 2022). Early log phase Hi5 cells were pelleted and resuspended to 4×10^6 cells/mL before adding 4 μg of polyethylenimine and 1 μg of noro-VP1 encoding pOpIE2 plasmid per million cells. After 6–10 hours, the volume was quadrupled and 48 hours after transfection, it was doubled again. As

there are no baculoviruses lysing the cells and releasing the produced noro-VLPs, they could be collected from the medium only after 9 days of expression. Alternatively, we collected noro-VLP after days of expression from the soluble fraction of the cell pellet after lysis by sonication. Unlike the optimized published protocols, we produced SpyTag-noro-VLP 2.0 in Hi5 cells with less than 30 passages and Hyclone SFM4 media.

4.2.3 Purification of norovirus-like particles

After the different versions of noro-VLP were released into the production medium, we needed to reduce its volume for further purification. The method for this was chosen depending on the starting volume and the planned final purification step. With ultracentrifugation, it is difficult to handle volumes larger than ~300 mL at a time, but on the other hand, automated tangential flow filtration alone cannot be used to reduce volume enough to continue directly into size-exclusion chromatography (SEC). When handling large expression volumes, concentration began with tangential flow filtration using ÄKTA Flux (Cytiva, USA) with 750 000 molecular weight cut-off (MWCO) hollow fiber. The concentrate from tangential flow filtration was either polished immediately by anion exchange chromatography or concentrated further by ultracentrifugation for SEC purification. Ultracentrifugation (175 000 g, 6–16 h) was done through 30 % sucrose cushion in PBS, where the large noro-VLPs are forced through the sucrose layer to pellet on the bottom of the tube and smaller molecules get stuck in the sucrose. After ultracentrifugation, noro-VLP was redissolved into a small volume of buffer, centrifuged, and sterile-filtered to remove any aggregates or contaminating microbes. When proceeding to anion exchange chromatography, the buffer was exchanged to low-salt phosphate buffer already during tangential flow filtration or ultracentrifugation.

Tangential flow filtration and ultracentrifugation both purified noro-VLP to a high degree, but because both are based on particle size, most of the similarly sized baculovirus ends up in the same fraction with the norovirus, and thus the fractions need further purification. We separated residual baculovirus from norovirus either by surface charge by binding the viruses on a HiTrap Q XL anion exchange column in pH 7.0 buffer with a conductivity of less than 5 mS/cm. When the bound proteins were eluted by raising NaCl concentration to 500 mM, noro-VLP eluted first starting from ~50 mM NaCl while the baculovirus still remained in the column and eluted

at ~250 mM NaCl. After concentrating noro-VLP to less than 5 mL with ultracentrifugation, we could alternatively run it through HiPrep 16/60 Sephacryl S-500 HR size-exclusion column (Cytiva, USA) in PBS. Here, the slightly larger baculovirus eluted faster through the column. Compared to anion exchange chromatography, SEC led to better recovery rates of noro-VLP and thus better yields. After purification, noro-VLP was concentrated to 1–8 mg/mL using VivaSpin Turbo spin tubes (10 000 MWCO, Sartorius) and sterile-filtered for storage and downstream applications. Noro-VLP was mostly stored at +4 °C during the project, which it can take unchanged for months, but also frozen and stored at -20 °C.

4.3 Antigen production

4.3.1 Antigen expression

All SpyCatcher-antigen fusion proteins used in this project were produced in *E. coli* grown in lysogeny broth (LB). All peptide fusion proteins (M2e, PEED, DIIG, SWG) were transformed in BL21 Star (Thermo Fisher Scientific) using heat shock (30 s, +42 °C) and expressed at +25 °C overnight after induction with 1 mM isopropyl β -D-1-thiogalactopyranoside (IPTG) at an optical density at 600 nm ($OD_{600\text{ nm}}$) of approximately 0.6. HA2, SpyCatcher-HA2 and SpyCatcher-P domain were expressed overnight at +18 °C after 1 mM IPTG induction at an $OD_{600\text{ nm}}$ of 0.6–0.8. The differences between BL21 Star (Thermo Fisher Scientific), C41 and C43 were minor, but we used C41 for their expression in the end.

4.3.2 Antigen purification

N-terminal HisTags were included in SpyCatcher-fused antigen and HA2 genes for Ni-NTA purification using the same protocol for all. After expression, we lysed the bacteria containing the antigens with an Emulsiflex-C3 homogenizer (Avestin, Canada) by running them twice through the extruder with 60–80 bar pressure. After centrifuging (15 000 g, 20 min), the soluble fraction of the lysate was loaded on HisTrap FF crude column (Cytiva, USA) in a pH 7.2 phosphate buffer containing 500 mM NaCl and 20 mM imidazole. Purifications were done using ÄKTA Purifier (Cytiva, USA) and Bio-Rad (USA) NGC automated chromatography instruments. To remove endotoxins bound to the proteins from lysed *E. coli*, the column was

washed with 0.1 % Triton X-114 before elution of target protein from the column. The proteins were eluted with gradually rising imidazole concentrations.

4.4 SpyCatcher/SpyTag conjugation

To decorate SpyTag-noro-VLP with SpyCatcher-fused antigens, they were mixed in neutral buffer solution and incubated at +4 °C overnight. SpyCatcher was added in 1.5–4 -fold molar excess to SpyTag-noro-VLP to ensure maximal conjugation efficiency. Unreacted SpyCatcher-antigen was removed from the mixture either by dialysis through 1 000 000 MWCO membrane or by size-exclusion chromatography. We also successfully used equimolar reactions with SpyTag-noro-VLP 2.0 to skip separating unreacted SpyCatcher-antigen. Because the bond that forms between SpyCatcher and SpyTag is covalent, the conjugation reaction can be observed as a mobility shift with sodium dodecyl sulfate polyacrylamide gel electrophoresis (SDS-PAGE) followed by total protein staining or Western blotting. Upon conjugation, the size of noro-VP1 increases by the size of the conjugated SpyCatcher-antigen, so in SDS-PAGE, a portion of the noro-VP1 band(s) move slower and end up higher on the gel. Conjugation efficiency was calculated as the densitometric mass of conjugated noro-VP1 bands divided by the sum of total noro-VP1 mass in an SDS-PAGE gel well.

4.5 Characterization and quality control of vaccine candidates

4.5.1 SDS-PAGE and Western blotting

SDS-PAGE was used throughout the project for comparing target protein quantities in expression optimization, tracking target protein from purification fractions, and for estimating protein purity in purified protein preparations. In an SDS-PAGE analysis, a sample of the protein fraction was mixed with SDS sample buffer and boiled for 5–10 minutes to unfold the proteins and run through a polyacrylamide gel. The overexpression efficiency of the SpyCatcher-antigens and noro-VLPs produced here were both sufficient for comparing overexpression conditions from cell lysates and for tracking target protein in purification fractions by total protein staining. For this, we used Any kD Mini-PROTEAN and Criterion TGX Stain-Free

Precast Gels (Bio-Rad) and only occasionally verified the smallest proteins by PageBlue total protein staining. For estimating the purity of final vaccine preparations, we used silver-staining with 500–1000 ng of total protein per well. For most applications, we used only protein batches estimated to be more than 90 % pure by densitometry. All SDS-PAGE gels were imaged with the ChemiDoc instrument and the accompanying Image Lab software (Bio-Rad). For densitometry analysis of conjugation efficiency or protein purity, we used Image Lab and Fiji ImageJ (Schindelin et al. 2012).

In addition to comparing the predicted size of target protein with its mobility and appearance in total protein staining after SDS-PAGE, we also used Western blotting for further confirmation of protein identity. In Western blotting, the proteins from a Stain-free SDS-PAGE gel were transferred to a 0.2 µm nitrocellulose membrane with Trans-blot Turbo (Bio-Rad) after imaging the gel. The membrane was then blocked with 5 % BSA in TBS + 0.05 % Tween 20 or EveryBlot (Bio-Rad), then incubated with a primary antibody to identify a select set of proteins on the membrane. During the project, we used an anti-HisTag antibody (1:5000, Thermo Fisher Scientific, USA, #ma1-21315) for identification of SpyCatcher-antigens that all had an N-terminal HisTag, a mouse anti-gp64 (1:2000, Santa Cruz Biotechnology, USA, #sc-65499) for detecting residual baculovirus, a mouse anti-influenza-M2 antibody (1:3000, Thermo Fisher Scientific, #ma1-082) for M2e peptide identification, and a rabbit polyclonal anti-diphtheria toxin antibody (1:2000, Abcam, USA, #ab151222). For confirming the presence of noro-VP1, we used mouse serum originating from in-house vaccine studies. The primary antibodies were finally detected with a fluorophore-conjugated secondary antibody and imaged with Odyssey CLx (LI-COR Biosciences, USA).

4.5.2 Mass spectrometry

Since mobility in SDS-PAGE often does not match the predicted mass of a protein exactly, we used mass spectrometry for further confirmation of the identities of the produced SpyCatcher-antigens. The masses of SpyCatcher-M2e and -HA2 were accurately measured with matrix-assisted laser desorption/ionization (MALDI) mass spectrometry analysis (Markku Varjosalo, University of Helsinki) and the masses of SpyCatcher-PEED, -DIIG and -SWG with electrospray ionization mass spectrometry (Janne Jänis, University of Eastern Finland).

4.5.3 Particle size and morphology

While SDS-PAGE tells us of the size of polypeptide chains connected to each other via covalent bonds in a protein assembly, most protein oligomers, like VLPs, depend on noncovalent bonds in their formation. During this project, we used dynamic light scattering (DLS) to track the oligomeric state of SpyCatcher-antigens and the assembling and size of noro-VLPs. The measurements were done with Zetasizer Nano ZS (Malvern Instruments, UK). Each result is based on cumulant analysis of three consecutive measurements with an instrument-optimized number (at least 10) of 10-second readings. All measurements were made at a scattering angle of 173° , at $+25^\circ\text{C}$.

Assembled noro-VLPs are large enough for direct observation in transmission electron microscopy. We used an F200 S/TEM (Jeol, Japan) to make estimates on the sizes of the different noro-VLPs and to compare their morphology. Before analysis with the microscope, we made carbon-coated copper mesh grids hydrophilic using the GloQube Plus glow discharge system (Quorum Technologies, UK) to help noro-VLPs distribute uniformly when adhering them on the grids. Residual phosphates were diluted and washed off with TBS and the grid-adhered noro-VLPs were stained with 1 % uranyl acetate.

4.5.4 Thermal stability measurements

To get an estimate of stability, we compared the thermal melting points of different noro-VLP versions to each other and to wild type noro-VLP. We used a quick small-scale technique called differential scanning fluorimetry (DSF) for this, as described in detail in (Niesen et al. 2007). In DSF, we mixed the protein under analysis with SYPRO Orange (Thermo Fisher Scientific, #S6650) and heated the mixture from $+25$ to $+110^\circ\text{C}$ at a rate of $2^\circ\text{C}/\text{min}$. The protein unfolds upon heating, which reveals hydrophobic regions from inside the protein. SYPRO Orange binds these regions and starts to fluoresce. Unfolding of the protein forms a peak in the plot of fluorescence intensity as a function of temperature, and the melting point of the protein can be derived from the inflection point of the rising side of the fluorescence peak with the Boltzmann equation.

We also used a similar stain-free method, called differential scanning calorimetry (DSC) for comparing melting points of different noro-VLPs. We did the DSC measurements with the GE Healthcare (USA) VP-Capillary. The instrument heats the protein sample and a reference buffer sample in insulated cells and compares the

amount of energy needed for the process. The disassembly of VLPs and unfolding of proteins are usually endothermic reactions, so heating the protein sample consumes more energy as compared to the reference sample. When the difference in heating power is plotted against increasing temperature, a melting curve is obtained. In DSC, the melting point is defined as the midpoint of the unfolding peak, which is obtained from the Levenberg-Marquardt non-linear least-squares fit on the data. Data analysis was done using MicroCal Origin 7.0 (Malvern Instruments). In DSC, we increased the temperature 2 °C/min and followed the samples from +20 to +110 °C.

4.5.5 Concentration measurements

When working with recombinant proteins, the concentration of protein and impurities in the sample are important things to consider. For rapid first estimate on protein concentration, we used a spectrophotometer to measure absorbance at 280 nm. For well-purified batches of small, soluble proteins with known primary sequences, absorbance can give a rather accurate estimate of protein concentration and the A260/280 ratio can be used to evaluate sample quality when the A260/280 ratio is known empirically for the given protein. Conversely, VLPs scatter light a lot in addition to absorbing it, which can lead to overestimated concentrations when assessed using A280, even when using a baseline correction at 340 nm. All in all, determination of protein concentration with UV has limitations and should be interpreted with care. Therefore, all reported protein concentrations in this work were measured with the Pierce bicinchoninic acid (BCA) assay (Thermo Fisher Scientific, #23252). During the project, most protein sample concentrations were initially measured with A280 for a quick estimation and later verified with BCA. Most noro-VLP sample concentrations turned out to be overestimates upon verification. When using the produced recombinant proteins in immunological experiments, we monitored levels of residual double-stranded DNA and bacterial endotoxins from the expression host or contaminating bacteria that often purify alongside the target proteins. DNA concentrations were measured with the Quant-iT dsDNA high sensitivity kit (Thermo Fisher Scientific, #Q33120) and for endotoxin measurement, we used the ToxinSensor chromogenic LAL endotoxin assay kit (GenScript, #L00350) and Endozyme II Go Strips (bioMérieux, France). Batches where the double-stranded DNA concentration exceeded 10 ng per immunization dose (Knezevic et al. 2008) or the endotoxin concentration exceeded 1.5 endotoxin units

(EU) per μg of protein (Makidon et al. 2008) were discarded or purified further. DNA was removed with Benzonase nuclease (Merck Group, Germany) followed by dialysis or SEC. Residual endotoxins were removed from HisTagged proteins with the Triton X-114 washing of column-bound protein as described above, but for noro-VLPs, we used EndoTrap HD resin (Lionex, Germany) that binds endotoxin specifically.

4.6 Preclinical experiments

During this PhD project, we produced and purified multiple vaccine candidates and tested the immunogenicity of the most promising of them in preclinical mouse experiments. We used only female BALB/c OlaHsd (Envigo, the Netherlands) and BALB/cJrj mice (Janvier Labs, France) to increase comparability to our previous research and to avoid fights between male mice in group housing and breeding. After arriving in the facility, the mice were acclimatized for a week and ear-marked before starting the experiments. During the experiments, we immunized the mice 2–4 times intramuscularly (I, II, IV) or subcutaneously (III, IV). Blood samples were collected from tail vein during the experiment and by heart puncture at termination. We also collected spleens and extracted the splenocytes by filtration, centrifugation, and washing, as described in (González-Rodríguez et al. 2022). All procedures were executed under anesthesia to reduce the animals' pain. The animal experiments were done according to the regulations and guidelines of the Finnish National Experiment Board, and under permission numbers ESAVI/10800/04.10.07/2016, ESAVI/6781/2018, ESAVI/16254/2019 and ESAVI/1408/2021.

The vaccine doses we used in immunizations were protein (missing in buffer control group) diluted in neutral saline buffer. 100 μg per dose of aluminum “Alhydrogel adjuvant 2%” (Invivogen, USA, #vac-alu-250; referred to here as $\text{Al}(\text{OH})_3$) was included in selected vaccine groups as an additional immune activator. When planning vaccine doses, we had to consider total protein mass, conjugation efficiency and the mass and molarity of conjugated antigen. An example for calculating antigen dose is provided below for vaccination group 4 in publication III.

$M(\text{SpyTag-noro-VLP})=61.01 \text{ kDa}$, $M(\text{SpyCatcher})=12.04 \text{ kDa}$, $M(\text{M2e})=2.76 \text{ kDa}$ and conjugation efficiency was 24 %, so the amount of M2e in a vaccine dose of 31 μg is calculated as follows:

$$24 \% \times 31 \mu\text{g} \times \frac{2.76 \text{ kDa}}{(61.01+12.04+2.76) \text{ kDa}} = 0.27 \mu\text{g}$$

4.7 Immunological studies

4.7.1 Antibody levels by ELISA

The main output from mouse immunizations was the number of antibodies against the used vaccine components. During the project, we measured the numbers of antibodies specific to SpyCatcher, SpyTag, SpyCatcher-M2e, SpyCatcher-HA2, influenza HA, HA2 and the M2e peptide, furin, PCSK9, and the PPC peptides PEED, DIIG and SWG, both as SpyCatcher fusions and as individual peptides. Comparable antibody end-point titers were obtained from enzyme-linked immunosorbent assays. The assay began with overnight coating of Maxisorp 96-well plates (Thermo Fisher Scientific, #439454) with the antigen under study. Unbound antigen was washed off, the well was blocked with BSA, and then 2-fold dilution series of mouse sera were applied on the wells. After washing unbound serum antibodies off, horseradish peroxidase (HRP) conjugated secondary antibody and o-phenylenediamine dihydrochloride (OPD) substrate (Merck Group, #P8412) were used to detect the bound serum antibodies. The HRP in the secondary antibody forms a colored product from the OPD substrate and H₂O₂, which is proportional to the amount of bound secondary antibody, and thus, to bound antibody from the serum. We used secondary antibodies recognizing all IgG antibodies (1:4000, Vector, USA, #PI-2000) and IgG1 or IgG2a (1:3000, Thermo Fisher Scientific, #A10685 and #A0551) subtypes specifically. Finally, endpoint-titers for each mouse serum were obtained by choosing the highest serum dilution that still has an absorbance value higher than the set positive cut-off value. The positive cut-off value was obtained from the lowest dilution measurements of naive mice as $(\text{mean absorbance}) + A \times (\text{standard deviation})$, where A is either a commonly used arbitrary factor of 3 or a statistically defined factor that depends on the desired confidence level (described in (Frey et al. 1998)). When studying antibodies against the small SpyTag peptide, we coated the well first with in-house recombinant wild type avidin and bound biotinylated SpyTag on the avidin molecules for better availability of the peptide for binding. After these steps, the assay proceeded as described above.

4.7.2 Cytokine levels after splenocyte activation by FluoroSpot

In publication III, we measured cytokine responses from antigen-stimulated splenocytes using FluoroSpot assay. We used the Mouse IFN- γ /IL-2/TNF FluoroSpotPLUS kit (Mabtech, Sweden, #FSP-414245-10) according to the kit's protocol to measure secreted IFN- γ , IL-2, and TNF simultaneously. Briefly, splenocytes frozen after extraction were thawed and counted to use 250 000 live cells in stimulation reactions with M2e or SpyTag peptide, noro-VLP or SpyCatcher or kit controls as stimulants under co-stimulation with anti-CD28 from the kit. Stimulation lasted overnight, after which the cells were removed, and the well-bound cytokines were detected with fluorophore-conjugated antibodies and quantitated with the IRIS reader at Mabtech. A positivity cut-off value was defined for each mouse separately as the mean spot count + 3 \times (standard deviation) of negative control stimulations for that mouse. This value was subtracted from each stimulation result to obtain the final value in spot-forming units per a million splenocytes.

4.7.3 Cytokine levels after splenocyte activation by ELISA

After the first immunization experiment in publication IV, the splenocytes were extracted from the mice as described above and a maximum of 2.5×10^6 cells per well were seeded on 24-well culture plates. The cells were stimulated with 5 μ g of anti-CD3 (Thermo Fisher Scientific), SpyTag-noro-VLP, SpyCatcher-PEED, SpyCatcher-DIIG, SpyCatcher-SWG, or SpyCatcher-P domain. After stimulation, the cells were cultured at +37 °C in RPMI-1640 (Lonza, Switzerland) with 10 % FBS, 1 % penicillin-streptomycin (Lonza), 1 % L-glutamine (Lonza), and 50 μ M β -mercaptoethanol. After 3 days, the supernatant was collected and frozen. Later, we measured cytokine concentrations from the supernatant with the ELISA kits for mouse IFN- γ , IL-2, and IL-13, according to the instructions (Thermo Fisher Scientific).

4.7.4 Flow cytometry

After the second immunization experiment in publication IV, the splenocytes were extracted and seeded onto 24-well plates as in stimulation studies and prepared for flow cytometry analysis. Instead of stimulation, the cells were incubated for 4 hours at +37 °C with 50 ng/mL phorbol-12-myristate 13-acetate (PMA, Merck Group),

1 µg/mL calcium ionophore (Merck Group), 1 µg/mL GolgiPlug, and 0.7 µL/mL GolgiStop (Becton, Dickinson and Company, USA). The cells were washed with RPMI-1640 and stored 18 hours at +4 °C. Subsequently, the cells were treated with FVS510 viability stain and a CD16/CD32 antibody mix (Thermo Fisher Scientific, Becton, Dickinson and Company) to block Fc receptors. Finally, the surfaces of the cells were stained with CD3 -FITC, CD8a -PerCP-Cy5.5, CD4-APC-Cy7 and CD19-BV786 antibodies, and IFNG-PE-Cy7 and TNF-PE-Cy7 (Thermo Fisher Scientific) antibodies were used with Cytofix/Cytoperm kit (Beckman Coulter, USA) for intracellular staining. The Beckman Coulter CytoFlex instrument was used for the flow cytometry.

4.7.5 Cytokine levels in mouse serum

In publication IV, we measured the levels of a set of cytokines in the frozen mouse sera in both immunization experiments. For this, we used the V-PLEX Plus Proinflammatory Panel 1 mouse kit (Meso Scale Discovery, USA). The analysis was done according to the kit's recommendations. This included washing the precoated plate, adding the sera as 2-fold dilutions (except the serum for a mouse from PBS group was diluted 1:4.2 due to low sample availability) and then finally adding the analytes from the kit according to instructions. MESO QuickPlex SQ 120MM was used for measuring the signals. We measured sera from 10/64≈16 % mice as duplicates. From the duplicate measurements, the standard deviation of the assay was 5.8 ± 9.6 % of the mean concentration in measurements above detection limit.

4.7.6 Statistical analyses

When considering group sizes for the animal immunization experiments, we used power calculations based on similar, earlier studies. For statistical analysis of ELISA data on antibody and cytokine levels and for FluoroSpot data, we used versions 8.3.0 and 9.0.0 of the GraphPad Prism software and version 25 of IBM SPSS. In all tests, we set $P < 0.05$ as statistically significant difference. Populations derived from all these tests were assumed not to be normally distributed, so we used the nonparametric Kruskal-Wallis test followed by Dunnett's test to test for differences between each vaccine group and the negative control group. Dunn's test was used to compare the means of each group to all others. The negative controls groups were either mice vaccinated with only buffer or with nondecorated noro-VLP, depending

on the test. In publication II, we used the Wilcoxon signed rank test and a paired samples t-test to compare IgG1 and IgG2a titers and mean absorbances within a group.

4.7.7 Noro-VLP histo-blood group antigen binding

We used an assay that measures binding of noro-VLP to the cellular receptor of norovirus as a tool to indirectly measure neutralization capability of the anti-norovirus antibodies formed during the first animal experiment in the project (II). The protocol is described in detail in (Malm 2018, Uusi-Kerttula 2014). Briefly, human blood group antigens (HBGA) from human blood group A saliva or pig gastric mucin were coated on 96-well half area polystyrene plates (Costar, Corning, USA). Noro-VLPs were pre-incubated with anti-noro mouse serum, control serum or buffer, and then bound on the HBGA. Bound noro-VLP was detected with an in-house human serum from volunteers. Half-maximal inhibitory concentration (IC₅₀) was calculated from dose-response analysis of several anti-noro serum dilutions.

4.7.8 Influenza neutralization assay

In publication II, we evaluated neutralizing capability of the anti-influenza sera obtained from mouse immunizations in a neutralization assay adapted from (Okunp 1990). Briefly, confluent Madin-Darby canine kidney (MDCK) in 96-well cell culture plates (Nunc) were infected using H1N1 A/Puerto Rico/8/1934 influenza virus stocks. The stocks were pre-incubated with buffer, mouse serum dilutions, human serum or with monoclonal anti-influenza HA2 antibody. The cells were covered with carboxymethylcellulose to limit virus diffusion. After ~20 hours incubation, the cells were fixed and infected cell clusters were detected by anti-HA antibody and HRP-conjugated secondary antibody.

4.7.9 Diphtheria proteolysis assay

To test if the furin-specific mouse sera created in publication IV would inhibit furin activity *in vitro*, we adapted a diphtheria toxin proteolysis assay from (Zhu et al. 2012). Furin is a protease that activates diphtheria toxin protein by cleaving it in two. Here,

we pre-incubated recombinant furin diluted mouse serum for 30 minutes at RT. Then we added 2 μg of diphtheria toxin and continued incubation for 60 minutes at +37 °C. We used a non-toxic version of diphtheria toxin with a G52E mutation (Abcam, #ab188505). After the incubation time, the reaction was stopped by boiling the sample in SDS-PAGE sample buffer. Here, we had to visualize diphtheria toxin and its cleaved parts by Western blotting, because the polypeptides that form IgG are of a very similar size compared to diphtheria toxin and its cleavage products.

5 SUMMARY OF THE RESULTS

5.1 Norovirus-like particle can self-assemble with C-terminal modifications

We employed several strategies to produce noro-VLPs with different C-terminal modifications. First, we used the Bac-to-Bac system to transpose the gene of SpyTag-noro-VLP into a baculovirus genome in bacteria (I), as reported earlier for HisTag-noro-VLP (Koho et al. 2015). After this, we moved SpyTag-noro-VLP and later constructs into the FlashBAC system (III), where the plasmid is transposed into a baculovirus genome directly in the insect cell, allowing us faster transition into making the baculovirus stock. Finally, WT-noro-VLP and SpyTag-noro-VLP 2.0 were produced with a baculovirus-free method by transfecting insect cells directly with an expression plasmid by aid of polyethyleneimine (PEI) (Lampinen, et al., unpublished data) (Korn et al. 2020), skipping directly to VLP production. For comparable noro-VLP constructs, each of these methods produced very similar yields (Table 1) but differed considerably by their repeatability and time consumption. Transient expression with a plasmid was easiest to do and Bac-to-Bac took the most time to achieve. With baculovirus-dependent methods, we had trouble with deteriorating baculovirus stocks that needed replenishing during the project and a couple instances where the baculovirus had mutated or amplified poorly, requiring a new transfection round.

During the thesis project, several purification strategies were tested to enhance the obtained noro-VLP yields and to improve practical aspects in their continuous production. We began with the anion exchange protocol reported in (Koho et al. 2012), but used Hi5 insect cells instead of Sf9 cells and ultracentrifugation through sucrose gradient instead of polyethylene glycol (PEG) precipitation for concentrating the VLPs into a pellet (I). In our hands, Hi5 always yielded better expression yields compared to Sf9, and we used Sf9 cells only for amplification and titration of baculovirus stocks. Since ultracentrifugation is not very scalable, we moved to using tangential flow filtration (TFF) to concentrate larger production batches down before loading them on sucrose cushions (III). This step reduced the hands-on time significantly and already purified the noro-VLP as smaller proteins

were mostly excluded from production supernatant. We also noticed that most residual baculovirus precipitates during TFF, which helps to remove the virus but caused blocking of the TFF membrane during runs. By freeze-thawing and centrifuging the supernatant before TFF, the purification pipeline becomes more flexible, and most precipitates could be removed before TFF. A tiny portion of noro-VLP also precipitates in freeze-thawing, but its concentration was negligible compared to precipitated baculovirus. As a polishing step, anion exchange was able to separate baculovirus from most noro-VLP versions (III) and yielded noro-VLP with up to 3-fold higher overall yield than reported in (Koho et al. 2012) (30 vs. 10 mg/L). However, we noticed that a lot of noro-VLP was lost in flow-through in all tested conditions that were able to separate baculovirus and therefore we later switched to size-exclusion chromatography (SEC). With this method, we were able to double the noro-VLP yield to up to 80 mg/L while removing the residual baculovirus efficiently. SEC is practical as a polishing step, since it can be used to switch to storage buffer simultaneously, whereas this is done in a separate dialysis step after ion exchange.

The first modified noro-VLP we produced during the project had a SpyTag001 fused to the C-terminus of noro-VP1 by a short linker of 4 amino acids (TSGG). Compared to WT-noro-VLP and the HisTag-noro-VLP (7 amino acid tag), the enlengthening of the C-terminal tag to 17 amino acid residues had no significant effect on the producibility, stability, self-assembly or purification performance of the noro-VLP. Replacing the original SpyTag001 with SpyTag003, but still using the same linker, did not lead to an increase in maximal conjugation efficiency of the noro-VLP (unpublished data). The expected increase in reaction speed in SpyTag003 vs. SpyTag001 (Keeble et al. 2019) is not relevant in the reaction concentration and time we have used SpyTag-noro-VLP with, so this was not thoroughly tested. The latest SpyCatcher-decoratable noro-VLP version has SpyTag003 separated from the C-terminus of noro-VP1 by a linear PAS-linker (Schlapschy et al. 2013) of 23 amino acid residues (Alkula, Lampinen, et al., unpublished data). All modified noro-VLPs were able to self-assemble into morphologically very similar VLPs and behaved in the same way in purification and downstream experiments, with no large differences in production yields.

In addition to the strategy of making noro-VLPs that can be decorated with SpyCatcher-fused antigens after their production, we also tried producing vaccine candidates with a small antigen genetically fused to the C-terminus of noro-VLP. Fusing the influenza M2e peptide (24 amino acids) to the C-terminus in place of SpyTag001 via the same linker did yield particles that seemed morphologically

identical to other noro-VLPs, but their production yields were almost halved with comparable purification strategies (III). We also fused some coronavirus antigens on the C-terminus of the noro-VLP (unpublished data). These were all whole protein domains instead of peptides and served as a good benchmark on the limits of the noro-VLP assembly mechanism. The 26 kDa receptor binding domain (RBD) of SARS-CoV-2 made the noro-VLP insoluble when attached to the C-terminal, and the 46 kDa dimeric nucleoprotein did the same. The dimerization domain of nucleoprotein (DD, 13 kDa) alone, however, was tolerated as a noro-VP1 fusion protein, and we obtained noro-VLP in particle-form with directly fused DD presented on the outside. Nevertheless, production yield was reduced 10-fold from SpyTag-noro-VLP, and anion exchange runs were unable to separate residual baculovirus from DD-noro-VLP. The noro-VLP has a strong self-assembly mechanism that tolerates peptide additions well, but protein-domain sized genetic fusions greatly benefit from conjugation via SpyCatcher-linkage by reducing the need for the optimization of expression systems.

Stability of a vaccine during transport, storage and even in the patient's body is crucial for its usability. As discussed above, norovirus is an extremely resilient virus, which we hoped would be conveyed to noro-VLPs. SpyTag-noro-VLP showed no measurable changes during a 5-month storage period in PBS at +4 °C (I). During this period, no aggregates were observed under visual inspection or by DLS. DLS showed no disassembly or size change of the particles, either. The SpyTags on noro-VLP surface retained their original reactivity during storage. At the same time, we stored SpyCatcher-M2e aliquots at -20 °C to use in conjugation for the storage experiment. After obtaining these results, we routinely stored the different noro-VLP versions in sterile-filtered PBS or TBS solutions at +4 °C successfully, in some cases for years. We also confirmed that the SpyTag-noro-VLP tolerates freeze-thaw cycles in case frozen storage would be necessary.

We compared the thermal stability of the modified noro-VLP versions to WT-noro-VLP by differential scanning fluorimetry (DSF) and differential scanning calorimetry (DSC). In DSF, SpyTag-noro-VLP seemed as stable as WT-noro-VLP (melting points, T_m , of +66–68 (vs. +68 °C, respectively (I, III)). Like WT-noro-VLP (Ausar et al. 2006; Shoemaker et al. 2010), SpyTag-noro-VLP is most stable in slightly acidic to neutral pH. In basic conditions exceeding pH 8, the particles are destabilized and disassembled. Under neutral pH, SpyTag-noro-VLP and M2e-noro-VLP showed the same thermal stability characteristics in salt concentrations between 60 and 300 mM (Figure 4A–B). Conjugation of the noro-VLP with SpyCatcher-fused influenza M2e or HA2 decreases its stability to T_m =+63 °C (I), and genetic

fusion of M2e on noro-VLP diminishes the melting point to +53 °C (III). Nevertheless, M2e-noro-VLP could be stored at +4 °C for months without observable deterioration. In DSC measurements, the unfolding curves of WT-noro-VLP and M2e-noro-VLP both had two closely associated peaks. The low temperature peak appeared at a temperature 4.5 degrees lower in the M2e-noro-VLP than in the WT-noro-VLP sample (67 vs. 72 °C), but the higher peaks only had a 1-degree difference between the two VLPs (74 vs. 75 °C) (Figure 4C–D).

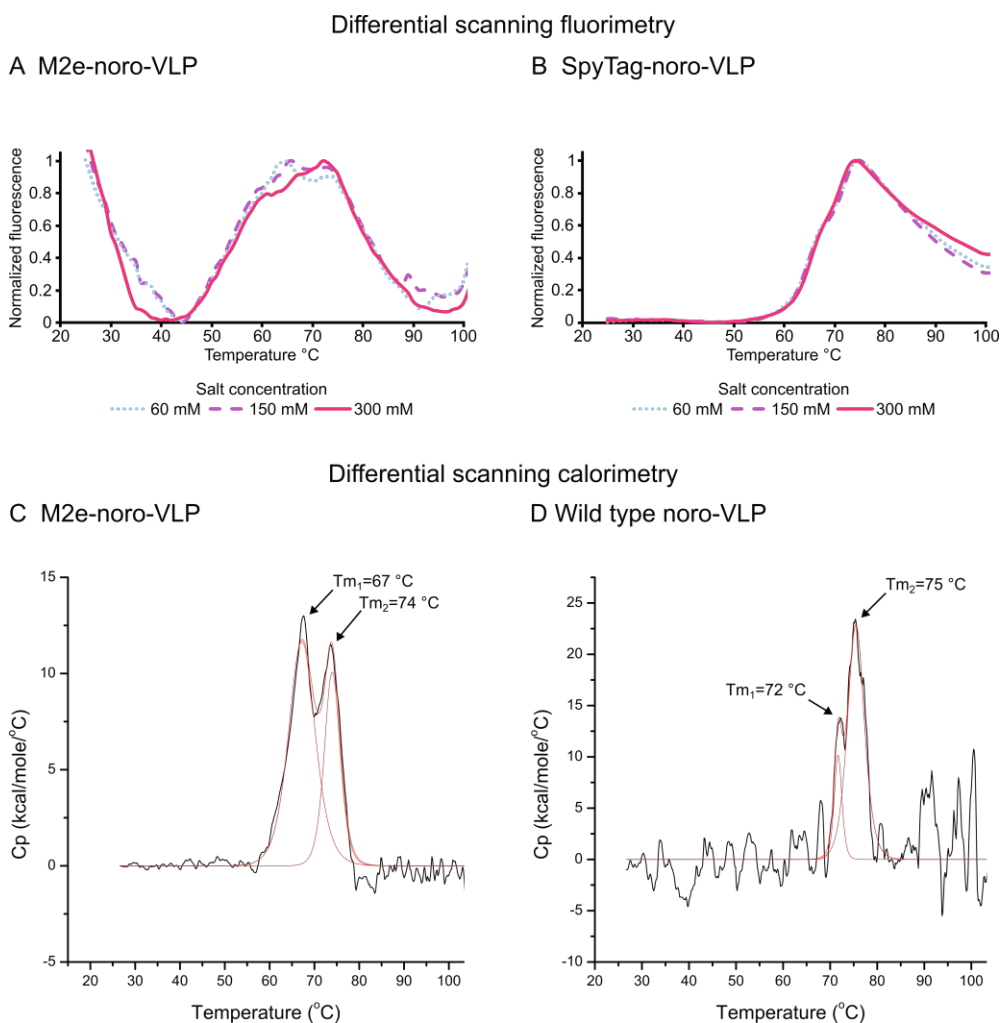


Figure 4. Norovirus-like particle stability studies. Differential scanning fluorimetry analysis of M2e-noro-VLP (A) and SpyTag-noro-VLP (B) in 60, 150, or 300 mM total salt concentration. Each graph here is averaged from three independent measurements. Differential scanning calorimetry analysis of M2e-noro-VLP (C) and wild type noro-VLP (D). The curves were fitted with Levenberg-Marquardt non-linear least-squares method. Adapted from publication III, used under CC BY 4.0.

5.2 SpyCatcher fused antigens

During the thesis project, we produced several different SpyCatcher-fused antigens from influenza virus (I) and PPC (IV) proteins. From influenza, we selected conserved parts of viral proteins, namely the ectodomain of the M2 ion channel

(M2e) and the stem part of HA (HA2). HA2 is a trimeric protein constructed from stem-associated fragments of HA1 fused to loops in HA2 from an H1N1 subtype of influenza (Mallajosyula et al. 2014). To construct experimental vaccine against self-antigen, we fused two peptide antigens from the LDL receptor binding site of PCSK9 to SpyCatcher. These peptides were selected from a similar VLP vaccine experiment (Crossey et al. 2015) and were completely conserved between human and mouse PCSK9. Furin P domain was selected to work as a furin-specific antigen, and a peptide from the active site of furin (SWG) to generate a pan-PPC response. Only 5 % of the amino acids differ in the P domains of mouse and human furin, while the active site peptide (of 14 amino acid residues) is fully conserved between the *FURIN* genes of the species and more than 85 % conserved between human *PCSK9* genes 1–7. All antigens were fused to the C-terminus of the original SpyCatcher that had a cleavable HisTag attached to its N-terminus for purification and identification of the proteins.

All SpyCatcher-antigens in this project were expressed in *E. coli*. After optimization of the expression conditions, they were bound on Ni-NTA column by their N-terminal HisTag, washed with Triton X-114 to remove residual bacterial endotoxin, and finally eluted and stored in PBS. Overall, all peptide-like antigens produced very efficiently in *E. coli* as SpyCatcher fusions, all exceeding 30 mg/L. Larger, protein domain antigen fusions were more difficult to produce, as expected. The trimeric influenza HA2 ministem produced to a yield of ~10 mg/L alone and as a SpyCatcher fusion. On the other hand, even with a slow expression strategy at an +18 °C temperature, most of SpyCatcher-P domain ended up in the insoluble fraction, with a final yield of only 1 mg/L of *E. coli* culture. This was still enough for purifying the antigen and preparing experimental amounts of vaccine, given to the ease of scaling up of *E. coli* cultures. Without SpyCatcher fusion, all of the P domain was found in the insoluble fraction (data not shown).

As expected, simplicity of purification of SpyCatcher-antigen was directly proportional to its overexpression rate. SpyCatcher-fused peptides all overexpressed very strongly and were purified to more than 90 % purity by a single affinity chromatography run. A single run was enough to purify SpyCatcher-HA2 and even SpyCatcher-P domain to the same purity level, but we needed to load cleared lysate from multi-liter volumes of culture. At this point, the lysate becomes viscous, requiring a lowered loading rate on the column. This slowed the purification process down somewhat but did not block HisTrap crude resin. After purification, the SpyCatcher-antigens were stored in PBS at -20 °C. All of them seemed stable for

months and showed no differences in SpyCatcher reactivity or aggregation status after freezing and thawing.

We confirmed the identity of each SpyCatcher-antigen with several methods during the project. In SDS-PAGE, the mobility of all of them matched the expected sizes well. When loaded in high concentrations, all antigens showed a minor band attributed to a dimer (Figure 5A–B). We also used a HisTag antibody to verify the presence of the N-terminal HisTag in the presumed bands in monomers, dimers and SpyTag-noro-VP1 conjugates. The presence of influenza M2e in SpyCatcher-M2e was verified similarly. As the peptide antigens were small and we had good monoclonal antibodies against only M2e, we used mass spectrometry to confirm that the small C-terminal had not been removed. The measured masses showed no peaks that could be attributed to truncated protein in any of the produced SpyCatcher-peptide antigens (I, IV).

5.3 SpyTag-noro-VLP tolerates conjugation of SpyCatcher-antigens

After producing and purifying the SpyTag-noro-VLP and SpyCatcher-antigen separately, the two components can be covalently conjugated together by simply mixing in solution, as described previously (Zakeri et al. 2012). The progress of the reaction can be followed by SDS-PAGE by the appearance of the band that matches the combined masses of noro-VP1 and SpyCatcher-antigen (Figure 5). We did all conjugations in the storage buffer of the components (PBS), and tried conjugation either for 1 hour at room temperature or overnight at +4 °C. The reaction continued after 1 hour but not anymore after ~18 hours, except when using very high concentrations of noro-VLP and a small SpyCatcher-antigen. With peptide antigens (e.g., SpyCatcher-M2e), we reported maximal conjugation efficiencies of 60 % (I), while the larger SpyCatcher-HA2 (I) and SpyCatcher-P domain (IV) reached 20 %. After publication of the conjugation efficiency tests, we noticed that SpyCatcher can continue making the isopeptide bonds even after boiling the SpyTag and SpyCatcher combination in SDS-PAGE sample buffer. Most likely this is because of refolding of SpyCatcher protein. In contrast, during boiling, the noro-VLP is denatured and disassembled into dimers or monomers and is unlikely to refold, let alone reassemble, in the presence of SDS, thus removing sterical restrictions of SpyCatcher/SpyTag binding. When repeating the SpyCatcher-M2e conjugation and

analyzing the efficiency immediately after boiling the sample, we estimated the efficiency at 24 % (Figure 5A–B).

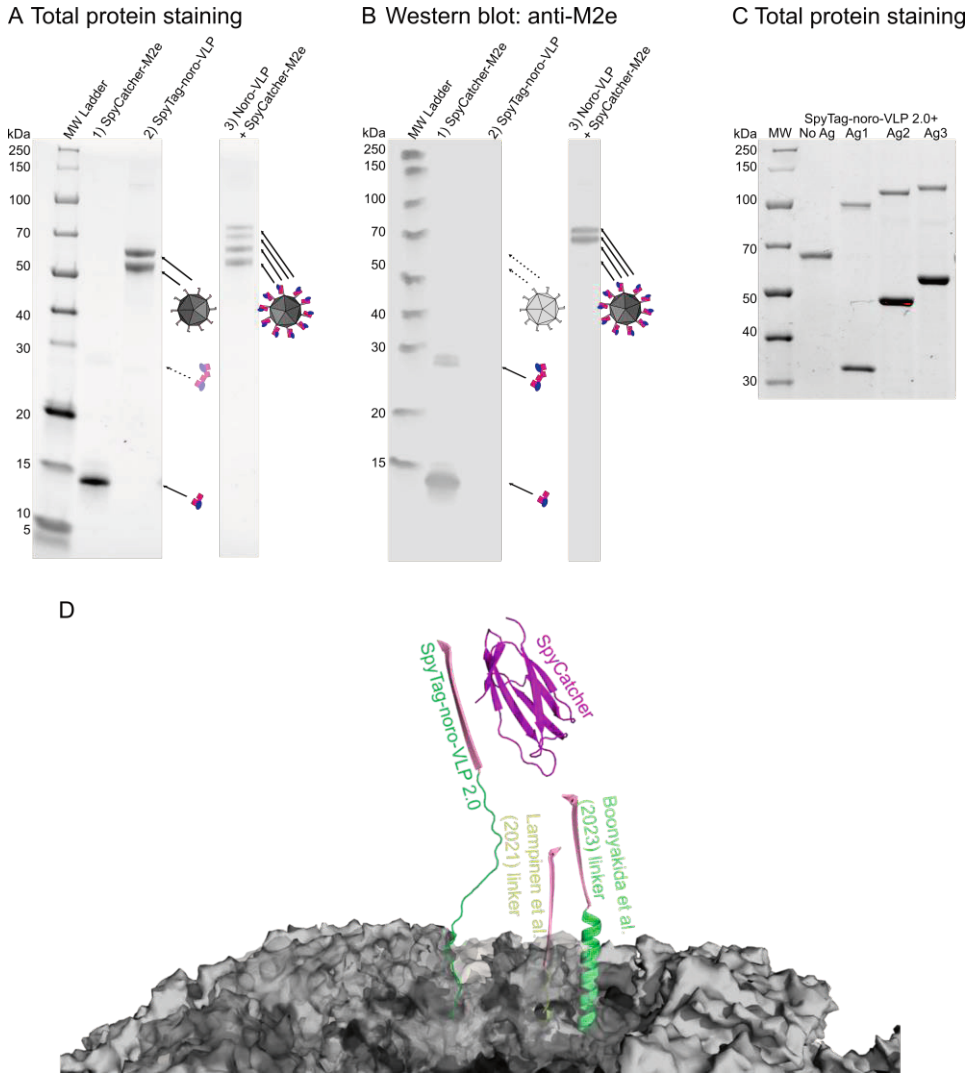


Figure 5. Conjugation of SpyCatcher-antigens on noro-VLP. A) Stain-Free total protein gel with approximately 1 μ g of total protein loaded in each well. SpyTag-noro-VP1 appears as a double band due to an N-terminal truncation. Upon conjugation, some of the SpyTag-noro-VLP double band moves upwards by the size of the conjugated SpyCatcher-M2e. B) The same gel blotted onto membrane for detection by M2 antibody. Only the conjugated noro-VLP double band is identified by the M2 antibody. A small amount of SpyCatcher-M2e is in dimeric form on the gel, despite boiling the sample. C) Conjugation of three differently sized SpyCatcher-antigens on SpyTag-noro-VLP 2.0. SpyCatcher was added in 3-fold molar concentration to the reactions. The size of SpyTag-noro-VLP 2.0 is 68 kDa, Ag1 is

~30 kDa, Ag2 is ~45 kDa and Ag3 is ~55 kDa. This batch of SpyTag-noro-VLP 2.0 was expressed in FlashBAC ULTRA baculovirus genome, so it is single-banded. D) The figure shows SpyTag (pink) fused to noro-VP1 C-terminus via three different linkers and an approaching SpyCatcher (purple), all in scale. In the original SpyTag-noro-VLP (limon), SpyTag was separated from noro-VP1 C-terminus only by a 4-amino-acid linker. The longer alpha helix linker by Boonyakida et al. may be enough to take SpyTag outside the protrusion domain. SpyTag-noro-VLP 2.0 has a linker (green) that is assumed to be almost linear here, and thus, takes SpyTag furthest from the noro-VLP core. Each binding spot, shown here with three SpyTags for clarity, contains five or six SpyTags (Figure 6B). RCSB PDB structures: norovirus: 1IHM (Prasad et al. 1999), SpyCatcher/SpyTag: 4MLS (Li et al. 2014). Panels A–B modified from publication III, used under CC BY 4.0, C–D modified from Alkula, Lampinen, et al., unpublished data.

The maximum conjugation efficiency of SpyTag-noro-VLP 2.0 was significantly enhanced as compared to the earlier versions of SpyTag-noro-VLP. This was probably due to the long and flexible linker that distances SpyTag from the valleys between the protruding domains of noro-VLP (Figure 5D). Further from the VLP core, sterical hindrance from the protruding domains and neighboring SpyCatcher-antigens is greatly reduced, allowing for more SpyCatcher-antigens to bind their SpyTag partners. Maximum conjugation efficiency was increased to more than 95 % with SpyTag-noro-VLP 2.0 (Figure 5C) (Alkula, Lampinen, et al., unpublished data). At the same time, another group developed a similar SpyTag-noro-VLP version with a longer alpha helix linker and enhanced conjugation efficiency (Boonyakida et al. 2023).

To ensure maximal conjugation efficiency, we made the conjugations with 1.5–3-fold molar excess of SpyCatcher-antigen as compared to SpyTag-noro-VLP. To separate the unconjugated SpyCatcher-antigen from the vaccine preparation, we dialyzed it out through a 1 000 000 Da MWCO membrane or separated it by SEC. Dialysis and SEC performed equally well in separation, but the high MWCO dialysis membrane was fragile and difficult to use, and the yield was better with SEC. We followed the disappearance of the free SpyCatcher-antigen band in SDS-PAGE after dialysis. The peptide SpyCatcher-antigens disappeared completely in dialysis (I, II, IV) and SEC (III), but some free SpyCatcher-HA2 (I) and SpyCatcher-P domain (IV) remained in the product even after dialysis. HA2, and possibly SpyCatcher-P domain as well, can form oligomers noncovalently and presumably remain attached to the VLPs through these bonds even without covalent SpyCatcher linkage.

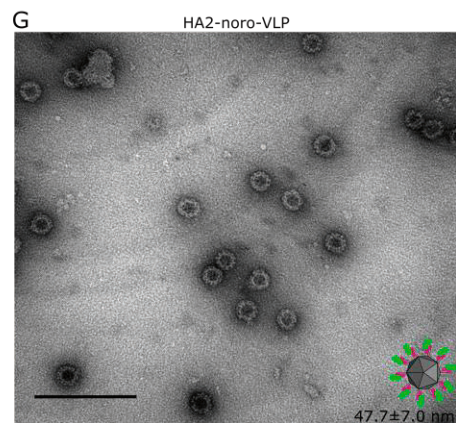
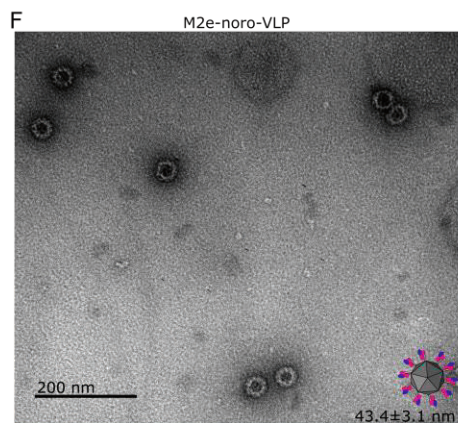
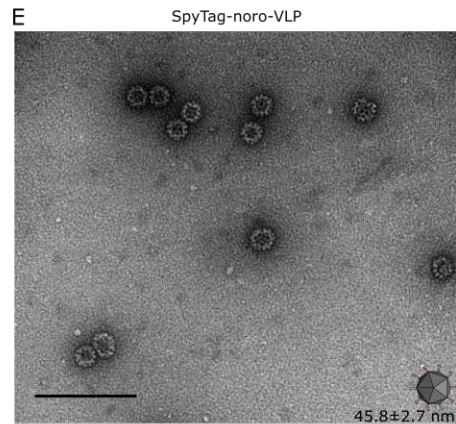
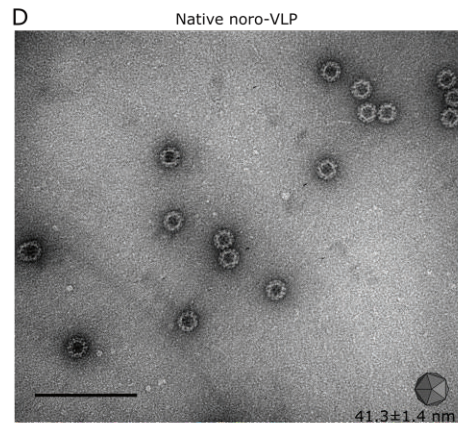
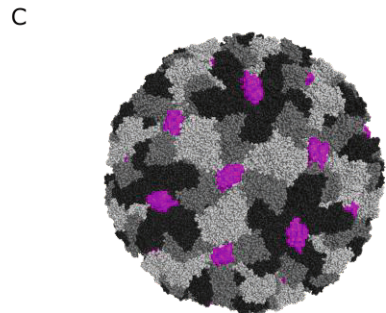
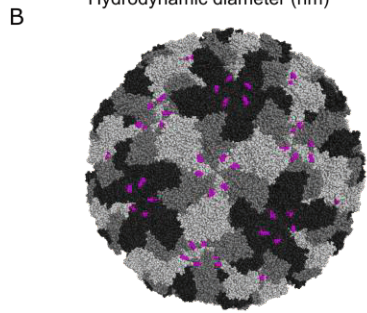
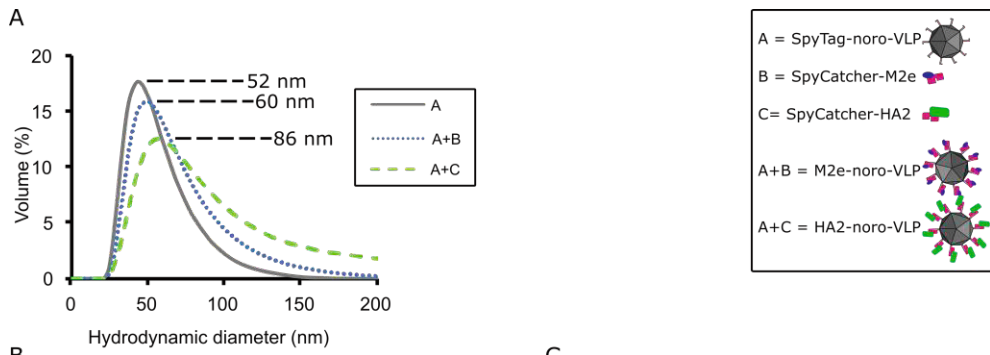


Figure 6. Size and morphology of norovirus-like particles. A) Dynamic light scattering analysis of SpyTag-noro-VLP and SpyTag-noro-VLP decorated with M2e and HA2. B) The noro-VLP is formed by 180 VP1 proteins, whose C-termini (purple) protrude from the surface in clusters of five or six. SpyTag (light purple) was genetically fused to the C-terminus of noro-VP1 via a 4-residue linker C) One SpyCatcher bound per cluster of SpyTags is shown for size comparison. The fusion protein models in B and C were constructed with the SynLinker web application (maintenance ceased since) and visualized with PyMOL software. The models are based on the following RCSB PDB structures: norovirus: 1IHM (Prasad et al. 1999), SpyCatcher: 4MLS (Li et al. 2014). D–E) Representative transmission electron microscopy pictures with arithmetic means of equivalent circle diameters \pm standard deviation of d native noro-VLP (n = 114), e SpyTag-noro-VLP (n = 112) and noro-VLP decorated with f M2e (n = 109) and g HA2 (n = 274). The scale bars are all 200 nm. 60,000 \times magnification was used for these pictures and analysis. Adapted from publication I, used under CC BY 4.0.

According to SDS-PAGE, the SpyTag-noro-VLP seems to conjugate well with the different SpyCatcher-antigens, but denaturing SDS-PAGE tells only of unfolded and disassembled polypeptides. We used dynamic light scattering (DLS) to check average particle sizes before and after conjugation. Decoration with SpyCatcher-M2e, SpyCatcher-P domain, and SpyCatcher-HA2 increased particle sizes in this order, according to the expected size of the SpyCatcher-antigen (I). Genetically fused M2e-noro-VLP was also larger in DLS than SpyTag-noro-VLP (54 vs. 49 nm) (III). Conversely, SpyTag-noro-VLP decorated with PPC-peptides via SpyCatcher slightly decreased in average size (IV). Transmission electron microscopy (TEM) showed that the same samples had large populations of the small \sim 23 nm particles that can be assumed to be 60-mers with T=1 symmetry according to literature (Devant and Hansman 2021; Jung et al. 2019). For the other vaccine candidates, this particle population was smaller or not observed at all. Based on the DLS size estimate of \sim 49 nm and the morphology by TEM, these GII.4 noro-VLPs were mostly 240-mers in T=4 symmetry (Figure 6), as suggested for the norovirus genotype GII.4 (Devant et al. 2019). 180-meric and 240-meric forms of noro-VLP seem very similar by morphology in TEM, but 180-mers should be \sim 40 nm by diameter. The conjugated SpyCatcher-antigens on top of noro-VLPs could not be readily visualized in TEM, maybe because even the largest of them were still rather small and globular and can probably fit in the valleys between noro-VLP protrusion domains.

5.4 Potential candidates for universal influenza vaccines

Influenza HA2 is a conserved part of the virus and a trimeric protein domain of around 16 kDa per monomer. Mice were immunized with HA2 presented on noro-

VLP via SpyCatcher linkage and as a SpyCatcher fusion without adjuvants. Based on ELISA analysis of their serum, the mice produced geometric mean titers (GMTs) of more than 10^4 of HA2-specific antibodies in groups that received SpyCatcher-HA2 alone or on noro-VLPs (Figure 7C). Still, the HA2-noro-VLP group generated a slightly higher mean titer with 68 % lower variance. The HA2-noro-VLP vaccine induced a balanced immune response generating high titers of IgG1 and IgG2a antibody subtypes in equal magnitudes (II). The antibodies were able to bind complete HA protein from the same influenza subtype, but in lower numbers compared to recombinant HA2 (II). In a cell-based neutralization assay, the produced anti-HA antibodies were unable to inhibit replication of a homotypic influenza virus. In summary, the unadjuvanted HA2-noro-VLP vaccine produced a strong and balanced, but non-neutralizing immune response.

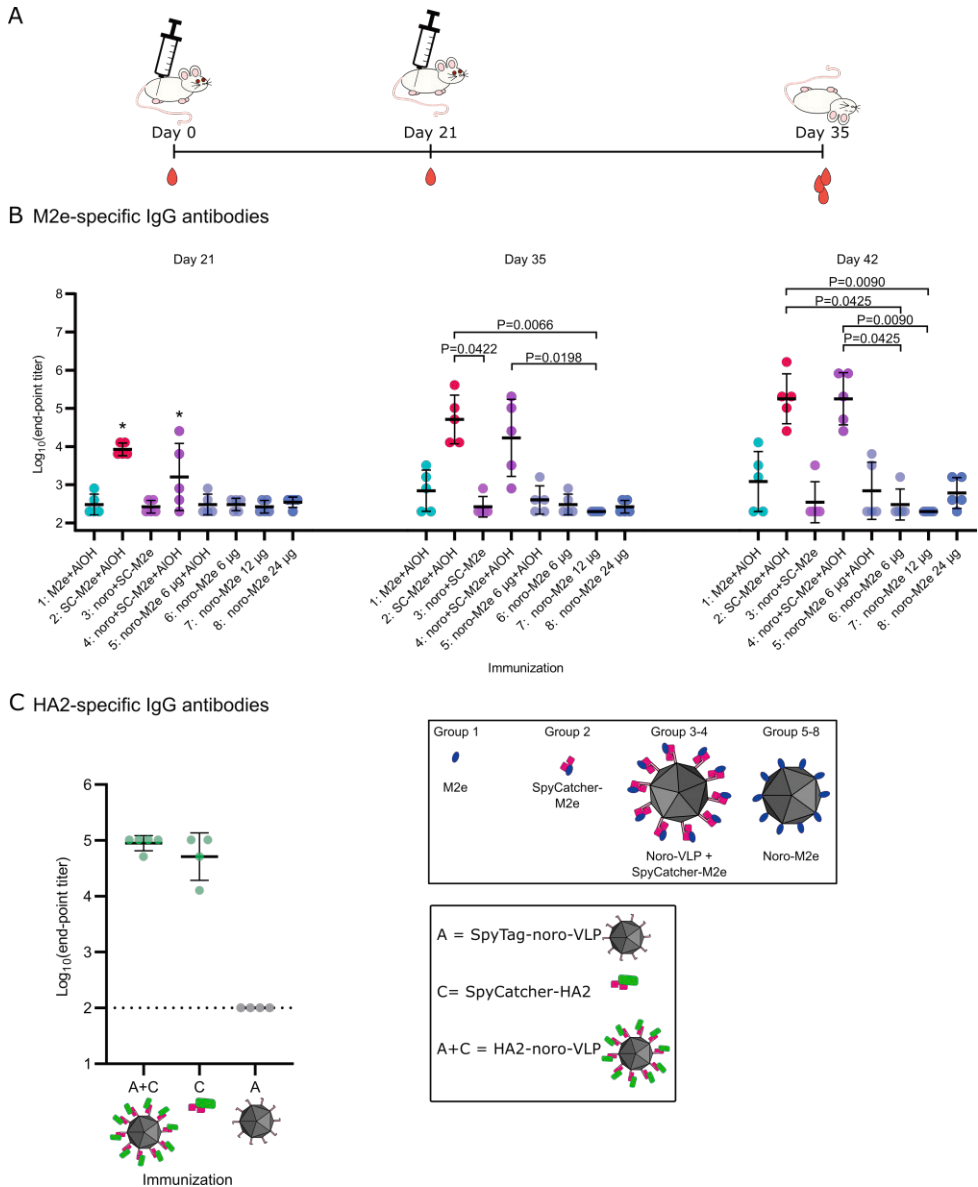


Figure 7. Antibodies generated by influenza vaccine candidates. A) A schematic showing the timeline of the vaccinations in BALB/c mice. We tested the immunogenicity of the vaccine candidates by injecting vaccine candidates twice and following the mice until day 35 (C) or day 42 (B). The injection was subcutaneous in the experiment in panel B and intramuscular in panel C. Log₁₀ transformations of IgG antibody end-point titers against M2e at different timepoints (B) and against HA2 on day 35 (C). Mean titers are represented by the thick line \pm standard deviation. P values are shown for groups with a difference with $P < 0.05$, determined by Dunn's test. Each dot represents a single mouse. Undetectable antibody levels were denoted with the titer corresponding to half of the lowest dilution assessed. Modified from publications I and III, used under CC BY 4.0.

We studied another universal influenza antigen called M2e during the project. It is a 24 amino acid peptide of 3 kDa. M2e presented on noro-VLP via SpyCatcher was compared to genetically fused M2e-noro-VLP (Table 3). When using M2e in immunizations either as SpyCatcher fusions or presented on noro-VLP via SpyCatcher without any added Al(OH)₃ adjuvant, we detected very few antibodies against M2e (Figure 7B) (I, II, III). When formulated with adjuvants, SpyCatcher-M2e produced very high titers of anti-M2e antibodies when conjugated on noro-VLP and also when introduced as soluble SpyCatcher-M2e (mean of 1.8×10^5 in both) (Figure 7B). However, cellular responses were slightly higher in groups where noro-VLP was present (III). Al(OH)₃ adjuvant skewed the immune response heavily towards humoral response, as seen by the low cytokine levels detected in FluoroSpot. Even adjuvanted, genetically fused M2e-noro-VLP generated only a low mean titer of 700 (Figure 7B). It should be noted that with an Al(OH)₃ adjuvant, even soluble M2e peptide was able to form a detectable antibody response (II), but it was used in a 50–160-fold larger dose than the successful noro-VLP conjugated and SpyCatcher-fused groups.

Table 3. M2e-based influenza vaccines and their doses used in the experiments. SC=SpyCatcher, Al(OH)₃=alum adjuvant. The colors match the group colors used in Figure 7. Modified from publication III, used under CC BY 4.0.

Group	Vaccine	Total protein dose (µg)	M2e dose (µg)	Noro-VLP dose (µg)	SpyCatcher dose
1 (Publication III)	M2e+Al(OH) ₃	1.1	1.1	0	0
2 (Publication III)	SC-M2e+Al(OH) ₃	1.5	0.3	0	1.2
3 (Publication III)	noro+SC-M2e	31	0.3	29	1.2
4 (Publication III)	noro+SC-M2e+Al(OH) ₃	31	0.3	29	1.2
5 (Publication III)	noro-M2e+Al(OH) ₃	6.0	0.3	5.7	0
6 (Publication III)	noro-M2e	6.0	0.3	5.7	0
7 (Publication III)	noro-M2e	12	0.5	11	0
8 (Publication III)	noro-M2e	24	1.1	23	0
9 (Publication III)	buffer+Al(OH) ₃	0	0	0	0
Publication I	noro+SC-M2e	50	1.1	43	4.8
Publication II	M2e+Al(OH) ₃	50	50	0	0

5.5 Potential candidates for furin vaccines (IV)

We wanted to study if noro-VLP presentation would be immunogenic enough to induce antibodies against endogenous (self) proteins in mice. To this end, we immunized mice with the peptides PEED and DIIG from the LDL receptor binding site of PCSK9, a peptide from near the active site of furin (SWG), and the furin P domain. All antigens were conjugated on noro-VLP via SpyCatcher and used in immunizations with no added adjuvant. The PCSK9 peptides generated detectable titers of PCSK9-binding antibodies (GMT of 280 for DIIG group and 980 for PEED) (Figure 8C). The furin active site peptide SWG failed to produce any detectable response against furin (Figure 8D). It is possible that the active site of furin would be unavailable for the serum antibodies in ELISA, but we got the same result when coating with a synthetic SWG peptide. Furin P domain (15 kDa) performed best, inducing furin-specific antibodies with the GMT of 1100 and a single mouse with a titer of 1.3×10^4 . To obtain higher titers of furin-specific antibodies, we studied P domain-noro-VLP further in another round of immunizations, now with a smaller dose, but with an $\text{Al}(\text{OH})_3$ adjuvant and two extra boosts. Here, the mice showed an even more variable result, and GMT was not increased further (IV). Surprisingly, a group containing only adjuvanted SpyCatcher-P domain fusion actually induced a stronger antibody response with a maximum titer of 4.1×10^5 and a GMT of 1.4×10^3 for the whole group. We incubated recombinant furin with the sera with the highest furin-specific antibodies to see if they would inhibit furin's activity *in vitro*. However, we did not see any difference in the ability of furin to process its protein substrate, diphtheria toxin, between vaccine groups (Data not shown).

All PPC-noro-VLP vaccines generated antigen-specific cell-mediated immune responses against SpyCatcher and noro-VLP, but the peptide antigens caused no detectable T cell signals in a recall assay (Figure 8E). In addition to a memory response, SpyCatcher-conjugated furin P domain seemed to generate non-specific activation in immune cells naive to these antigens. Importantly, the growth rate and health of the mice was not evidently disturbed (Figure 8B), even though humoral self-immune responses were observed in the animals.

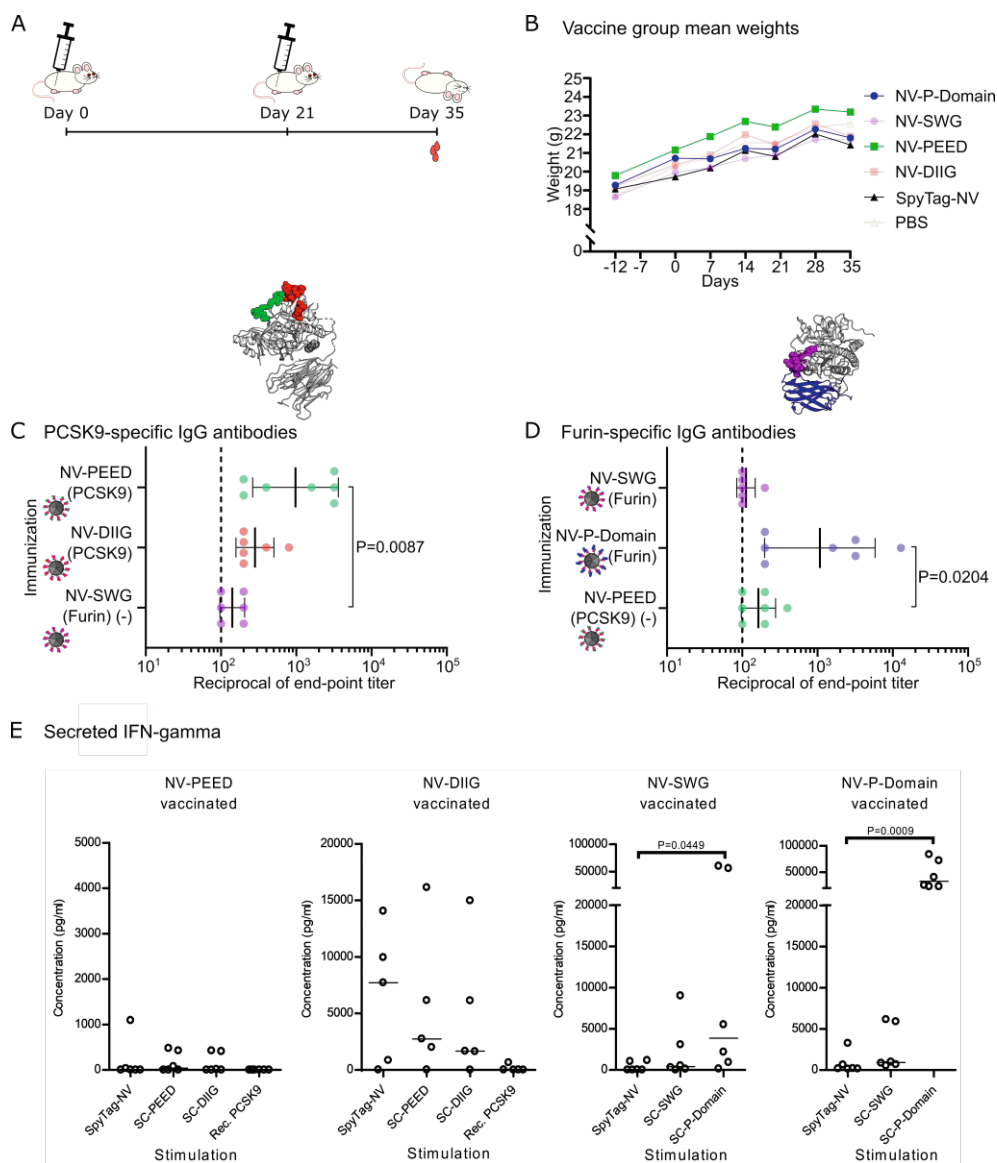


Figure 8. Unadjuvanted PPC-coated noro-VLPs induce the production of PCSK9 and furin-specific IgGs. A) A schematic overview of the immunization experiment. 8-week-old BALB/c mice (n=6, all females) were injected twice i.m. with PPC-decorated noro-VLPs, SpyTag-noro-VLP or PBS at days 0 and 21. On day 35 the animals were euthanized, and blood and spleen collected for analysis. B) The arithmetic mean mass of mice in different vaccination groups during the experiment is represented as a function of time. C–D) End-point antibody titers were measured using ELISA. Plates were coated with the corresponding protein and the IgG antibody titers against recombinant PCSK9 (C) and recombinant furin (D) are shown. The end-point titer is the reciprocal of the lowest serum dilution that gives a significantly higher absorbance as compared to negative control mouse group (SpyTag-

noro-VLP) serum diluted 1:200. Mean titer \pm standard deviation is depicted. Differences in means were tested with Kruskal-Wallis test followed by Dunnet's test and the significant adjusted P values are shown. As an additional negative control (-), we used serum from a group naive to the protein tested. Each dot represents a single mouse. Undetectable antibody levels were denoted with the reciprocal titer 100 (vertical dashed line). E) Splenocytes were isolated from mice immunized with PPC-decorated noro-VLP and the cells were stimulated *in vitro* for 3 days at 37 °C. The culture media was collected after 3 days and the IFN- γ concentrations quantified using ELISA. The antigen-specificity of the IFN- γ response is shown for noro-VLP-PEED, noro-VLP-DIIG, noro-VLP-SWG and noro-VLP-P domain vaccinated mice. Scatter dot plot with median is shown for each group. Nonparametric Kruskal-Wallis one way ANOVA followed by Dunnet/Dunn's test was used in panels A and B and the Mann-Whitney U test in panel C for the statistical evaluation of differences. Modified from publication IV.

5.6 Tagged and decorated noro-VLPs work as potential norovirus vaccines

An added benefit to using the noro-VLP as a vaccine platform is the possibility of inducing relevant anti-noro immune responses as a “side effect” of the vaccine. In the vaccine experiments described above, all mouse groups that received noro-VLP generated remarkably high titers of norovirus antibodies. The noro-VLP-specific GMTs ranged from 4.5×10^4 (IV) to 2.9×10^6 (III). Fusing SpyTag or M2e on the C-terminal had little effect on the generation of responses against norovirus but adding Al(OH)₃ to the preparation increased the titers (Figure 9A). Interestingly, conjugation of noro-VLP with the furin active site peptide SWG increased anti-norovirus titers significantly compared to SpyTag-noro-VLP alone but produced no detectable furin antibodies (IV). Other conjugated noro-VLP groups had insignificant differences that seemed to correlate with the dose of noro-VLP given to each group.

The ability of norovirus antibodies to block the binding of noro-VLP to its receptor, the histo-blood group antigen (HBGA), correlates well with their virus neutralization ability. The IC₅₀ values of mice immunized with SpyTag-noro-VLP, HA2-noro-VLP or M2e-noro-VLP did not differ significantly from a comparable mouse group immunized with WT-noro-VLP in blocking of homologous or heterologous strain of noro-VLP (Figure 9B). In conclusion, conjugated noro-VLP vaccines work as well as norovirus vaccines as unconjugated noro-VLPs based on the same strain.

A Noro-VLP-specific IgG antibodies

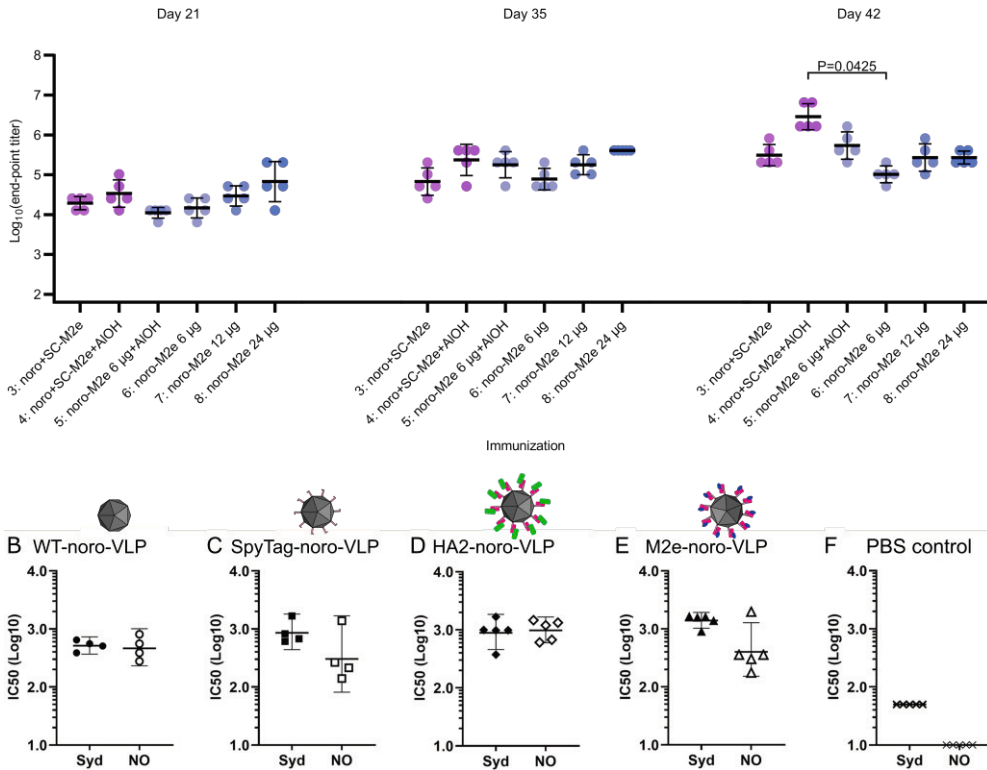


Figure 9. Norovirus-specific antibody responses. A) Total IgG responses at different time points. Log₁₀ transformations of IgG antibody end-point titers against noro-VLP, as assessed in ELISA. Mean titers are represented by the thick line \pm standard deviation. P values are shown for groups with a difference with $P < 0.05$, determined by Dunn's test. Each dot represents a single mouse. Undetectable antibody levels were denoted with the titer 200 (half of the lowest dilution assessed) Induction of NoV blocking (neutralizing) antibodies by decorated NoV VLP formulations. B) Homologous and heterologous blockage of NoV Sydney (Syd) and NoV New Orleans (NO) VLP binding to HBGAs present in pig gastric mucin (PGM) by serum antibodies following two immunizations with NoV VLPs (A), SpyTagged NoV VLPs (B), NoV VLPs decorated with HA2 (C), NoV VLPs decorated with M2e (D) or carrier only (E). Half maximal inhibitory concentration (IC₅₀) of each mouse is shown. Each symbol represents an individual animal. Bars indicate geometric mean values of the experimental groups with 95% confidence intervals. A titer of 50 (1.7 log₁₀) was assigned for sera with no detectable genotype-specific antibodies, being a half of the initial serum dilution in homologous blocking assay. A titer of 10 (log₁₀) was assigned for sera with no detectable cross-reactive antibodies, being a half of the initial serum dilution in heterologous blocking assay. Adapted from publications II and III, used under CC BY 4.0.

5.7 SpyCatcher fusion enhances immune responses

Substantial immune responses were formed against SpyCatcher in all vaccine preparations that contained it. The strength of the anti-SpyCatcher immune response depended on the other components in the preparation. SpyCatcher-M2e raised significantly more anti-SpyCatcher antibodies when conjugated on the noro-VLP than when injected alone, but the opposite was true for the influenza HA2 vaccine candidates (I). Then again, when Al(OH)₃ was added in each group, SpyCatcher-M2e formed more SpyCatcher antibodies without any noro-VLP presentation (III). The immunogenicity of SpyCatcher also activated the immune system against its fusion proteins. Fusing M2e on SpyCatcher generated equal titers of anti-M2e antibodies to noro-VLP presentation via SpyCatcher and more than soluble M2e peptide alone, when all groups were adjuvanted (III). SpyCatcher-P domain was also immunogenic for many of the tested mice when formulated with Al(OH)₃ adjuvant, even though furin P domain is endogenous in mice (IV). Only insignificant immune responses were detected against SpyTag in the immunization groups tested in publication III.

6 DISCUSSION

6.1 VLP based vaccines offer many benefits over conventional technologies

Even before the SARS-CoV-2 pandemic, top epidemiologists warned us repeatedly about the ever-increasing rate and seriousness of global pandemics. The latest pandemic brought a brief surge of resources and fast-forwarded mRNA vaccines, which were under study since the late 1980s (Verbeke et al. 2019), from the bench to the clinic in record time. Still, it seems that the next dangerous world-wide pandemic is more a question of when than if, and that we will face pandemic diseases ever more often in the future (Clifford Astbury et al. 2023). To survive these upcoming perils, we need more efficient, better storable, and more flexible vaccine technologies, which can be quickly applied to address any emerging threat. At the same time, novel immunomodulatory techniques can be implemented to treat old diseases in new ways. In this project, we developed a modifiable vaccine platform based on the norovirus-like particle and decorated it with clinically relevant antigens of various shapes and sizes. To do this, we utilized SpyCatcher/SpyTag conjugation methods to present influenza antigens and proprotein convertase self-antigens on the surface of the noro-VLP.

The main tool against influenza is still the traditional inactivated whole influenza virus vaccine grown in chicken eggs. This technology is as simple to use now as it was in the 1940s but comes with many restrictions. The vaccines pose a problem for people with egg allergies and avian influenza epidemics threaten the availability of eggs. Working with live viruses is always an infection risk and requires specialized facilities. The virus cultivation process is slow, which means that the optimal properties of the next flu season's vaccine need to be predicted six months beforehand (Hannoun 2013). Some years, the prediction fails badly, and the vaccine does not match the circulating virus and is ineffective. There are a few recombinantly produced options now, like Flublok (Sanofi Pasteur, France). Flublok is made of adjuvanted whole HA protein of the currently circulating strain, but recombinant production is much faster, allowing for better matching than in the egg-cultivated vaccines. Then again, whole HA vaccines also direct the immune responses against

the fast-mutating parts of influenza virus, so annual revaccination is still needed to protect against escape mutants.

Vaccines based on virus-like particles offer important advantages over ones based on soluble proteins or whole viruses. VLPs contain no viral genome, so they cannot cause infection at the production facility or in the patient, like e.g. the live attenuated polio vaccine has in rare cases (Wringe et al. 2008). Virus-like particles are potent immune activators by themselves due to their size (20–200 nm) which is optimal for uptake in antigen-presenting cells and for direct draining into lymph nodes (Bachmann and Jennings 2010). By cross-presentation, antigens linked to VLPs are presented to cytotoxic T cells more often than soluble antigens (Quan et al. 2016). The surface proteins on VLPs are close to each other and presented in a repetitive manner, allowing for B cell receptor cross-linking and direct T cell-independent activation of B cells (Dintzis et al. 1983, 1989). The high immunogenicity of VLPs can lower the required dose of vaccine and/or adjuvant, potentially reducing side effects of vaccination. The hepatitis B VLP was the first one discovered and it has been used to vaccinate against hepatitis since the 1980s (Mohsen and Bachmann 2022). The first malaria vaccine was recently approved for clinical use (Mosquirix, GSK, UK). The vaccine is a chimeric VLP vaccine which consists of a malaria antigen presented on hepatitis B VLPs for increased immunogenicity.

Mosquirix is made by genetic fusion of the antigen on the VLP surface, but a lot of research effort has recently been into modular vaccines, where the VLP and antigen components are produced independently and conjugated together after VLP assembly and antigen folding. The SpyCatcher/SpyTag and related technologies are particularly promising in making a vaccine like this and they have already entered clinical trials for prevention of SARS-CoV-2 and against cytomegalovirus in 2023 (<https://spybiotech.com>; accessed 17.9.2023). In academic research, there are dozens of publications utilizing this technology for VLP decoration (<http://www.howarthgroup.org/info>; accessed 17.9.2023). The main benefit of modular decoration is that it requires less optimization compared to genetic fusion and is more controllable than chemical conjugation (Brune and Howarth 2018). Also, if several vaccine products based on the same modular VLP platform would be approved for clinical use, it would allow the formation of a common stockpile of the VLP that could be then decorated with any antigen whenever needed. Sharing a common immunogenic VLP platform and formulation technique should also expedite the currently rate-limiting process of getting new vaccine products approved by authorities.

6.2 The norovirus-like particle as a vaccine platform

During this thesis project, we have produced several versions of the noro-VLP. The recombinant production of noro-VLP is efficient and easily scalable, and it works in a range of eukaryotic expression systems from yeast to silkworms and plants (Boonyakida et al. 2022; Mason et al. 1996; Xia et al. 2007). Here, we obtained excellent yields of the SpyTagged noro-VLP in the scalable insect cell expression system. For lab scale, ultracentrifugation and size-exclusion chromatography were the most adaptable purification methods, but we proved that the industrially scalable tangential flow filtration and ion exchange chromatography work well for noro-VLPs, provided that they are optimized properly for each version of noro-VLP. We observed that the SpyTag-noro-VLP shows very similar stability characteristics to WT-noro-VLP (I, III), which can be stored at room temperature for at least 7 days (Huhti et al. 2010). In refrigerator temperatures, the SpyTag-noro-VLP could be stored for months, which is important for its use as a vaccine, especially if making large stockpiles of the vaccine platform.

We compared the thermal stability of modified noro-VLPs to one another and the wild type noro-VLP. According to differential scanning fluorimetry (DSF), SpyTag does not reduce thermal stability of the particle ($T_m = +67^\circ\text{C}$ vs $+68^\circ\text{C}$ in wild type (WT) noro-VLP), but C-terminal fusion of M2e lowers T_m to $+53^\circ\text{C}$. For laboratory storage at $+4$ or -20°C , this makes no difference in practice, but may affect vaccine use in regions with poor refrigeration possibilities. Lowered thermal stability of M2e-noro-VLP was confirmed in differential scanning calorimetry (DSC), where we observed two unfolding peaks for M2e-noro-VLP and WT-noro-VLP. The lower temperature peak (T_{m1}) was markedly lowered in M2e-noro-VLP ($+67$ vs. $+72^\circ\text{C}$), but the higher temperature peak (T_{m2}) only had a single degree difference ($+74$ vs. $+75^\circ\text{C}$). An earlier study on WT-noro-VLP disassembly observed the same two unfolding peaks by DSC (Ausar et al. 2006). There, they compared T_{m1} to the unfolding peak of norovirus protruding (P) domain subparticles, and suggested that T_{m1} matches the unfolding of P domain of VP1, even though there was a 10-degree difference between the T_m values. In this model, T_{m2} was associated with the shell (S) domain, and the domains of VP1 unfold separately. Because in M2e-noro-VLP, we have modified the C-terminus of P domain and left S domain untouched, the fact that we observed a larger effect on the proposed P domain unfolding peak would match the model well. Another explanation for the two peaks would be that T_{m1} is associated with the disassembly

of the capsids and T_{m2} with the subsequent unfolding of the capsid proteins. The T_{m1} of WT-noro-VLP is close to the temperature where noro-VLP was seen to start disassembling by TEM (+72 vs. +65 °C) (Ausar et al. 2006). Neither of the models of disassembly can be ruled out before further biophysical studies, for example DSC analysis of noro S subparticles.

The noro-VLP was successfully decorated with protein antigens with different properties. The SpyTags on the noro-VLP surface concentrate into clusters of 5 or 6 that lie in valleys between the protrusion domains. Based on the structure of norovirus, it may be possible to fit 2–3 SpyCatchers in the valleys, but with larger fusion partners of SpyCatcher, the number is further reduced. This would translate into a maximum conjugation efficiency of 33–60 %. During the project, we realized that SpyCatcher reactions continue even after boiling in SDS-PAGE, probably due to it refolding. If this conclusion is true, the refolded SpyCatcher could form covalent bonds with SpyTag on unfolded and disassembled noro-VP1 with greatly reduced sterical restrictions. Therefore, the conjugation efficiencies of 60 % we reported in publications I and II for SpyCatcher-M2e may be overestimated. When we repeated SpyCatcher-M2e conjugation on noro-VLP 1.0 and analyzed it on SDS-PAGE immediately after boiling, we estimated a conjugation efficiency of 24 % (III). Later, we developed SpyTag-noro-VLP 2.0 with a longer linker between SpyTag and the C-terminus of noro-VP1. This version could reach conjugation efficiencies of more than 95 % with small SpyCatcher fusion proteins (Alkula, Lampinen, et al. unpublished data). Independently, another group published a SpyTag-noro-VLP version with maximal conjugation efficiency increased to 63 % with an alpha helical linker (Boonyakida et al. 2023). Their alpha helix linker was a few amino acids shorter than the one in SpyTag-noro-VLP 2.0 and also more compact than the PAS linker (assumed to be almost linear (Schlapschy et al. 2013)) in SpyTag-noro-VLP 2.0, which may be why their SpyTag-noro-VLP reached lower maximum conjugation efficiencies. Boonyakida et al. reported that a linker comparable to the one in SpyTag-noro-VLP 1.0 yielded a maximal conjugation efficiency of 35 %, which is in line with what we found in publication III. Other modular VLP platforms often have the SpyCatcher on the VLP surface (e.g. (Brune et al. 2016), which could also increase conjugation efficiency, but at the same time, could reduce the yield and stability of noro-VLP. While we were able to produce M2e-noro-VLP in insect cells efficiently, the M2e perhaps starts to be on the larger end of possible fusion partners on the noro-VLP, based on the lowered yield and thermal stability (III). On the other hand, a similar enlengthened linker that enabled better conjugation efficiency in SpyTag-noro-VLP 2.0 could also stabilize larger fusion partners in future studies.

According to my literature search, whole noro-VLP has been heavily studied as a norovirus vaccine, but not before in immunological studies that aim for a chimeric vaccine. As discussed in Chapter 2.2, the noro-VLP is formed by 60, 180, or 240 full-length VP1 proteins. VP1 can be divided to the protruding (P) and shell (S) domains that can be used to form smaller P and S subparticles. Both subparticle types can be produced efficiently in *E. coli*, and they have generated promising results as antigen carriers (Jiang et al. 2015; Tan et al. 2011; Xia et al. 2011, 2018). P domain subparticles are 12-mers or 24-mers, and S subparticles are 60-mers. The full-length noro-VLP has been considered as a norovirus vaccine for decades already, but no licensed vaccine exists yet. Based on their HBGA binding and blocking ability, the SpyTag-noro-VLP and its antigen-decorated forms function as norovirus vaccines as well as the corresponding WT-noro-VLP (II). The HBGA blocking assay correlates with norovirus neutralization well and may even underestimate the virus blocking efficiency of antibodies (Ettayebi et al. 2016). Therefore, application of the SpyTag-noro-VLP as a vaccine platform would also help reduce the burden of the most prevalent “stomach flu”.

6.3 Novel influenza vaccine candidates developed during the project

Influenza vaccines have been in the market all around the world for decades now. Most in current use are based on inactivated virus grown in chicken eggs, but these vaccines have limitations and suffer from severe ineffectiveness during some flu seasons. New vaccine types against influenza are developed continuously, and a recombinant HA protein vaccine is already on the market (Flublok, Sanofi Pasteur). Even though recombinant protein expression is faster than egg-based virus cultivation, it will be a huge investment to build facilities large enough to recombinantly produce the vaccines needed to replace the huge number of egg-based influenza vaccine doses used each year. Also, all current recombinant influenza vaccines target the same rapidly mutating parts of influenza as egg-based vaccines do, and thus require yearly renewal to stay effective. Heavy research efforts are directed to create a more broadly reactive, longer lasting, “universal” influenza vaccine. Promising research includes display of HA from many influenza strains on the same VLP (Prabakaran et al., 2010; Pushko et al., 2011; Schwartzman et al., 2015), chimeric HA (Carter et al., 2016), and conserved influenza antigens (Ben-Yedidia,

2011; Krammer, 2015; Wiersma, Rimmelzwaan, & de Vries, 2015). Many solutions like this have progressed to clinical trials, but none have entered the market yet.

In publication I, we tested the immunogenicity of the modular noro-VLP platform in presenting the most studied universal influenza vaccine candidates M2e and HA2. Both antigens were successfully produced as SpyCatcher fusions and conjugated on the noro-VLP. The HA2 ministem was based on HA2 from A/Puerto Rico/8/34 (H1N1) influenza virus fused with stem-associated fragments of HA1 from the same influenza subtype (Mallajosyula et al. 2014). The antigen previously generated promising titers in mice (Valkenburg et al. 2016), but performed worse in ferrets (Sutton et al. 2017), when used in soluble form at a higher, adjuvanted dose. Even the SpyCatcher-fused soluble HA2 vaccine produced higher antibody titers in mice than the previously tested formulations (I), which suggests that here SpyCatcher has a higher immunogenic effect than the CpG7909 adjuvant used earlier (Mallajosyula et al. 2014). Noro-VLP presentation slightly increased the titers and reduced variance within the mouse group. The immune response was also well-balanced between the humoral and cellular immunity (II). On the other hand, the acquired antibodies were not neutralizing (II), unlike some obtained with soluble HA2 ministem proteins (Mallajosyula 2014, Deng 2018). Earlier challenge studies have shown that non-neutralizing antibodies can be protective (Bommakanti et al. 2010, Bommakanti 2012), so challenge studies would still need to be executed with the otherwise promising HA2-noro-VLP vaccines to learn more about their biological significance.

In the first unadjuvanted experiment, we observed few M2e-specific antibodies but strong responses against noro-VLP and SpyCatcher when immunizing mice with SpyCatcher-decorated M2e-noro-VLP (I, II). We thought that SpyCatcher may somehow block M2e antibodies from forming in this vaccine group, so we prepared a genetically fused version of M2e-noro-VLP. M2e-noro-VLP produced well and formed stable particles, but it was not very good at raising M2e-specific immune responses. In an Al(OH)₃ adjuvanted group, we measured an appreciable mean titer against M2e, but three mice had undetectable antibodies, indicating poor repeatability. Surprisingly, the SpyCatcher-fused M2e generated strong anti-M2e responses when given in soluble, adjuvanted format. In the earlier experiment, this vaccine candidate produced no detectable M2e response (II).

Similar genetically fused M2e peptide vaccines based on hepatitis B VLPs (Neirynek et al., 1999), bacteriophage AP205 VLPs (Tissot et al., 2010) and on norovirus P-subparticles (Xia et al., 2011) have been reported to work better. In the noro-VLP, the C-termini are located in valleys surrounded by protruding domains

(Figure 5D). In the tested M2e-noro-VLP construct, we only have a short (TS) linker between the C-terminus, which positions the M2e peptides between noro-VLP protrusions, potentially limiting the access of large proteins. In future studies, this could be circumvented by fusing multiple peptides in succession to a VLP carrier, as described earlier in (Kim et al., 2013; Lee et al., 2018; Lee et al., 2019) or by separating M2e from noro-VP1 C-terminus by an enlengthened linker, like the one used in SpyTag-noro-VLP 2.0.

Even a very strong immune response against the well-conserved M2e would not be enough for preventing influenza infections altogether. As discussed in Chapter 2.3.1, there are only a few M2 channels in an influenza virion (Zebedee and Lamb 1988), and they are poorly accessible beneath the head domains of HA and NA. to prevent infection, anti-M2e vaccines should be combined with a neutralizing influenza vaccine. After a cell has already been infected with influenza virus, the virus needs to adjust the pH of the cell, which is done by expressing the M2 proton channel vigorously on the cell membrane. This enables targeting of the cells by M2e-specific immune responses (Hashemi et al. 2012). M2e antibodies can aid in clearance of infected cells through antibody-enhanced natural killer cell or macrophage cytotoxicity, Fc opsonization or possibly prevent budding of new virions (Lee et al. 2018). The most successful adjuvanted SpyCatcher-conjugated M2e-noro-VLP or soluble SpyCatcher-M2e could be combined into the HA2-noro-VLP vaccines and a commercial vaccine against HA head domain (like Flublok) to produce a universal influenza vaccine that could potentially block acute infection and give broad protection from escape mutants. As neutralization was not observed for the HA2-noro-VLP vaccine candidates and M2e antibodies are even theoretically unable to neutralize influenza, this combination vaccine should be evaluated in challenge studies.

6.4 Endogenous proprotein convertase vaccine candidates

Vaccination has long been one of the most important tools in fighting infectious disease, but latest advancements in the field of vaccine technologies have led to studies that aim to bring vaccination to treat noncommunicable illness, as well. The most deadly groups of noncommunicable disease in the world are cancer and cardiovascular disease (<https://www.who.int/news-room/fact-sheets/detail/the-top-10-causes-of-death>; 9.11.2023) and new vaccines are in development against them both. For example, a breast cancer vaccine based on HER2 presented on

AP205 bacteriophage VLP induced high titers of antibodies against HER2 and reduced growth of breast cancer tumors in mice (Palladini et al. 2018). Many cancer cells overexpress the anti-apoptotic HER2 on their membranes, so cancer inhibition works through its binding and inhibition. Similarly, PCSK9 has been targeted in several preclinical vaccine trials to inhibit endogenous PCSK9 and thus increase the number of active LDL receptors, which leads to reduced blood cholesterol. Both HER2 and PCSK9 have been validated as drug targets in clinically approved therapeutic antibody treatments (e.g., trastuzumab, Roche, Switzerland and evolocumab, Amgen, respectively). Active immunization against them could potentially induce the patient's body to produce similar antibodies with a single immunization for years and replace expensive and frequent antibody injections.

We wanted to see if the noro-VLP vaccine platform could be utilized to produce modern self-vaccines against endogenous proteins. Two peptide antigens from the LDL receptor binding site of PCSK9 were fused to SpyCatcher and conjugated to noro-VLP surface. The chosen peptides were similar to ones that had produced promising results in an earlier VLP vaccine study (Crossey et al. 2015) and its recent continuation with bivalent VLP vaccine (Fowler et al. 2023). At the same time, we produced novel vaccine candidates against a related PPC protein, furin, by similarly decorating noro-VLP with the whole P domain of furin. Furin has also been targeted by inhibitory therapeutic agents in a preclinical setting to prevent pathogen activity (Sarac et al. 2004; Shiryayev et al. 2007) and in phase II trials to treat ovarian cancer (Rocconi et al. 2021), but to our knowledge, it has not been considered yet as a target of vaccination.

The PCSK9 peptide antigens were both able to produce antibody responses against PCSK9 when mice were injected with them presented on the noro-VLP. The response levels were at least an order of magnitude lower than induced by the Q β -VLP-based vaccine candidates they were derived from (Crossey et al. 2015), but this may be explained by the differences in the setup of the experiment. The noro-VLP vaccine candidates generated detectable antibody levels with only two immunizations and no conventional adjuvants, while the Q β vaccine candidates were injected into mice three times with Freund's incomplete adjuvant.

The furin-specific P domain vaccine candidate generated a promising antibody in the first immunization experiment with it, but surprisingly, the same effect could not be detected in a repeated immunization with added Al(OH)₃ adjuvant. This time, four immunizations were needed to reach similar titers. We switched from intramuscular to the subcutaneous route for practical reasons for the second immunization experiment, which has been reported to lead to lower humoral

response (Mohan et al. 2010). The groups that received half or all of their immunizations in soluble SpyCatcher-P domain generated the highest furin-specific titers in the study, but even these groups included many mice with nondetectable responses. Although the IgG signals observed in individual mice grew to high levels in the experiments, these sera were not able to inhibit the processing of diphtheria toxin by recombinant furin *in vitro*. Inhibition of furin activity by purified P domain specific nanobodies has been reported (Zhu et al. 2012), but it is possible that the mouse serum samples also contain other PPCs, whose activity in the assay cannot be ruled out. Importantly, we showed that P domain vaccine candidates can generate antibody responses against endogenous furin, but the biological significance of these antibodies will need to be studied further in future experiments.

Vaccines against endogenous proteins activate the immune system to attack parts of the patient's own proteins, so they rightfully raise questions about the risk to cause autoimmune disease by vaccination. B cell (i.e., antibody) responses are regarded safer and more desirable when developing self-vaccines as compared to T cell responses (Toth et al. 2020). To evaluate T cell memory responses, we stimulated splenocytes extracted from PPC vaccinated mice with the vaccine components and measured the cytokines secreted by the cells. Here, we observed specific memory responses against noro-VLP, but not against any of the peptide-like antigens, indicating that the immune responses against PCSK9 at least were limited to antibody responses. In this *in vitro* recall assay, stimulation by SpyCatcher-P domain seemed to cause some unspecific cytokine secretion, but we observed no changes in cytokine levels in the serum of the mice with P domain antibody responses, or changes in the unstimulated splenocytes extracted from them. If the mice had a chronic inflammation due to autoimmune disease, we would have expected changes in the activation status and number of their immune cells (Collins et al. 2011). The mice also showed no apparent adverse effects or weight loss during the experiment that could be linked to their immunization, so we concluded that the generated immune responses were safe to the animals.

6.5 The immunogenicity of SpyCatcher

SpyCatcher is based on a protein found from a common human pathogen, the bacterium *Streptococcus pyogenes*. As such, it is not surprising that it would be immunogenic in mammals, but this has not been very thoroughly studied considering the number of papers in the field of immunology that utilize the

technology. Antibodies were formed against the SpyCatcher-fused AP205 bacteriophage platform, but significantly less after its conjugation with SpyTag-fused antigens (Brune et al. 2016). We did not note such blocking of SpyCatcher immunogenicity by its conjugation in our immunizations. Then again, Brune et al. did not study antibodies against SpyCatcher alone, but conjugated to the VLP, so their conclusion is the sum of VLP- and SpyCatcher-specific antibodies. According to our results, SpyCatcher is so immunogenic that fusion to it may be enough to transform even small peptide antigens into effective vaccines without any VLP presentation. Conversely, we detected very low SpyTag-specific immune responses (III). SpyCatcher is a very soluble, stable and *E. coli* expressible protein, and the yields of many antigens are increased when produced as SpyCatcher fusions (Thrane et al. 2016), so this option should be considered for antigens where VLP presentation seems to produce little benefit. However, cell-dependent responses were enhanced by presenting the SpyCatcher fusion on the noro-VLP (III). Modified versions of SpyCatcher resemble less the original bacterial protein, which can be seen in the lower reactivity of human sera to them (Rahikainen et al. 2021) and in reduced immunogenicity in mice (Liu et al. 2014).

7 CONCLUSIONS

During this PhD thesis project, we explored the properties of noro-VLP as an antigen carrier and as a vaccine platform. We engineered several iterations of modifiable noro-VLP that can be easily decorated with other proteins, including antigens, through use of SpyCatcher/SpyTag technology. The efficient production and purification methods developed during the project allow for easy and scalable expression of the noro-VLP vaccine platform and its use in testing novel SpyCatcher-fused antigens. Importantly for a vaccine platform, the SpyTagged noro-VLP retains most of the stability and storability found in native noroviruses and can be stored in a common refrigerator for months. SpyTagged noro-VLP also seems to retain its immunological properties, indicating that vaccines made with the platform would work as norovirus vaccines as a “side effect” of immunizing against the carried antigen.

To demonstrate its applicability to clinically relevant problem, we decorated the noro-VLP with universal influenza antigens M2e and HA2. Universal influenza antigens are designed to induce an immune reaction that would protect against multiple strains of influenza for a long period of time. HA2 here represents a trimeric, whole protein domain, while M2e is a small peptide. In mouse immunizations, the HA2 antigen raised high titers of IgG antibodies that specifically bound whole influenza HA and especially HA2 but were not neutralizing in an *in vitro* assay. Vaccine candidates based on the large influenza HA2 antigen were very effective even without conventional adjuvants, but with M2e, we obtained a response against the antigen only after combining the vaccine candidates with added alum adjuvant, Al(OH)₃. Even adjuvanted M2e peptide alone could form M2e-specific antibodies in mice with high enough doses, but by fusing M2e with SpyCatcher and then conjugating them on noro-VLP, the mice generated strong M2e-specific immune responses with 50-fold smaller protein doses. Both HA2 and M2e-based influenza vaccines seem promising by themselves, and their combination could potentially work as an efficient universal influenza vaccine. SpyCatcher-M2e worked as an effective influenza vaccine even without noro-VLP conjugation, but cellular responses seemed to be increased by noro-VLP. Another kind of adjuvant could still

be tried if cell responses are desired in the vaccine candidates, since $\text{Al}(\text{OH})_3$ is known to boost humoral responses over cellular responses.

Finally, we explored the capabilities of the noro-VLP in inducing immune responses against endogenous proprotein convertase proteins. The immune system is naturally tolerant to its own proteins, so to turn it to inhibit them in diseases where this is needed, one needs strong accompanying immune boosting signals. In these experiments, mice formed antibodies against two peptide-like fragments of their own protein, PCSK9. In this way, they functioned better with the noro-VLP than the previously tested M2e peptide. We were also able to raise antibodies against endogenous furin in mice, but the response levels were varied — some mice did not respond at all, some formed strong antibody responses against furin. Most importantly, even though we were able to form humoral immune responses against the endogenous proteins of mice, they showed no apparent adverse effects. This study proves that it is possible to generate antibody responses against endogenous furin, but in future studies, the biological impact of these novel anti-furin responses by vaccination should still be investigated.

8 REFERENCES

- Andersson, J., D. Q. Tran, M. Pesu, T. S. Davidson, H. Ramsey, J. J. O'Shea, and E. M. Shevach. 2008. "CD4+FoxP3+ Regulatory T Cells Confer Infectious Tolerance in a TGF- β -Dependent Manner." *Journal of Experimental Medicine* 205. doi: 10.1084/jem.20080308.
- Arrieta, A., T. F. Page, E. Veledar, and K. Nasir. 2017. "Economic Evaluation of PCSK9 Inhibitors in Reducing Cardiovascular Risk from Health System and Private Payer Perspectives." *PLoS ONE* 12. doi: 10.1371/journal.pone.0169761.
- Atmar, R. L., and M. K. Estes. 2006. "The Epidemiologic and Clinical Importance of Norovirus Infection." *Gastroenterology Clinics of North America* 35. doi: 10.1016/j.gtc.2006.03.001.
- Ausar, S. F., T. R. Foubert, M. H. Hudson, T. S. Vedvick, and C. R. Middaugh. 2006. "Conformational Stability and Disassembly of Norwalk Virus-like Particles. Effect of pH and Temperature." *The Journal of Biological Chemistry* 281. doi: 10.1074/jbc.M603313200.
- Bachmann, M. F., and G. T. Jennings. 2010. "Vaccine Delivery: A Matter of Size, Geometry, Kinetics and Molecular Patterns." *Nature Reviews Immunology* 10. doi: 10.1038/nri2868.
- Ball, J. P., M. J. Springer, Y. Ni, I. Finger-Baker, J. Martinez, J. Hahn, J. F. Suber, A. V. DiMarco, J. D. Talton, and R. R. Cobb. 2017. "Intranasal Delivery of a Bivalent Norovirus Vaccine Formulated in an in Situ Gelling Dry Powder." *PLoS ONE* 12. doi: 10.1371/journal.pone.0177310.
- Belizário, J. E., J. M. Neyra, and M. F. Setúbal Destro Rodrigues. 2018. "When and How NK Cell-Induced Programmed Cell Death Benefits Immunological Protection against Intracellular Pathogen Infection." *Innate Immunity* 24. doi: 10.1177/1753425918800200.
- Bertolotti-Ciarlet, A., S. E. Crawford, A. M. Hutson, and M. K. Estes. 2003. "The 3' End of Norwalk Virus mRNA Contains Determinants That Regulate the Expression and Stability of the Viral Capsid Protein VP1: A Novel Function for the VP2 Protein." *Journal of Virology* 77. doi: 10.1128/JVI.77.21.11603-11615.2003.
- Bommakanti, G., M. P. Citron, R. W. Hepler, C. Callahan, G. J. Heidecker, T. A. Najar, X. Lu, J. G. Joyce, J. W. Shiver, D. R. Casimiro, J. ter Meulen, X. Liang, and R. Varadarajan. 2010. "Design of an HA2-Based Escherichia Coli Expressed Influenza Immunogen That Protects Mice from Pathogenic Challenge." *Proceedings of the National Academy of Sciences of the United States of America* 107. doi: 10.1073/pnas.1007465107.

- Boonyakida, J., I. M. Khoris, F. Nasrin, and E. Y. Park. 2023. "Improvement of Modular Protein Display Efficiency in SpyTag-Implemented Norovirus-like Particles." *Biomacromolecules* 24. doi: 10.1021/acs.biomac.2c01150.
- Boonyakida, J., D. I. S. Utomo, F. N. Soma, and E. Y. Park. 2022. "Two-Step Purification of Tag-Free Norovirus-like Particles from Silkworm Larvae (*Bombyx Mori*)." *Protein Expression and Purification* 190. doi: 10.1016/j.pep.2021.106010.
- Bouvier, N. M., and P. Palese. 2008. "The Biology of Influenza Viruses." *Vaccine* 26. doi: 10.1016/j.vaccine.2008.07.039.
- Braun, E., and D. Sauter. 2019. "Furin-Mediated Protein Processing in Infectious Diseases and Cancer." *Clinical and Translational Immunology* 8. doi: 10.1002/cti2.1073.
- Bretscher, P., and M. Cohn. 1970. "A Theory of Self-Nonself Discrimination." *Science* 169. doi: 10.1126/science.169.3950.1042.
- Brewer, J. M., M. Conacher, A. Satoskar, H. Bluethmann, and J. Alexander. 1996. "In Interleukin-4-Deficient Mice, Alum Not Only Generates T Helper 1 Responses Equivalent to Freund's Complete Adjuvant, but Continues to Induce T Helper 2 Cytokine Production." *European Journal of Immunology* 26. doi: 10.1002/eji.1830260915.
- Brown, J. R., K. Gilmour, and J. Breuer. 2016. "Norovirus Infections Occur in B-Cell-Deficient Patients." *Clinical Infectious Diseases: An Official Publication of the Infectious Diseases Society of America* 62. doi: 10.1093/cid/ciw060.
- Brune, K. D., and M. Howarth. 2018. "New Routes and Opportunities for Modular Construction of Particulate Vaccines: Stick, Click, and Glue." *Frontiers in Immunology* 9. doi: 10.3389/fimmu.2018.01432.
- Brune, K. D., D. B. Leneghan, I. J. Brian, A. S. Ishizuka, M. F. Bachmann, S. J. Draper, S. Biswas, and M. Howarth. 2016. "Plug-and-Display: Decoration of Virus-Like Particles via Isopeptide Bonds for Modular Immunization." *Scientific Reports* 6. doi: 10.1038/srep19234.
- Buldun, C. M., J. X. Jean, M. R. Bedford, and M. Howarth. 2018. "SnoopLigase Catalyzes Peptide–Peptide Locking and Enables Solid-Phase Conjugate Isolation." *Journal of the American Chemical Society* 140. doi: 10.1021/jacs.7b13237.
- Carey, B., M. K. Staudt, D. Bonaminio, J. C. M. van der Loo, and B. C. Trapnell. 2007. "PU.1 Redirects Adenovirus to Lysosomes in Alveolar Macrophages, Uncoupling Internalization from Infection." *Journal of Immunology* 178. doi: 10.4049/jimmunol.178.4.2440.
- Casella, C. R., and T. C. Mitchell. 2008. "Putting Endotoxin to Work for Us: Monophosphoryl Lipid A as a Safe and Effective Vaccine Adjuvant." *Cellular and Molecular Life Sciences* 65. doi: 10.1007/s00018-008-8228-6.
- Chackerian, B., M. R. Durfee, and J. T. Schiller. 2008. "Virus-like Display of a Neo-Self Antigen Reverses B Cell Anergy in a B Cell Receptor Transgenic Mouse Model." *Journal of Immunology* 180. doi: 10.4049/jimmunol.180.9.5816.

- Chackerian, B., and K. M. Frieze. 2016. "Moving towards a New Class of Vaccines for Non-Infectious Chronic Diseases." *Expert Review of Vaccines* 15. doi: 10.1586/14760584.2016.1159136.
- Chen, B. J., G. P. Leser, D. Jackson, and R. A. Lamb. 2008. "The Influenza Virus M2 Protein Cytoplasmic Tail Interacts with the M1 Protein and Influences Virus Assembly at the Site of Virus Budding." *Journal of Virology* 82. doi: 10.1128/JVI.01184-08.
- Chen, C., Z. Nagy, E. Luning Prak, and M. Weigert. 1995a. "Immunoglobulin Heavy Chain Gene Replacement: A Mechanism of Receptor Editing." *Immunity* 3. doi: 10.1016/1074-7613(95)90064-0.
- Chen, J., S. A. Wharton, W. Weissenhorn, L. J. Calder, F. M. Hughson, J. J. Skehel, and D. C. Wiley. 1995b. "A Soluble Domain of the Membrane-Anchoring Chain of Influenza Virus Hemagglutinin (HA2) Folds in Escherichia Coli into the Low-pH-Induced Conformation." *Proceedings of the National Academy of Sciences of the United States of America* 92. doi: 10.1073/pnas.92.26.12205.
- Cheung, T. K., Y. Guan, S. S. Ng, H. Chen, C. H. Wong, J. S. Peiris, and L. L. Poon. 2005. "Generation of Recombinant Influenza A Virus without M2 Ion-Channel Protein by Introduction of a Point Mutation at the 5' End of the Viral Intron." *The Journal of General Virology* 86. doi: 10.1099/vir.0.80727-0.
- Chuan, Y. P., T. Rivera-Hernandez, N. Wibowo, N. K. Connors, Y. Wu, F. K. Hughes, L. H. L. Lua, and A. P. J. Middelberg. 2013. "Effects of Pre-Existing Anti-Carrier Immunity and Antigenic Element Multiplicity on Efficacy of a Modular Virus-like Particle Vaccine." *Biotechnology and Bioengineering* 110. doi: 10.1002/bit.24907.
- Ciampor, F., P. M. Bayley, M. V. Nermut, E. M. Hirst, R. J. Sugrue, and A. J. Hay. 1992. "Evidence That the Amantadine-Induced, M2-Mediated Conversion of Influenza A Virus Hemagglutinin to the Low pH Conformation Occurs in an Acidic Trans Golgi Compartment." *Virology* 188. doi: 10.1016/0042-6822(92)90730-d.
- Clifford Astbury, C., K. M. Lee, R. Mcleod, R. Aguiar, A. Atique, M. Balolong, J. Clarke, A. Demeshko, R. Labonté, A. Ruckert, P. Sibal, K. C. Togño, A. M. Viens, M. Wiktorowicz, M. K. Yambayamba, A. Yau, and T. L. Penney. 2023. "Policies to Prevent Zoonotic Spillover: A Systematic Scoping Review of Evaluative Evidence." *Globalization and Health* 19. doi: 10.1186/s12992-023-00986-x.
- Cohen, J., A. Pertsemlidis, I. K. Kotowski, R. Graham, C. K. Garcia, and H. H. Hobbs. 2005. "Low LDL Cholesterol in Individuals of African Descent Resulting from Frequent Nonsense Mutations in PCSK9." *Nature Genetics* 37. doi: 10.1038/ng1509.
- Collins, E. L., L. D. Jager, R. Dabelic, P. Benitez, K. Holdstein, K. Lau, M. I. Haider, H. M. Johnson, and J. Larkin III. 2011. "Inhibition of SOCS1-/- Lethal Autoinflammatory Disease Correlated to Enhanced Peripheral Foxp3+ Regulatory T Cell Homeostasis." *The Journal of Immunology* 187. doi: 10.4049/jimmunol.1003819.

- Corti, D., J. Voss, S. J. Gamblin, G. Codoni, A. Macagno, D. Jarrossay, S. G. Vachieri, D. Pinna, A. Minola, F. Vanzetta, C. Silacci, B. M. Fernandez-Rodriguez, G. Agatic, S. Bianchi, I. Giacchetto-Sasselli, L. Calder, F. Sallusto, P. Collins, L. F. Haire, N. Temperton, J. P. Langedijk, J. J. Skehel, and A. Lanzavecchia. 2011. "A Neutralizing Antibody Selected from Plasma Cells That Binds to Group 1 and Group 2 Influenza A Hemagglutinins." *Science* 333. doi: 10.1126/science.1205669.
- Cory, S., and J. M. Adams. 1980. "Deletions Are Associated with Somatic Rearrangement of Immunoglobulin Heavy Chain Genes." *Cell* 19. doi: 10.1016/0092-8674(80)90386-4.
- Costantini, V., E. K. Morantz, H. Browne, K. Ettayebi, X.-L. Zeng, R. L. Atmar, M. K. Estes, and J. Vinjé. 2018. "Human Norovirus Replication in Human Intestinal Enteroids as Model to Evaluate Virus Inactivation." *Emerging Infectious Diseases* 24. doi: 10.3201/eid2408.180126.
- Couceiro, J. N., J. C. Paulson, and L. G. Baum. 1993. "Influenza Virus Strains Selectively Recognize Sialyloligosaccharides on Human Respiratory Epithelium; the Role of the Host Cell in Selection of Hemagglutinin Receptor Specificity." *Virus Research* 29. doi: 10.1016/0168-1702(93)90056-s.
- Crossey, E., M. J. A. Amar, M. Sampson, J. Peabody, J. T. Schiller, B. Chackerian, and A. T. Remaley. 2015. "A Cholesterol-Lowering VLP Vaccine That Targets PCSK9." *Vaccine* 33. doi: 10.1016/j.vaccine.2015.09.044.
- Deng, L., K. J. Cho, W. Fiers, and X. Saelens. 2015. "M2e-Based Universal Influenza A Vaccines." *Vaccines* 3. doi: 10.3390/vaccines3010105.
- Desdouts, M., D. Polo, C. Le Menec, S. Strubbia, X.-L. Zeng, K. Ettayebi, R. L. Atmar, M. K. Estes, and F. S. Le Guyader. 2022. "Use of Human Intestinal Enteroids to Evaluate Persistence of Infectious Human Norovirus in Seawater." *Emerging Infectious Diseases* 28. doi: 10.3201/eid2807.220219.
- Devant, J. M., and G. S. Hansman. 2021. "Structural Heterogeneity of a Human Norovirus Vaccine Candidate." *Virology* 553. doi: 10.1016/j.virol.2020.10.005.
- Devant, J. M., G. Hofhaus, D. Bhella, and G. S. Hansman. 2019. "Heterologous Expression of Human Norovirus GII.4 VP1 Leads to Assembly of T=4 Virus-like Particles." *Antiviral Research* 168. doi: 10.1016/j.antiviral.2019.05.010.
- Didierlaurent, A. M., S. Morel, L. Lockman, S. L. Giannini, M. Bisteau, H. Carlsen, A. Kielland, O. Vosters, N. Vanderheyde, F. Schiavetti, D. Larocque, M. Van Mechelen, and N. Garçon. 2009. "AS04, an Aluminum Salt- and TLR4 Agonist-Based Adjuvant System, Induces a Transient Localized Innate Immune Response Leading to Enhanced Adaptive Immunity." *Journal of Immunology* 183. doi: 10.4049/jimmunol.0901474.
- Dintzis, R. Z., M. H. Middleton, and H. M. Dintzis. 1983. "Studies on the Immunogenicity and Tolerogenicity of T-Independent Antigens." *Journal of Immunology* 131. doi: 10.4049/jimmunol.131.5.2196.
- Dintzis, R. Z., M. Okajima, M. H. Middleton, G. Greene, and H. M. Dintzis. 1989. "The Immunogenicity of Soluble Haptenated Polymers Is Determined by Molecular Mass and Hapten Valence." *Journal of Immunology* 143. doi: 10.4049/jimmunol.143.4.1239.

- Donaldson, E. F., L. C. Lindesmith, A. D. LoBue, and R. S. Baric. 2010. "Viral Shape-Shifting: Norovirus Evasion of the Human Immune System." *Nature Reviews Microbiology* 8. doi: 10.1038/nrmicro2296.
- Dranoff, G. 2004. "Cytokines in Cancer Pathogenesis and Cancer Therapy." *Nature Reviews Cancer* 4. doi: 10.1038/nrc1252.
- Draper, S. J., and J. L. Heeney. 2010. "Viruses as Vaccine Vectors for Infectious Diseases and Cancer." *Nature Reviews Microbiology* 8. doi: 10.1038/nrmicro2240.
- Ebrahimi, S. M., and M. Tebianian. 2011. "Influenza A Viruses: Why Focusing on M2e-Based Universal Vaccines." *Virus Genes* 42. doi: 10.1007/s11262-010-0547-7.
- Essalmani, R., J. Jain, D. Susan-Resiga, U. Andréo, A. Evagelidis, R. M. Derbali, D. N. Huynh, F. Dallaire, M. Laporte, A. Delpal, P. Sutto-Ortiz, B. Coutard, C. Mapa, K. Wilcoxon, E. Decroly, T. Nq Pham, É. A. Cohen, and N. G. Seidah. 2022. "Distinctive Roles of Furin and TMPRSS2 in SARS-CoV-2 Infectivity." *Journal of Virology* 96. doi: 10.1128/jvi.00128-22.
- Ettayebi, K., S. E. Crawford, K. Murakami, J. R. Broughman, U. Karandikar, V. R. Tenge, F. H. Neill, S. E. Blutt, X. L. Zeng, L. Qu, B. Kou, A. R. Opekun, D. Burrin, D. Y. Graham, S. Ramani, R. L. Atmar, and M. K. Estes. 2016. "Replication of Human Noroviruses in Stem Cell-Derived Human Enteroids." *Science* 353. doi: 10.1126/science.aaf5211.
- Fierer, J. O., G. Veggiani, and M. Howarth. 2014. "SpyLigase Peptide-Peptide Ligation Polymerizes Affibodies to Enhance Magnetic Cancer Cell Capture." *Proceedings of the National Academy of Sciences of the United States of America* 111. doi: 10.1073/pnas.1315776111.
- Fowler, A., K. K. A. Van Rompay, M. Sampson, J. Leo, J. K. Watanabe, J. L. Usachenko, R. Immareddy, D. M. Lovato, J. T. Schiller, A. T. Remaley, and B. Chackerian. 2023. "A Virus-like Particle-Based Bivalent PCSK9 Vaccine Lowers LDL-Cholesterol Levels in Non-Human Primates." *Npj Vaccines* 8. doi: 10.1038/s41541-023-00743-6.
- Frey, A., J. Di Canzio, and D. Zurakowski. 1998. "A Statistically Defined Endpoint Titer Determination Method for Immunoassays." *Journal of Immunological Methods* 221. doi: 10.1016/s0022-1759(98)00170-7.
- Fulcher, D. A., and A. Basten. 1994. "Reduced Life Span of Anergic Self-Reactive B Cells in a Double-Transgenic Model." *Journal of Experimental Medicine* 179. doi: 10.1084/jem.179.1.125.
- Furuta, M., H. Yano, A. Zhou, Y. Rouillé, J. J. Holst, R. Carroll, M. Ravazzola, L. Orci, H. Furuta, and D. F. Steiner. 1997. "Defective Prohormone Processing and Altered Pancreatic Islet Morphology in Mice Lacking Active SPC2." *Proceedings of the National Academy of Sciences* 94. doi: 10.1073/PNAS.94.13.6646.
- Glass, P. J., L. J. White, J. M. Ball, I. Leparc-Goffart, M. E. Hardy, and M. K. Estes. 2000. "Norwalk Virus Open Reading Frame 3 Encodes a Minor Structural Protein." *Journal of Virology* 74. doi: 10.1128/jvi.74.14.6581-6591.2000.

- González-Rodríguez, M. I., N. Nurminen, L. Kummola, O. H. Laitinen, S. Oikarinen, A. Parajuli, T. Salomaa, I. Mäkelä, M. I. Roslund, A. Sinkkonen, H. Hyöty, I. S. Junntila, and ADELE Research Group. 2022. "Effect of Inactivated Nature-Derived Microbial Composition on Mouse Immune System." *Immunity, Inflammation and Disease* 10. doi: 10.1002/iid3.579.
- Guex, N., and M. C. Peitsch. 1997. "SWISS-MODEL and the Swiss-PdbViewer: An Environment for Comparative Protein Modeling." *Electrophoresis* 18. doi: 10.1002/elps.1150181505.
- Hannoun, C. 2013. "The Evolving History of Influenza Viruses and Influenza Vaccines." *Expert Review of Vaccines* 12. doi: 10.1586/14760584.2013.824709.
- Hashemi, H., S. Pouyanfard, M. Bandehpour, Z. Noroozbabaei, B. Kazemi, X. Saelens, and T. Mokhtari-Azad. 2012. "Immunization with M2e-Displaying T7 Bacteriophage Nanoparticles Protects against Influenza A Virus Challenge." *PLoS ONE* 7. doi: 10.1371/journal.pone.0045765.
- Hodgkin, P. D., W. R. Heath, and A. G. Baxter. 2007. "The Clonal Selection Theory: 50 Years since the Revolution." *Nature Immunology* 8. doi: 10.1038/ni1007-1019.
- Hong, M., P. S. Lee, R. M. B. Hoffman, X. Zhu, J. C. Krause, N. S. Laursen, S. Yoon, L. Song, L. Tussey, J. E. Crowe, A. B. Ward, and I. A. Wilson. 2013. "Antibody Recognition of the Pandemic H1N1 Influenza Virus Hemagglutinin Receptor Binding Site." *Journal of Virology* 87. doi: 10.1128/jvi.01388-13.
- Hozumi, N., and S. Tonegawa. 1976. "Evidence for Somatic Rearrangement of Immunoglobulin Genes Coding for Variable and Constant Regions." *Proceedings of the National Academy of Sciences of the United States of America* 73. doi: 10.1073/pnas.73.10.3628.
- Huhti, L., V. Blazevic, K. Nurminen, T. Koho, V. P. Hytönen, and T. Vesikari. 2010. "A Comparison of Methods for Purification and Concentration of Norovirus GII-4 Capsid Virus-like Particles." *Archives of Virology* 155. doi: 10.1007/s00705-010-0768-z.
- Hutchings, M. I., A. W. Truman, and B. Wilkinson. 2019. "Antibiotics: Past, Present and Future." *Current Opinion in Microbiology* 51. doi: 10.1016/j.mib.2019.10.008.
- Ikonen, E. 2008. "Cellular Cholesterol Trafficking and Compartmentalization." *Nature Reviews Molecular Cell Biology* 9. doi: 10.1038/nrm2336.
- Janeway, C. A., and R. Medzhitov. 2002. "Innate Immune Recognition." *Annual Review of Immunology* 20. doi: 10.1146/annurev.immunol.20.083001.084359.
- Jaron, M., M. Lehky, M. Zarà, C. N. Zaydowicz, A. Lak, R. Ballmann, P. A. Heine, E. V. Wenzel, K.-T. Schneider, F. Bertoglio, S. Kempter, R. W. Köster, S. S. Barbieri, J. van den Heuvel, M. Hust, S. Dübel, and M. Schubert. 2022. "Baculovirus-Free SARS-CoV-2 Virus-like Particle Production in Insect Cells for Rapid Neutralization Assessment." *Viruses* 14. doi: 10.3390/v14102087.

- Jegerlehner, A., M. Wiesel, K. Dietmeier, F. Zabel, D. Gatto, P. Saudan, and M. F. Bachmann. 2010. "Carrier Induced Epitopic Suppression of Antibody Responses Induced by Virus-like Particles Is a Dynamic Phenomenon Caused by Carrier-Specific Antibodies." *Vaccine* 28. doi: 10.1016/j.vaccine.2010.02.103.
- Jiang, L., R. Fan, S. Sun, P. Fan, W. Su, Y. Zhou, F. Gao, F. Xu, W. Kong, and C. Jiang. 2015. "A New EV71 VP3 Epitope in Norovirus P Particle Vector Displays Neutralizing Activity and Protection in Vivo in Mice." *Vaccine* 33. doi: 10.1016/j.vaccine.2015.10.104.
- Jones, M. K., M. Watanabe, S. Zhu, C. L. Graves, L. R. Keyes, K. R. Grau, M. B. Gonzalez-Hernandez, N. M. Iovine, C. E. Wobus, J. Vinjé, S. A. Tibbetts, S. M. Wallet, and S. M. Karst. 2014. "Enteric Bacteria Promote Human and Mouse Norovirus Infection of B Cells." *Science* 346. doi: 10.1126/science.1257147.
- Jung, J., T. Grant, D. R. Thomas, C. W. Diehnelt, N. Grigorieff, and L. Joshua-Tor. 2019. "High-Resolution Cryo-EM Structures of Outbreak Strain Human Norovirus Shells Reveal Size Variations." *Proceedings of the National Academy of Sciences* 116. doi: 10.1073/pnas.1903562116.
- Kaddoura, R., B. Orabi, and A. M. Salam. 2020. "Efficacy and Safety of PCSK9 Monoclonal Antibodies: An Evidence-Based Review and Update." *Journal of Drug Assessment* 9. doi: 10.1080/21556660.2020.1801452.
- Kapikian, A. Z., R. G. Wyatt, R. Dolin, T. S. Thornhill, A. R. Kalica, and R. M. Chanock. 1972. "Visualization by Immune Electron Microscopy of a 27-Nm Particle Associated with Acute Infectious Nonbacterial Gastroenteritis." *Journal of Virology* 10. doi: 10.1128/JVI.10.5.1075-1081.1972.
- Karlsson Hedestam, G. B., R. A. M. Fouchier, S. Phogat, D. R. Burton, J. Sodroski, and R. T. Wyatt. 2008. "The Challenges of Eliciting Neutralizing Antibodies to HIV-1 and to Influenza Virus." *Nature Reviews Microbiology* 6. doi: 10.1038/nrmicro1819.
- Keeble, A. H., A. Banerjee, M. P. Ferla, S. C. Reddington, I. N. A. K. Anuar, and M. Howarth. 2017. "Evolving Accelerated Amidation by SpyTag/SpyCatcher to Analyze Membrane Dynamics." *Angewandte Chemie* 56. doi: 10.1002/anie.201707623.
- Keeble, A. H., P. Turkki, S. Stokes, I. N. A. Khairil Anuar, R. Rahikainen, V. P. Hytönen, and M. Howarth. 2019. "Approaching Infinite Affinity through Engineering of Peptide-Protein Interaction." *Proceedings of the National Academy of Sciences* 116.
- Kimble, B., G. R. Nieto, and D. R. Perez. 2010. "Characterization of Influenza Virus Sialic Acid Receptors in Minor Poultry Species." *Virology Journal* 7. doi: 10.1186/1743-422X-7-365.
- Klimpel, K. R., S. S. Molloy, G. Thomas, and S. H. Leppla. 1992. "Anthrax Toxin Protective Antigen Is Activated by a Cell Surface Protease with the Sequence Specificity and Catalytic Properties of Furin." *Proceedings of the National Academy of Sciences of the United States of America* 89. doi: 10.1073/pnas.89.21.10277.
- Knezevic, I., G. Stacey, and J. Petricciani. 2008. "WHO Study Group on Cell Substrates for Production of Biologicals, Geneva, Switzerland, 11–12 June 2007." *Biologicals* 36. doi: 10.1016/j.biologicals.2007.11.005.

- Koho, T., T. O. Ihalainen, M. Stark, H. Uusi-Kerttula, R. Wieneke, R. Rahikainen, V. Blazevic, V. Marjomaki, R. Tampe, M. S. Kulomaa, and V. P. Hytonen. 2015. "His-Tagged Norovirus-like Particles: A Versatile Platform for Cellular Delivery and Surface Display." *European Journal of Pharmaceutics and Biopharmaceutics* 96. doi: 10.1016/j.ejpb.2015.07.002.
- Koho, T., T. Mantyla, P. Laurinmaki, L. Huhti, S. J. Butcher, T. Vesikari, M. S. Kulomaa, and V. P. Hytonen. 2012. "Purification of Norovirus-like Particles (VLPs) by Ion Exchange Chromatography." *Journal of Virological Methods* 181. doi: 10.1016/j.jviromet.2012.01.003.
- Kopf, M., M. F. Bachmann, and B. J. Marsland. 2010. "Averting Inflammation by Targeting the Cytokine Environment." *Nature Reviews Drug Discovery* 9. doi: 10.1038/nrd2805.
- Korn, J., D. Schäckermann, T. Kirmann, F. Bertoglio, S. Steinke, J. Heisig, M. Ruschig, G. Rojas, N. Langreder, E. V. Wenzel, K. D. R. Roth, M. Becker, D. Meier, J. van den Heuvel, M. Hust, S. Dübel, and M. Schubert. 2020. "Baculovirus-Free Insect Cell Expression System for High Yield Antibody and Antigen Production." *Scientific Reports* 10. doi: 10.1038/s41598-020-78425-9.
- Kotowski, I. K., A. Pertsemliadis, A. Luke, R. S. Cooper, G. L. Vega, J. C. Cohen, and H. H. Hobbs. 2006. "A Spectrum of PCSK9 Alleles Contributes to Plasma Levels of Low-Density Lipoprotein Cholesterol." *American Journal of Human Genetics* 78. doi: 10.1086/500615.
- Krammer, F. 2019. "The Human Antibody Response to Influenza A Virus Infection and Vaccination." *Nature Reviews Immunology* 19. doi: 10.1038/s41577-019-0143-6.
- Kumlin, U., S. Olofsson, K. Dimock, and N. Arnberg. 2008. "Sialic Acid Tissue Distribution and Influenza Virus Tropism." *Influenza and Other Respiratory Viruses* 2. doi: 10.1111/j.1750-2659.2008.00051.x.
- Lee, Y. T., E. J. Ko, Y. Lee, K. H. Kim, M. C. Kim, Y. N. Lee, and S. M. Kang. 2018. "Intranasal Vaccination with M2e5x Virus-like Particles Induces Humoral and Cellular Immune Responses Conferring Cross-Protection against Heterosubtypic Influenza Viruses." *PLoS ONE* 13. doi: 10.1371/journal.pone.0190868.
- Leiding, T., J. Wang, J. Martinsson, W. F. DeGrado, and S. P. Årsköld. 2010. "Proton and Cation Transport Activity of the M2 Proton Channel from Influenza A Virus." *Proceedings of the National Academy of Sciences of the United States of America* 107. doi: 10.1073/pnas.1009997107.
- Leren, T. P. 2004. "Mutations in the PCSK9 Gene in Norwegian Subjects with Autosomal Dominant Hypercholesterolemia." *Clinical Genetics* 65. doi: 10.1111/j.0009-9163.2004.0238.x.
- Li, L., J. O. Fierer, T. A. Rapoport, and M. Howarth. 2014. "Structural Analysis and Optimization of the Covalent Association between SpyCatcher and a Peptide Tag." *Journal of Molecular Biology* 426. doi: 10.1016/j.jmb.2013.10.021.
- Li, Z., Y. Zhao, Y. Li, and X. Chen. 2021. "Adjuvantation of Influenza Vaccines to Induce Cross-Protective Immunity." *Vaccines* 9. doi: 10.3390/vaccines9020075.

- Lin, Y., L. Fengling, W. Lianzhu, Z. Yuxiu, and J. Yanhua. 2014. "Function of VP2 Protein in the Stability of the Secondary Structure of Virus-like Particles of Genogroup II Norovirus at Different pH Levels: Function of VP2 Protein in the Stability of NoV VLPs." *Journal of Microbiology* 52. doi: 10.1007/s12275-014-4323-6.
- Lindesmith, L. C., E. F. Donaldson, and R. S. Baric. 2011. "Norovirus GII.4 Strain Antigenic Variation." *Journal of Virology* 85. doi: 10.1128/JVI.01364-10.
- Lirussi, D., S. F. Weissmann, T. Ebensen, U. Nitsche-Gloy, H. B. G. Franz, and C. A. Guzmán. 2021. "Cyclic Di-Adenosine Monophosphate: A Promising Adjuvant Candidate for the Development of Neonatal Vaccines." *Pharmaceutics* 13. doi: 10.3390/pharmaceutics13020188.
- Liu, C., J. X. Chin, and D.-Y. Lee. 2015. "SynLinker: An Integrated System for Designing Linkers and Synthetic Fusion Proteins." *Bioinformatics* 31. doi: 10.1093/bioinformatics/btv447.
- Liu, Z., H. Zhou, W. Wang, W. Tan, Y.-X. Fu, and M. Zhu. 2014. "A Novel Method for Synthetic Vaccine Construction Based on Protein Assembly." *Scientific Reports* 4. doi: 10.1038/srep07266.
- LoBue, A. D., L. Lindesmith, B. Yount, P. R. Harrington, J. M. Thompson, R. E. Johnston, C. L. Moe, and R. S. Baric. 2006. "Multivalent Norovirus Vaccines Induce Strong Mucosal and Systemic Blocking Antibodies against Multiple Strains." *Vaccine* 24. doi: 10.1016/j.vaccine.2006.03.080.
- Lu, L. L., T. J. Suscovich, S. M. Fortune, and G. Alter. 2018. "Beyond Binding: Antibody Effector Functions in Infectious Diseases." *Nature Reviews Immunology* 18. doi: 10.1038/nri.2017.106.
- Makidon, P. E., A. U. Bielinska, S. S. Nigavekar, K. W. Janczak, J. Knowlton, A. J. Scott, N. Mank, Z. Cao, S. Rathinavelu, M. R. Beer, J. E. Wilkinson, L. P. Blanco, J. J. Landers, and J. R. Baker. 2008. "Pre-Clinical Evaluation of a Novel Nanoemulsion-Based Hepatitis B Mucosal Vaccine." *PLoS ONE* 3. doi: 10.1371/journal.pone.0002954.
- Mallajosyula, V. V., M. Citron, F. Ferrara, X. Lu, C. Callahan, G. J. Heidecker, S. P. Sarma, J. A. Flynn, N. J. Temperton, X. Liang, and R. Varadarajan. 2014. "Influenza Hemagglutinin Stem-Fragment Immunogen Elicits Broadly Neutralizing Antibodies and Confers Heterologous Protection." *Proceedings of the National Academy of Sciences of the United States of America* 111. doi: 10.1073/pnas.1402766111.
- Marini, A., Y. Zhou, Y. Li, I. J. Taylor, D. B. Leneghan, J. Jin, M. Zaric, D. Mekhaieel, C. A. Long, K. Miura, and S. Biswas. 2019. "A Universal Plug-and-Display Vaccine Carrier Based on HBsAg VLP to Maximize Effective Antibody Response." *Frontiers in Immunology* 10. doi: 10.3389/fimmu.2019.02931.
- Martin, K., and A. Helenius. 1991. "Nuclear Transport of Influenza Virus Ribonucleoproteins: The Viral Matrix Protein (M1) Promotes Export and Inhibits Import." *Cell* 67. doi: 10.1016/0092-8674(91)90576-k.

- Mason, H. S., J. M. Ball, J. J. Shi, X. Jiang, M. K. Estes, and C. J. Arntzen. 1996. "Expression of Norwalk Virus Capsid Protein in Transgenic Tobacco and Potato and Its Oral Immunogenicity in Mice." *Proceedings of the National Academy of Sciences* 93. doi: 10.1073/pnas.93.11.5335.
- Masuda, A., J. Man Lee, T. Miyata, S. Sato, A. Masuda, M. Taniguchi, R. Fujita, H. Ushijima, K. Morimoto, T. Ebihara, M. Hino, K. Kakino, H. Mon, and T. Kusakabe. 2023. "High Yield Production of Norovirus GII.4 Virus-like Particles Using Silkworm Pupae and Evaluation of Their Protective Immunogenicity." *Vaccine* 41. doi: 10.1016/j.vaccine.2022.12.015.
- Mohanan, D., B. Slütter, M. Henriksen-Lacey, W. Jiskoot, J. A. Bouwstra, Y. Perrie, T. M. Kündig, B. Gander, and P. Johansen. 2010. "Administration Routes Affect the Quality of Immune Responses: A Cross-Sectional Evaluation of Particulate Antigen-Delivery Systems." *Journal of Controlled Release* 147. doi: 10.1016/j.jconrel.2010.08.012.
- Mohsen, M. O., and M. F. Bachmann. 2022. "Virus-like Particle Vaccinology, from Bench to Bedside." *Cellular & Molecular Immunology* 19. doi: 10.1038/s41423-022-00897-8.
- Niesen, F. H., H. Berglund, and M. Vedadi. 2007. "The Use of Differential Scanning Fluorimetry to Detect Ligand Interactions That Promote Protein Stability." *Nature Protocols* 2. doi: 10.1038/nprot.2007.321.
- Odegard, V. H., and D. G. Schatz. 2006. "Targeting of Somatic Hypermutation." *Nature Reviews Immunology* 6. doi: 10.1038/nri1896.
- Palladini, A., S. Thrane, C. M. Janitzek, J. Pihl, S. B. Clemmensen, W. A. de Jongh, T. M. Clausen, G. Nicoletti, L. Landuzzi, M. L. Penichet, T. Balboni, M. L. Ianzano, V. Giusti, T. G. Theander, M. A. Nielsen, A. Salanti, P.-L. Lollini, P. Nanni, and A. F. Sander. 2018. "Virus-like Particle Display of HER2 Induces Potent Anti-Cancer Responses." *OncoImmunology* 7. doi: 10.1080/2162402X.2017.1408749.
- Prasad, B. V. V., M. E. Hardy, T. Dokland, J. Bella, M. G. Rossmann, and M. K. Estes. 1999. "X-Ray Crystallographic Structure of the Norwalk Virus Capsid." *Science* 286. doi: 10.1126/science.286.5438.287.
- Qin, G., K. Yu, T. Shi, C. Luo, G. Li, W. Zhu, and H. Jiang. 2010. "How Does Influenza Virus a Escape from Amantadine?" *The Journal of Physical Chemistry.B* 114. doi: 10.1021/jp911588y.
- Quan, F. S., Y. T. Lee, K. H. Kim, M. C. Kim, and S. M. Kang. 2016. "Progress in Developing Virus-like Particle Influenza Vaccines." *Expert Review of Vaccines* 15. doi: 10.1080/14760584.2016.1175942.
- Rahikainen, R., P. Rijal, T. K. Tan, H.-J. Wu, A.-M. C. Andersson, J. R. Barrett, T. A. Bowden, S. J. Draper, A. R. Townsend, and M. Howarth. 2021. "Overcoming Symmetry Mismatch in Vaccine Nanoassembly through Spontaneous Amidation." *Angewandte Chemie* 133. doi: 10.1002/ange.202009663.
- Rahikainen, R., S. K. Vester, P. Turkki, C. P. Janosko, A. Deiters, V. P. Hytönen, and M. Howarth. 2023. "Visible Light-Induced Specific Protein Reaction Delineates Early Stages of Cell Adhesion." *Journal of the American Chemical Society* 145. doi: 10.1021/jacs.3c07827.

- Renjifo, X., S. Wolf, P.-P. Pastoret, H. Bazin, J. Urbain, O. Leo, and M. Moser. 1998. "Carrier-Induced, Hapten-Specific Suppression: A Problem of Antigen Presentation?" *The Journal of Immunology* 161. doi: 10.4049/jimmunol.161.2.702.
- Rocconi, R. P., S. A. Ghamande, M. A. Barve, E. E. Stevens, P. Aaron, L. Stanbery, E. Bognar, L. Manning, J. J. Nemunaitis, D. M. O'Malley, T. J. Herzog, B. J. Monk, and R. L. Coleman. 2021. "Maintenance Vigil Immunotherapy in Newly Diagnosed Advanced Ovarian Cancer: Efficacy Assessment of Homologous Recombination Proficient (HRP) Patients in the Phase IIb VITAL Trial." *Journal of Clinical Oncology* 39. doi: 10.1200/JCO.2021.39.15_suppl.5502.
- Roebroek, A. J., L. Umans, I. G. Pauli, E. J. Robertson, F. van Leuven, W. J. Van de Ven, and D. B. Constam. 1998. "Failure of Ventral Closure and Axial Rotation in Embryos Lacking the Proprotein Convertase Furin." *Development* 125. doi: 10.1242/dev.125.24.4863.
- Rossmann, J. S., and R. A. Lamb. 2011. "Influenza Virus Assembly and Budding." *Virology* 411. doi: 10.1016/j.virol.2010.12.003.
- Ruskowitz, E. R., B. G. Munoz-Robles, A. C. Strange, C. H. Butcher, S. Kurniawan, J. R. Filteau, and C. A. DeForest. 2023. "Spatiotemporal Functional Assembly of Split Protein Pairs through a Light-Activated SpyLigation." *Nature Chemistry* 15. doi: 10.1038/s41557-023-01152-x.
- Ruvoën-Clouet, N., G. Belliot, and J. Le Pendu. 2013. "Noroviruses and Histo-Blood Groups: The Impact of Common Host Genetic Polymorphisms on Virus Transmission and Evolution." *Reviews in Medical Virology* 23. doi: 10.1002/rmv.1757.
- Sahin, U., K. Karikó, and Ö. Türeci. 2014. "mRNA-Based Therapeutics — Developing a New Class of Drugs." *Nature Reviews Drug Discovery* 13. doi: 10.1038/nrd4278.
- Sanchez-Trincado, J. L., M. Gomez-Perosanz, and P. A. Reche. 2017. "Fundamentals and Methods for T- and B-Cell Epitope Prediction." *Journal of Immunology Research* 2017. doi: 10.1155/2017/2680160.
- Sarac, M. S., J. R. Peinado, S. H. Leppla, and I. Lindberg. 2004. "Protection against Anthrax Toxemia by Hexa-d-Arginine In Vitro and In Vivo." *Infection and Immunity* 72. doi: 10.1128/IAI.72.1.602-605.2004.
- Sato, S., N. Matsumoto, K. Hisaie, and S. Uematsu. 2020. "Alcohol Abrogates Human Norovirus Infectivity in a pH-Dependent Manner." *Scientific Reports* 10. doi: 10.1038/s41598-020-72609-z.
- Saxena, M., P. J. Coloe, and P. M. Smooker. 2009. "Influence of Promoter, Gene Copy Number, and Preexisting Immunity on Humoral and Cellular Responses to a Vected Antigen Delivered by a Salmonella Enterica Vaccine." *Clinical and Vaccine Immunology* 16. doi: 10.1128/CVI.00253-08.
- Saxena, M., T. T. H. Van, F. J. Baird, P. J. Coloe, and P. M. Smooker. 2013. "Pre-Existing Immunity against Vaccine Vectors – Friend or Foe?" *Microbiology* 159. doi: 10.1099/mic.0.049601-0.

- Scamuffa, N., G. Siegfried, Y. Bontemps, L. Ma, A. Basak, G. Cherel, F. Calvo, N. G. Seidah, and A.-M. Khatib. 2008. "Selective Inhibition of Proprotein Convertases Represses the Metastatic Potential of Human Colorectal Tumor Cells." *The Journal of Clinical Investigation* 118. doi: 10.1172/JCI32040.
- Schindelin, J., I. Arganda-Carreras, E. Frise, V. Kaynig, M. Longair, T. Pietzsch, S. Preibisch, C. Rueden, S. Saalfeld, B. Schmid, J.-Y. Tinevez, D. J. White, V. Hartenstein, K. Eliceiri, P. Tomancak, and A. Cardona. 2012. "Fiji: An Open-Source Platform for Biological-Image Analysis." *Nature Methods* 9. doi: 10.1038/nmeth.2019.
- Schlapschy, M., U. Binder, C. Börger, I. Theobald, K. Wachinger, S. Kisling, D. Haller, and A. Skerra. 2013. "PASylation: A Biological Alternative to PEGylation for Extending the Plasma Half-Life of Pharmaceutically Active Proteins." *Protein Engineering, Design and Selection* 26. doi: 10.1093/protein/gzt023.
- Schrödinger, L., and W. DeLano. 2020. "PyMOL." Retrieved (<http://www.pymol.org/pymol>).
- Seidah, N. G., and A. Prat. 2012. "The Biology and Therapeutic Targeting of the Proprotein Convertases." *Nature Reviews. Drug Discovery* 11. doi: 10.1038/nrd3699.
- Shakya, M., and I. Lindberg. 2021. "Mouse Models of Human Proprotein Convertase Insufficiency." *Endocrine Reviews* 42. doi: 10.1210/ENDREV/BNAA033.
- Sharif, N., S. Ahmed, M. N. Sharif, K. Alzahrani, M. Alsuwat, F. Alzahrani, S. Khandakar, N. Monifa, s Okitsu, Md. A. K. Parvez, H. Ushijima, and Dr. S. Dey. 2023. "High Prevalence of Norovirus GII.4 Sydney among Children with Acute Gastroenteritis in Bangladesh, 2018 to 2021." *Journal of Infection and Public Health*. doi: 10.1016/j.jiph.2023.05.002.
- Sheng, J., S. Lei, L. Yuan, and X. Feng. 2017. "Cell-Free Protein Synthesis of Norovirus Virus-like Particles." *RSC Advances* 7. doi: 10.1039/C7RA03742B.
- Shiryaev, S. A., A. G. Remacle, B. I. Ratnikov, N. A. Nelson, A. Y. Savinov, G. Wei, M. Bottini, M. F. Rega, A. Parent, R. Desjardins, M. Fugere, R. Day, M. Sabet, M. Pellicchia, R. C. Liddington, J. W. Smith, T. Mustelin, D. G. Guiney, M. Lebl, and A. Y. Strongin. 2007. "Targeting Host Cell Furin Proprotein Convertases as a Therapeutic Strategy against Bacterial Toxins and Viral Pathogens." *The Journal of Biological Chemistry* 282. doi: 10.1074/jbc.M703847200.
- Shoemaker, G. K., E. Van Duijn, S. E. Crawford, C. Utrecht, M. Baclayon, W. H. Roos, G. J. L. Wuite, M. K. Estes, B. V. V. Prasad, and A. J. R. Heck. 2010. "Norwalk Virus Assembly and Stability Monitored by Mass Spectrometry." *Molecular & Cellular Proteomics* 9. doi: 10.1074/mcp.M900620-MCP200.
- Siegfried, G., J. Descarpentrie, S. Evrard, and A. M. Khatib. 2020. "Proprotein Convertases: Key Players in Inflammation-Related Malignancies and Metastasis." *Cancer Letters* 473. doi: 10.1016/J.CANLET.2019.12.027.
- Slamon, D. J., G. M. Clark, S. G. Wong, W. J. Levin, A. Ullrich, and W. L. McGuire. 1987. "Human Breast Cancer: Correlation of Relapse and Survival with Amplification of the HER-2/Neu Oncogene." *Science* 235. doi: 10.1126/science.3798106.

- Stieneke-Gröber, A., M. Vey, H. Angliker, E. Shaw, G. Thomas, C. Roberts, H. D. Klenk, and W. Garten. 1992. "Influenza Virus Hemagglutinin with Multibasic Cleavage Site Is Activated by Furin, a Subtilisin-like Endoprotease." *The EMBO Journal* 11. doi: 10.1002/j.1460-2075.1992.tb05305.x.
- Sutton, T. C., S. Chakraborty, V. V. A. Mallajosyula, E. W. Lamirande, K. Ganti, K. W. Bock, I. N. Moore, R. Varadarajan, and K. Subbarao. 2017. "Protective Efficacy of Influenza Group 2 Hemagglutinin Stem-Fragment Immunogen Vaccines." *NPJ Vaccines* 2. doi: 10.1038/s41541-017-0036-2.
- Syed, Y. Y. 2022. "RTS,S/AS01 Malaria Vaccine (Mosquirix®): A Profile of Its Use." *Drugs & Therapy Perspectives* 38. doi: 10.1007/s40267-022-00937-3.
- Szewczyk, B., K. Bienkowska-Szewczyk, and E. Krol. 2014. "Introduction to Molecular Biology of Influenza a Viruses." *Acta Biochimica Polonica* 61. doi: 10.18388/abp.2014_1857.
- Tan, M., P. Huang, M. Xia, P.-A. Fang, W. Zhong, M. McNeal, C. Wei, W. Jiang, and X. Jiang. 2011. "Norovirus P Particle, a Novel Platform for Vaccine Development and Antibody Production." *Journal of Virology* 85. doi: 10.1128/jvi.01835-10.
- Tangye, S. G., and D. M. Tarlinton. 2009. "Memory B Cells: Effectors of Long-Lived Immune Responses." *European Journal of Immunology* 39. doi: 10.1002/eji.200939531.
- Thomas, G. 2002. "Furin at the Cutting Edge: From Protein Traffic to Embryogenesis and Disease." *Nature Reviews.Molecular Cell Biology* 3. doi: 10.1038/nrm934.
- Thrane, S., C. M. Janitzek, S. Matondo, M. Resende, T. Gustavsson, W. A. de Jongh, S. Clemmensen, W. Roeffen, de Vegte van, G. J. van Gemert, R. Sauerwein, J. T. Schiller, M. A. Nielsen, T. G. Theander, A. Salanti, and A. F. Sander. 2016. "Bacterial Superglue Enables Easy Development of Efficient Virus-like Particle Based Vaccines." *Journal of Nanobiotechnology* 14. doi: 10.1186/s12951-016-0181-1.
- Tian, S., Q. Huang, Y. Fang, and J. Wu. 2011. "FurinDB: A Database of 20-Residue Furin Cleavage Site Motifs, Substrates and Their Associated Drugs." *International Journal of Molecular Sciences* 12. doi: 10.3390/IJMS12021060.
- Tissot, A. C., P. Maurer, J. Nussberger, R. Sabat, T. Pfister, S. Ignatenko, H.-D. Volk, H. Stocker, P. Müller, G. T. Jennings, F. Wagner, and M. F. Bachmann. 2008. "Effect of Immunisation against Angiotensin II with CYT006-AngQb on Ambulatory Blood Pressure: A Double-Blind, Randomised, Placebo-Controlled Phase IIa Study." *The Lancet* 371. doi: 10.1016/S0140-6736(08)60381-5.
- Toth, S., D. Pella, and J. Fedacko. 2020. "Vaccines Targeting PSCK9 for the Treatment of Hyperlipidemia." *Cardiology and Therapy* 9. doi: 10.1007/s40119-020-00191-6.
- Tsuneoka, M., K. Nakayama, K. Hatsuzawa, M. Komada, N. Kitamura, and E. Mekada. 1993. "Evidence for Involvement of Furin in Cleavage and Activation of Diphtheria Toxin." *The Journal of Biological Chemistry* 268.

- Turley, C. B., R. E. Rupp, C. Johnson, D. N. Taylor, J. Wolfson, L. Tussey, U. Kavita, L. Stanberry, and A. Shaw. 2011. "Safety and Immunogenicity of a Recombinant M2e-Flagellin Influenza Vaccine (STF2.4xM2e) in Healthy Adults." *Vaccine* 29. doi: 10.1016/j.vaccine.2011.05.041.
- Turpeinen, H., Z. Ortutay, and M. Pesu. 2013. "Genetics of the First Seven Proprotein Convertase Enzymes in Health and Disease." *Current Genomics* 14. doi: 10.2174/1389202911314050010.
- Valkenburg, S. A., V. V. Mallajosyula, O. T. Li, A. W. Chin, G. Carnell, N. Temperton, R. Varadarajan, and L. L. Poon. 2016. "Stalking Influenza by Vaccination with Pre-Fusion Headless HA Mini-Stem." *Scientific Reports* 6. doi: 10.1038/srep22666.
- Veggiari, G., T. Nakamura, M. D. Brenner, R. V. Gayet, J. Yan, C. V. Robinson, and M. Howarth. 2016. "Programmable Polyproteins Built Using Twin Peptide Superglues." *Proceedings of the National Academy of Sciences of the United States of America* 113. doi: 10.1073/pnas.1519214113.
- Verbeke, R., I. Lentacker, S. C. De Smedt, and H. Dewitte. 2019. "Three Decades of Messenger RNA Vaccine Development." *Nano Today* 28. doi: 10.1016/j.nantod.2019.100766.
- Vester, S. K., R. Rahikainen, I. N. A. Khairil Anuar, R. A. Hills, T. K. Tan, and M. Howarth. 2022. "SpySwitch Enables pH- or Heat-Responsive Capture and Release for Plug-and-Display Nanoassembly." *Nature Communications* 13. doi: 10.1038/s41467-022-31193-8.
- White, J., A. Helenius, and M.-J. Gething. 1982. "Haemagglutinin of Influenza Virus Expressed from a Cloned Gene Promotes Membrane Fusion." *Nature* 300. doi: 10.1038/300658a0.
- White, L. J., M. E. Hardy, and M. K. Estes. 1997. "Biochemical Characterization of a Smaller Form of Recombinant Norwalk Virus Capsids Assembled in Insect Cells." *Journal of Virology* 71.
- Wringe, A., P. E. M. Fine, R. W. Sutter, and O. M. Kew. 2008. "Estimating the Extent of Vaccine-Derived Poliovirus Infection." *PLoS ONE* 3. doi: 10.1371/journal.pone.0003433.
- Xia, M., T. Farkas, and X. Jiang. 2007. "Norovirus Capsid Protein Expressed in Yeast Forms Virus-like Particles and Stimulates Systemic and Mucosal Immunity in Mice Following an Oral Administration of Raw Yeast Extracts." *Journal of Medical Virology* 79. doi: 10.1002/jmv.20762.
- Xia, M., P. Huang, C. Sun, L. Han, F. S. Vago, K. Li, W. Zhong, W. Jiang, J. S. Klassen, X. Jiang, and M. Tan. 2018. "Bioengineered Norovirus S60 Nanoparticles as a Multifunctional Vaccine Platform." *ACS Nano* 12. doi: 10.1021/acs.nano.8b02776.
- Xia, M., M. Tan, C. Wei, W. Zhong, L. Wang, M. McNeal, and X. Jiang. 2011. "A Candidate Dual Vaccine against Influenza and Noroviruses." *Vaccine* 29. doi: 10.1016/j.vaccine.2011.07.139.

- Zakeri, B., J. O. Fierer, E. Celik, E. C. Chittock, U. Schwarz-Linek, V. T. Moy, and M. Howarth. 2012. "Peptide Tag Forming a Rapid Covalent Bond to a Protein, through Engineering a Bacterial Adhesin." *Proceedings of the National Academy of Sciences of the United States of America* 109. doi: 10.1073/pnas.1115485109.
- Zebedee, S. L., and R. A. Lamb. 1988. "Influenza A Virus M2 Protein: Monoclonal Antibody Restriction of Virus Growth and Detection of M2 in Virions." *Journal of Virology* 62. doi: 10.1128/JVI.62.8.2762-2772.1988.
- Zhang, D. W., T. A. Lagace, R. Garuti, Z. Zhao, M. McDonald, J. D. Horton, J. C. Cohen, and H. H. Hobbs. 2007. "Binding of Proprotein Convertase Subtilisin/Kexin Type 9 to Epidermal Growth Factor-like Repeat A of Low Density Lipoprotein Receptor Decreases Receptor Recycling and Increases Degradation." *The Journal of Biological Chemistry* 282. doi: 10.1074/jbc.M702027200.
- Zhu, F.-C., Y.-H. Li, X.-H. Guan, L.-H. Hou, W.-J. Wang, J.-X. Li, S.-P. Wu, B.-S. Wang, Z. Wang, L. Wang, S.-Y. Jia, H.-D. Jiang, L. Wang, T. Jiang, Y. Hu, J.-B. Gou, S.-B. Xu, J.-J. Xu, X.-W. Wang, W. Wang, and W. Chen. 2020. "Safety, Tolerability, and Immunogenicity of a Recombinant Adenovirus Type-5 Vectedored COVID-19 Vaccine: A Dose-Escalation, Open-Label, Non-Randomised, First-in-Human Trial." *Lancet (London, England)* 395. doi: 10.1016/S0140-6736(20)31208-3.
- Zhu, J., J. Declercq, B. Roucourt, G. H. Ghassabeh, S. Meulemans, J. Kinne, G. David, A. J. Vermorken, W. J. de Ven, I. Lindberg, S. Muyltermans, and J. W. Creemers. 2012. "Generation and Characterization of Non-Competitive Furin-Inhibiting Nanobodies." *The Biochemical Journal* 448. doi: 10.1042/BJ20120537.

ORIGINAL COMMUNICATIONS

- I Lampinen, V; Heinimäki, S; Laitinen, OH; Pesu, M; Hankaniemi, MM*; Blazevic, V*; Hytönen, VP*. Modular vaccine platform based on the norovirus-like particle. *Journal of Nanobiotechnology* 19 (2021). <https://doi.org/10.1186/s12951-021-00772-0>
- II Heinimäki, S; Lampinen, V; Tamminen, K; Hankaniemi, MM; Malm, M; Hytönen, VP; Blazevic, V. Antigenicity and immunogenicity of HA2 and M2e influenza virus antigens conjugated to norovirus-like, VP1 capsid-based particles by the SpyTag/SpyCatcher technology. *Virology* 566 (2022). <https://doi.org/10.1016/j.virol.2021.12.001>
- III Lampinen, V; Gröhn, S; Soppela, S; Hytönen, VP; Hankaniemi, MM. SpyTag/Catcher display of influenza M2e peptide on norovirus-like particle provides stronger immunization than direct genetic fusion. *Frontiers in Cellular and Infection Microbiology* 13 (2023). <https://doi.org/10.3389/fcimb.2023.1216364>
- IV Lampinen, V; Ojanen, MJT; Muñoz Caro, F; Gröhn, S; Hankaniemi, MM; Pesu, M; Hytönen, VP. Experimental VLP vaccine displaying a furin antigen elicits autoantibodies and is well tolerated in mice. Submitted manuscript.

* Equal contribution

PUBLICATION

I

Modular vaccine platform based on the norovirus-like particle

Lampinen V, Heinimäki S, Laitinen OH, Pesu M, Hankaniemi MM*, Blazevic V*,
Hytönen VP*

Journal of Nanobiotechnology. 2021; 19

doi: 10.1186/s12951-021-00772-0

Publication reprinted with the permission of the copyright holders (CC BY 4.0).

RESEARCH

Open Access



Modular vaccine platform based on the norovirus-like particle

Vili Lampinen¹, Suvi Heinimäki², Olli H. Laitinen¹, Marko Pesu^{1,3}, Minna M. Hankaniemi^{1*†}, Vesna Blazevic^{2*†} and Vesa P. Hytönen^{1,3*†}

Abstract

Background: Virus-like particle (VLP) vaccines have recently emerged as a safe and effective alternative to conventional vaccine technologies. The strong immunogenic effects of VLPs can be harnessed for making vaccines against any pathogen by decorating VLPs with antigens from the pathogen. Producing the antigenic pathogen fragments and the VLP platform separately makes vaccine development rapid and convenient. Here we decorated the norovirus-like particle with two conserved influenza antigens and tested for the immunogenicity of the vaccine candidates in BALB/c mice.

Results: SpyTagged noro-VLP was expressed with high efficiency in insect cells and purified using industrially scalable methods. Like the native noro-VLP, SpyTagged noro-VLP is stable for months when refrigerated in a physiological buffer. The conserved influenza antigens were produced separately as SpyCatcher fusions in *E. coli* before covalent conjugation on the surface of noro-VLP. The noro-VLP had a high adjuvant effect, inducing high titers of antibody production against the antigens presented on its surface.

Conclusions: The modular noro-VLP vaccine platform presented here offers a rapid, convenient and safe method to present various soluble protein antigens to the immune system for vaccination and antibody production purposes.

Keywords: VLP, Vaccine, Influenza, SpyCatcher, Virus

Background

Out of all medical inventions, vaccination has doubtless had the largest impact on global health, but this mature invention still has potential for improvement. A well-known example of this is the influenza vaccine, which because of the rapid evolution of influenza virus surface proteins, needs reformulation for each season [1]. Influenza has imposed a considerable disease burden

worldwide for hundreds of years and it still constitutes a constant threat to public health. On a global scale, WHO estimates the yearly death toll of influenza infections between 290,000 and 650,000 [2], while emerging pandemic strains threaten the lives of millions. To avoid the current need of annual vaccination, we need a universal influenza vaccine that targets conserved regions that mutate at a slower pace in the virus. Most influenza vaccines in use today are still produced as whole virus vaccines in chicken eggs, using the same technology that has been in use since 1946 [3]. This suffices against the particular strain chosen for production, but more modern approaches are needed for rapid and dependable production of vaccines that work against multiple strains of influenza.

Virus-like particles (VLPs) have recently shown great promise as flexible, safe and effective modern vaccines.

*Correspondence: minna.hankaniemi@tuni.fi; vesna.blazevic@tuni.fi; vesa.hytonen@tuni.fi

[†]Minna M. Hankaniemi, Vesna Blazevic and Vesa P. Hytönen contributed equally to this work

¹ Faculty of Medicine and Health Technology, Tampere University, 33014 Tampere, Finland

² Vaccine Development and Immunology/Vaccine Research Center, Faculty of Medicine and Health Technology, Tampere University, Tampere, Finland

Full list of author information is available at the end of the article



© The Author(s) 2021. This article is licensed under a Creative Commons Attribution 4.0 International License, which permits use, sharing, adaptation, distribution and reproduction in any medium or format, as long as you give appropriate credit to the original author(s) and the source, provide a link to the Creative Commons licence, and indicate if changes were made. The images or other third party material in this article are included in the article's Creative Commons licence, unless indicated otherwise in a credit line to the material. If material is not included in the article's Creative Commons licence and your intended use is not permitted by statutory regulation or exceeds the permitted use, you will need to obtain permission directly from the copyright holder. To view a copy of this licence, visit <http://creativecommons.org/licenses/by/4.0/>. The Creative Commons Public Domain Dedication waiver (<http://creativecommons.org/publicdomain/zero/1.0/>) applies to the data made available in this article, unless otherwise stated in a credit line to the data.

They are virus-genome-free particles that are similar in size and shape to the respective viruses. This makes VLPs incapable of infection but still very effective in mounting immune responses [4]. VLPs are produced by recombinant expression of structural virus proteins, followed by their spontaneous assembly into particles. In addition to the elementary idea of replacing inactivated virus vaccines with their safer and more producible VLP counterparts, VLP technology can be harnessed against any pathogen by decorating VLPs with antigens from heterologous pathogens. The simplest way to do this is to genetically fuse the antigens to a virus capsid protein that participates in forming the VLP. However, as this often hinders either VLP or antigen assembly, it requires laborious and time-intensive planning and optimization individually for each antigen tested [5]. Using a modular system, wherein the antigen and VLP are produced separately and conjugated together only after that, circumvents these problems. Both native and decorated VLP vaccines, such as vaccines against human papilloma virus and malaria [Gardasil (MSD, Ireland), and Mosquirix H-W-2300 (GSK, UK), respectively], are already in clinical use, which demonstrates the commercial feasibility and medical potential of VLP technology. The modular VLP vaccine approach is not yet in clinical use, but with the research reported here, we aim to append to previous research on the subject and bring it closer to clinical testing.

We have previously demonstrated that the norovirus-like particle (noro-VLP) shows exceptional producibility and stability, even when displaying C-terminal HisTags on its surface for simple non-covalent and modular decoration [6]. Now, we developed this idea further by displaying SpyTags on the noro-VLP and covalently decorating it with SpyCatcher conjugation technology [7]. With this modular system, we can produce and purify SpyCatcher-fused antigen separately from the SpyTag-noro-VLP and then decorate the noro-VLP via isopeptide bonds forming spontaneously between SpyTag and SpyCatcher. To test a medically relevant application of this flexible molecular platform, we produced two conserved influenza antigens as SpyCatcher fusions to present them on the noro-VLP. The noro-VLP was decorated with the ectodomain of influenza matrix-2 ion channel protein (M2e) and a minimized stem-fragment of hemagglutinin glycoprotein 2 (HA2), and the immunogenicity of the decorated particles was tested in BALB/c mice. Both protein fragments are highly conserved across different influenza strains from a long time span [8]. A vaccine that can create an immune response against these conserved influenza protein sequences could protect against many pathogenic influenza strains without annual renewal [9, 10]. Generating such a response has proven near

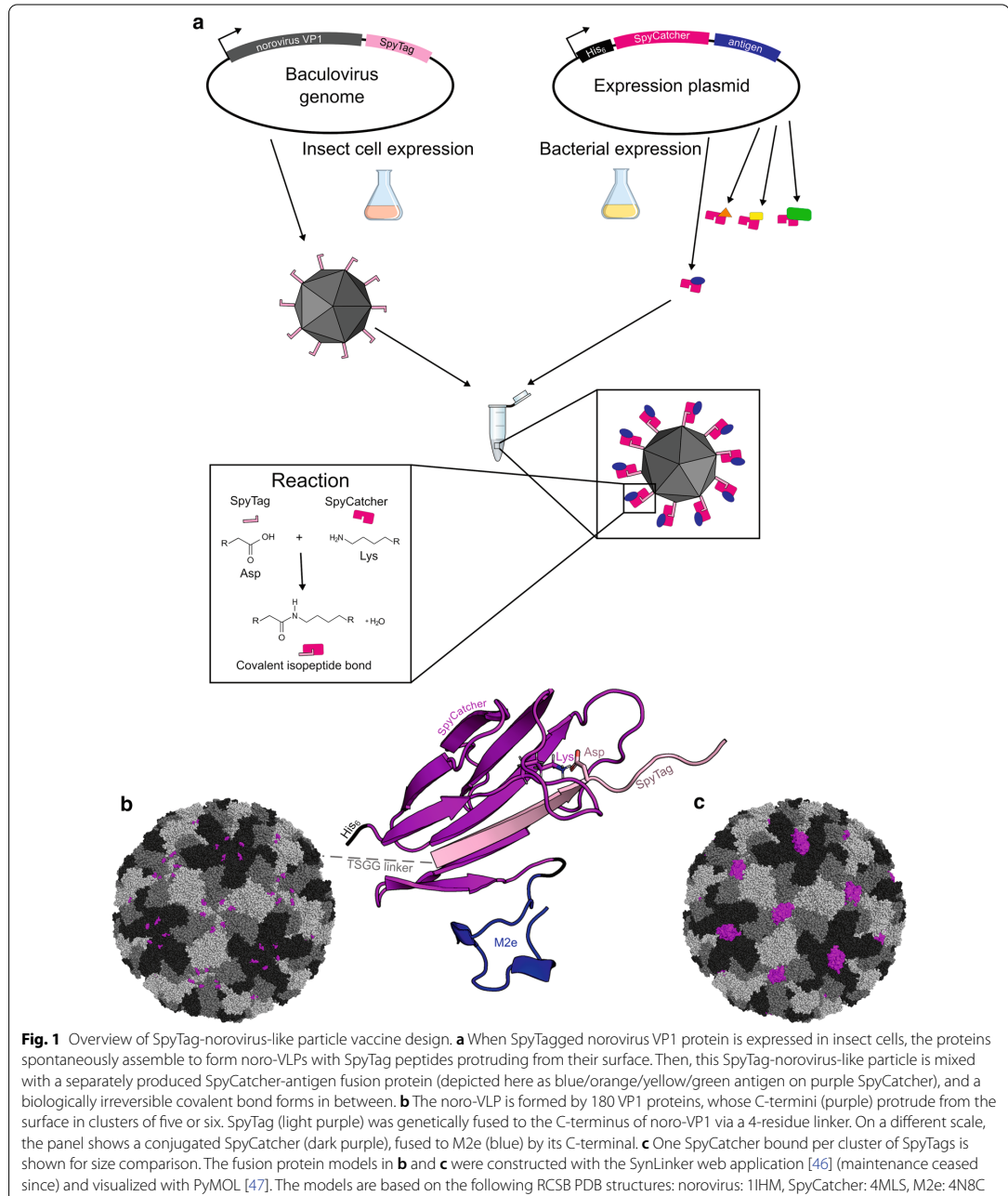
impossible when vaccinating with or getting infected by natural viruses, presumably because both conserved regions are immunogenically dominated by the highly variable regions in the highly immunogenic and prominent head domains of HA and neuraminidase (NA) proteins. When fused to a VLP, only the desired conserved antigen fragments are displayed in an immunogenic way. The M2e peptide and the trimeric HA2 protein domain are disparate antigens physically, so successful conjugation of them both on the noro-VLP holds great promise for wide use of the noro-VLP platform in biotechnology.

Results

Production of SpyTagged norovirus-like particles and SpyCatcher fusion proteins

To create norovirus-like particles decorated with influenza antigens, we expressed and purified SpyTagged norovirus-like particles (SpyTag-noro-VLPs) separately from SpyCatcher-fused antigens before conjugating the components together (overview in Fig. 1). The best SpyTag-noro-VLP yields were obtained by infecting Hi5 insect cells with SpyTag-noro-VLP-expressing baculovirus at a multiplicity of infection (MOI) value of 1 and proceeding to the first crude purification step directly after collecting the expressed protein. Both tangential flow filtration (TFF) and ultracentrifugation through a sucrose gradient separated most protein impurities from the VLP (data not shown). After this crude purification, SpyTag-noro-VLPs could be stored at +4 °C for ≥ 5 months without apparent change in morphology, homogeneity, concentration or conjugation efficiency of the product. However, a polishing ion exchange step is required to separate the similarly sized baculovirus from the SpyTag-noro-VLP [11]. After anion exchange chromatography purification, the SpyTag-noro-VLP yields were 10–30 mg/L of insect cell culture, with a purity of >95% (Fig. 2a), as determined by densitometry analysis from silver-stained SDS-PAGE gel. Anion exchange chromatography removed all detectable baculovirus from the product (determined by anti-gp64 western blotting, Additional file 1: Figure S1), making it suitable for vaccination purposes.

We expressed influenza M2e and HA2 as SpyCatcher-fusion proteins in *E. coli* and purified them with Ni-NTA affinity chromatography. For M2e, we chose the human influenza virus consensus sequence of the first 24 N-terminal amino acids of influenza matrix-2 [10], while HA2 here is the minimized, pre-fusion stem region of influenza hemagglutinin, first reported in [12]. Like the original authors, we included a foldon trimerization domain to the C-terminal of HA2 to support its natural trimerization. A proteolytically cleavable HisTag was included in the N-terminus of SpyCatcher in both fusion proteins to allow purification and detection. The amino



acid sequences of the proteins produced in this study are shown in Additional File 1: Table S1. The single-step affinity chromatography purification yielded > 30 mg/L of

SpyCatcher-M2e and > 10 mg/L of SpyCatcher-H1F. Both antigens were > 95% pure (by SDS-PAGE densitometry analysis, Fig. 2a) after total protein staining. By including

(See figure on next page.)

Fig. 2 Conjugation of norovirus-like particles. **a** Silver-stained SDS-PAGE gel of the vaccine components. The noro-VLP appears as a double band between the 70 and 50 kDa markers. All wells contain approximately 250 ng of protein. **b** Western blot analysis of noro-VLP decorated with the influenza antigens. The HisTag in the N-termini of SpyCatcher fusion proteins is recognized by mouse anti-HisTag antibody. **c** Dynamic light scattering analysis of SpyTag-noro-VLP and SpyTag-noro-VLP decorated with M2e and HA2. Numerical data shown in Additional file 1: Figure S4. Representative transmission electron microscopy pictures with arithmetic means of equivalent circle diameters \pm standard deviation of **d** native noro-VLP ($n = 114$), **e** SpyTag-noro-VLP ($n = 112$) and noro-VLP decorated with **f** M2e ($n = 109$) and **g** HA2 ($n = 274$). The scale bars are all 200 nm. 60,000 \times magnification was used for these pictures and analysis

a detergent washing step into the affinity chromatography protocol, we removed most endotoxins from these *E. coli*-expressed proteins to make them usable as vaccine components.

According to dynamic light scattering (DLS) analysis, SpyTag-noro-VLP and SpyCatcher-H1F were very monodisperse (polydispersity index (PDI) < 0.2) and soluble in PBS after purification. SpyCatcher-M2e showed a PDI of over 0.8 in DLS, which would indicate it being a very polydisperse sample, but on the other hand, visual inspection showed no aggregates even in our high concentration samples. In transmission electron microscopy analysis, the produced SpyTag-noro-VLPs showed a similar size and morphology as compared to native noro-VLPs (Fig. 2d, e). MALDI-MS analysis confirmed that SpyCatcher-M2e and SpyCatcher-H1F were intact and had the predicted masses of 14 and 31 kDa, respectively (Additional file 1: Figure S2).

Decoration of norovirus-like particles with SpyCatcher-fused antigens

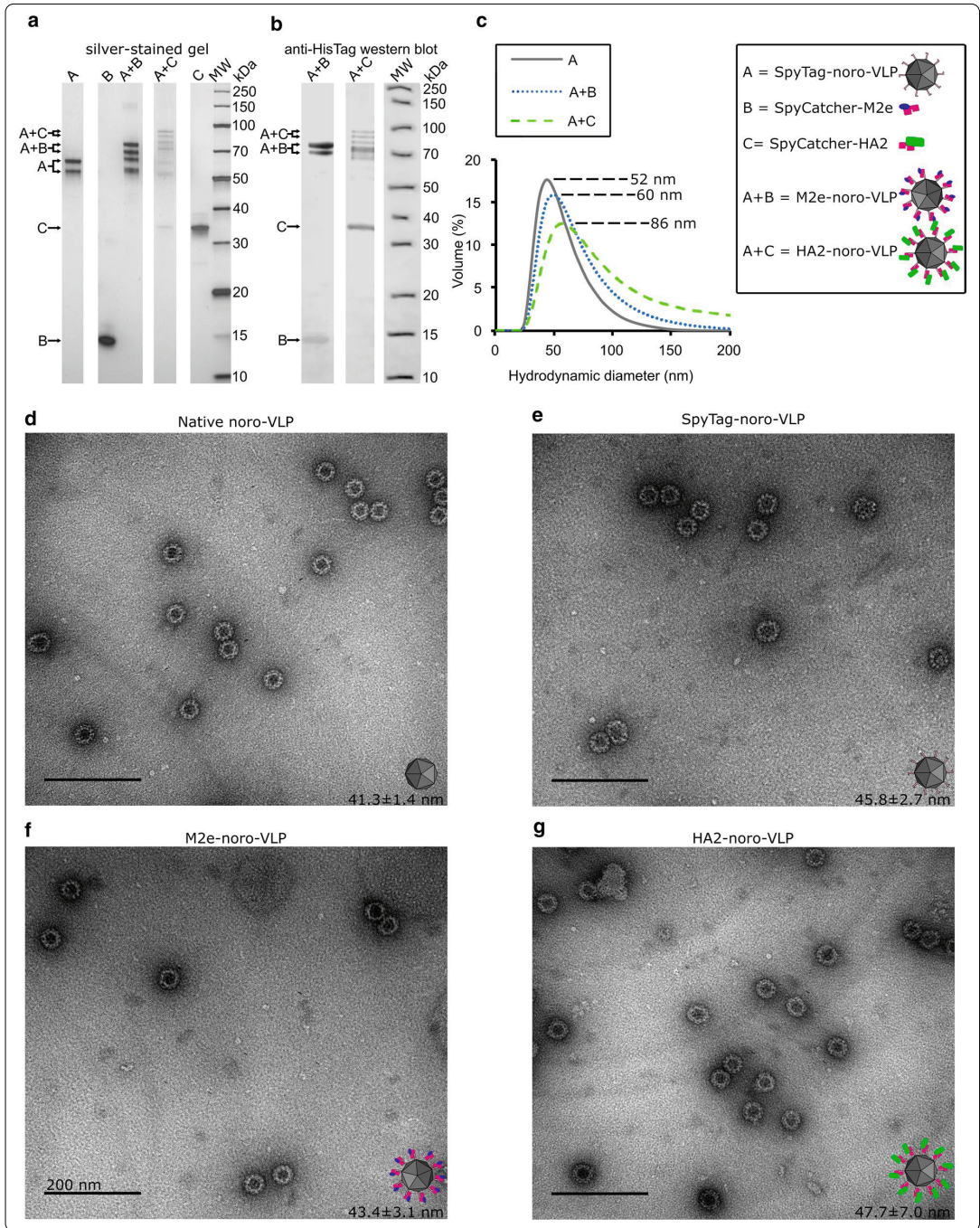
The SpyTag-noro-VLPs were decorated with SpyCatcher-fused influenza antigens by mixing the components together in PBS buffer, as described in [13]. The conjugation efficiency was estimated from SDS-PAGE gel by densitometry. Decoration with SpyCatcher-M2e or SpyCatcher-H1F moves the noro-VLP-specific double band upwards by 14 or 31 kDa, respectively (Fig. 2a). This matches the sizes of the SpyCatcher fusion proteins. In both cases, approximately half of the VP1 proteins in the product are covalently conjugated with antigen. Since noro-VLP consists of 180 VP1 proteins [14], 50% conjugation efficiency equals 90 SpyCatcher-antigen molecules per particle. By performing multiple independent conjugation reactions, we noted that the reaction proceeds to the end in 2 h at RT or overnight at +4 °C. The HisTag in the N-terminus of SpyCatcher-fusion protein is visualized in conjugated VLP bands in anti-HisTag western blot, whereas unconjugated VLP is invisible in these wells (Fig. 2b). All detectable unbound SpyCatcher-M2e is separated in dialysis, but some noncovalently bound SpyCatcher-HA2 can be seen in the gel even after dialysis. Moreover, an extra double band can be seen in the HA2-noro-VLP well between the expected conjugation bands and noro-VLP bands.

In TEM, no obvious differences between native, tagged or decorated particles were initially recognized (Fig. 2d–g), but a particle size distribution measurement from TEM images revealed a measurable increase in particle size in HA2-decorated particles. DLS shows a 15% increase in hydrodynamic diameter when SpyTag-noro-VLPs are decorated with SpyCatcher-M2e and a 65% increase with SpyCatcher-HA2 (Fig. 2c). The low molecular weight of SpyCatcher-M2e could explain why it is not detected in TEM. Decorating the particles also increases the polydispersity index from 0.107 to 0.167 in DLS, but volume distribution still shows only a single, slightly wider peak. Even though the SpyCatcher-antigen fusion proteins were produced in *E. coli*, Triton X-114 washing of the produced proteins reduced the endotoxin content to acceptable levels [15]. All immunogens used in vaccination had an endotoxin content of < 0.054 EU/ μ g (Table 1) and < 0.18 ng dsDNA/ μ g of protein.

SpyTagged noro-VLPs are exceptionally stable and convenient to store

Like the native noro-VLP and norovirus itself, also SpyTag-noro-VLP shows remarkable stability. Due to the influence of temperature on vaccine stability, the stability of the vaccines was evaluated by differential scanning fluorimetry (DSF). DSF measurements showed that SpyTag-noro-VLP's melting temperature (T_m) of +66(\pm 0.1) °C in pH 7.4 PBS is very close to that of native noro-VLP's +68(\pm 0.1) °C (Fig. 3b). Our comparison of the native and SpyTagged noro-VLP under pH 3, 5.5 and 8 (Additional file 1: Figure S5) confirmed that SpyTag destabilizes the noro-VLP only in the slightest and that noro-VLP is most stable at mildly acidic to neutral pH. This conforms with earlier studies on noro-VLP stability [16]. Conjugating noro-VLP with M2e or HA2 lowered its T_m further to +63(\pm 0.1) °C (Fig. 3c). HA2-noro-VLP shows signs of a second unfolding peak near SpyCatcher-HA2's own T_m of +35(\pm 0.1) °C.

In series of DLS measurements, a SpyTag-noro-VLP sample did not show any signs of aggregation or disintegration during a five-month follow-up (Fig. 3a). During the study, we stored the purified SpyTag-noro-VLP in PBS at +4 °C. In seven months, we did not observe a change in conjugation efficiency (Fig. 3e). For the stability experiment, SpyCatcher-M2e aliquots were stored at



–20 °C and thawed each month before the conjugation reaction.

Although the vaccine components are easy to store on their own, we noticed that after conjugation, HA2-conjugated noro-VLP lost some of its stability. During storage of conjugated HA2-noro-VLP vaccine sample, the largest bands on SDS-PAGE disappeared after 76 days at +4 °C (Additional file 1: Figure S3). At the same time, prominence of a 13-kDa band, unrecognized by anti-HisTag antibodies, increased. Addition of 1 µg/mL aprotinin and leupeptin protease inhibitors into a parallel sample prevented these changes. By 40 days, the changes in SDS-PAGE appearance were not yet apparent, meaning that the phenomenon should not influence the immunizations. It should be noted that these observations were made with samples wherein the unreacted H1F was still unseparated from the mixture.

Decorated norovirus-like particles induce strong antibody responses

To study the immunogenicity of the purified and decorated noro-VLPs, we used them to immunize female BALB/c mice intramuscularly. Groups of 4–5 mice were injected twice with M2e or HA2 decorated noro-VLPs or with control samples, with a 3-week interval. We used ELISA to analyze the IgG antibody responses in mice sera. Mice vaccinated with SpyCatcher-HA2 produced high titers ($>10^4$) of HA2-specific antibodies, regardless of whether HA2 was presented on noro-VLP or introduced alone as a SpyCatcher fusion protein (Fig. 4b). The mean titer was slightly higher in the HA2-noro-VLP group ($p=0.40$) and noro-VLP presentation of HA2 decreased the deviation in the immune response between mice by 68%. Presenting the M2e peptide on noro-VLP via SpyCatcher linkage produced no detectable M2e-specific antibodies (not shown). Instead, the antibody titers seen in Fig. 4c are more likely to recognize SpyCatcher.

By cross testing our SpyCatcher fusion proteins, we can estimate the titer of antibodies formed against the common factor of the vaccine components—SpyCatcher. Antibodies against SpyCatcher were produced, but it is not clear if noro-VLP presentation enhanced their formation or not. SpyCatcher-M2e on noro-VLP induced more SpyCatcher-antibodies than SpyCatcher-M2e alone ($p=0.036$) (Fig. 4c), but conversely, SpyCatcher-HA2 raised more antibodies against SpyCatcher than HA2-noro-VLP ($p=0.032$) (Fig. 4d).

Discussion

While COVID-19 has recently eclipsed seasonal influenza as a viral threat, it still serves as a shocking reminder of the insurance that functional virus vaccines provide us.

Table 1 Vaccine groups and doses used in the immunization experiment

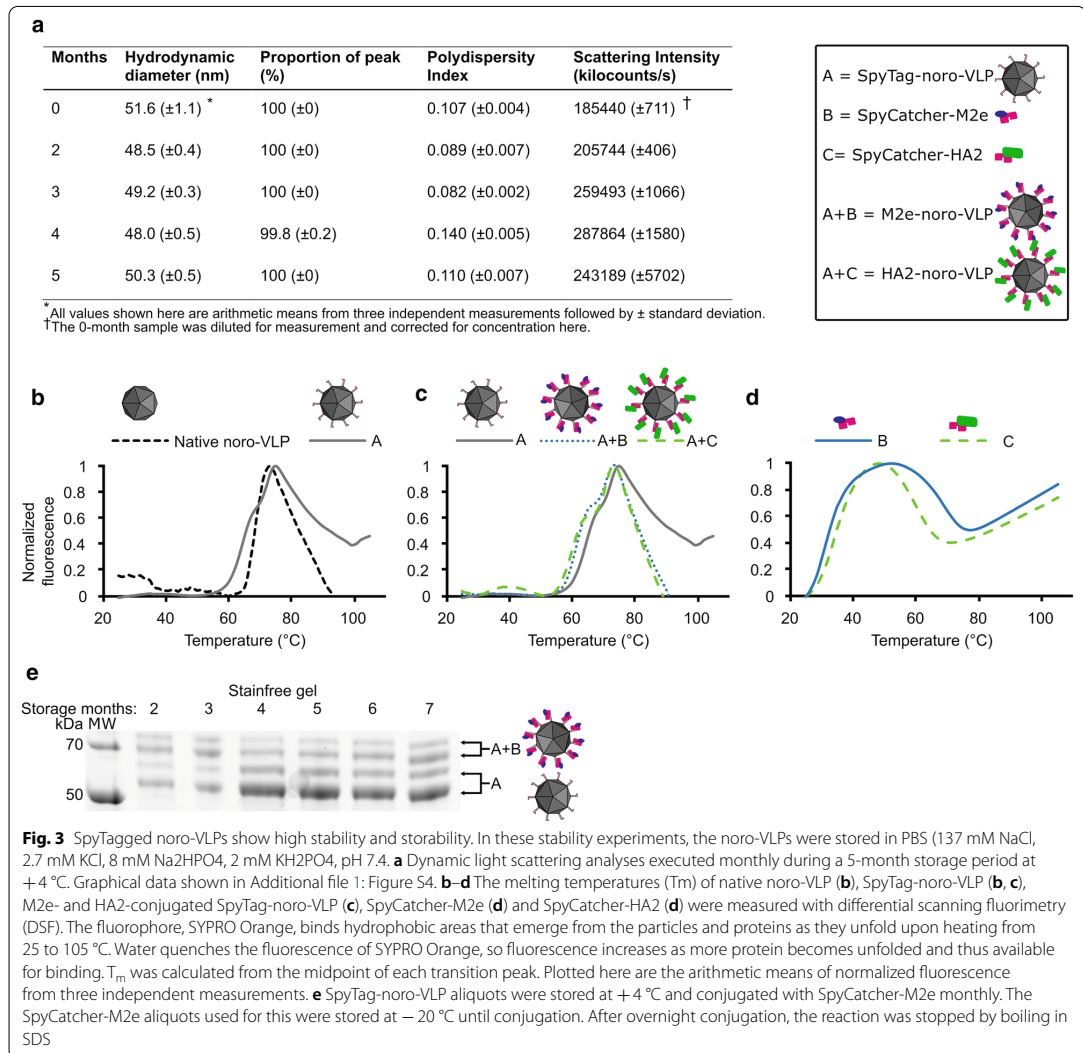
Group	Mice/group (n)	Vaccine	Total protein dose (µg)	Antigen ^a dose (µg)	Endotoxin dose (EU)
I	4	SpyTag-noro-VLP ^b	25	24.3	< 1
II	4	SpyCatcher-HA2	25	12.5	< 0.4
III	5	HA2-noro-VLP	15	1.3	< 0.6
IV	4	SpyCatcher-M2e	100	24.3	< 5.4
V	5	M2e-noro-VLP	50	1.2	< 0.4

^a The dose of the underlined antigen molecule is estimated in this column, as described in the text

^b Norovirus-like particle

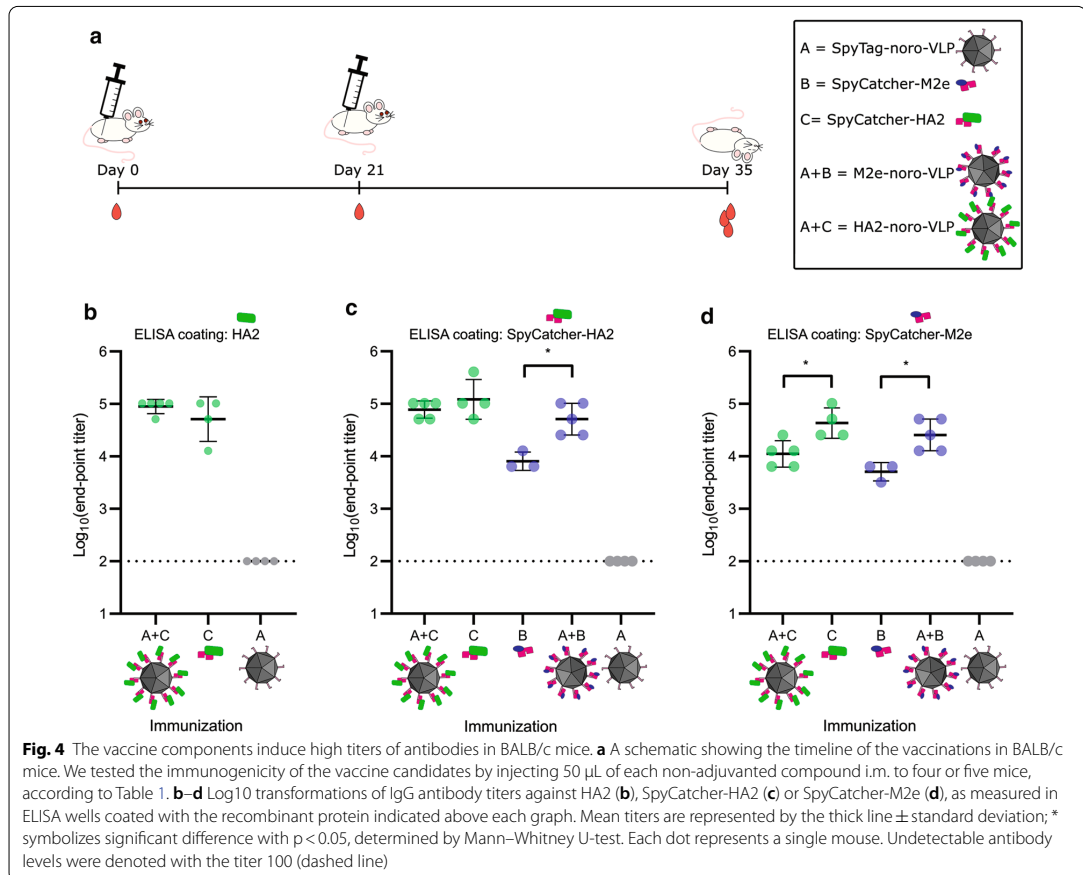
Although it has been more than 70 years since the first influenza vaccine, most vaccines are still made with the same egg-based manufacture technology. The procedure is simple and usually functional, but also poses several problems, including egg allergy-related side effects, limitations in egg availability and requiring work with live, infectious viruses [3]. Even though influenza is used as a well-known example here, credible alternative vaccine technologies to any whole pathogen vaccine have arrived only recently in the form of DNA, RNA and recombinant protein vaccines. While all nucleic acid vaccines for influenza remain exclusively in research use, the first recombinant influenza vaccine called Flublok (Sanofi Pasteur, Lyon, France) was approved for commercial use in the USA in 2013. Flublok is comprised of recombinant full-length, wild-type HA protein. It does not provide any broader immunity than conventional, egg-based influenza vaccines, but avoids problems related to virus safety and egg allergies and availability. Additionally, generation of a new vaccine product with recombinant technology can be significantly faster [17]. Most recombinant proteins, including influenza HA in Flublok, are too small to be very immunogenic without addition of strong adjuvants [18]. Recombinantly produced VLPs, on the other hand, assemble into a virus-sized particle that can drain into lymph nodes and cross-link B-cell receptors, generating strong immune responses even without added adjuvants [4].

The recently developed SpyCatcher/SpyTag conjugation has been used before for presenting SpyTagged malaria antigens on SpyCatcher-decorated bacteriophage AP205 VLPs [13]. In the present study, we adapted the SpyCatcher/SpyTag technology for decorating the exceptionally stable norovirus-like particle. The methods described here can be used to establish large-scale



production of vaccine-grade SpyTag-noro-VLPs and SpyCatcher fusion proteins. Production of two SpyCatcher-fused influenza antigens succeeded in high efficiency in a simple *E. coli* batch production system. This was expected, as SpyCatcher has been shown to be a tenaciously folding protein that can even enhance the solubility of its fusion partners [19]. Arrays of SpyCatcher fusion proteins have been successfully produced in different systems after the publication of the technology (e.g. [19–21]). SpyCatcher functions as N- or C-terminal or even internal loop fusions [7], which makes our vaccine

platform compatible with the vast majority of soluble protein antigens. The SpyTag-noro-VLP was decorated with SpyCatcher fusion proteins by simply mixing the components together in solution. In this study, we used PBS, in which noro-VLP remains stable for months (Fig. 3 and [22]), but SpyCatcher works in a range of different buffers and conditions [7]. Generating each new vaccine in an identical way as SpyCatcher fusions presented on noro-VLP would expedite the regulatory process compared to a different vaccine formula for each generation or kind of pathogen.



Efficient and scalable production is imperative for a functional vaccine platform, since it needs to be manufactured quickly in enormous quantities against emerging epidemics and pandemics. The norovirus-like particle production methods presented here and before [23] do not require specialized virus-outbreak-safe facilities and they are fully scalable even to industrial level with standard cell culture and protein purification equipment. To exemplify, it has been estimated that to achieve global herd immunity against the current COVID-19 pandemic, close to 5 billion vaccine doses are needed. Given a typical VLP vaccine dose of 120 μg (e.g. Gardasil, MSD, Ireland), this would mean a whopping 24 million liters of insect cell culture, even with no boosts and a yield of 10–30 mg. Although this sounds like a large volume and an immense effort, it is still vastly more realistic than the 4–8 billion infected chicken eggs it would take to produce this number of vaccine doses the traditional way [24].

Decoration of noro-VLPs worked well with methods described previously [7, 13, 19] with a simple M2e peptide and a complicated, trimeric HA2 protein. With noro-VLP, the conjugation efficiency was estimated to be up to 50%, instead of close to 100% that has been reported with other SpyCatcher-VLP systems [13, 19]. Based on the X-ray structure of noro-VLP (Fig. 1, panels B–C), we predicted that up to three SpyCatcher molecules can fit into one SpyTag cluster on the SpyTag-noro-VLP. The clusters contain five or six C-termini, hence five or six SpyTags, which would translate into a maximum conjugation efficiency of $\sim 60\%$. This equals 108 antigen molecules per particle, which is in line with similar VLP platforms [19, 25, 26].

We used SDS-PAGE to measure the mobility shift caused by conjugation of the vaccine components and densitometry to compare the ratios of unconjugated and conjugated noro-VLP bands. In SDS-PAGE, covalently bound peptides (e.g. proteins conjugated via SpyCatcher/

SpyTag) are expected to form a single band and noncovalently bound peptide complexes (e.g. the 180 proteins that form the noro-VLP together) to separate into their peptide components. In SDS-PAGE gels, the noro-VLP double band moved upwards by the size of its SpyCatcher-antigen partner (Fig. 2a). The noro-VLP double band is caused by an N-terminal truncation [27], which means that both the full length and truncated forms have SpyTag in their C-termini. Both forms participate in forming the particle. M2e conjugation behaved as expected on gel. However, HA2-noro-VLP shows up as the expected double band at 92/89 kDa, but also as a double band near 75/72 kDa. All four conjugation bands are recognized by anti-HisTag antibody (Fig. 2b), which indicates that SpyCatcher's N-terminal HisTag must be included in these forms as well. We hypothesize that partial cleavage takes place after conjugation of the trimeric HA2-SpyCatcher on SpyTag-noro-VLP, cutting loose some of covalently conjugated HA2 and leaving only SpyCatcher on some binding spots on the noro-VLP. On the other hand, we also observed that some SpyCatcher-HA2 remains in the vaccine product after vigorous dialysis, so some of the protein may bind the large noro-VLP only through noncovalent means via its foldon trimerization domain. Based on the immunization results, enough HA2 remained bound on the noro-VLP for producing anti-HA2 antibodies.

Earlier research shows that native noro-VLPs are exceptionally stable and easy to store [22], which probably derives from the known perseverance of the pathogenic norovirus. This study confirms that the same aspects apply to the SpyTag-noro-VLP. The SpyTag-noro-VLP can be stored at +4 °C for months in a simple PBS buffer without any additives. This is important for making large stockpiles of the vaccine platform to secure supply in an emergency. For example, in developing countries, continuous refrigeration is not always possible, so storage of noro-VLP at room temperature should still be investigated. Since the native noro-VLP can already survive 7 days at room temperature [22], noro-VLP is a promising platform for stabilization studies. For example, stabilization via added disulfide bonds and formalin treatment has increased the thermostability of many VLPs before [28]. Formalin treatment of Coxsackievirus VLPs improved both their stability and immunogenicity [29], which demonstrates the importance stability can have on the clinical applicability of vaccines.

As a downside to this vaccine platform, SpyCatcher fusion proteins are not as stable as the noro-VLP, according to their melting temperatures (Fig. 3d), so we stored these in frozen form. Fusing the M2e peptide or HA2 on SpyCatcher apparently lowered its melting temperature from +49 °C [30] to +31 or +35 °C, respectively. The

effect of these fusions on the observed melting temperature of SpyCatcher seems stronger than fusion of beta lactamase [31]. Also, we noticed degradation of conjugated HA2-noro-VLP during its storage at +4 °C after 76 days. A minor protease contamination, most likely from *E. coli*, could explain this observation. It should still be investigated if further purification steps could resolve the issue altogether. On the other hand, the process seems to be visible only after over a month of storage, so it is possible to still use antigens like described above if administration is done within a month after conjugation. The dialysis step would be impossible to do in the clinic, but SpyCatcher conjugation should proceed to the end within minutes also with equimolar concentrations, especially with more optimized SpyCatcher versions [7, 21, 30]. Conjugation could be done in situ for example by mixing of two pre-prepared vaccine component solutions with a dual chamber syringe.

In the ongoing effort to make a universal influenza vaccine, recombinant vaccines containing conserved peptides and protein domains from M2 and HA have been studied extensively. HA is natively formed by six non-covalently bound HA1 and HA2 polypeptides, so recombinant expression of the conserved stem domain is not trivial. The problem was solved by engineering a construct that fused the structurally and immunologically important stem fragments of HA1 into the gene of HA2 to make a single soluble polypeptide, capable of forming a trimer that mimics the native stem domain of HA [12]. The authors immunized mice with this HA ministem based on H1 influenza, together with the respective antigen from an H5 influenza strain. The vaccine protected mice from influenza strains H1, H3 and H5, which was the broadest protective effect reported thus far [9], but the results could not be repeated in ferrets [32]. The group proposed that the HA ministem vaccine candidates need "enhancement" to be effective in large, outbred species (like humans), which motivated us to test their antigen as a noro-VLP conjugate. We executed immunogenicity tests in a similar setting. SpyCatcher-HA2 and HA2-noro-VLP (this study) and HA2 alone [12] all raised high antibody titers, but SpyCatcher-HA2 and HA2-noro-VLP were able to do so without added adjuvant and with 2- or 20-fold smaller antigen doses, respectively. Noro-VLP display showed a trend towards higher antibody titers as compared to SpyCatcher-HA2 and with lower variation. From this indirect comparison, it can be deduced that especially noro-VLP display and even SpyCatcher conjugation alone have adjuvant effects surpassing or at least comparable to CpG7909 (TriLink BioTechnologies, USA), used by Mallajosyula et al. Additionally, bacterial endotoxins were not removed or measured from the *E. coli* produced antigens in the earlier

reports, so the adjuvant load might have been high in these immunization tests. Therefore, our HA2 vaccine candidate represents a product closer to clinical use.

In this study, we observed no M2e-specific antibodies even when vaccinating mice with noro-VLP decorated with the M2e peptide. Instead, all antibodies we detected in the mouse sera in ELISA seemed to identify the SpyCatcher conjugation protein. Anti-SpyCatcher antibodies are to be expected, since SpyCatcher is derived from a common human pathogen, *Streptococcus pyogenes* [7], and the immunogenicity of the full-length protein has been noted in previous immunization studies [33]. Nevertheless, we expected to also find M2e-specific antibodies, since it has been shown to be immunogenic with similar platforms [34, 35]. Both papers presented N-terminally fused M2e, whereas we fused M2e to the C-terminus of SpyCatcher (Additional file 1: Table S1). As M2e represents the N-terminus of the influenza M2 protein, this change in topology might be problematic for natural folding, although some protective antibodies have been obtained also from M2e presented in internal loops [36]. Directing immunity against the peptide presented on the noro-VLP could work better with 3–5 tandem repeats of the peptide, as in [36, 37]. Now that we have shown that noro-VLP tolerates C-terminal HisTag [6] and SpyTag fusion well, we should next investigate direct genetic fusion of M2e, removing the immunogenic SpyCatcher from the product. Another way to remove SpyCatcher and still maintain a modular system would be to test the SnoopLigase 3-part conjugation technology with the noro-VLP [38].

M2e and HA stem vaccines both work in a distinct mechanism as compared to conventional influenza vaccines, which makes studying their neutralizing effect more complicated. HA2-stem-directed antibodies mediate neutralization of influenza by inhibiting membrane fusion [12], while M2e antibodies are thought to mainly work against infected cells that express M2e on their membrane [10]. Neither block influenza from binding its host cell receptors, like whole virus vaccines, which means that the convenient hemagglutination assay usually used for estimating neutralization capacity of influenza vaccines will not work in this case. Cell-based or challenge studies with live influenza virus should still be executed to further assess the antibodies we obtained.

Conclusions

In this study, we constructed a modular vaccine platform based on the noro-VLP. The SpyTagged noro-VLP can be decorated with SpyCatcher fused antigens by simply mixing the components together in a variety of solutions. We established efficient, scalable and easily modifiable production and purification methods for the

SpyTag-noro-VLP platform and two prototype antigens. Important for a vaccine platform, our studies demonstrate that the SpyTag-noro-VLP is stable and that it can be stored at normal refrigerator temperature for months. We decorated the noro-VLP with two conserved influenza antigens, aiming for a universal influenza vaccine. In mouse immunization experiments, the decorated noro-VLPs raised high titers of IgG antibodies against HA2 and SpyCatcher proteins. Presentation of HA2 on noro-VLP showed a trend towards higher antibody titers compared to soluble SpyCatcher-HA2 alone. In conclusion, the SpyTag-noro-VLP vaccine platform offers a convenient and promising method to rapidly produce vaccine candidates out of various protein domain antigens, but further research is still needed to confirm compatibility of the noro-VLP platform with peptide antigens.

Methods

Construction of expression plasmids

The genes for SpyCatcher-fused influenza M2e or HA2 antigens were codon-optimized for *E. coli* expression and synthesized by GenScript (USA). The sequence of N- and C-terminally truncated, 84-amino-acid-long SpyCatcher [39], was used in the constructs. We included an N-terminal HisTag in SpyCatcher and made it cleavable by including a TEV protease site. The antigens were fused to the C-terminus of SpyCatcher via a two-residue (LE) linker, which makes up an XhoI restriction site on the DNA level and allows for convenient replacement of the antigen. For the ELISA assays, we ordered a plasmid encoding HA2 without the SpyCatcher fusion. GenScript prepared it by restriction-ligation and subcloning of the SpyCatcher-HA2 plasmid. The amino acid sequences of the proteins produced during this study are shown in Additional file 1: Table S1. The genes were subcloned into the pET-11b (+) plasmid under the strong T7 promoter and sequence-verified.

To construct a gene encoding SpyTag-noro-VLP, the DNA sequence of SpyTag was inserted into the C-terminus of VP1 from norovirus strain Hu/GII.4/Sydney/NSW0514/2012/AU (GenBank accession no. AFV08795). SpyTag is separated from VP1 by a 4-residue linker (TSGG), containing a unique SpeI restriction site. GeneArt (Germany) codon-optimized the SpyTag-noro-VLP gene for insect cell expression and synthesized and subcloned it into the pFastBac Dual vector, under the polyhedrin promoter. High-titer baculovirus stock expressing the SpyTag-noro-VLP gene was produced in Sf9 insect cells with the standard Bac-to-Bac protocol (Thermo Fisher Scientific, USA). Baculovirus titers were determined with the BacPAK Baculovirus Rapid Titer Kit (Takara Bio, Japan, #631406).

Expression and purification of SpyTagged norovirus-like particles

The SpyTag-noro-VLP-expressing baculovirus stock was used to infect Hi5 insect cells at a cell density of 2×10^6 cells/mL with a multiplicity of infection value of 1. The production medium was collected 4–6 days post infection and clarified by vacuum-filtering through Nalgene Rapid flow 0.2 μm filter (Thermo Fisher Scientific, USA, #566-0020) with the help of SartoClear Dynamics Lab FilterAid (Sartorius, Germany, SDLV-0500-10C-2). The clarified production medium was loaded on 30% sucrose cushions in PBS and centrifuged for 16–22 h in 104,000–175,000g. The resulting pellets were dissolved in sterile PBS and the concentrated SpyTag-noro-VLP was diluted in 20 mM phosphate buffer (pH 7.0) until conductivity reached < 5 mS/cm.

Next, the diluted supernatant was loaded on a pre-packed 5 mL HiTrap Q XL anion exchange column (GE Healthcare, USA, 17-5159-01) using a flow rate of 2 mL/min. The flow rate was raised to 3 mL/min for the rest of the chromatography purification. Weakly bound proteins were washed out with 5 column volumes (CV) of binding buffer (50 mM phosphate buffer, pH 7.0). The rest of proteins in the column were eluted by linearly increasing the concentration of elution buffer (binding buffer with 1 M NaCl) over 20 CV. The VLP-containing fractions were pooled, concentrated to 1–2 mg/mL and simultaneously buffer exchanged to PBS (pH 7.2) with VivaSpin Turbo 15 10,000 molecular weight cut-off (MWCO) PES tubes (Sartorius, Germany, #VS15T02). The product was sterile-filtered and stored at $+4$ °C until further use.

Expression and purification of SpyCatcher-fused influenza antigens

After sequential optimization of the most important parameters (strain, induction time point, temperature), BL21 Star (DE3) *E. coli* (Thermo Fisher Scientific, USA, #C601003) expressed the SpyCatcher-M2e fusion protein at $+25$ °C overnight. Induction was done with 1 mM IPTG when optical density ($\text{OD}_{600\text{nm}}$) reached ~ 0.6 . The bacteria were pelleted by centrifugation (10 min, 4000 g), resuspended in binding buffer (20 mM PBS, 20 mM imidazole, 500 mM NaCl; pH 7.4) and lysed with Avestin Emulsiflex C3 (ATA Scientific, Australia) homogenizer (2 rounds, 80 bar). The lysates were clarified by centrifugation (20,000g, 20 min, $+4$ °C) and loaded on an affinity column (5 mL HisTrap FF crude; GE Healthcare, USA, #17528601). Residual endotoxins were washed from the column-bound proteins with 50 CV 0.1% Triton X-114 in binding buffer (as described in [40]), and the target proteins were eluted with imidazole. We optimized SpyCatcher-H1F production likewise. After induction with 1 mM IPTG at $\text{OD}_{600\text{nm}} \approx 0.8$, it was expressed in C41

E. coli at $+18$ °C overnight and purified identically. Both proteins were dialyzed thrice into PBS with gradually decreasing concentrations of imidazole and EDTA, concentrated with appropriate VivaSpin columns if needed and, finally, flash-frozen for storage at -80 °C.

Conjugation of antigens on norovirus-like particles

The purified SpyTag-noro-VLPs were mixed with a two-fold molar excess of SpyCatcher-fused influenza antigens and incubated for 2 h at RT or overnight at $+4$ °C. To remove unreacted SpyCatcher-antigen, the product was dialyzed four times using Spectra/Por 1000 kDa MWCO membrane (Spectrum laboratories, USA, #131486) in at least 200-fold volume of PBS.

Characterization of purified proteins and particles

The size and polydispersity of the produced proteins and particles were measured by dynamic light scattering (DLS) with the Zetasizer Nano ZS (Malvern Instruments, UK). Protein purity and conjugation efficiency were estimated by densitometry analysis of Stain-free (Bio-Rad, USA) or silver stained SDS-PAGE gels with the Image Lab software (Bio-Rad, USA). For confirming the identity of the purified influenza antigens, we transferred the proteins from gel onto membrane with the semi-dry Trans-blot Turbo system (Bio-Rad, USA). The affinity tags in the proteins were identified by a mouse monoclonal anti-HisTag antibody (1:5000, Thermo Fisher Scientific, USA, #ma1-21315). The absence of baculovirus in the purified VLPs was confirmed with mouse monoclonal anti-gp64 antibody (1:2000, Santa Cruz Biotechnology, USA, #sc-65499). The bound primary antibodies were visualized by IRDye 800CW goat anti-mouse IgG (1:20,000, LI-COR Biosciences, USA, #926–32210) secondary antibody and the Odyssey CLx instrument (LI-COR Biosciences, USA).

F200 S/TEM (Jeol, Japan) transmission electron microscope (TEM) was used to examine the morphology and size of noro-VLPs after negative staining with 1% uranyl acetate. For size distribution analysis, images of $n > 100$ particles of each class were measured with Fiji ImageJ software [41] by manually outlining each particle, using the software's area function and calculating the diameter of an equivalent circle based on the area. Before analysis, the image files and folders were encoded to blind the measurer. Pierce BCA protein assay (Thermo Fisher Scientific, USA, #23252) was used to measure total protein concentrations in preparations. Endotoxin concentrations were determined with Pierce LAL Chromogenic Endotoxin Quantitation Kit (Thermo Fisher Scientific, USA, #88282). The amount of residual DNA was measured with the Quant-iT dsDNA high sensitivity kit (Thermo Fisher Scientific, USA, #Q33120).

The thermal and pH stability of the decorated VLP particles was characterized by differential scanning fluorimetry (DSF), as described in [42]. Briefly, SYPRO Orange (Thermo Fisher Scientific, USA, S6650), a fluorescence dye that binds to hydrophobic amino acid residues, was used to analyze the unfolding or denaturation of the VLPs to study the conformational stability of the vaccines. The fluorescence intensity of the dye in the presence of the vaccines was plotted as a function of the temperature, and melting temperatures (T_m) of the vaccines were derived from the inflection points of the transition curve using the Boltzmann equation [43]. Before pH stability studies, native and SpyTagged noro-VLP were dialyzed three times (final dialysis overnight) into 20 mM phosphate-citrate buffer, pH 3, 5.5 or 8.

Immunizations

Specific pathogen-free female BALB/c OlaHsd mice, aged 6 weeks (Envigo, Horst, the Netherlands), were randomly divided into five groups (I–V, 4–5 mice/experimental group) and acclimatized under controlled specific conditions for a week before starting the study. The animals were immunized at study weeks 0 and 3 intramuscularly (i.m.) at the right caudal thigh muscle with SpyTagged noro-VLPs, influenza antigens presented on noro-VLPs or SpyCatcher-fused influenza antigens (Table 1). I.m. injection was chosen to mimic human influenza vaccines currently in use, but at the same time it restricted our maximum dose volume to 50 μ L. Our hypothesis at the time was that the SpyCatcher-antigen proteins by themselves would be very poor as immunogens, so we tried rather high doses of them to be able to claim so. The antigen doses indicated in Table 1 were calculated by multiplying total protein dose (measured by BCA) with the proportion of the antigen protein in the preparation, considering the estimated conjugation efficiency and the antigen's mass, compared to the mass of other proteins in the particle system. For example, HA2-noro-VLP was diluted in PBS to the concentration of 0.3 mg/mL to reach a total protein mass of 15 μ g in a dose sized 50 μ L. Based on SDS-PAGE densitometry, 51% of all protein in the HA2-noro-VLP preparation was HA2-noro-VP1, while the rest was unconjugated noro-VP1. The molecular masses of noro-VP1, SpyCatcher and HA2 are 61, 15.50 and 15.48 kDa, respectively. Thus, the specific mass of HA2 in the dose can be calculated as follows: $51\% * 15\mu\text{g} * (\frac{15.48\text{kDa}}{(61+15.50+15.48)\text{kDa}}) = 1.3\mu\text{g}$. No external adjuvants were included in any vaccine formulation. Immunizations were performed under general anesthesia by inhalation of isoflurane (Attane vet, Vet Medic Animal Health Oy, Parola, Finland, #AP/DRUGS/220/96). Whole blood was collected at the time of sacrifice (study week 5) and processed according to the previously published procedure [44].

ELISA

Sera of individual mice were tested in enzyme-linked immunosorbent assay (ELISA) for the presence IgG antibodies against HA2, Spycatcher-HA2 and Spycatcher-M2e, as described earlier [45]. Briefly, half-area polystyrene 96-well-plates (Corning Inc., #3690) were coated with 50 ng of HA2 or 500 ng of SpyCatcher-fused protein per well. Antigen-specific IgG antibodies in the sera were detected with horseradish peroxidase-conjugated anti-mouse IgG (Sigma-Aldrich, Cat. A4416) and SIGMA FAST OPD substrate (Sigma-Aldrich, Cat. P9187). Optical densities at 490 nm (OD_{490}) were measured with a microplate reader (Victor², PerkinElmer, USA). Endpoint titers were defined as the reciprocal of the highest serum dilution with an OD_{490} above the positivity cut-off value ($>0.1 OD_{490}$ unit). The difference between non-parametric observations in independent vaccine groups was determined with the Mann–Whitney U test. For data analysis, we used GraphPad Prism software, version 8.4.2, and defined that $p < 0.05$ indicates statistically significant difference.

Supplementary Information

The online version contains supplementary material available at <https://doi.org/10.1186/s12951-021-00772-0>.

Additional file 1: Figures S1–S5 and Table S1. The figures provide additional results and graphical presentations from characterization of the used vaccine candidates and their components. The amino acid sequences of the used vaccine components are listed in Table S1.

Acknowledgements

The technical assistance and guidance given by Niklas Kähkönen, Ulla Kiiskinen, Merja Jokela, Sanna Kavén and Eeva Jokela is gratefully acknowledged. This work made use of Tampere Microscopy Center facilities at Tampere University. Mari Honkanen from TMC in particular deserves our gratitude for her efforts in providing training on the TEM instrument. We acknowledge Biocenter Finland for infrastructure support.

Authors' contributions

VB, VH and OL conceived the original idea for the project. VB, VH, OL and MH developed the idea together into the final research plan. MH, VH, OL and VL designed all experiments except for the immunizations and immunological studies. VL produced the vaccines and performed most experiments in the supervision of MH, VH and MP. VL, MH, VH and OL analyzed and interpreted the results. VB designed the immunizations and immunological studies together with SH. SH performed these tests and analyses. SH and VB analyzed and interpreted the results. VL drafted the manuscript and figures. All authors discussed the results and commented on the manuscript to help shape its final version. All authors read and approved the final manuscript.

Funding

We thank the foundations for Research on Viral diseases, V.A. Kotilainen and Onni and Hilja Tuovinen for the grants they provided to support the early steps of this work, the Academy of Finland for financial support [Projects 309455 (MH) and 295814 (MP)]. The work was also funded by the Competitive State Research Financing of the Expert Responsibility Area of Tampere University Hospital (MP), the Competitive State Research Financing of the Expert Responsibility Area of Fimlab Laboratories, Tays Support Foundation (MP), Tampere Tuberculosis Foundation (MP) and the Cancer Society of Finland (MP).

Availability of data and materials

The datasets used and/or analyzed during the current study are available from the corresponding author on reasonable request.

Ethics approval and consent to participate

Experimental procedures conducted were in accordance with the regulations and guidelines of the Finnish National Experiment Board (Permission number ESAVI/10800/04.10.07/2016). All efforts were made to minimize animal suffering and to reduce the number of animals used. The welfare of the animals was monitored throughout the experiment.

Consent for publication

Not applicable.

Competing interests

The authors declare that they have no competing interests.

Author details

¹ Faculty of Medicine and Health Technology, Tampere University, 33014 Tampere, Finland. ² Vaccine Development and Immunology/Vaccine Research Center, Faculty of Medicine and Health Technology, Tampere University, Tampere, Finland. ³ Fimlab Laboratories, Tampere, Finland.

Received: 27 August 2020 Accepted: 8 January 2021

Published online: 19 January 2021

References

- Kang SM, Kim MC, Compans RW. Virus-like particles as universal influenza vaccines. *Expert Rev Vaccines*. 2012;11:995–1007. <https://doi.org/10.1586/erv.12.70>.
- WHO. Influenza (Seasonal). 2018. [https://www.who.int/news-room/fact-sheets/detail/influenza-\(seasonal\)](https://www.who.int/news-room/fact-sheets/detail/influenza-(seasonal)). Accessed 14 May 2020.
- Hannoun C. The evolving history of influenza viruses and influenza vaccines. *Expert Rev Vaccines*. 2013;12(9):1085–94. <https://doi.org/10.1586/14760584.2013.824709>.
- Mohsen MO, Zha L, Cabral-Miranda G, Bachmann MF. Major findings and recent advances in virus-like particle (VLP)-based vaccines. *Semin Immunol*. 2017;34:123–32. <https://doi.org/10.1016/j.smim.2017.08.014>.
- Mateu MG. Virus engineering: functionalization and stabilization. *Protein Eng Des Sel*. 2011;24(1–2):53–63. <https://doi.org/10.1093/protein/gzq069>.
- Koho T, Ihalainen TO, Stark M, Uusi-Kerttula H, Wieneke R, Rahikainen R, et al. His-tagged norovirus-like particles: a versatile platform for cellular delivery and surface display. *Eur J Pharm Biopharm*. 2015;96:22–31. <https://doi.org/10.1016/j.ejpb.2015.07.002>.
- Zakeri B, Fierer JO, Celik E, Chittock EC, Schwarz-Linek U, Moy VT, et al. Peptide tag forming a rapid covalent bond to a protein, through engineering a bacterial adhesion. *Proc Natl Acad Sci U S A*. 2012;109:690. <https://doi.org/10.1073/pnas.1115485109>.
- Ebrahimi SM, Tebianian M. Influenza A viruses: why focusing on M2e-based universal vaccines. *Virus Genes*. 2011;42:1–8. <https://doi.org/10.1007/s11262-010-0547-7>.
- Valkenburg SA, Mallajosyula VV, Li OT, Chin AW, Carnell G, Temperton N, et al. Stalking influenza by vaccination with pre-fusion headless HA minisystem. *Sci Rep*. 2016;6:22666. <https://doi.org/10.1038/srep22666>.
- Deng L, Cho KJ, Fiers W, Saelens X. M2e-Based Universal Influenza A Vaccines. *Vaccines (Basel)*. 2015;3:105–36. <https://doi.org/10.3390/vaccines3010105>.
- Huhti L, Tamminen K, Vesikari T, Blazevic V. Characterization and immunogenicity of norovirus capsid-derived virus-like particles purified by anion exchange chromatography. *Arch Virol*. 2013;158:933–42. <https://doi.org/10.1007/s00705-012-1565-7>.
- Mallajosyula VV, Citron M, Ferrara F, Lu X, Callahan C, Heidecker GJ, et al. Influenza hemagglutinin stem-fragment immunogen elicits broadly neutralizing antibodies and confers heterologous protection. *Proc Natl Acad Sci U S A*. 2014;111:2514. <https://doi.org/10.1073/pnas.1402766111>.
- Brune KD, Leneghan DB, Brian IJ, Ishizuka AS, Bachmann MF, Draper SJ, et al. Plug-and-Display: decoration of Virus-Like Particles with isopeptide bonds for modular immunization. *Sci Rep*. 2016;6:19234. <https://doi.org/10.1038/srep19234>.
- Prasad BV, Rothnagel R, Jiang X, Estes MK. Three-dimensional structure of baculovirus-expressed Norwalk virus capsids. *J Virol*. 1994;68(8):5117–25. <https://doi.org/10.1128/JVI.68.8.5117-5125.1994>.
- Brito LA, Singh M. Acceptable levels of endotoxin in vaccine formulations during preclinical research. *J Pharm Sci*. 2011;100(1):34–7. <https://doi.org/10.1002/jps.22267>.
- Ausar SF, Foubert TR, Hudson MH, Vedvick TS, Middaugh CR. Conformational stability and disassembly of Norwalk virus-like particles Effect of pH and temperature. *J Biol Chem*. 2006;281(28):19478–88. <https://doi.org/10.1074/jbc.M603313200>.
- Traynor K. First recombinant flu vaccine approved. *Am J Health Syst Pharm*. 2013;70:382. <https://doi.org/10.2146/news130016>.
- Quan FS, Lee YT, Kim KH, Kim MC, Kang SM. Progress in developing virus-like particle influenza vaccines. *Expert Rev Vaccines*. 2016;15:1281–93. <https://doi.org/10.1080/14760584.2016.1175942>.
- Thrane S, Janitzek CM, Matondo S, Resende M, Gustavsson T, de Jongh WA, et al. Bacterial superglue enables easy development of efficient virus-like particle based vaccines. *J Nanobiotechnol*. 2016;14:30. <https://doi.org/10.1186/s12951-016-0181-1>.
- Pardee K, Slomovic S, Nguyen PQ, Lee JW, Donghia N, Burrill D, et al. Portable, on-demand biomolecular manufacturing. *Cell*. 2016;167(1):248–59. <https://doi.org/10.1016/j.cell.2016.09.013>.
- Keeble AH, Turkki P, Stokes S, Anuar IN, Rahikainen R, Hytönen VP, et al. Approaching infinite affinity through engineering of peptide–protein interaction. *Proc Natl Acad Sci USA*. 2019;116(52):26523–33. <https://doi.org/10.1073/pnas.1909653116>.
- Huhti L, Blazevic V, Nurminen K, Koho T, Hytönen VP, Vesikari T. A comparison of methods for purification and concentration of norovirus GII-4 capsid virus-like particles. *Arch Virol*. 2010;155(11):1855–8. <https://doi.org/10.1007/s00705-010-0768-z>.
- Koho T, Koivunen MR, Oikarinen S, Kummola L, Mäkinen S, Mahonen AJ, et al. Coxsackievirus B3 VLPs purified by ion exchange chromatography elicit strong immune responses in mice. *Antiviral Res*. 2014;104:93–101. <https://doi.org/10.1016/j.antiviral.2014.01.013>.
- Milián E, Kamen AA. Current and emerging cell culture manufacturing technologies for influenza vaccines. *Biomed Res Int*. 2015;2015:504831. <https://doi.org/10.1155/2015/504831>.
- Marini A, Zhou Y, Li Y, Taylor IJ, Leneghan DB, Jin J, et al. A Universal plug-and-display vaccine carrier based on HBsAg VLP to maximize effective antibody response. *Front Immunol*. 2019;10:2931. <https://doi.org/10.3389/fimmu.2019.02931>.
- Sharma J, Shephardson K, Johns LL, Wellham J, Avera J, Schwarz B, et al. A self-adjuvanted, modular, antigenic vlp for rapid response to influenza virus variability. *ACS Appl Mater Interfaces*. 2020;12(16):18211–24. <https://doi.org/10.1021/acsmi.9b21776>.
- Koho T, Huhti L, Blazevic V, Nurminen K, Butcher SJ, Laurinmäki P, et al. Production and characterization of virus-like particles and the P domain protein of GII.4 norovirus. *J Virol Methods*. 2012;179:1–7. <https://doi.org/10.1016/j.jviromet.2011.05.009>.
- Rohovie MJ, Nagasawa M, Swartz JR. Virus-like particles: Next-generation nanoparticles for targeted therapeutic delivery. *Bioeng Transl Med*. 2017;2(1):43–57. <https://doi.org/10.1002/btm2.10049>.
- Hankaniemi MM, Stone VM, Andrejef T, Heinimäki S, Siiofy-Khojine A, Marjomäki V, et al. Formalin treatment increases the stability and immunogenicity of coxsackievirus B1 VLP vaccine. *Antiviral Res*. 2019;171:104595. <https://doi.org/10.1016/j.antiviral.2019.104595>.
- Keeble AH, Banerjee A, Ferla MP, Reddington SC, Anuar IN, Howarth M. Evolving accelerated amidation by spytag/spycatcher to analyze membrane dynamics. *Angew Chem Int Ed*. 2017;56(52):16521–5. <https://doi.org/10.1002/anie.201707623>.
- Schoene C, Fierer JO, Bennett SP, Howarth M. SpyTag/SpyCatcher cyclization confers resilience to boiling on a mesophilic enzyme. *Angew Chem Int Ed Engl*. 2014;53(24):6101–4. <https://doi.org/10.1002/anie.201402519>.
- Sutton TC, Chakraborty S, Mallajosyula VVA, Lamirande EW, Ganti K, Bock KW, et al. Protective efficacy of influenza group 2 hemagglutinin stem-fragment immunogen vaccines. *NPJ Vaccines*. 2017;35:2. <https://doi.org/10.1038/s41541-017-0036-2>.
- Liu Z, Zhou H, Wang W, Tan W, Fu YX, Zhu M. A novel method for synthetic vaccine construction based on protein assembly. *Sci Rep*. 2014;4:7266. <https://doi.org/10.1038/srep07266>.

34. Tissot AC, Renhofa R, Schmitz N, Cielens I, Meijerink E, Ose V, et al. Versatile virus-like particle carrier for epitope based vaccines. *PLoS ONE*. 2010. <https://doi.org/10.1371/journal.pone.0009809>.
35. Ibañez LI, Roose K, De Filette M, Schotsaert M, De Sloovere J, Roels S, et al. M2e-displaying virus-like particles with associated RNA promote T helper 1 type adaptive immunity against influenza A. *PLoS ONE*. 2013;5(3):e9809. <https://doi.org/10.1371/journal.pone.0059081>.
36. De Filette M, Min Jou W, Birkett A, Lyons K, Schultz B, Tonkyro A, et al. Universal influenza A vaccine: optimization of M2-based constructs. *Virology*. 2005;337(1):149–61. <https://doi.org/10.1016/j.virol.2005.04.004>.
37. Yong CY, Yeap SK, Ho KL, Omar AR, Tan WS. Potential recombinant vaccine against influenza A virus based on M2e displayed on nodaviral capsid nanoparticles. *Int J Nanomed*. 2015;10:2751–63. <https://doi.org/10.2147/IJN.S77405>.
38. Andersson AC, Buldun CM, Pattinson DJ, Draper SJ, Howarth M. Snoop-Ligase peptide-peptide conjugation enables modular vaccine assembly. *Sci Rep*. 2019;9(1):4625. <https://doi.org/10.1038/s41598-019-40985-w>.
39. Li L, Fierer JO, Rapoport TA, Howarth M. Structural analysis and optimization of the covalent association between SpyCatcher and a peptide Tag. *J Mol Biol*. 2014;426(2):309–17. <https://doi.org/10.1016/j.jmb.2013.10.021>.
40. Reichelt P, Schwarz C, Donzeau M. Single step protocol to purify recombinant proteins with low endotoxin contents. *Protein Expr Purif*. 2006;46(2):483–8. <https://doi.org/10.1016/j.pep.2005.09.027>.
41. Schindelin J, Arganda-Carreras I, Frise E, Kaynig V, Longair M, Pietzsch T, et al. Fiji: an open-source platform for biological-image analysis. *Nat Methods*. 2012;9(7):676–82. <https://doi.org/10.1038/nmeth.2019>.
42. Hankaniemi MM, Stone VM, Sioofy-Khojine A, Heinimäki S, Marjomäki V, Hyöty H, et al. A comparative study of the effect of UV and formalin inactivation on the stability and immunogenicity of a Coxsackievirus B1 vaccine. *Vaccine*. 2019;37(40):5962–71. <https://doi.org/10.1016/j.vaccine.2019.08.037>.
43. Niesen FH, Berglund H, Vedadi M. The use of differential scanning fluorimetry to detect ligand interactions that promote protein stability. *Nat Protoc*. 2007;2(9):2212–21. <https://doi.org/10.1038/nprot.2007.321>.
44. Tamminen K, Huhti L, Koho T, Lappalainen S, Hytonen VP, Vesikari T, et al. A comparison of immunogenicity of norovirus GI-4 virus-like particles and P-particles. *Immunology*. 2012;135(1):89–99. <https://doi.org/10.1111/1/j.1365-2567.2011.03516.x>.
45. Blazevic V, Lappalainen S, Nurminen K, Huhti L, Vesikari T. Norovirus VLPs and rotavirus VP6 protein as combined vaccine for childhood gastroenteritis. *Vaccine*. 2011;29(45):8126–33. <https://doi.org/10.1016/j.vaccine.2011.08.026>.
46. Liu C, Chin JX, Lee D. SynLinker: an integrated system for designing linkers and synthetic fusion proteins. *Bioinformatics*. 2015;31(22):3700–2. <https://doi.org/10.1093/bioinformatics/btv447>.
47. The PyMOL Molecular Graphics System, Version 2.3.4 Schrödinger, LLC.

Publisher's Note

Springer Nature remains neutral with regard to jurisdictional claims in published maps and institutional affiliations.

Ready to submit your research? Choose BMC and benefit from:

- fast, convenient online submission
- thorough peer review by experienced researchers in your field
- rapid publication on acceptance
- support for research data, including large and complex data types
- gold Open Access which fosters wider collaboration and increased citations
- maximum visibility for your research: over 100M website views per year

At BMC, research is always in progress.

Learn more biomedcentral.com/submissions



PUBLICATION II

Antigenicity and immunogenicity of HA2 and M2e influenza virus antigens conjugated to norovirus-like, VP1 capsid-based particles by the SpyTag/SpyCatcher technology

Heinimäki S, Lampinen V, Tamminen K, Hankaniemi MM, Malm M, Hytönen VP, Blazevic V

Virology. 2022; 566
doi: 10.1016/j.virol.2021.12.001

Publication reprinted with the permission of the copyright holders (CC BY 4.0).



Antigenicity and immunogenicity of HA2 and M2e influenza virus antigens conjugated to norovirus-like, VP1 capsid-based particles by the SpyTag/SpyCatcher technology

Suvi Heinimäki^{a,*}, Vili Lampinen^b, Kirsi Tamminen^a, Minna M. Hankaniemi^b, Maria Malm^a, Vesa P. Hytönen^{b,c}, Vesna Blazevic^a

^a Vaccine Development and Immunology/Vaccine Research Center, Faculty of Medicine and Health Technology, Tampere University, Tampere, Finland

^b Protein Dynamics Group, Faculty of Medicine and Health Technology, Tampere University, Tampere, Finland

^c Finlab Laboratories, Tampere, Finland

ARTICLE INFO

Keywords:

Norovirus
Virus-like particle
VLP
Platform
Vaccine
HA2
M2e
Influenza virus
SpyTag/SpyCatcher

ABSTRACT

Virus-like particles (VLPs) modified through different molecular technologies are employed as delivery vehicles or platforms for heterologous antigen display. We have recently created a norovirus (NoV) VLP platform, where two influenza antigens, the extracellular domain of matrix protein M2 (M2e) or the stem domain of the major envelope glycoprotein hemagglutinin (HA2) are displayed on the surface of the NoV VLPs by SpyTag/SpyCatcher conjugation. To demonstrate the feasibility of the platform to deliver foreign antigens, this study examined potential interference of the conjugation with induction of antibodies against conjugated M2e peptide, HA2, and NoV VLP carrier. High antibody response was induced by HA2 but not M2e decorated VLPs. Furthermore, HA2-elicited antibodies did not neutralize the homologous influenza virus *in vitro*. Conjugated NoV VLPs retained intact receptor binding capacity and self-immunogenicity. The results demonstrate that NoV VLPs could be simultaneously used as a platform to deliver foreign antigens and a NoV vaccine.

1. Introduction

In the absence of an effective vaccine, new and reemerging pathogens such as influenza viruses and coronaviruses can cause rapidly spreading epidemics or pandemics with extensive morbidity and mortality rates (Jin et al., 2020). Modern vaccine technologies provide tools to develop novel vaccines containing only the essential antigenic parts of the pathogens to address the safety and production challenges encountered with traditional vaccines derived from live attenuated or inactivated whole pathogens (Karch and Burkhard, 2016). (Poly)saccharides, protein domains or even short immunodominant peptides derived from viruses or bacteria might be sufficient to induce protective immunity when displayed on the surface of larger carriers (Tan et al., 2011; Tinto et al., 2015).

Self-assembling non-infectious protein-derived nanoparticles, such as virus-like particles (VLPs), have emerged as an attractive technology in vaccine development. The intrinsic immunogenic properties of the VLPs make them promising stand-alone vaccine candidates for many diseases (Karch and Burkhard, 2016). These particles can also be

exploited as delivery vehicles or platforms for heterologous antigen display (Kushnir et al., 2012), conjugating vaccine antigens to nanoparticle scaffold through different coupling approaches including genetic fusion (Neiryneck et al., 1999), chemical cross-linking (Peacey et al., 2007) or isopeptide bioconjugation (e.g. the SpyTag–SpyCatcher technology) (Brune et al., 2016). Nanoparticles with repetitive structures enable expression of conjugated foreign antigens on the particle surface at high density and thus more potent antigen presentation and induction of immune responses (Fifis et al., 2004). This approach allows rapid and simple modification of the selected vaccine antigens, facilitating the development of novel vaccines in the threat of (re)emerging pandemics without a need for laborious and time-consuming pathogen cultivation and inactivation/attenuation processes. Several chimeric VLPs or other subviral particles carrying different drug substances and vaccine antigens have been created from e.g. hepatitis viruses (Neiryneck et al., 1999), human papillomavirus (Murata et al., 2009), murine polyomavirus (Wibowo et al., 2013), rotavirus (Peralta et al., 2009; Tamminen et al., 2021; Philip and Patton, 2021), as well as bacteriophages (Tissot et al., 2010), and some of these have been demonstrated to be

* Corresponding author. Vaccine Development and Immunology/Vaccine Research Center, Tampere University, Arvo Ylpön katu 34, FI-33520, Tampere, Finland.
E-mail address: suvi.heinimaki@tuni.fi (S. Heinimäki).

auspicious vaccine candidates in different stages of clinical trials.

Norovirus (NoV) is a common cause of acute gastroenteritis, affecting millions of people across all age groups worldwide. The current NoV vaccine development relies mainly on extensively studied ~30–40 nm VLPs (Atmar et al., 2011; Blazevic et al., 2011) formed by a shell (S) and a protruding domain (P) of a major capsid protein VP1 (Prasad et al., 1999). The feasibility of NoV VLPs as antigen carriers has been tested by non-covalent conjugation of foreign antigens to VLPs exploiting the affinity between polyhistidine-tag and *tris*-nitrilotriacetic acid (Koho et al., 2015). Further, two ~20 nm NoV derived subviral particles, P or S particles, consisting of only P or S domain of VP1, have been successfully implemented as platforms for presentation of short peptide epitopes and large protein antigens (Xia et al., 2018; Jiang et al., 2015). The platform technology, including NoV P particles, has been applied in the development of universal influenza vaccine candidates (Neiryck et al., 1999; Xia et al., 2011) able to induce broadly cross-protective immune responses against highly conserved regions of influenza viruses, aiming at substituting the current seasonal influenza vaccines that provide only strain-specific protection and are inefficient in protection against antigenically distinct strains (Jazayeri and Poh, 2019). Thereby, the influenza antigens employed are mostly based on the proximal stem domain of the major envelope glycoprotein hemagglutinin (HA2) or the extracellular domain of matrix protein M2 (M2e), HA2 inducing broadly neutralizing and cross-protective antibodies (Lee et al., 2013; Darricarrère et al., 2021; Nachbagauer et al., 2021) and M2e cross-protective antibodies and enabling activation of CD8⁺ T cells (Neiryck et al., 1999; Deng et al., 2015).

We have recently constructed a stable modular vaccine platform based on NoV VLPs using the isopeptide-bond-forming SpyCatcher/SpyTag pair and the two universal influenza vaccine antigens as model antigens (Lampinen et al., 2021). Both, HA2 fragment and M2e peptide, were demonstrated to be successfully presented by the NoV VLP platform, and NoV VLPs conjugated with HA2 or M2e were immunogenic in mice inducing antibodies against SpyCatcher fused influenza antigens, providing the first evidence of NoV VLP platform feasibility. The present study was aimed to further investigate induction of influenza-specific immune responses and functionality of the induced immunity as well as the effect of SpyTag/SpyCatcher conjugation on NoV-specific immunity.

2. Materials and methods

2.1. Antigenic formulations

NoV capsid VLPs derived from strains GII.4 Sydney (Syd; 2012, GenBank accession no AFV08795.1), GII.4 New Orleans (NO; 2010, accession no GU445325) and GII.12 (1998, acc. no. AJ277618) were produced in insect cells using baculovirus expression vector system as previously described (Blazevic et al., 2011). The VLPs were purified by ultracentrifugation through discontinuous sucrose gradients (10–60%) (Huhti et al., 2010) and consecutive ultrafiltration method (Tamminen et al., 2020) and confirmed for purity, antigenicity, and morphology with the procedures described in detail elsewhere (Blazevic et al., 2011; Tamminen et al., 2020). NoV VLPs were employed as antigens in immunological assays and NoV Syd VLPs were also used as control vaccine antigens in animal immunizations.

NoV VLPs were decorated with M2e or HA2 influenza antigens employing a modification (Lampinen et al., 2021) of SpyTag/SpyCatcher strategy originally described by Brune and colleagues (Brune et al., 2016). Briefly, for modular VLP formation, SpyTagged NoV GII.4 Syd VLPs (NoV VLP-SpyTag) were expressed and purified separately from SpyCatcher-fused antigens prior to conjugation of the components via spontaneous isopeptide bond formation. SpyTagged NoV VLPs were produced by expression of baculovirus recombinants in insect cells and purified by tangential flow filtration and ultracentrifugation through a 30% sucrose cushion as well as anion exchange chromatography

(Lampinen et al., 2021). Instead, SpyCatcher-fused M2e (SpyCatcher-M2e) and HA2 (SpyCatcher-HA2) as well as HA2 without the SpyCatcher fusion (rHA2) were equipped with polyhistidine-tag, expressed in *E. coli* and purified with Ni-NTA affinity chromatography. M2e and HA2 antigens were derived from the human influenza A virus consensus sequence of the first 24 N-terminal amino acids (aa) of matrix protein M2 (Neiryck et al., 1999; Deng et al., 2015) and the influenza A virus H1N1 HA (A/Puerto Rico/8/34 subtype) stem fragment (140 aa) consisting of aa 18–41 and aa 290–323 of subunit HA1 and aa 41–113 of subunit HA2 connected by GSA and GSAGSA linkers (Mallajosyula et al., 2014). Each SpyTag/SpyCatcher component was confirmed for stability, morphology, size, purity, and identity as demonstrated in our recent publication (Lampinen et al., 2021).

A 23-mer consensus peptide (SLLTEVETPIRNEWGCRNDSSD) derived from M2e protein of human H1N1, H2N2 and H3N2 influenza A viruses (Deng et al., 2015) was synthesized by Synpeptide Co. Ltd. (Shanghai, China). Recombinant HA (rHA, extracellular domain (aa 1–528) of HA, Influenza A, subtype H1N1 A/Puerto Rico/8/1934) was purchased from Sino Biological (Beijing, China). The influenza type A virus, A/PR/8 [A/Puerto Rico/8/34(H1N1)], cultured in embryonated hen eggs (Blazevic et al., 2000), was used in focus reduction neutralization assay.




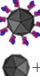

2.2. Mouse immunizations

Immunogenicity of the NoV VLPs conjugated with influenza HA2 or M2e antigens was assessed in randomly divided pathogen-free seven-weeks-old female BALB/c mice (Envigo, Horst, the Netherlands), acclimatized under controlled specific conditions for one week prior to experiments. Native NoV VLPs, SpyTagged NoV VLPs, a mixture of SpyCatcher-fused M2e and native NoV VLPs, M2e peptide formulated with Al(OH)₃ (Alhydrogel; InvivoGen, Toulouse, France) as well as carrier only (PBS; Lonza, Verviers, Belgium) served as control groups. Animals (4–5 mice/group) were immunized twice with intramuscular (im) injection into the right caudal thigh muscle at a 3-week interval (study weeks 0 and 3). Table 1 shows the employed antigenic formulations as well as the doses of immunogens in each experimental group. All immunizations were performed under isoflurane (Attane Vet®, Vet Medic Animal Health Oy, Parola, Finland) generated inhalation anesthesia. Mice were euthanized at study week 5 and whole blood was collected from each mouse. The serum was separated by centrifugation as previously described (Tamminen et al., 2012) and stored at –20 °C until further analysis.

2.3. Measurement of NoV-specific antibody responses

Antibody responses generated against NoV VLPs were determined by measuring NoV GII.4 Syd type-specific IgG antibody levels in serum samples of individual mice by enzyme-linked immunosorbent assay (ELISA) according to previously published procedures (Blazevic et al., 2011; Tamminen et al., 2012) and as outlined here. Half-area polystyrene plates (Corning Inc, Corning, NY) were coated with 50 ng of NoV Syd VLPs per well and anti-NoV IgG antibodies in serially twofold diluted serum specimens were detected with horseradish peroxidase (HRP)-conjugated goat anti-mouse IgG and FAST OPD-substrate (both purchased from Sigma-Aldrich, St Louis, MO). Optical density (OD) values at 490 nm (OD₄₉₀) were measured by a microplate reader (Victor², Perkin Elmer, Waltham, MA). Endpoint titers were expressed as the reciprocal of the highest serum dilution giving an OD₄₉₀ value above the set cut-off value (mean OD₄₉₀ of the negative control mice + 3 × SD and >0.1 OD₄₉₀). Negative samples were assigned with a reciprocal titer half of the starting dilution for statistical purposes. The results are expressed as geometric mean titers (GMTs) with 95% confidence intervals (CI).

Table 1
Experimental and control immunization groups.

Group	n of mice	Test article	Dose (μ g) Total	Dose (μ g) VLP ^a	Dose (μ g) HA2 ^a	Dose (μ g) M2e ^a	Graphical Structure
I	4	NoV VLP	10	10	–	–	
II	4	NoV VLP-SpyTag	25	25	–	–	
III	5	NoV VLP-HA2 (NoV VLP-SpyTag-SpyCatcher-HA2)	15	10	1.3	–	
IV	5	NoV VLP-M2e (NoV VLP-SpyTag-SpyCatcher-M2e)	50	40	–	1.2	
V	5	NoV VLP + SpyCatcher-M2e (mix)	10 + 100	10	–	12	
VI	4	M2e + Al(OH) ₃	50 + 100	–	–	50	–
VII	4	PBS	0	–	–	–	–

VLP, virus-like particle; HA2, hemagglutinin 2; M2e, extracellular domain of matrix protein M2, PBS, phosphate buffered saline.

^a Approximate molecular sizes: VLP 58 kD, HA2 16.5 kD, M2e 2.5 kD.

2.4. NoV VLP binding and blocking assays

The ability of SpyTagged NoV VLPs to bind to cellular binding ligands, histo-blood group antigens (HBGAs), was examined using two sources of HBGAs: pig gastric mucin (PGM) type III (Sigma Chemicals, St Louis, MO) and human type A saliva. HbGA binding assays were conducted using procedures described in detail elsewhere (Malm et al., 2018; Uusi-Kerttula et al., 2014). In brief, 96-well half-area polystyrene plates (Costar, Corning, NY) were coated with 2.5 μ g/mL PGM or 1:3000 diluted type A saliva from adult volunteers with previously determined ABO phenotype (Uusi-Kerttula et al., 2014). Binding of serially twofold diluted NoV GII.4 Syd VLPs, SpyTagged NoV GII.4 Syd VLPs as well as NoV GII.12 control VLPs (0.8–0.05 μ g/mL) was detected using human anti-NoV GII.4 or GII.12 detection serum collected from voluntary laboratory personnel (Nurminen et al., 2011) and the corresponding anti-human IgG HRP-conjugate (Novex; Thermo Fisher Scientific, Fremont, CA) followed by FAST OPD substrate. Results are expressed as the mean OD₄₉₀ of duplicate wells. OD₄₉₀ > 1.0 was interpreted as a strong binding (Uusi-Kerttula et al., 2014). Positive reactivity was defined as a mean OD₄₉₀ > 0.2.

To determine neutralization ability of NoV-specific antibodies, the ability of serum antibodies to inhibit the binding of NoV VLPs to HBGA, a blocking assay was conducted as a surrogate test for neutralization using PGM as the source of HBGAs (Malm et al., 2017). Briefly, NoV GII.4 Syd and GII.4 NO VLPs were preincubated with mouse sera serially diluted 2-fold from 1:100 (homologous GII.4 Syd blocking) or 1:20 (heterologous GII.4 NO blocking) and added to PGM coated plates. The PGM bound VLPs were detected with a combination of human GII.4 positive serum and anti-human HRP-conjugated secondary antibody according to the HBGA binding assays described above. The maximum binding (OD₄₉₀) was determined with VLPs without serum preincubation. The blocking indexes (%) were calculated as 100% – [(OD₄₉₀ sample/OD₄₉₀ max. binding) × 100%]. Half maximal inhibitory concentration (IC₅₀) of the blocking data was calculated from sigmoidal dose–response analysis of nonlinear data for each serum demonstrating \geq 50% blockade. A serum sample failing to block \geq 50% of the binding was considered negative for blocking antibodies and was assigned with the reciprocal titer of half of the starting dilution. The blocking data are expressed as the GMTs of the IC₅₀ values with 95% CI.

2.5. Measurement of influenza-specific antibody responses

Induction of influenza-specific immune responses by HA2 and M2e vaccine formulations was investigated in ELISA assays (Lampinen et al., 2021; Heinimäki et al., 2020). Anti-HA2, -HA and -M2e total IgG as well

as anti-HA2 and -HA IgG subtype antibodies were measured in the sera of mice as described above for NoV-specific responses (section 2.3), but the microtiter plates were coated with rHA2 (50 ng/well), rHA (50 ng/well), or M2e peptide (500 ng/well) and detection of antigen-specific antibodies were accomplished with a combination of anti-mouse IgG, IgG1 (Invitrogen, Carlsbad, CA) or IgG2a (Invitrogen) HRP conjugate and FAST OPD or TMB (Vector Laboratories, Burlingame, CA) substrate. TMB substrate was employed in detection of responses against rHA and M2e peptide. In those cases, the OD values were measured at 450 nm (OD₄₅₀) instead of 490 nm used for OPD.

2.6. Influenza focus reduction neutralization assay

To evaluate the neutralizing activity of the sera against influenza virus, a focus reduction neutralization assay was established by modifying the published procedures (Okuno et al., 1990). Madin-Darby canine kidney (MDCK) cells (Sigma-Aldrich) maintained in Minimum Essential Medium (MEM, Gibco) supplemented with 1% L-Glutamin, 1% PenStrep and 10% FBS (all from Sigma-Aldrich) were seeded (30000 cells/well) in 96-well cell-culture microplates (Nunc) and cultivated at +37 °C, 5% CO₂ until the cells reached confluency (2–3 d). Mouse sera diluted 1:25 were preincubated with ~100 focus forming units (ffu) per well of influenza virus stock (H1N1 A/Puerto Rico/8/1934) for 2 h at +37 °C. A repository serum originating from an adult volunteer described in NoV binding assay in the paragraph 2.4 (diluted 1:25) and monoclonal HA2 antibody (20 μ g/mL, Takara Bio, Kusatsu, Japan) were used as positive controls in the assay. The virus-serum mixes were then transferred (50 μ l/well) on top of MDCK monolayers and incubated for 1 h at +37 °C and 5% CO₂. Virus lacking serum and blank wells containing medium only were included in each plate. After incubation, the virus inocula were removed and the MEM washed cells were covered with an overlay (0.8% carboxymethylcellulose in MEM). The plates were incubated for ~20 h at +37 °C and 5% CO₂. Next day, the cells were fixed with 10% formalin and permeabilized with 1% Triton-X-100 (Sigma-Aldrich) followed by immunocolorimetric staining of the infected cells using 1:2000 diluted rabbit anti-HA IgG (Syno Biologicals) reacting with 1:3000 diluted anti-rabbit IgG-HRP (Abcam, Cambridge, UK). The infected cells were visualized using TrueBlue substrate (Sera Care, Milford, MA) and the foci were counted visually under an inverted light microscope (Nikon, Tokyo, Japan). The results are expressed as ffu/well.

2.7. Statistical analyses

Kruskal-Wallis H-test was used to compare the non-parametric

observations (the end-point titers and the IC_{50} values) between independent groups. The Wilcoxon signed-rank test was used to compare the non-parametric observations within a single experimental group (IgG1 and IgG2a titers). Paired samples *t*-test was used to assess the statistical differences of the mean OD-values (IgG1 and IgG2a levels) within a single experimental group. Statistical analyses were conducted using IBM SPSS statistics (SPSS, Chicago, USA) version 25. Statistical significance was defined at $p < 0.05$.

3. Results

3.1. NoV-specific immune responses

3.1.1. The induction of NoV-specific antibodies

The ability of conjugated VLPs to induce NoV-specific antibodies compared with the native VLPs was evaluated in an ELISA (Fig. 1). Mice receiving either native NoV VLPs (Fig. 1A), SpyTagged VLPs (Fig. 1B) or HA2 (Fig. 1C) or M2e (Fig. 1D) -conjugated VLPs generated a robust NoV-specific IgG response. Although different doses of VLPs were employed in different immunization groups (10–40 μ g, Table 1), appreciably high GMTs (reciprocal titer $>4.9 \log_{10}$) were detected in all groups receiving any of the VLP formulations. The conjugated VLPs induced comparable levels of antibodies to those observed with native VLPs ($p = 0.102$). This indicates that conjugation of VLPs with SpyTag or subsequent decoration of SpyTagged VLPs with influenza antigens did not impair induction of antibodies against NoV. Control mice receiving carrier only were negative for anti-NoV IgG antibodies (Fig. 1E).

3.1.2. Functionality of SpyTagged VLPs

To assess the effect of SpyTag insertion on NoV VLP functionality and integrity, ability of the conjugated antigen to bind HBGA receptors, was examined by binding of native (Fig. 2A) and conjugated VLPs (Fig. 2B) to PGM and human type A saliva. SpyTagged VLPs showed similar binding profile to native VLPs, both VLP preparations interacting equally efficiently with PGM and saliva in two repeated experiments. The results demonstrate that VLPs retained receptor binding capacity despite the SpyTag conjugation. As expected (Uusi-Kerttula et al., 2014), GII.12 VLPs used as a negative control failed to bind to the HBGAs tested in this binding assay (Fig. 2C).

3.1.3. Neutralization activity of the NoV-specific IgG

The ability of the induced antibodies to neutralize NoV was examined by measuring blocking activity of the immune sera against homologous NoV GII.4 Syd and heterologous NoV GII.4 NO VLPs with PGM-based HBGA blocking assay. All experimental groups receiving VLP formulations developed antibodies with strong homologous blocking ability with GMTs of IC_{50} values of 516 (95% CI 383–689) for native VLPs (Fig. 3A), 869 (95% CI 463–1631) for SpyTagged VLPs (Fig. 3B), 903 (95% CI 483–1688) for HA2-conjugated VLPs (Fig. 3C) and 1399

(95% CI 1268–1544) for M2e-conjugated VLPs (Fig. 3D). Although the highest blocking activity was observed in mice immunized with the M2e-conjugated VLPs, a group administered with the highest VLP dose (Table 1), the difference in the IC_{50} values between all four VLP groups tested was not statistically significant ($p = 0.059$). Similarly, comparable magnitudes of cross-blocking antibodies were detected in groups receiving native VLPs or any of the conjugated VLPs. The respective cross-blocking GMTs were 470 (95% CI 248–891) for native VLPs (Fig. 3A), 324 (95% CI 80–1302) for SpyTagged VLPs (Fig. 3B), 423 (95% CI 149–1203) for HA2-conjugated VLPs (Fig. 3C), and 991 (95% CI 843–1164) for M2e-conjugated VLPs (Fig. 3D). The negative control mice did not induce any blocking antibodies (Fig. 3E). Based on these results, display of SpyTag peptides on NoV VLPs or conjugation of influenza antigens on VLP via SpyTag/Catcher technology had no effect on ability of VLPs to generate NoV neutralizing antibodies.

3.2. Influenza-specific immune responses

3.2.1. Antibody responses against HA2

To examine induction of antibodies directed against HA2 displayed on NoV VLPs, the sera of mice immunized with HA2-conjugated VLPs were assayed for the presence of HA2-specific total IgG and IgG subtype antibodies. Strong IgG response against rHA2 with a GMT of $4.9 \log_{10}$ was detected after administration with HA2-conjugated VLPs, the IgG titers of individual mice ranging from 4.7 to $5.0 \log_{10}$ (Fig. 4A). Further, anti-HA2 IgG subtype analyses (IgG1 and IgG2a as hallmarks of respective Th2 and Th1 responses), showed induction of a mixed and balanced Th2- (Fig. 4B) and Th1-type (Fig. 4C) immune response with equally high magnitudes ($p = 0.492$) of IgG1 (GMT $4.9 \log_{10}$, 95% CI $4.8 \log_{10}$ – $5.1 \log_{10}$) and IgG2a (GMT $4.9 \log_{10}$, 95% CI $4.5 \log_{10}$ – $5.1 \log_{10}$) antibodies. Negative control mice receiving SpyTagged VLPs had no IgG (Fig. 4D), IgG1 (Fig. 4E) or IgG2a (Fig. 4F) antibodies against rHA2. Mice administered with M2e-conjugated VLPs were negative for anti-rHA2 antibodies (data not shown).

3.2.2. Antibody responses against HA

To investigate functionality of the induced HA2-specific antibodies, the immune sera were further assayed for the presence of IgG, IgG1, and IgG2a antibodies reactive with complete rHA-protein. As expected, HA2-conjugated VLPs induced responses against rHA (Fig. 5A). However, the level of the antibodies (OD 1.072 ± 0.248 at a 1:100 dilution) was considerably lower than the level detected against rHA2 (OD 2.806 ± 0.019 , Fig. 4A). Further, determination of anti-HA IgG subtypes confirmed a mixed Th2- (OD 0.459 ± 0.230) and Th1-type (OD 0.715 ± 0.352) response (Fig. 5A). Although VLPs conjugated with HA2 seemed to skew the HA-response slightly towards Th1-type, the difference was not significant ($p = 0.642$). No HA-specific IgG, IgG1 or IgG2a antibodies were detected in the sera of negative control mice receiving SpyTagged VLPs (Fig. 5A).

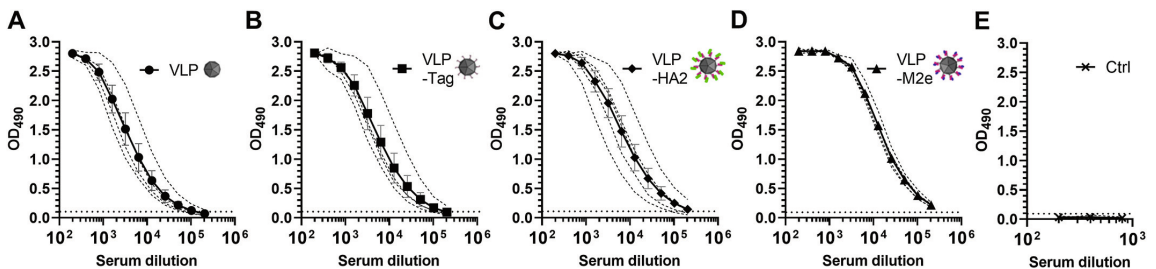


Fig. 1. Norovirus (NoV) -specific serum IgG antibody responses induced by conjugated NoV VLP formulations. Antibodies against homologous NoV Sydney VLP antigen in sera of mice following two immunizations with NoV VLPs (A), SpyTagged VLPs (B), NoV VLPs conjugated with HA2 (C), NoV VLPs conjugated with M2e (D) or carrier only (E). Shown are individual titration curves of each mouse (dashed lines) and mean titration curves (\pm SEM) of the experimental groups (solid lines with symbols). Horizontal dotted lines indicate the cut-off level ($OD_{490} \geq 0.1$).

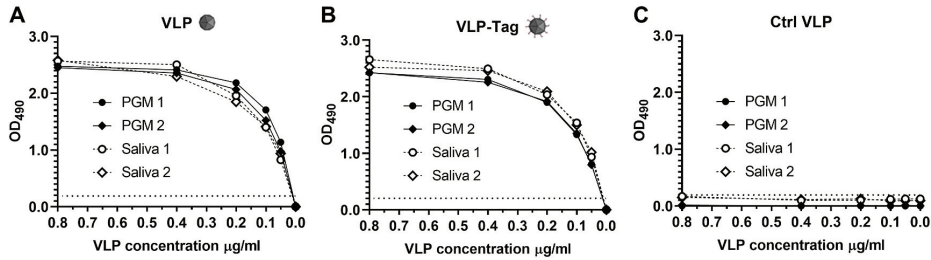


Fig. 2. Effect of SpyTag conjugation on NoV GII.4 Sydney VLP binding to different histo-blood group antigens (HBGAs). Binding of native NoV VLPs (A), SpyTagged NoV VLPs (B) and NoV GII.12 control VLPs (C) to HBGAs present in pig gastric mucin (PGM) and type A saliva (Saliva) was determined at different VLP concentrations in two independent experiments. Shown are OD₄₉₀ values of two repeated experiments (1 and 2).

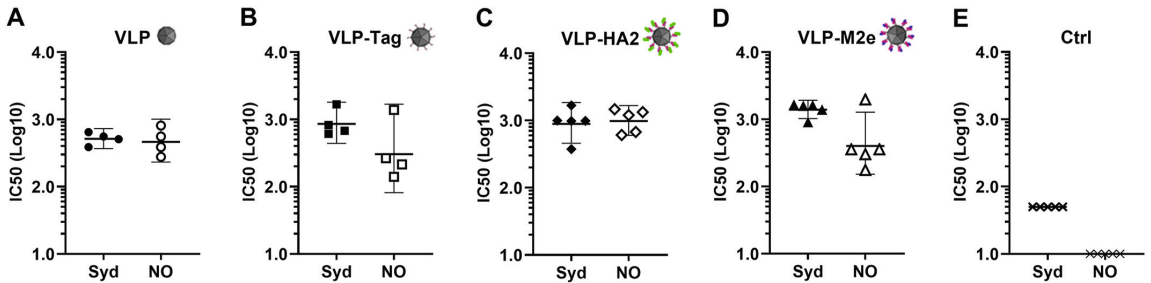


Fig. 3. Induction of NoV blocking (neutralizing) antibodies by decorated NoV VLP formulations. Homologous and heterologous blockage of NoV Sydney (Syd) and NoV New Orleans (NO) VLP binding to HBGAs present in pig gastric mucin (PGM) by serum antibodies following two immunizations with NoV VLPs (A), SpyTagged NoV VLPs (B), NoV VLPs decorated with HA2 (C), NoV VLPs decorated with M2e (D) or carrier only (E). Half maximal inhibitory concentration (IC₅₀) of each mouse is shown. Each symbol represents an individual animal. Bars indicate geometric mean values of the experimental groups with 95% confidence intervals. A titer of 50 (1.7 log₁₀) was assigned for sera with no detectable genotype-specific antibodies, being a half of the initial serum dilution in homologous blocking assay. A titer of 10 (log₁₀) was assigned for sera with no detectable cross-reactive antibodies, being a half of the initial serum dilution in heterologous blocking assay.

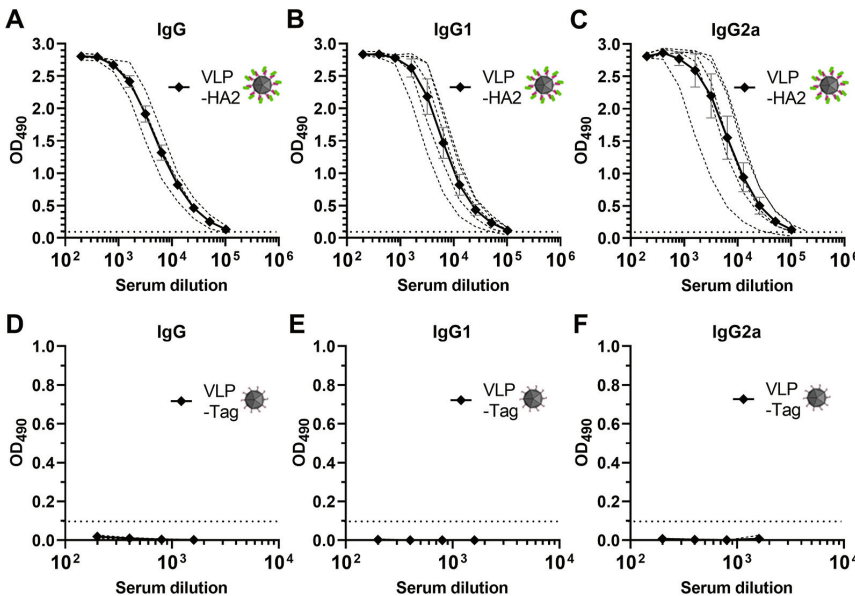


Fig. 4. Induction of influenza HA2-specific IgG and IgG subtype antibody responses. The sera of mice immunized twice with NoV VLPs decorated with HA2 (A–C) or SpyTagged NoV VLPs (D–F) were tested for IgG (A, D), IgG1 (B, E) and IgG2a (C, F) antibodies against rHA2. Shown are individual titration curves of each mouse (dashed lines) and mean titration curves (±SEM) of the experimental groups (solid lines with symbols). Horizontal dotted lines indicate the cut-off level (OD₄₉₀ ≥ 0.1).

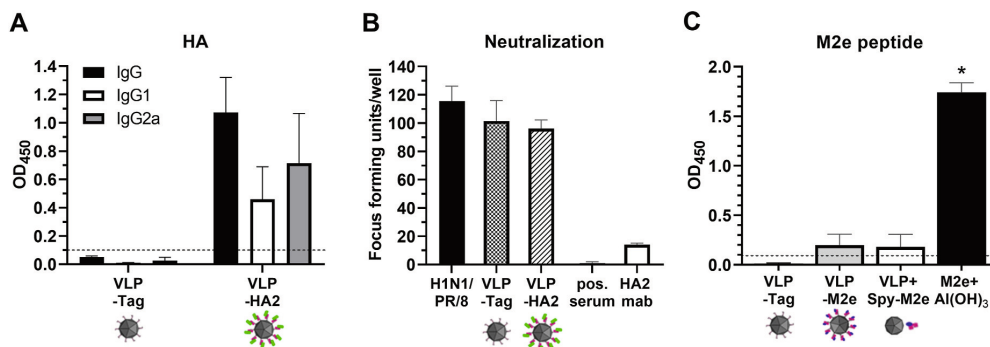


Fig. 5. Influenza-specific immune responses. (A) Induction of IgG, IgG1 and IgG2a antibody responses against whole rHA-domain following two immunizations of mice with SpyTagged NoV VLPs or NoV VLPs decorated with HA2. Group mean OD₄₅₀ values (\pm SEM) of 1:100 diluted sera are shown. (B) Neutralizing antibodies against influenza A virus following two immunizations of mice with SpyTagged NoV VLPs or NoV VLPs decorated with HA2. Blocking of influenza A virus H1N1 PR/8 infection by serum antibodies was tested in a focus reduction neutralization assay. Virus (H1N1 PR/8) without test sample, serum from influenza A virus seropositive human donor (pos. serum) and HA2 monoclonal antibody (HA2 mAb) served as assay controls. Results are expressed as focus forming units (ffu) 20 h post-infection. Shown are group mean ffu (\pm SEM) of 1:25 diluted sera. Development of serum IgG antibody responses against M2e peptide (C) following two immunizations with SpyTagged NoV VLPs, NoV VLPs decorated with M2e, mixture of NoV VLPs and SpyCatcher-M2e or M2e peptide formulated with Al(OH)₃. Group mean OD₄₅₀ values (\pm SEM) of 1:100 diluted sera are shown. The horizontal dotted lines indicate the cut-off values for the assays (OD₄₅₀ \geq 0.1). * indicates statistically significant ($p > 0.05$) differences between the groups.

3.2.3. Induction of neutralizing antibodies against influenza A virus

Ability of antibodies induced by HA2-conjugated VLPs to neutralize influenza A virus H1N1 PR/8 (homologous to the HA2 used for VLP conjugation) was tested in focus reduction neutralization assay (Fig. 5B). Sera of mice immunized with HA2-conjugated VLPs were unable to reduce the replication of the influenza A virus H1N1 PR/8, as only $16.7 \pm 5.3\%$ reduction in ffu was detected. Similar result ($12.1 \pm 12.6\%$ reduction) was observed with sera of negative control mice receiving SpyTagged VLPs. Instead, the known positive human serum as well as HA2 monoclonal antibody, employed as assay controls, conferred strong neutralization with $99.1 \pm 0.9\%$ and $87.9 \pm 1\%$ reductions in ffu. These results show that the antibodies induced by HA2-conjugated VLPs did not exhibit neutralizing activity against influenza A virus.

3.2.4. IgG responses against M2e

To examine the effect of conjugation on induction of antibodies directed against M2e displayed on NoV VLPs, the sera of mice immunized with different M2e vaccine formulations were assayed for the presence of M2e-specific IgG. The IgG responses of mice receiving M2e-conjugated VLPs were compared to the responses induced by SpyCatcher-M2e co-delivered with native VLPs as a mixture or to those obtained with alum-adjuvanted M2e peptide. Testing of immune sera against M2e peptide indicated that extremely low IgG responses were induced by M2e-conjugated VLPs (OD 0.198 ± 0.111) as well as SpyCatcher-M2e in combination with native VLPs (OD 0.180 ± 0.126), antibody levels being significantly lower ($p = 0.016$) than the levels induced by M2e peptide formulated with Al(OH)₃ (OD 1.742 ± 0.097) (Fig. 5C). These results demonstrate that neither conjugation of M2e to VLPs nor coadministration of SpyCatcher linked M2e with VLPs improved the development of antibody response against M2e peptide. Sera of negative control mice immunized with SpyTagged VLPs did not react with M2e peptide (Fig. 5C).

4. Discussion

Particulate delivery platforms for presentation of heterologous antigens are considered as next generation vaccines and the first vaccine based on Hepatitis B surface antigen (HBsAg) nanoparticles carrying a T cell epitope of the *Plasmodium falciparum* malaria parasite (Mosquirix®) has been recently approved for clinical use (Tinto et al.,

2015). Despite extensive research on the potential of various nanoparticles acting as vaccine platforms, the applicability of the VLPs formed by a VP1 capsid protein of NoV as antigen carriers has not been thoroughly studied. However, the successful presentation of several foreign antigens inserted into the surface loops of NoV VP1 capsid-derived subviral P domain (Tan et al., 2011; Jiang et al., 2015; Xia et al., 2011) or the hinge of S domain (Xia et al., 2018) supports the potential of NoV VLPs to act as a vaccine platform. These VLPs can be easily produced in baculovirus-insect cell expression system at high quantities. In addition, NoV VLPs have been considered as vaccine candidates against NoV infection and disease (Atmar et al., 2011; Blazevic et al., 2011). We have previously described a nanocarrier platform based on NoV VLPs and non-covalent chemical conjugation of a C-terminal polyhistidine-tag projecting out of the VLP surface (Koho et al., 2015). Subsequently, we created a NoV VLP platform, where the M2e or HA2 of influenza A virus were successfully displayed on the surface of NoV VLPs as model antigens by exploiting SpyTag/SpyCatcher conjugation technology (Lampinen et al., 2021). This versatile technology allows decoration of different particles irreversibly with virtually any protein or peptide antigen that can be produced separately in standard expression systems. To demonstrate further the feasibility of this vaccine platform to deliver foreign antigens as well as to serve as a NoV vaccine, we examined potential interference of SpyTag/SpyCatcher conjugation with induction of antibodies directed to conjugated universal influenza antigens, M2e peptide and HA2, as well as NoV VLP carrier.

We have recently demonstrated that C-terminally SpyTagged NoV VLPs exhibit uniform size, good thermal stability, and indistinguishable morphology to native VLPs as determined by dynamic light scattering, differential scanning fluorimetry and electron microscopy (Lampinen et al., 2021). In here, we have further demonstrated a strong and unaltered binding profile of SpyTagged VLPs to HBGAs, putative cellular receptors for NoV (Harrington et al., 2002; Marionneau et al., 2002). Furthermore, the conjugated NoV VLPs retained comparable antigenicity and immunogenicity to their native counterpart, as addressed by induction of equal amounts of NoV-specific antibodies *in vivo* in mice, including antibodies with the potential to prevent binding of VLPs to HBGAs. These blocking antibodies are considered an indirect indication of neutralization and the best correlate of protection against NoV infection (Reeck et al., 2010). This data indicates that insertion of SpyTag to the C-terminus of VLPs did not mask important antigenic and

receptor binding sites on the P domain of NoV VLPs. Importantly, conjugation of SpyTagged VLPs with SpyCatcher fused influenza M2e or HA2 antigens did not alter significantly immune responses against NoV either. Congruent with our observations, the conjugation of polyhistidine-tag or other antigens to the C-terminus of NoV VLPs (Koho et al., 2015) or to surface loops of NoV P particles (Tan et al., 2011; Xia et al., 2011) have not affected the particle assembly, receptor binding or antigenic capacity, thus supporting the notion of NoV VLPs as a potent vaccine platform.

Generation of strong HA2-specific antibody response by NoV VLPs conjugated with HA2, the headless HA stem antigen consisting mainly of HA2 subunit (Mallajosyula et al., 2014), demonstrated high immunogenicity of the antigen. In addition, a moderate response to the complete recombinant HA protein, containing also the highly variable and prominent head domain HA1, was detected. While the NoV-HA2 construct was immunogenic, the induced antibodies were unable to neutralize homologous H1N1 PR/8 influenza A virus *in vitro*. This may suggest that HA2 as presented by SpyTag/SpyCatcher conjugation on NoV VLPs was structurally different from the HA stem structure in the native influenza virus particle. Some reports have shown induction of neutralizing antibodies by HA2 stalk (Mallajosyula et al., 2014; Deng et al., 2018), while others have demonstrated a lack of neutralization *in vitro* (Bommakanti et al., 2010, 2012), the latter of which corroborating our observations. This does not necessarily imply an unprotective nature of the induced antibodies, as HA2 immunization has been demonstrated to protect mice *in vivo* from lethal virus challenge in the absence of *in vitro* neutralization (Bommakanti et al., 2010, 2012).

Although neutralizing antibodies are generally considered a correlate of vaccine-induced protective immunity against influenza virus, also non-neutralizing antibodies could confer protection or recovery from disease. HA2-induced protection can be mediated by antibody-dependent effector functions such as antibody-dependent cell-mediated cytotoxicity or complement-dependent cellular cytotoxicity (Bommakanti et al., 2010, 2012). Immunization of mice with viral replicon particle vectors expressing influenza virus HA has failed to induce significant neutralizing and IgG1 antibodies while stimulating IgG2a antibodies, which correlate with clearance of virus and increased protection against lethal influenza challenge (Huber et al., 2006). In the present study, HA2 decorated VLPs elicited robust IgG1 and IgG2a responses, demonstrating a mixed Th2/Th1 response against HA2. The IgG2a antibody subtype has been demonstrated to be important in host defense against different viral infections in mice (Nimmerjahn and Ravetch, 2006) due to the ability of the antibody to activate the complement system (Klaus et al., 1979) and stimulate antibody-dependent cell-mediated cytotoxicity (Kipps et al., 1985).

Antibodies directed to M2e are involved in viral clearance by binding to infected cells expressing M2e on their surface (Deng et al., 2015). Surprisingly, our results show that C-terminal conjugation of a short M2e peptide to NoV VLPs as a SpyCatcher fusion did not result in significant induction of anti-M2e IgG response in immunized mice, which is inconsistent with the strong immunogenicity of M2e following conjugation to various other nanocarriers (Neirynek et al., 1999; Tissot et al., 2010; Xia et al., 2011). The discrepancies in our results compared with the previously published ones could be due to the conjugation technique employed, as usually genetic fusion was used to display the M2e epitope (Neirynek et al., 1999; Tissot et al., 2010; Xia et al., 2011). It may be that SpyTag/SpyCatcher conjugation did not enable correct presentation of the M2e antigen on the surface of NoV VLPs. Further, M2e representing the N-terminus of the influenza M2 protein, may require a free N-terminus for proper presentation and induction of immunity, as demonstrated with some short peptides being unable to generate antibodies if directly fused to the C-terminus of a carrier (Taxt et al., 2010). Indeed,

high levels of M2e antibodies were detected, when M2e was coupled to N-terminus of Hepatitis B virus core antigen or bacteriophage AP205 (Neirynek et al., 1999; Tissot et al., 2010). Finally, the large SpyCatcher conjugation protein, derived from a common human pathogen, *Streptococcus pyogenes* (Zakeri et al., 2012), may exhibit immunodominant nature, overwhelming or hindering the responses against the smaller and poorly immunogenic M2e epitope. Very high immunogenicity of SpyCatcher was noticed in our recent study, where antibodies induced by M2e-decorated VLPs or SpyCatcher-fused M2e cross-reacted with SpyCatcher fused HA2 and vice versa (Lampinen et al., 2021). Short peptides with sizes of ~20 aa will likely require a different conjugation methodology. Therefore, experiments with genetic fusion of the short peptides to NoV VLPs are currently in progress.

In conclusion, our data shows that SpyTagged NoV VLPs can be exploited as a platform to deliver foreign antigens in the form of longer polypeptides while preserving receptor binding capacity and excellent self-immunogenicity. Thus, NoV VLPs may not only serve as a carrier but also as a NoV vaccine offering new insights in the design of combination vaccines. However, the SpyTag/SpyCatcher conjugation technology, while not significantly affecting the autologous antigenicity or immunogenicity of NoV VLPs, will require further research to ensure presentation of heterologous antigens on the NoV VLPs in the correct native structure.

Funding

This work was financially supported by Research on Viral diseases, V.A. Kotilainen, and Onni and Hilja Tuovinen, Tampere University Graduate School, and Academy of Finland [Projects 309455 and 335870]. The work was also funded by the Competitive State Research Financing of the Expert Responsibility Area of Fimlab Laboratories, and the Cancer Society of Finland.

Declaration of competing interest

The authors declare that they have no known competing financial interests or personal relationships that could have appeared to influence the work reported in this paper.

CRedit authorship contribution statement

Suvi Heinimäki: Methodology, Formal analysis, Investigation, Data curation, Visualization, Writing – original draft, Writing – review & editing. **Vili Lampinen:** Methodology, Investigation, Visualization, Funding acquisition, Writing – review & editing. **Kirsi Tamminen:** Methodology, Formal analysis, Visualization, Writing – original draft, Writing – review & editing. **Minna M. Hankaniemi:** Methodology, Investigation, Funding acquisition, Writing – review & editing. **Maria Malm:** Methodology, Writing – review & editing. **Vesa P. Hytönen:** Conceptualization, Investigation, Funding acquisition, Writing – review & editing. **Vesna Blazevic:** Conceptualization, Investigation, Visualization, Funding acquisition, Project administration, Writing – original draft, Writing – review & editing.

Acknowledgements

Technical assistance given by Eeva Jokela, Sanna Kavén and Nina Koivisto from Vaccine development and immunology group/Vaccine Research Center of Tampere University is gratefully acknowledged. We also express our gratitude to members of the animal facility at Tampere University. We acknowledge infrastructure support by Biocenter Finland.

References

- Atmar, R.L., Bernstein, D.I., Harro, C.D., Al-Ibrahim, M.S., Chen, W.H., Ferreira, J., Estes, M.K., Graham, D.Y., Opekun, A.R., Richardson, C., et al., 2011. Norovirus vaccine against experimental human Norwalk Virus illness. *N. Engl. J. Med.* 365, 2178. <https://doi.org/10.1056/NEJMoal101245>.
- Blazevic, V., Trubey, C.M., Shearer, G.M., 2000. Comparison of in vitro immunostimulatory potential of live and inactivated influenza viruses. *Hum. Immunol.* 61, 845–849. [https://doi.org/10.1016/s0198-8859\(00\)00170-1](https://doi.org/10.1016/s0198-8859(00)00170-1).
- Blazevic, V., Lappalainen, S., Nurminen, K., Huhti, L., Vesikari, T., 2011. Norovirus VLPs and rotavirus VP6 protein as combined vaccine for childhood gastroenteritis. *Vaccine* 29, 8126. <https://doi.org/10.1016/j.vaccine.2011.08.026>.
- Bommakanti, G., Citron, M.P., Hepler, R.W., Callahan, C., Heidecker, G.J., Najjar, T.A., Lu, X., Joyce, J.G., Shiver, J.W., Casimiro, D.R., et al., 2010. Design of an HA2-based Escherichia coli expressed influenza immunogen that protects mice from pathogenic challenge. *Proc. Natl. Acad. Sci. U. S. A.* 107, 13701–13706. <https://doi.org/10.1073/pnas.1007465107>.
- Bommakanti, G., Lu, X., Citron, M.P., Najjar, T.A., Heidecker, G.J., ter Meulen, J., Varadarajan, R., Liang, X., 2012. Design of Escherichia coli-expressed stalk domain immunogens of H1N1 hemagglutinin that protect mice from lethal challenge. *J. Virol.* 86, 13434–13444. <https://doi.org/10.1128/JVI.01429-12>.
- Brune, K.D., Leneghan, D.B., Brian, I.J., Ishizuka, A.S., Bachmann, M.F., Draper, S.J., Biswas, S., Howarth, M.P., 2016. Plug-and-Display: decoration of Virus-Like Particles via isopeptide bonds for modular immunization. *Sci. Rep.* 6, 19234. <https://doi.org/10.1038/srep19234>.
- Darricarrère, N., Qiu, Y., Kanekiyo, M., Creanga, A., Gillespie, R.A., Moin, S.M., Saleh, J., Sancho, J., Chou, T.-H., Zhou, Y., et al., 2021. Broad neutralization of H1 and H3 viruses by adjuvanted influenza HA stem vaccines in nonhuman primates. *Sci. Transl. Med.* 13, eabe5449. <https://doi.org/10.1126/scitranslmed.abe5449>.
- Deng, L., Cho, K.J., Fiers, W., Saelens, X., 2015. M2e-Based universal influenza A vaccines. *Vaccines* 3, 105–136. <https://doi.org/10.3390/vaccines3010105>.
- Deng, L., Mohan, T., Chang, T.Z., Gonzalez, G.X., Wang, Y., Kwon, Y.M., Kang, S.M., Compans, R.W., Champion, J.A., Wang, B.Z., 2018. Double-layered protein nanoparticles induce broad protection against divergent influenza A viruses. *Nat. Commun.* 9, 359. <https://doi.org/10.1038/s41467-017-02725-4>.
- Fifis, T., Gnavrellis, A., Criméan-Irwin, B., Pieters, G.A., Li, J., Mottram, P.L., McKenzie, I.F., Plebanski, M., 2004. Size-dependent immunogenicity: therapeutic and protective properties of nano-vaccines against tumors. *J. Immunol.* 173, 3148. <https://doi.org/10.4049/jimmunol.173.5.3148>.
- Harrington, P.R., Linds Smith, L., Yount, B., Moe, C.L., Baric, R.S., 2002. Binding of Norwalk virus-like particles to ABH histo-blood group antigens is blocked by antisera from infected human volunteers or experimentally vaccinated mice. *J. Virol.* 76, 12335. <https://doi.org/10.1128/jvi.76.23.12335-12343.2002>.
- Heinimäki, S., Tamminen, K., Hytonen, V.P., Malm, M., Blazevic, V., 2020. Rotavirus inner capsid VP6 acts as an adjuvant in formulations with particulate antigens only. *Vaccines* 8. <https://doi.org/10.3390/vaccines8030365>.
- Huber, V.C., McKeon, R.M., Brackin, M.N., Miller, L.A., Keating, R., Brown, S.A., Makarova, N., Perez, D.R., Macdonald, G.H., McCullers, J.A., 2006. Distinct contributions of vaccine-induced immunoglobulin G1 (IgG1) and IgG2a antibodies to protective immunity against influenza. *Clin. Vaccine Immunol.* 13, 981–990. <https://doi.org/10.1128/CVI.00156-06>.
- Huhti, L., Blazevic, V., Nurminen, K., Koho, T., Hytonen, V.P., Vesikari, T., 2010. A comparison of methods for purification and concentration of norovirus GII-4 capsid virus-like particles. *Arch. Virol.* 155, 1855. <https://doi.org/10.1007/s00705-010-0768-z>.
- Jazayeri, S.D., Poh, C.L., 2019. Development of Universal Influenza Vaccines Targeting Conserved Viral Proteins, vol. 7. *Vaccines*. <https://doi.org/10.3390/vaccines7040169>.
- Jiang, L., Fan, R., Sun, S., Fan, P., Su, W., Zhou, Y., Gao, F., Xu, F., Kong, W., Jiang, C., 2015. A new EV71 VP3 epitope in norovirus P particle vector displays neutralizing activity and protection in vivo in mice. *Vaccine* 33, 6596–6603. <https://doi.org/10.1016/j.vaccine.2015.10.104>.
- Jin, Y., Yang, H., Ji, W., Wu, W., Chen, S., Zhang, W., Duan, G., 2020. Virology, epidemiology, pathogenesis, and control of COVID-19. *Viruses* 12. <https://doi.org/10.3390/v12040372>.
- Karch, C.P., Burkhard, P., 2016. Vaccine technologies: from whole organisms to rationally designed protein assemblies. *Biochem. Pharmacol.* 120, 1–14. <https://doi.org/10.1016/j.bcp.2016.05.001>.
- Kipps, T.J., Parham, P., Punt, J., Herzenberg, L.A., 1985. Importance of immunoglobulin isotype in human antibody-dependent, cell-mediated cytotoxicity directed by murine monoclonal antibodies. *J. Exp. Med.* 161, 1–17. <https://doi.org/10.1084/jem.161.1.1>.
- Klaus, G.G., Pepsy, M.B., Kitajima, K., Askonas, B.A., 1979. Activation of mouse complement by different classes of mouse antibody. *Immunology* 38, 687–695.
- Koho, T., Ihalaainen, T.O., Stark, M., Uusi-Kerttula, H., Wieneke, R., Rahikainen, R., Blazevic, V., Marjomäki, V., Tampe, R., Kulomaa, M.S., et al., 2015. His-tagged norovirus-like particles: a versatile platform for cellular delivery and surface display. *Eur. J. Pharm. Biopharm.* 96, 22–31. <https://doi.org/10.1016/j.ejpb.2015.07.002>.
- Kushnir, N., Streetfield, S.J., Yusibov, V., 2012. Virus-like particles as a highly efficient vaccine platform: diversity of targets and production systems and advances in clinical development. *Vaccine* 31, 58. <https://doi.org/10.1016/j.vaccine.2012.10.083>.
- Lampinen, V., Heinimäki, S., Laitinen, O.H., Pesu, M., Hankaniemi, M.M., Blazevic, V., Hytonen, V.P., 2021. Modular vaccine platform based on the norovirus-like particle. *J. Nanobiotechnol.* 19, 25. <https://doi.org/10.1186/s12951-021-00772-0>.
- Lee, J.S., Chowdhury, M.Y., Moon, H.J., Choi, Y.K., Talactac, M.R., Kim, J.H., Park, M.E., Son, H.Y., Shin, K.S., Kim, C.J., 2013. The highly conserved HA2 protein of the influenza A virus induces a cross protective immune response. *J. Virol Methods* 194, 280–288. <https://doi.org/10.1016/j.jviro.2013.08.022>.
- Mallajosyula, V.V., Citron, M., Ferrara, F., Lu, X., Callahan, C., Heidecker, G.J., Sama, S. P., Flynn, J.A., Temperton, N.J., Liang, X., et al., 2014. Influenza hemagglutinin stem-fragment immunogen elicits broadly neutralizing antibodies and confers heterologous protection. *Proc. Natl. Acad. Sci. U. S. A.* 111, E2514–E2523. <https://doi.org/10.1073/pnas.1402766111>.
- Malm, M., Heinimäki, S., Vesikari, T., Blazevic, V., 2017. Rotavirus capsid VP6 tubular and spherical nanostructures act as local adjuvants when co-delivered with norovirus VLPs. *Clin. Exp. Immunol.* 189, 331. <https://doi.org/10.1111/cei.12977>.
- Malm, M., Tamminen, K., Vesikari, T., Blazevic, V., Norovirus, G.I.I., 2018. 17 virus-like particles bind to different histo-blood group Antigens and cross-react with genogroup II-specific mouse sera. *Viral Immunol.* <https://doi.org/10.1089/vim.2018.0115>.
- Marionneau, S., Ruvoen, N., Le Moullac-Vaidy, B., Clement, M., Cailleau-Thomas, A., Ruiz-Palacois, G., Huang, P., Jiang, X., Le Pendu, J., 2002. Norwalk virus binds to histo-blood group antigens present on gastroduodenal epithelial cells of secretor individuals. *Gastroenterology* 122, 1967. <https://doi.org/10.1053/gast.2002.33661>.
- Murata, Y., Lightfoote, P.M., Rose, R.C., Walsh, E.E., 2009. Antigenic presentation of heterologous epitopes engineered into the outer surface-exposed helix 4 loop region of human papillomavirus L1 capsomeres. *Virol. J.* 6, 81. <https://doi.org/10.1186/1743-422X-6-81>.
- Nachbagger, R., Feser, J., Naficy, A., Bernstein, D.I., Guptill, J., Walter, E.B., Berlanda-Scorza, F., Stadlbauer, D., Wilson, P.C., Aydllo, T., et al., 2021. A chimeric hemagglutinin-based universal influenza virus vaccine approach induces broad and long-lasting immunity in a randomized, placebo-controlled phase I trial. *Nat. Med.* 27, 106–114. <https://doi.org/10.1038/s41591-020-1118-7>.
- Neiryneck, S., Deroo, T., Saelens, X., Vanlandschoot, P., Jou, W.M., Fiers, W., 1999. A universal influenza A vaccine based on the extracellular domain of the M2 protein. *Nat. Med.* 5, 1157–1163. <https://doi.org/10.1038/13484>.
- Nimmerjahn, F., Ravetch, J.V., 2006. Fcγamma receptors: old friends and new family members. *Immunity* 24, 19–28. <https://doi.org/10.1016/j.immuni.2005.11.010>.
- Nurminen, K., Blazevic, V., Huhti, L., Rasanen, S., Koho, T., Hytonen, V.P., Vesikari, T., 2011. Prevalence of norovirus GII-4 antibodies in Finnish children. *J. Med. Virol.* 83, 525. <https://doi.org/10.1002/jmv.21990>.
- Okuno, Y., Tanaka, K., Baba, K., Maeda, A., Kunita, N., Ueda, S., 1990. Rapid focus reduction neutralization test of influenza A and B viruses in microtiter system. *J. Clin. Microbiol.* 28, 1308–1313.
- Peacey, M., Wilson, S., Baird, M.A., Ward, V.K., 2007. Versatile RHDV virus-like particles: incorporation of antigens by genetic modification and chemical conjugation. *Biotechnol. Bioeng.* 98, 968–977. <https://doi.org/10.1002/bit.21518>.
- Peralta, A., Molinari, P., Taboga, O., 2009. Chimeric recombinant rotavirus-like particles as a vehicle for the display of heterologous epitopes. *Virol. J.* 6, 192. <https://doi.org/10.1186/1743-422X-6-192>.
- Philip, A.A., Patton, J.T., 2021. Rotavirus as an expression platform of domains of the SARS-CoV-2 spike protein. *Vaccines* 9, 449.
- Prasad, B.V., Hardy, M.E., Dokland, T., Bella, J., Rossmann, M.G., Estes, M.K., 1999. X-ray crystallographic structure of the Norwalk virus capsid. *Science* 286, 287.
- Reeck, A., Kavanagh, O., Estes, M.K., Opekun, A.R., Gilger, M.A., Graham, D.Y., Atmar, R.L., 2010. Serological correlate of protection against norovirus-induced gastroenteritis. *J. Infect. Dis.* 202, 1212. <https://doi.org/10.1093/infdis/jiq656>.
- Tamminen, K., Huhti, L., Koho, T., Lappalainen, S., Hytonen, V.P., Vesikari, T., Blazevic, V., 2012. A comparison of immunogenicity of norovirus GII-4 virus-like particles and P-particles. *Immunology* 135, 89. <https://doi.org/10.1111/j.1365-2567.2011.03516.x>.
- Tamminen, K., Heinimäki, S., Vesikari, T., Blazevic, V., 2020. Rotavirus VP6 adjuvant effect on norovirus GII-4 virus-like particle uptake and presentation by bone marrow-derived dendritic cells in vitro and in vivo. *J. Immunol. Res.* 2020, 3194704. <https://doi.org/10.1155/2020/3194704>.
- Tamminen, K., Heinimäki, S., Gröhn, S., Blazevic, V., 2021. Fusion protein of rotavirus VP6 and SARS-CoV-2 receptor binding domain induces T cell responses. *Vaccines* 9. <https://doi.org/10.3390/vaccines9070733>.
- Tan, M., Huang, P.W., Xia, M., Fang, P.A., Zhong, W.M., McNeal, M., Wei, C., Jiang, W., Jiang, X., 2011. Norovirus P particle, a novel platform for vaccine development and antibody production. *J. Infect. Dis.* 205, 753–764. <https://doi.org/10.1128/JVI.01835-10>.
- Text, A., Aasland, R., Sommerfelt, H., Nataro, J., Puntervoll, P., 2010. Heat-stable enterotoxin of enterotoxigenic Escherichia coli as a vaccine target. *Infect. Immun.* 78, 1824–1831. <https://doi.org/10.1128/iai.01397-09>.
- Tinto, H., D'Alessandro, U., Sorgho, H., Valea, I., Tahita, M.C., Kabore, W., Kiemde, F., Lompo, P., Ouedraogo, S., Derra, K., et al., 2015. Efficacy and safety of RTS,S/AS01 malaria vaccine with or without a booster dose in infants and children in Africa: final results of a phase 3, individually randomised, controlled trial. *Lancet* 386, 31–45. [https://doi.org/10.1016/s0140-6736\(15\)60721-8](https://doi.org/10.1016/s0140-6736(15)60721-8).
- Tissot, A.C., Renhofs, R., Schmitz, N., Cielen, I., Meijerink, E., Ose, V., Jennings, G.T., Sautan, P., Pumpens, P., Bachmann, M.F., 2010. Versatile virus-like particle carrier for epitope based vaccines. *PLoS One* 5, e9809. <https://doi.org/10.1371/journal.pone.0009809>.
- Uusi-Kerttula, H., Tamminen, K., Malm, M., Vesikari, T., Blazevic, V., 2014. Comparison of human saliva and synthetic histo-blood group antigens usage as ligands in norovirus-like particle binding and blocking assays. *Microb. Infect.* 16, 472. <https://doi.org/10.1016/j.micinf.2014.02.010>.
- Wibowo, N., Chuan, Y.P., Lua, L.H.L., Middelberg, A.P.J., 2013. Modular engineering of a microbially-produced viral capsomere vaccine for influenza. *Chem. Eng. Sci.* 103, 12–20. <https://doi.org/10.1016/j.ces.2012.04.001>.

- Xia, M., Tan, M., Wei, C., Zhong, W., Wang, L., McNeal, M., Jiang, X., 2011. A candidate dual vaccine against influenza and noroviruses. *Vaccine* 29, 7670. <https://doi.org/10.1016/j.vaccine.2011.07.139>.
- Xia, M., Huang, P., Sun, C., Han, L., Vago, F.S., Li, K., Zhong, W., Jiang, W., Klassen, J.S., Jiang, X., et al., 2018. Bioengineered norovirus S60 nanoparticles as a multifunctional vaccine platform. *ACS Nano* 12, 10665–10682. <https://doi.org/10.1021/acsnano.8b02776>.
- Zakeri, B., Fierer, J.O., Celik, E., Chittock, E.C., Schwarz-Linek, U., Moy, V.T., Howarth, M., 2012. Peptide tag forming a rapid covalent bond to a protein, through engineering a bacterial adhesin. *Proc. Natl. Acad. Sci. U. S. A.* 109, E690–E697. <https://doi.org/10.1073/pnas.1115485109>.

PUBLICATION
III

SpyTag/Catcher display of influenza M2e peptide on norovirus-like particle provides stronger immunization than direct genetic fusion

Lampinen V, Gröhn S, Soppela S, Hytönen VP, Hankaniemi MM

Frontiers in Cellular and Infection Microbiology. 2023; 13
doi: 10.3389/fcimb.2023.1216364

Publication reprinted with the permission of the copyright holders (CC BY 4.0).



OPEN ACCESS

EDITED BY

Antonio Roldao,
Instituto de Biologia e Tecnologia
Experimental (iBET), Portugal

REVIEWED BY

John T. Bates,
University of Mississippi Medical Center,
United States
Matthew D. Moore,
University of Massachusetts Amherst,
United States

*CORRESPONDENCE

Minna M. Hankaniemi
✉ minna.hankaniemi@tuni.fi
Vesa P. Hytönen
✉ vesa.hytonen@tuni.fi

[†]These authors have contributed
equally to this work and share
last authorship

RECEIVED 03 May 2023

ACCEPTED 05 June 2023

PUBLISHED 22 June 2023

CITATION

Lampinen V, Gröhn S, Soppela S,
Blazevic V, Hytönen VP and
Hankaniemi MM (2023) SpyTag/SpyCatcher
display of influenza M2e peptide on
norovirus-like particle provides stronger
immunization than direct genetic fusion.
Front. Cell. Infect. Microbiol. 13:1216364.
doi: 10.3389/fcimb.2023.1216364

COPYRIGHT

© 2023 Lampinen, Gröhn, Soppela, Blazevic,
Hytönen and Hankaniemi. This is an open-
access article distributed under the terms of
the Creative Commons Attribution License
(CC BY). The use, distribution or
reproduction in other forums is permitted,
provided the original author(s) and the
copyright owner(s) are credited and that
the original publication in this journal is
cited, in accordance with accepted
academic practice. No use, distribution or
reproduction is permitted which does not
comply with these terms.

SpyTag/SpyCatcher display of influenza M2e peptide on norovirus-like particle provides stronger immunization than direct genetic fusion

Vili Lampinen^{1,2}, Stina Gröhn², Saana Soppela², Vesna Blazevic³,
Vesa P. Hytönen^{1,4*†} and Minna M. Hankaniemi^{2*†}

¹Protein Dynamics, Faculty of Medicine and Health Technology, Tampere University, Tampere, Finland, ²Virology and Vaccine Immunology, Faculty of Medicine and Health Technology, Tampere University, Tampere, Finland, ³Vaccine Development and Immunology/Vaccine Research Center, Faculty of Medicine and Health Technology, Tampere University, Tampere, Finland, ⁴Fimlab Laboratories, Tampere, Finland

Introduction: Virus-like particles (VLPs) are similar in size and shape to their respective viruses, but free of viral genetic material. This makes VLP-based vaccines incapable of causing infection, but still effective in mounting immune responses. Noro-VLPs consist of 180 copies of the VP1 capsid protein. The particle tolerates C-terminal fusion partners, and VP1 fused with a C-terminal SpyTag self-assembles into a VLP with SpyTag protruding from its surface, enabling conjugation of antigens via SpyCatcher.

Methods: To compare SpyCatcher-mediated coupling and direct peptide fusion in experimental vaccination, we genetically fused the ectodomain of influenza matrix-2 protein (M2e) directly on the C-terminus of norovirus VP1 capsid protein. VLPs decorated with SpyCatcher-M2e and VLPs with direct M2e fusion were used to immunize mice.

Results and discussion: We found that direct genetic fusion of M2e on noro-VLP raised few M2e antibodies in the mouse model, presumably because the short linker positions the peptide between the protruding domains of noro-VLP, limiting its accessibility. On the other hand, adding aluminum hydroxide adjuvant to the previously described SpyCatcher-M2e-decorated noro-VLP vaccine gave a strong response against M2e. Surprisingly, simple SpyCatcher-fused M2e without VLP display also functioned as a potent immunogen, which suggests that the commonly used protein linker SpyCatcher-SpyTag may serve a second role as an activator of the immune system in vaccine preparations. Based on the measured anti-M2e antibodies and cellular responses, both SpyCatcher-M2e as well as M2e presented on the noro-VLP via SpyTag/Catcher show potential for the development of universal influenza vaccines.

KEYWORDS

influenza, norovirus, SpyCatcher, virus-like particle, norovirus (NoV), conjugation, fusion protein, cell mediated and humoral immunity

1 Introduction

Influenza has been, and still is, one of the most prevalent microbial diseases tormenting humankind. Though an influenza infection rarely hospitalizes healthy adults, it can lead to serious and even fatal complications, especially in the young and elderly. On a global scale, WHO estimates between 3 and 5 million infections with serious complications and 290 000–650 000 deaths due to influenza every year ([https://www.who.int/news-room/fact-sheets/detail/influenza-\(seasonal\)](https://www.who.int/news-room/fact-sheets/detail/influenza-(seasonal)); accessed 28.4.2023). Influenza is widespread among mammals and birds, and due to its segmented genome, influenza occasionally goes through a genetic shift between strains from different host species that allows the hybrid strain unparalleled transmissibility, causing pandemics (Wolfe et al., 2007).

Effective vaccines against influenza exist, but due to the fast evolution rates of the RNA virus, these need annual renewal to keep up. A long-lasting, universal influenza vaccine has been the target of heavy research efforts for decades, but none have reached the clinic yet. The most promising universal influenza vaccine candidates direct the immune response against conserved parts of the influenza virus. The ectodomain of Matrix 2 proton channel is only 24 amino acid residues long, but it is >90% conserved across different influenza strains (Ebrahimi and Tebianian, 2011), making it an attractive target for a universal influenza vaccine.

Short peptides, like M2e, are not very immunogenic by themselves, so they must be attached to an immunogenic carrier, such as a virus capsid protein. The spontaneous assembly of viral proteins into virus-like particles (VLPs) enables multivalent presentation of target antigens on the VLP surface, which can increase the efficiency of the B-cell response against small peptides, independent of T-cells (Chackerian et al., 2008). Most VLPs have diameters (10–200 nm) that are optimal for uptake by antigen-presenting cells and for direct drainage into the lymphatic system (Bachmann and Jennings, 2010).

Our previous studies on norovirus-like particles (norovirus-VLPs) have revealed that they are particularly robust and easy to modify, produce and store (Koho et al., 2015; Lampinen et al., 2021). Norovirus-VLPs consist of 180 repeats of the single capsid protein, VP1 (Prasad et al., 1994), that assemble to form the norovirus-VLP so that C-terminal extensions are presented on the particle surface (Koho et al., 2015). In earlier experiments, we utilized this by genetically fusing SpyTag on the norovirus-VLP C-terminus and then covalently conjugating the SpyTags with SpyCatcher-fused influenza M2e peptides (Lampinen et al., 2021; Heinimäki et al., 2022). SpyTag and SpyCatcher are two halves of a split protein system that spontaneously reforms *via* a covalent isopeptide bond upon contact in a variety of conditions (Zakeri et al., 2012). The system has been used successfully in many labs for decoration of VLPs for vaccination (e.g. (Brune et al., 2016; Thrane et al., 2016; Rahikainen et al., 2021)).

Previously, we immunized mice with unadjuvanted SpyCatcher-M2e-decorated norovirus-VLP, but few anti-M2e antibodies were formed (Heinimäki et al., 2022). This led us to suspect that the *Streptococcus pyogenes* bacteria-derived SpyCatcher may mask the small M2e peptide from the immune system, so here,

we produced a form of norovirus-VLP that presents influenza M2e as a direct genetic fusion on its C-termini (Figure 1). We immunized mice subcutaneously with the genetically fused M2e-norovirus-VLP, SpyCatcher-M2e alone and, also, SpyCatcher-M2e-decorated norovirus-VLP in doses comparable to the earlier experiments with and without an Al(OH)₃ adjuvant. The present study shows a dramatic enhancement to the anti-M2e immune response of the SpyCatcher-M2e-decorated norovirus-VLP vaccine candidate tested before, apparently due to the addition of alum adjuvant. The group immunized with adjuvanted soluble SpyCatcher-M2e also generated high titers of anti-M2e antibodies, making both vaccines attractive candidates for further development of universal influenza vaccines. We were able to produce and purify the genetically fused M2e-norovirus-VLP, but mice immunized with it produced less anti-M2e antibodies compared to SpyCatcher-M2e immunized animals. On the other hand, norovirus-VLP-displayed M2e showed higher cellular responses compared to simple SpyCatcher-M2e fusion, which supports further studies on norovirus-VLP presented influenza M2e peptide.

2 Results

2.1 Norovirus-VLP tolerates direct fusion of M2e

We produced SpyTag-norovirus-VLP in insect cells as described previously (Lampinen et al., 2021), but utilized size-exclusion chromatography as a new method for removing the residual baculovirus (Supplementary Figure 1). Compared to the anion exchange method used earlier for this purpose, we were able to almost double the VLP production yield from 10–30 to 40–80 mg/L. After setting up the production and purification methods for the SpyTag-norovirus-VLP, the same protocol was utilized to produce and purify a norovirus-VLP with genetically fused influenza M2e peptide in its C-terminus. In gel electrophoresis, M2e-norovirus-VLP (calculated mass 62 150 Da) was detected as a clear, single band slightly larger than SpyTag-norovirus-VLP (60 867 Da) in size, as expected (Figure 2A). M2e-norovirus-VLP was produced with yields of approximately 25 mg/L with this protocol, which is comparable to the SpyTag-norovirus-VLP yields reported with anion exchange purification (Lampinen et al., 2021).

We conjugated SpyCatcher-M2e on SpyTag-norovirus-VLP as described earlier, now with a conjugation efficiency of 24%. The monoclonal anti-influenza-M2 antibody recognized the SpyCatcher-fusion of M2e covalently bound to norovirus-VLP as well as the genetic fusion between M2e and norovirus-VLP1 (Figure 2B). Dynamic light scattering confirmed that M2e-fused norovirus-VLP1 can assemble into homogenic particles (hydrodynamic diameter=54 nm; PdI=0.178 ± 0.008) that seem slightly larger than SpyTag-norovirus-VLPs (49 nm; PdI=0.118 ± 0.016) (Figure 2C). According to negative staining transmission electron microscopy, M2e-norovirus-VLP is indistinguishable in morphology from wild type norovirus-VLPs (Figure 2D) (Jiang et al., 1992; Ausar et al., 2006; Lampinen et al., 2021), which is expected given that the small fusion partner is positioned into a valley between protruding domains, based on the

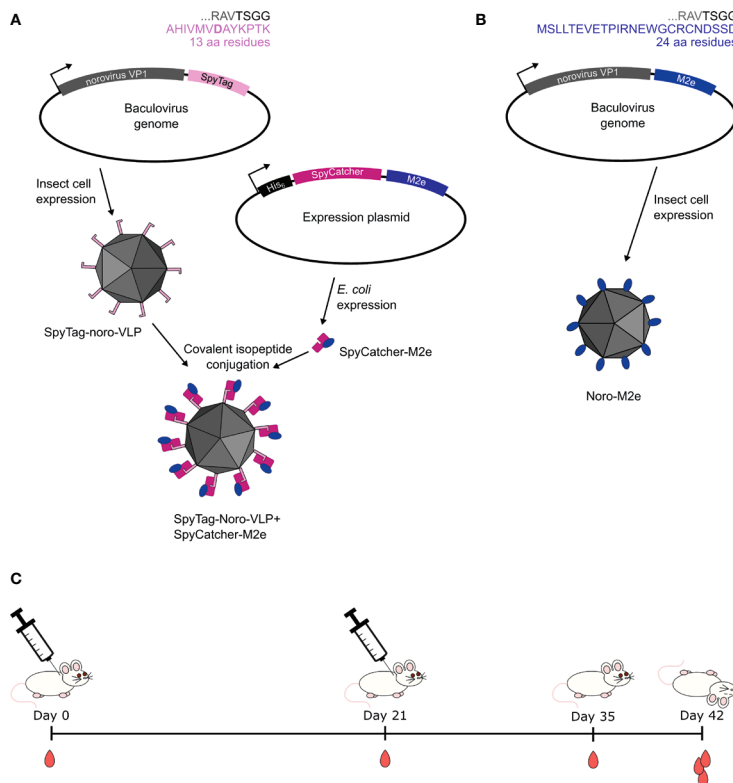


FIGURE 1

Design of vaccines used in this study. (A) Earlier studies (Lampinen et al., 2021) show that when a 13-amino-acid SpyTag is genetically fused to the C-terminus of noro-VP1, the tag is available on the outside of the assembled norovirus-like particle. SpyCatcher with a fused protein antigen can be separately expressed in a bacterial system and mixed with SpyTag-noro-VLP to yield decorated VLP. (B) A 24-amino-acid M2e peptide was genetically fused to the C-terminus of noro-VLP for producing noro-VLPs displaying the M2e peptide in insect cells. (C) We injected these vaccine preparations twice in BALB/c mice with their control groups and compared the produced immune responses at different time points in the study.

noro-VLP crystal structure (RCSB PDB ID: 1IHM (Prasad et al., 1999)). All recombinant proteins used in vaccinations were purified to >95% purity and confirmed to contain <700 pg dsDNA and <1.5 EU endotoxins per μg of vaccine antigen, meeting the criteria set for preclinical experimental vaccines.

The influenza M2e peptide (24 aa) is almost double in size compared to SpyTag (13 aa), so we wanted to see if attaching such a large fusion partner to noro-VLP would affect its thermal stability. Differential scanning fluorimetry (DSF, a.k.a. thermofluor) analysis of SpyTag-noro-VLP and M2e-noro-VLP side by side showed that M2e-noro-VLP disassembly and unfolding indeed begins at a lower temperature compared to SpyTag-noro-VLP (Supplementary Figures 2A, B). Its melting temperature (T_m) of $53.2 \pm 0.5^\circ\text{C}$ is 14.3°C lower than that of SpyTag-noro-VLP ($67.5 \pm 0.6^\circ\text{C}$) ($n=3$). We observed no changes in the unfolding profile and melting point of either SpyTag-noro-VLP or M2e-noro-VLP in salt concentrations of 60, 150 and 300 mM. However, despite significant destabilization as compared to SpyTag-noro-VLP, the thermal stability of M2e-noro-VLP is sufficient to tolerate long storage periods in typical conditions and no signs of unfolding were

observed upon storage for several months at $+4^\circ\text{C}$ (data not shown). The melting curve of M2e-noro-VLP obtained from DSF is broadened and perhaps hints at a two-step unfolding mechanism. This model was further supported by differential scanning calorimetry (DSC) analysis, where M2e-noro-VLP showed a clear biphasic unfolding trace. The lower T_{m1} ($67.18 \pm 0.07^\circ\text{C}$) of M2e-noro-VLP was 4.5°C lower than the T_{m1} measured for wild type noro-VLP ($71.68 \pm 0.16^\circ\text{C}$) (Supplementary Figures 2C, D). Accordingly, DSC showed a 1.0°C reduction between the T_{m2} of M2e-noro-VLP and the T_{m2} of wild type noro-VLP (74.07 ± 0.05 vs. $75.07 \pm 0.11^\circ\text{C}$).

2.2 M2e immune responses are strengthened by protein fusion and adjuvant

To assess the influence of different methods of influenza M2e presentation on its immunogenicity, mice were immunized with various antigen compositions. We then assessed the levels of IgG

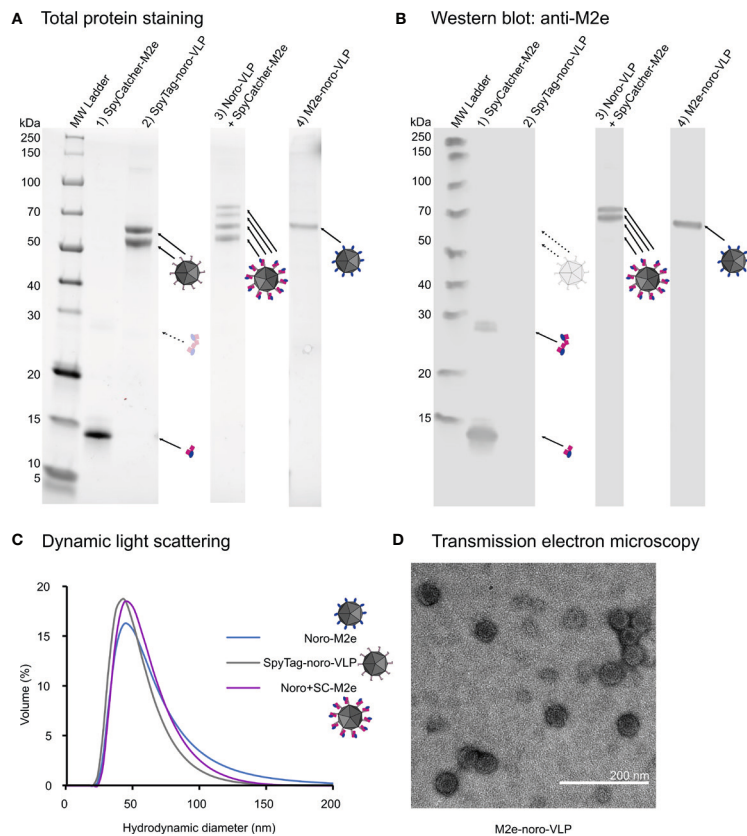


FIGURE 2

Characterization of the produced vaccine antigens. (A) An image of a Stainfree total protein gel with approximately 1 μg of total protein loaded in each well. SpyTag-noro-VLP appears as a double band due to an N-terminal truncation, which is not seen in M2e-noro-VLP. Upon conjugation, some of the SpyTag-noro-VLP double band moves upwards by the size of the conjugated SpyCatcher-M2e. (B) The same gel blotted onto membrane for detection by M2 antibody. Only the conjugated noro-VLP double band is identified by the M2 antibody. A small amount of SpyCatcher-M2e is in dimeric form on the gel, despite boiling the sample. (C) Dynamic light scattering results of the hydrodynamic sizes of different noro-VLPs from the volume-based distribution. The mean peak sizes are 49 nm for SpyTag-noro-VLP, 54 nm for noro-VLP+SpyCatcher-M2e and 58 nm for M2e-noro-VLP. (D) A representative image of M2e-noro-VLP in transmission electron microscopy.

antibodies formed against the peptide, the noro-VLP carrier and SpyCatcher linker protein at different time points in the animal experiment. At day 0, we detected no antibodies against any of the tested antigens (data not shown). Overall, IgG levels increased with time, especially after the second immunization at day 21 (Figure 3).

To evaluate if the vaccination could be potentiated with adjuvant, vaccination group 4 (G4: M2e presented on noro-VLP via SpyCatcher), was given $\frac{1}{4}$ of the M2e dose compared to our previous experiment (Lampinen et al., 2021; Heinimäki et al., 2022), but the vaccine was adsorbed on $\text{Al}(\text{OH})_3$ adjuvant. This resulted in a significant increase in the amount of anti-M2e antibodies after a single immunization compared to non-adsorbed vaccine. On day 42, the geometric mean end-point titer (GMT) of G4 was $1.8 \cdot 10^5$, compared to a titer of 100 obtained without adjuvant (Heinimäki et al., 2022). Surprisingly, adjuvanted SpyCatcher-M2e was equally good at raising anti-M2e antibodies as M2e presented on noro-VLP via SpyCatcher (also showing GMT of $1.8 \cdot 10^5$). In contrast to our

initial hypothesis, M2e-noro-VLP was not nearly as effective in directing the immune response towards the presented M2e peptide as SpyCatcher-conjugated M2e on noro-VLP or even SpyCatcher-M2e alone. The adjuvanted M2e-noro-VLP group 5 reached a GMT of 700, while the mice vaccinated with unadjuvanted M2e-noro-VLP had almost undetectable levels of anti-M2e antibodies (G6: 300, G7: 200, G8: 610).

Very high titers ($>1 \cdot 10^5$) of anti-noro antibodies were formed by all noro-VLP-containing vaccines after two immunizations, regardless of the presence of M2e antigen, SpyCatcher or adjuvant. Therefore, it seems likely that display of foreign antigens does not compromise the potential of the noro-VLPs as a vaccine against norovirus, as shown earlier in a similar context (Heinimäki et al., 2022). Conversely, SpyCatcher response was 5-fold stronger when presented without noro-VLP (G2: $5.0 \cdot 10^6$ vs. G4: $1.1 \cdot 10^6$). Furthermore, anti-noro response seemed less dependent on adjuvant as compared to M2e response, but still,

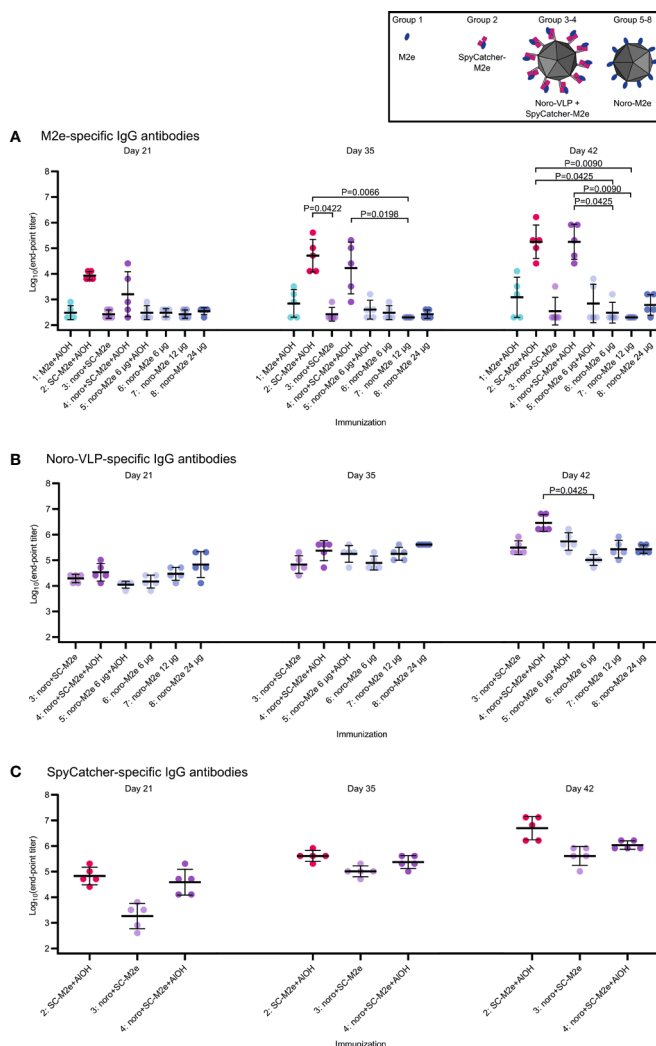


FIGURE 3

Total IgG responses at different time points. Log₁₀ transformations of IgG antibody end-point titers against M2e peptide (A), noro-VLP (B) or SpyCatcher (C), as assessed in ELISA wells coated with the peptide or protein indicated above each graph. Mean titers are represented by the thick line ± standard deviation. P values are shown for groups with a difference with $P < 0.05$, determined by Dunn's test. Each dot represents a single mouse. Undetectable antibody levels were denoted with the titer 200 (half of the lowest dilution assessed).

increases in the antibody response were observed in groups with Al(OH)₃ compared to groups without it (G4: 2.9×10^6 vs. G3: 3.1×10^5 and G5: 5.4×10^5 vs. G6: 1.0×10^5).

We previously used a noro-VLP dose of 43 μg to immunize mice with antigen-decorated noro-VLP (Table 1). To find the optimal dosing for strong immunity, we evaluated the antibody response with different antigen doses. Immunization with an 11-μg dose of noro-VLP (G7: 2.7×10^5) showed a trend of increasing anti-noro antibodies over those obtained with a dose of 6 μg (G6: 1.0×10^5), but no large difference could be seen when increasing noro-VLP dosage over 11 μg (G3: 3.2×10^5 and G8: 2.7×10^5).

While SpyCatcher/Tag system has been utilized widely, to our knowledge, no one has evaluated the immunogenicity of the SpyTag peptide. Even in the presence of adjuvant, GMT of IgG response against SpyTag was $< 1 \times 10^3$, and no cellular response was observed, either (Supplementary Figure 3).

Detectable IgG responses against M2e, SpyCatcher and noro-VLP antigens were also subtyped. As a generalization, IgG1 antibodies are associated with Th2-type antibody-mediated response, while IgG2a antibodies are more related to Th1-type cellular immune response (Mosmann and Coffman, 1989). Formulating antigens with Al(OH)₃ boosted IgG1 responses at

TABLE 1 Vaccination groups and doses used in this study and in two related studies.

Group	Vaccine	Total protein dose (μg)	M2e dose (μg)	Noro-VLP dose (μg)	SpyCatcher dose (μg)
1	M2e+Al(OH) ₃	1.06	1.1	0.0	0.0
2	SC-M2e+Al(OH) ₃	1.5	0.3	0.0	1.2
3	noro+SC-M2e	31.0	0.3	28.6	1.2
4	noro+ SC-M2e+Al(OH) ₃	31.0	0.3	28.6	1.2
5	noro-M2e+Al(OH) ₃	6.0	0.3	5.7	0.0
6	noro-M2e	6.0	0.3	5.7	0.0
7	noro-M2e	12.0	0.5	11.4	0.0
8	noro-M2e	24.0	1.1	22.8	0.0
9	Buffer+Al(OH) ₃	0	0	0	0
Lampinen et al., 2021	Noro+SC-M2e	50	1.1	42.8	4.8
Heinimäki et al., 2022	M2e+Al(OH) ₃	50	50	0	0

The doses of M2e, noro-VLP and SpyCatcher are calculated by comparing its mass to other proteins in the preparation and considering conjugation efficiency where applicable. A detailed explanation of dose calculation is provided in Materials and Methods 4.3. Highlight colors refer to the study group colors used in Figures 3–5.

the expense of IgG2a responses for all the studied antigens (Figure 4), as expected (Brewer et al., 1996). Adjuvant-free antibody responses were slightly biased towards IgG1.

2.3 Presence of noro-VLP strengthens the cellular immune response

We analyzed the cytokine responses (IFN- γ , TNF- α , IL-2) elicited by the vaccine candidates by FluoroSpot assay (Figure 5). The numbers of M2e-reactive IFN- γ - and IL-2-secreting splenocytes in mice immunized with SpyCatcher-M2e-decorated noro-VLPs (G3: arithmetic means of 38 and 302, respectively) were significantly higher than those measured for the adjuvanted M2e peptide group (G1: 0 and 23). However, formulating SpyCatcher-M2e-decorated noro-VLPs with Al(OH)₃ adjuvant decreased the cytokine responses (IFN- γ (G3 vs. G4): 38 vs. 0, TNF- α (G3 vs. G4): 110 vs. 26, IL-2 (G3 vs. G4): 302 vs. 60). The presence of noro-VLP led to a trend of improved cytokine responses in comparison to group 1 immunized with M2e peptide and Al(OH)₃ formulation, whose means cell numbers were 0, 4 and 23 for IFN- γ , TNF- α and IL-2, respectively. Negligible cytokine secretion could be detected in the group of mice immunized with Al(OH)₃-formulated SpyCatcher-M2e when stimulated with M2e (Figure 5A). Both IFN- γ and IL-2 responses were negligible in FluoroSpot analyses when using SpyCatcher or noro-VLP as stimulants (Supplementary Figure 4). We did observe some TNF- α signals here, but these appeared also in the buffer control group splenocytes, possibly related either to reactions of innate immune cells in the spleen to the stimulants or to unspecific inflammation responses due to handling of the splenocytes.

3 Discussion

Attempts to use M2e peptide to obtain protective immunization against various influenza strains stems from the high conservation

rate of the peptide. However, it has turned out somewhat challenging to induce strong immunization with this antigen. In our previous study, we used influenza M2e peptide displayed on noro-VLP via SpyCatcher/SpyTag conjugation to immunize mice via the intramuscular route, but these mice generated only low levels of anti-M2e antibodies. To assess if the SpyCatcher linker, originating from *S. pyogenes*, was dominating the immune response over the small M2e peptide, we now eliminated the linker from the vaccine candidate by preparing M2e presented on noro-VLP via genetic fusion. The resulting immune response was compared to that obtained with M2e SpyCatcher-conjugated on Spy-tagged noro-VLP (Figure 1).

We produced SpyTag-noro-VLP and M2e-noro-VLP in insect cells with the help of baculovirus vector as reported earlier (Lampinen et al., 2021), but now utilized size exclusion chromatography (SEC) instead of ion exchange for the separation of residual baculovirus. The method worked well, increasing noro-VLP production yield up to 2-fold and separating baculovirus (200–400 nm in length (Boucias and Pendland, 2012)) from the smaller norovirus-like particle (~40 nm (White et al., 1997; Lampinen et al., 2021)) efficiently. In Western blot analysis of SEC elution fractions, baculovirus transmembrane protein gp64 was observed both before and after the noro-VLP peaks, probably reflecting intact baculovirus in the early fractions and soluble gp64 released from disassembled baculovirus eluting after noro-VLP. The main perk of SEC over ion exchange chromatography is that modifications made on the VLP surface do not affect the purification parameters. For example, replacing SpyTag with M2e on noro-VP1 C-terminus may have changed the charge of the VLP surface enough that ion exchange elution buffer would have required optimization. However, for large-scale manufacturing of noro-VLPs, optimization of ion exchange chromatography protocol would be worth the trouble for being more scalable than SEC.

Even though M2e is almost double in size as a fusion partner compared to SpyTag, noro-VLP self-assembled efficiently despite the direct C-terminal fusion of M2e. We were not quite able to reach

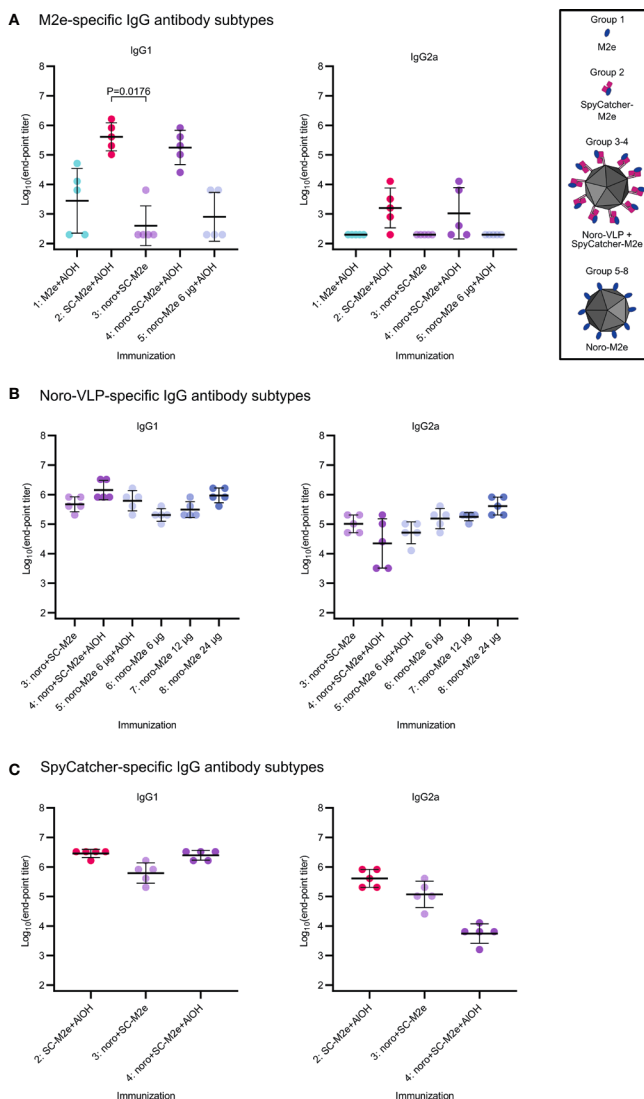
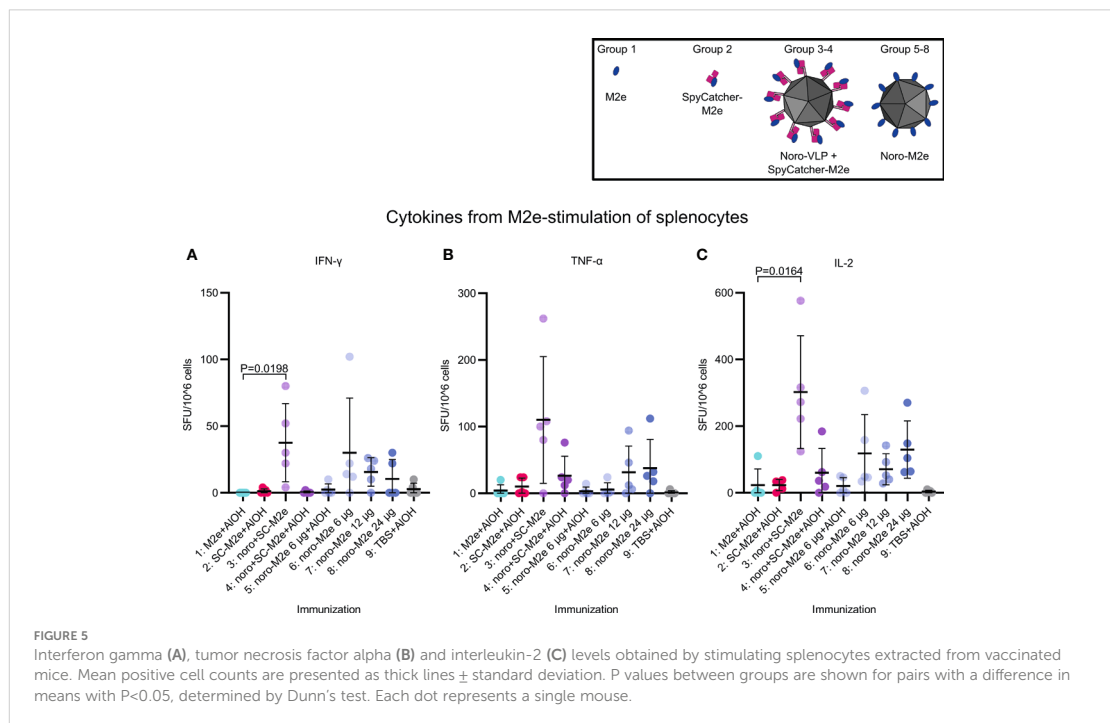


FIGURE 4

IgG antibody subtype comparison on day 42 (sacrifice). Log₁₀ transformations of IgG antibody end-point titers against M2e peptide (A), noro-VLP (B) or SpyCatcher (C), as assessed in ELISA wells coated with the peptide or protein indicated above each graph. Here, only mice with detectable total IgG antibodies were measured, unmeasured mice were denoted with the titer 200 and unmeasured groups were omitted from the graphs. Mean titers are represented by the thick line \pm standard deviation. P values between groups are shown for pairs with a difference in means with $P < 0.05$, determined by Dunn's test. Each dot represents a single mouse. Undetectable antibody levels were denoted with the titer 200 (half of the lowest dilution assessed).

the superb yields of SpyTag-noro-VLP (40–80 mg/L), but with an optimized purification protocol involving SEC, we obtained >95% pure M2e-noro-VLP with yields exceeding 20 mg/L. In electrophoresis, we noted that M2e-noro-VLP appears as a clear, single-band protein, even though our (Koho et al., 2015; Lampinen et al., 2021) and many other labs' (Jiang et al., 1992; White et al., 1997; Bertolotti-Ciarlet et al., 2002; Tan et al., 2004) noro-VLP preparations were double-banded. This reflects the use of different

baculovirus genomes in VLP expression (Lampinen et al., unpublished results). The thermal stability of M2e-noro-VLP ($T_m=53^\circ\text{C}$ according to DSF) was lower as compared to SpyTag-noro-VLP ($T_m=67^\circ\text{C}$) and wild type noro-VLP ($T_m=68^\circ\text{C}$) (Lampinen et al., 2021), but still sufficient for good storage stability in typical conditions. We encountered no deterioration of M2e-noro-VLP upon storage for months at $+4^\circ\text{C}$, which is a clear advantage for a vaccine candidate. The melting curve of M2e-noro-



VLP measured with DSC suggested a 2-step unfolding mechanism. This was also observed for wild type noro-VLP (WT). In line with DSF, the measured thermal transitions were lower for the particle with M2e fusion partner ($T_{m1}(M2e)=67^{\circ}\text{C}$, $T_{m1}(WT)=72^{\circ}\text{C}$; $T_{m2}(M2e)=74^{\circ}\text{C}$, $T_{m2}(WT)=75^{\circ}\text{C}$). Based on these stability studies and earlier studies on the disassembly of wild type noro-VLPs (Ausar et al., 2006), we suggest an unfolding model where the M2e peptide destabilizes the noro-VLP particle in a way that makes it disassemble at a lower temperature compared to VLP without a peptide fusion, producing the distinct T_{m1} peak. The melting temperature of the T_{m2} peak is very close to that of wild type noro-VLP and could be related to unfolding of disassembled VP1 monomers, where a terminal fusion peptide is likely to have only a minor contribution. Confirming the model would require further biophysical studies.

SpyCatcher-M2e was conjugated on the outside of SpyTag-noro-VLPs and conjugation efficiency was measured by mobility shift assay using polyacrylamide gel electrophoresis (PAGE), as described earlier (Lampinen et al., 2021). Here, we observed a conjugation efficiency of 24%, even though SpyCatcher-M2e was added in excess to the reaction. In our previous study, we reported an efficiency of 50% for the conjugation. This phenomenon was evaluated with multiple control experiments, where we noticed that storing mixtures of sodium dodecyl sulphate (SDS)-denatured SpyCatcher and noro-VLP for prolonged periods before PAGE analysis led to overestimation of conjugation efficiency (data not shown). Therefore, it appears that SpyCatcher can renature to some extent in the presence of SDS, and thus the conjugation may

proceed even after SDS/heat treatment. In favor of this hypothesis, previous studies have shown that certain heat-denatured proteins are able to refold slowly in the presence of SDS (Kaspersen et al., 2017). Future studies should assess the exact conditions required for SpyCatcher refolding and its dynamics.

Even though M2e-noro-VLP was easy to produce and proved structurally stable, it was not very effective in inducing immune responses against M2e in mice. The strong M2e-response elicited by SpyCatcher-M2e (group 2) and the poor immunological performance of M2e-noro-VLPs proves our initial hypothesis wrong, as SpyCatcher does not seem to mask M2e from the immune system at all. Two mice in the adjuvanted M2e-noro-VLP group (group 5) reached titers of $>3 \times 10^3$, but then again, three mice had undetectable anti-M2e antibody levels at day 42, indicating that this vaccine preparation is too poorly immunogenic to generate a repeatable immune reaction. M2e-noro-VLP fared slightly better in generating cell-mediated immune responses against M2e than the SpyCatcher-M2e group, but conversely, for cell responses the presence of $\text{Al}(\text{OH})_3$ was detrimental. Higher antibody titers were reported with similar genetic fusions of M2e peptide on hepatitis B VLPs (Neirynek et al., 1999), bacteriophage AP205 VLPs (Tissot et al., 2010) and on norovirus P-particles (Xia et al., 2011). The C-termini of noro-VLPs are located in valleys between the surrounding protruding domains, which positions the M2e peptides (equipped with only a short linker in our construct) between noro-VLP protrusions, potentially limiting the access of large proteins. In future studies, this could be potentially circumvented by fusing multiple peptides in

succession to a VLP carrier, as described in (Kim et al., 2013; Lee et al., 2018; Lee et al., 2019) or by separating M2e from noro-VP1 C-terminus by an elongated linker like the one introduced recently (Boonyakida et al., 2023). Boonyakida et al. used the linker to allow more space between noro-VP1 C-terminus and SpyTag, enhancing conjugation rates for SpyCatcher-fused proteins. Accordingly, a longer linker between noro-VP1 and M2e and/or multiple repeats of M2e may help to increase the anti-M2e immune responses in future experiments, but this can be expected to further destabilize noro-VLP and possibly disturb VLP assembly, and therefore, it can lead to lower yields.

Using SpyTag/Catcher-mediated M2e peptide display on noro-VLPs probably leaves SpyCatcher in between protruding domains but most likely carries M2e itself to the outside of noro-VLP. By formulating the vaccines with Al(OH)₃ adjuvant, we were able to generate biologically relevant anti-M2e antibody levels in groups 2 and 4 that contain SpyCatcher-M2e alone or presented on noro-VLPs, respectively (Figure 3A). Without adjuvant, neither preparation was able to generate anti-M2e antibodies (Heinimäki et al., 2022). Vaccine candidates in groups 2 and 4 both seem promising as M2e-based influenza vaccines, as both generate equal anti-M2e antibody levels. Based on anti-SpyCatcher antibodies found in human serum samples (Rahikainen et al., 2021), we speculate that response against SpyCatcher could also produce some protection against the pathogenic bacterium *S. pyogenes*. Using a longer linker as described above could increase conjugation rates with SpyCatcher-M2e, thus increasing M2e/noro-VLP ratio and M2e density on particle surface in the vaccine candidate, which may be essential for more effective anti-M2e responses to occur. SpyCatcher-M2e would be simpler to manufacture, but on the other hand, vaccines containing noro-VLP generate substantial responses against norovirus, adding another clinical benefit.

Generating a strong response against the well-conserved M2e is great for an efficient influenza vaccine, but alone, it is not enough for protecting against influenza infections. The ectodomain of M2 protrudes only slightly out of the virion membrane and the concentration of M2 in an influenza virion is low (Zebedee and Lamb, 1988). Therefore, anti-M2e vaccines should be combined with a neutralizing influenza vaccine to prevent infection altogether. Anti-M2e response is most useful when cells have already been infected — e.g., because a virus strain has drifted too far from the one used in the neutralizing vaccine component to be completely neutralized. Cells infected with influenza virus express the M2 proton channel vigorously on their membrane to adjust their pH, which makes them easy targets for a broadly armed immune response against M2e (Hashemi et al., 2012). The M2e antibodies can aid in clearance of infected cells through antibody-enhanced natural killer cell or macrophage cytotoxicity, Fc opsonization or possibly prevent budding of new virions (Lee et al., 2019). In the case of influenza virus, the complement system is not only an antibody-dependent mediator of these protective mechanisms, but has been reported to be required for protection mediated by anti-M2e vaccines (Kim et al., 2018).

Prevention of serious influenza infection has been shown in challenge studies in the mouse and the ferret model (Neirynek et al., 1999; Fan et al., 2004; Tissot et al., 2010). A thorough, long-lasting protection against multiple strains of influenza virus and also against norovirus could be achieved by combining the most

successful candidates in this study with an HA stem vaccine (Lampinen et al., 2021). Effective neutralizing effect against current strains can be added by mixing these with a commercial influenza vaccine, like Flublok (Sanofi Pasteur, France). Challenge studies should be conducted to test the *in vivo* protection capabilities of the influenza vaccine candidates reported here.

To our knowledge, immune responses against the SpyTag component have not been measured in earlier preclinical studies using the SpyCatcher/Tag conjugation system. Here, we measured a mild antibody response against SpyTag (the original version published in (Zakeri et al., 2012)) in vaccine group 4 containing SpyCatcher, noro-VLP and Al(OH)₃. Surprisingly, SpyTag-noro-VLP alone was weakest in inducing anti-SpyTag antibodies, suggesting that incorporation into the SpyCatcher enhances the immunogenicity of SpyTag. As SpyTag is only 13 amino acid residues long, we bound biotinylated SpyTag on avidin for presentation to serum antibodies in ELISA. This approach proved essential for making the antigen available, as direct coating of the peptide on wells yielded no signal at all.

The clearance of influenza infection depends on the cooperation of CD4⁺ helper T lymphocytes, CD8⁺ cytotoxic T lymphocytes, and antibody-producing B lymphocytes (Heer et al., 2008). Therefore, vaccination should also induce cellular immune responses, instead of relying exclusively on antibody-mediated responses. In this study, we observed that even though the adjuvanted SpyCatcher-M2e (G2) and noro-VLP+SpyCatcher-M2e (G4) groups were effective in raising anti-M2e antibodies, these groups did not raise very strong cellular responses against M2e. In comparison, the vaccine group that received noro-VLP+SpyCatcher-M2e without Al(OH)₃ elicited more robust cellular responses. This finding seems to demonstrate that Al(OH)₃ can boost the antibody response with the expense of the cellular immune response. Future optimization of used adjuvant would be needed for a more balanced antibody and cellular mediated immune response. The commercial adjuvant system 04 (AS04) which consists of Al(OH)₃ together with monophosphoryl lipid A (MPLA) could be considered in future experiments. MPLA has been shown to act as a TLR4 agonist and to promote IFN- γ production by antigen-specific CD4⁺ T cells, skewing the immune response toward a Th1 type direction (Casella and Mitchell, 2008; Didierlaurent et al., 2009).

In conclusion, our study demonstrates that display of influenza M2e on noro-VLP enhances its immunogenic capacity. Surprisingly, direct SpyCatcher-M2e fusion appears efficient in boosting the immunization against M2e. We, however, observed that conjugation of SpyCatcher-M2e on SpyTag-noro-VLP was beneficial for cellular immune responses in mice. Overall, the modular SpyTag-noro-VLP system appears a robust platform for optimization of experimental vaccine compositions.

4 Materials and methods

4.1 Preparation of vaccine antigens

Norovirus-like particle displaying C-terminal SpyTag (only original SpyTag version, published in Zakeri et al., 2012, was used in

this study; SpyTag-noro-VLP: Addgene plasmid #165989) was produced as described previously (Lampinen et al., 2021), but for the removal of residual baculovirus, we used size-exclusion chromatography (SEC) instead of anion exchange chromatography. The norovirus VP1 gene was from norovirus strain Hu/GIL4/Sydney/NSW0514/2012/AU (GenBank accession no. AFV08795). Briefly, baculovirus (*Autographa californica* multiple nucleopolyhedrovirus, genome bMON14272 from DH10Bac (Thermo Fisher Scientific, USA, #10361012)) containing the target gene was amplified in Sf9 cells (Thermo Fisher Scientific, #11496015) and subsequently used to infect High Five insect cells (Thermo Fisher Scientific, #B85502). 4–6 days after infecting insect cells with baculovirus, the SpyTag-noro-VLP was concentrated from the supernatant by ultracentrifugation (175 000 g, 6–16 h) through a sucrose cushion. After ultracentrifugation, residual baculovirus was removed by SEC using the ÄKTA Purifier instrument and HiPrep 16/60 Sephacryl S-500 HR column (Cytiva, USA, #28935606). SpyCatcher-M2e (Only original SpyCatcher version, published in Zakeri et al., 2012, was used in this study; M2e sequence according to consensus of human influenza sequences, MSLLTVEVETPIRNEWGCRCNDSSD; Addgene plasmid #165990) was expressed in *E. coli* as explained in (Lampinen et al., 2021) and conjugated on SpyTag-noro-VLP by adding a 2-fold molar excess of SpyCatcher-M2e and incubating overnight. Excess SpyCatcher-M2e was removed by another round of SEC, using the setting described above, instead of dialysis. The same M2e sequence was used in all preparations in this study.

For production of direct fusion between norovirus VP1 and M2e, SpyTag in the 3' end of SpyTag-noro-VLP gene was replaced by influenza M2e (Addgene plasmid #201192) and the expression cassette was subcloned into pOET5.1 vector (Oxford Expression Technologies, UK, #200106), under the polyhedrin late promoter by GenScript (USA). In the expression construct, M2e peptide is separated from the norovirus VP1 C-terminus by a 4-amino-acid linker (TSGG). M2e-noro-VLP was produced and purified as described above for SpyTag-noro-VLP, except that we used FlashBAC ULTRA baculovirus genome (Oxford Expression Technologies, UK, #100150) to produce the baculovirus. The M2e (Proteogenix, France) and SpyTag (AHIVMVDAYKPTK, original version published in Zakeri et al., 2012) peptides used for ELISA coating and splenocyte stimulation were chemically synthesized and purified to >85% purity by GenScript. The SpyTag peptide used for splenocyte stimulation was cleared of endotoxins by GenScript.

4.2 Characterization of recombinant protein and nanoparticle antigens

Protein purity and conjugation efficiency were estimated by densitometric analysis of Any kD Stain-free SDS-PAGE gels (#4568126 and #5678125) with the Image Lab software (Bio-Rad, USA). Conjugation efficiency was defined as the densitometric weight of noro-VP1/SpyCatcher conjugate divided by the weight of all noro-VP1 bands. We used the PageRuler Unstained Broad Range Protein Ladder (Thermo Fisher, #26630) as molecular weight marker. For Western blotting, we transferred the gel-separated proteins onto nitrocellulose membrane using Trans-blot Turbo

(Bio-Rad). The presence of M2e was confirmed with an anti-influenza-M2 antibody (1:3000, Thermo Fisher, #ma1-082). A mouse monoclonal anti-gp64 antibody (1:2000, Santa Cruz Biotechnology, USA, #sc-65499) was used to verify the absence of residual baculovirus in the purified noro-VLPs. The bound primary antibodies were visualized by IRDye 800CW goat anti-mouse IgG secondary antibody (1:20 000, LI-COR Biosciences, USA, #926–32210) and the Odyssey CLx instrument (LI-COR Biosciences, USA). We measured protein concentrations using the Pierce BCA protein assay (Thermo Fisher Scientific, #23252). Endotoxin concentrations were determined with ToxinSensor Chromogenic LAL Endotoxin Assay Kit (GenScript, #L00350) and the amount of residual DNA was measured with the Quant-iT dsDNA high sensitivity kit (Thermo Fisher Scientific, #Q33120).

We used dynamic light scattering (DLS) analysis with the Zetasizer Nano ZS (Malvern Instruments, UK) to measure the size and polydispersity of produced nanoparticles and proteins. F200 S/TEM (Jeol, Japan) transmission electron microscope was used to examine the morphology of noro-M2e after negative staining with 1% uranyl acetate. We compared the thermal stability of noro-M2e to that of SpyTag-noro-VLP with differential scanning fluorimetry (DSF), as described in detail elsewhere (Niesen et al., 2007). The DSF analyses were performed in phosphate buffer with different salt concentrations (50 mM Na₂HPO₄/NaH₂PO₄, 10/100/250 mM NaCl, pH 7.2), always using 4 µg VLP per reaction.

We used the VP-Capillary differential scanning calorimetry (DSC) instrument (GE Healthcare, USA) to measure the disassembly and unfolding of wild type noro-VLP at a concentration of 0.2 mg/mL in Tris-buffered saline (50 mM Tris-Cl, 150 mM NaCl, pH 7.4). We tried the same concentration for M2e-noro-VLP but were not able to get detectable unfolding signal before we increased concentration to 1.8 mg/mL, here dissolved in phosphate-buffered saline (PBS: 10 mM Na₂HPO₄, 1.8 mM KH₂PO₄, 137 mM NaCl, 2.7 mM KCl, pH 7.4). In all DSC measurements, we heated the samples from 20 to 110°C at a rate of 2°C/min. Feedback mode was set to “None”, and the filter period to 5 s. The T_m values were obtained from the midpoints of peak curves obtained by subtracting the buffer measurement baseline from measurement data and then fitting the curve with the Levenberg-Marquardt non-linear least-squares method. Data analysis was done using the MicroCal Origin 7.0 software (Malvern Instruments, UK). The results are averaged from two independent measurements.

4.3 Animal experiments

To evaluate the immunogenicity of the antigens, we randomly divided specific pathogen-free female BALB/cJrj mice (Janvier Labs, France) into groups of five animals (Table 1). Only female mice were used due to them being better adapted to group housing than male mice. In a previous study (Xia et al., 2011), the response had a standard deviation of 25 000 (unitless). If the true difference in the experimental and control antibody titer means is 50 000 in groups of 5 mice each, we would be able to reject the null hypothesis that the

population means of the experimental and control groups are equal with a probability (power) of 0.85. The Type I error probability associated with this test is 0.05. The mice were acclimatized for a week before the first immunization (day 0), at which point they were 6 weeks old. The mice received a subcutaneous injection of 150 μ L interscapularly at days 0 and 21. M2e doses were matched for each group according to Table 1, considering the size of M2e peptide compared to its carrier protein(s) and conjugation efficiency. An example of calculating M2e dose in a vaccine preparation for group 4 is provided below. $M(\text{SpyTag-noro-VLP})=61.01$ kDa, $M(\text{SpyCatcher})=12.04$ kDa, $M(\text{M2e})=2.76$ kDa and conjugation efficiency was 24%.

$$24\% * 31\mu\text{g} * \frac{2.76 \text{ kDa}}{(61.01 + 12.04 + 2.76) \text{ kDa}} = 0.27\mu\text{g}$$

We used “Alhydrogel adjuvant 2%” (Invivogen, USA, #vac-alu-250) $\text{Al}(\text{OH})_3$ as an adjuvant in the vaccination groups indicated in Table 1. In the adjuvanted groups, we added 100 μg of $\text{Al}(\text{OH})_3$ per dose.

We collected blood samples from tail veins at days 0, 21, 33 and 36 under inhalation anesthesia by isoflurane (Attane vet, Vet Medic Animal Health, Finland, #AP/DRUGS/220/96). At sacrifice on day 42, we collected whole blood by heart puncture and separated the serum with blood collection tubes (Thermo Fisher Scientific, #365968). We also collected spleens and extracted the splenocytes as described in (González-Rodríguez et al., 2022). The pre-clinical experiments were executed in accordance with the regulations and guidelines of the Finnish National Experiment Board (Permission number ESAVI/1408/2021). All efforts were made to minimize animal suffering and to reduce the number of animals used. The welfare of the animals was monitored throughout the experiment and Animal Research: Reporting of *In Vivo* Experiments (ARRIVE) guidelines were followed. Laboratory animal usage permission (Regional State Administrative Agency, Pirkanmaa, Finland; decision number ESAVI/1408/2021) covers all mouse experiments described here.

4.4 Serum analyses

The total IgG antibody levels against influenza M2e, noro-VLP and SpyTag were assessed with enzyme-linked immunosorbent assays (ELISA) from mouse serum samples, as described earlier (Blazevic et al., 2011). Briefly, Maxisorp 96-well-plates (Thermo Fisher Scientific, #439454) were coated with 50 ng of M2e peptide, SpyTag-noro-VLP or SpyCatcher protein fused with an unrelated peptide per well. For measuring anti-SpyTag antibodies, we coated the wells first with 250 ng of in-house wild type avidin (expressed recombinantly in *E. coli*) and then attached biotinylated SpyTag on the avidin for better availability of the peptide. After blocking the wells with bovine serum albumin and adding the serially diluted mouse sera from the immunization experiment, antigen-bound IgG antibodies in the sera were detected with horseradish peroxidase-conjugated horse anti-mouse monoclonal antibody (mAb) (1:4000, Vector, USA, #PI-2000) and OPD substrate (Merck, USA, #P8412). We used an in-house anti-noro-VLP mouse antiserum, a

monoclonal mouse anti-His antibody (1:160 000, Thermo Fisher Scientific, #ma1-21315) and a monoclonal mouse anti-M2 antibody (1:600 000, Thermo Fisher, #ma1-082) as positive controls. Optical densities at 490 nm (OD490) were measured with a microplate reader (Victor Nivo, PerkinElmer, USA). Endpoint titers were defined as the reciprocal of the highest serum dilution with an OD490 above the positivity cut-off value. The positive cut-off value was defined as the (mean absorbance) + 4.105*(standard deviation) of buffer+ $\text{Al}(\text{OH})_3$ group sera at dilution 1:400. Multiplication with 4.105 gives a confidence level of 99% with 5 mice in the negative control group (Frey et al., 1998). All ELISA analyses were performed in duplicate and at least two independent experiments were performed, so all endpoint titers in this experiment are estimated from averages of at least four measurements.

4.5 Immune cell analyses

Cryopreserved splenocytes from vaccinated mice were thawed in splenocyte incubation medium consisting of RPMI 1640 Medium supplemented with GlutaMAX (Thermo Fisher Scientific, #61870-010), 500 U Penicillin-Streptomycin (Sigma-Aldrich, #P0781), 10% FBS (Sigma-Aldrich, #F9665), and 25 mM HEPES (Sigma-Aldrich, #H0887) and rested for 1 h at 37°C in a humidified incubator with 5% CO_2 .

Simultaneous secretion of IFN- γ , IL-2, and TNF- α was analyzed with Mouse IFN- γ /IL-2/TNF- α FluoroSpot^{PLUS} kit (Mabtech, Sweden, #FSP-414245-10). We set up the assay in duplicate under sterile conditions and tested the splenocytes of individual mice separately according to the manufacturer’s instructions. Briefly, we washed plates pre-coated with mAbs AN18, 1A12, and MT1C8/23C9 from the kit with sterile PBS and blocked the plates with splenocyte incubation medium. After blocking, we added 1 μg of stimulant (antigen) diluted in splenocyte incubation medium together with 250 000 splenocytes to each well and incubated the plates at 37°C in a humidified incubator with 5% CO_2 overnight. Concanavalin A (Sigma-Aldrich, #C5275) (2 μg /well) and splenocyte incubation medium were used as positive and negative controls, respectively. Additionally, anti-CD28 mAb (1:1000) from the kit was used as a co-stimulator in each well to enhance antigen-specific responses, as recommended by the manufacturer. After the overnight incubation, we removed the cells by washing the plates with sterile PBS. We diluted the detection antibodies in PBS containing 0.1% bovine serum albumin (BSA) and added the BAM-tagged anti-IFN- γ mAb (1:200), biotinylated anti-IL-2 mAb (1:500), and WASP-tagged anti-TNF- α mAb (1:200) from the kit to the plates. The plates were then incubated for 2 hours at room temperature (RT) and washed with sterile PBS. Subsequently, anti-BAM-490, Streptavidin-550, and anti-WASP-640 fluorophore conjugates (diluted 1:200 in PBS-0.1% BSA) were added to the plates, which were incubated for 1 hour at RT. Then, we washed the plates with sterile PBS and added Fluorescence enhancer. After a 15-minute incubation at RT, we removed the Fluorescence enhancer and the bottom seals from the plates and dried the plates. Plates were then shipped to Mabtech for automated spot analysis with Mabtech IRIS FluoroSpot reader and the numbers of

cytokine-secreting cells specifically activated by a stimulant were received as a readout. For each mouse and stimulant used, we calculated an average of the duplicate wells and subtracted the positivity cut-off value. We defined the positivity cut-off value for each mouse separately as the average number of spots in the negative control wells $+3 \times$ (standard deviation). The final frequencies of responding cells were expressed as the number of spot-forming units/ 10^6 splenocytes.

4.6 Statistical analyses

For statistical analyses, we used GraphPad Prism version 8.3.0 and defined that $p < 0.05$ indicates statistically significant difference. To estimate differences in mean end-point titers and mean spot counts between vaccine groups and the negative control group, we used Kruskal-Wallis followed by Dunnett's test. For the ELISA data, we used the corresponding mouse serum at day 0 as the control group, whereas the buffer immunized group served as a negative control for FluoroSpot data. We also compared the means of each group to all other groups with the Dunn's test.

Data availability statement

The raw data supporting the conclusions of this article will be made available by the authors, without undue reservation.

Ethics statement

The animal study was reviewed and approved by the Finnish National Experiment Board. Laboratory animal usage permission (Regional State Administrative Agency, Pirkanmaa, Finland; decision number ESAVI/1408/2021) covers all mouse experiments described here.

Author contributions

VL, MH, VH and VB contributed to conception and design of the study. VL produced the vaccines and performed most experiments in the supervision of MH and VH. SG and SS participated in the animal experiment, performed the cellular immunology assays and analyzed their results. VL drafted the first manuscript draft and figures, while SG wrote sections of the manuscript. All authors discussed the results and commented on the manuscript to help shape its final version. All authors read and approved the final manuscript.

References

Ausar, S. F., Foubert, T. R., Hudson, M. H., Vedvick, T. S., and Middaugh, C. R. (2006). Conformational stability and disassembly of Norwalk virus-like particles. effect of pH and temperature. *J. Biol. Chem.* 281, 19478–19488. doi: 10.1074/jbc.M603313200

Funding

This work received funding from Tampere University Graduate School (VL, SG, SS), Finnish Foundation for Technology Promotion (VL), Instrumentarium Science Foundation (SS) and Tampere Tuberculosis Foundation (VL, MH, SG). We also acknowledge Academy of Finland (#335870, MH), Cancer Foundation Finland (VH) and Sigrid Juselius Foundation (VH) for financial support.

Acknowledgments

The technical assistance and guidance given by Niklas Kähkönen, Merja Jokela and Ulla Kiiskinen is gratefully acknowledged. We would like to thank Jalmari Malm, Lena Brouwer and Lena Klümper for their help in performing the immunological analyses and also Jonna Alkula and Angelika Pölläniemi for particle stability studies. We thank Professor Ilkka Junttila for help in preparing the revised version. This work made use of Tampere Microscopy Center facilities at Tampere University. We acknowledge Biocenter Finland for infrastructure support.

Conflict of interest

Author VH has consultive employment with Fimlab Laboratories. The remaining authors declare that the research was conducted in the absence of any commercial or financial relationships that could be construed as a potential conflict of interest.

Publisher's note

All claims expressed in this article are solely those of the authors and do not necessarily represent those of their affiliated organizations, or those of the publisher, the editors and the reviewers. Any product that may be evaluated in this article, or claim that may be made by its manufacturer, is not guaranteed or endorsed by the publisher.

Supplementary material

The Supplementary Material for this article can be found online at: <https://www.frontiersin.org/articles/10.3389/fcimb.2023.1216364/full#supplementary-material>

Bachmann, M. F., and Jennings, G. T. (2010). Vaccine delivery: a matter of size, geometry, kinetics and molecular patterns. *Nat. Rev. Immunol.* 10, 787–796. doi: 10.1038/nri2868

- Bertolotti-Ciarlet, A., White, L. J., Chen, R., Prasad, B. V. V., and Estes, M. K. (2002). Structural requirements for the assembly of Norwalk virus-like particles. *J. Virol.* 76, 4044–4055. doi: 10.1128/JVI.76.8.4044-4055.2002
- Blazevic, V., Lappalainen, S., Nurminen, K., Huhti, L., and Vesikari, T. (2011). Norovirus VLPs and rotavirus VP6 protein as combined vaccine for childhood gastroenteritis. *Vaccine* 29, 8126–8133. doi: 10.1016/j.vaccine.2011.08.026
- Boonyakida, J., Khoris, I. M., Nasrin, F., and Park, E. Y. (2023). Improvement of modular protein display efficiency in spytag-implemented norovirus-like particles. *Biomacromolecules* 24, 308–318. doi: 10.1021/acs.biomac.2c01150
- Boucias, D. G., and Pendland, J. C. (1998). *Principles of insect pathology* (New York, NY, USA: Springer Science & Business Media). doi: 10.1007/978-1-4615-4915-4
- Brewer, J. M., Conacher, M., Satoskar, A., Bluethmann, H., and Alexander, J. (1996). In interleukin-4-deficient mice, alum not only generates T helper 1 responses equivalent to Freund's complete adjuvant, but continues to induce T helper 2 cytokine production. *Eur. J. Immunol.* 26, 2062–2066. doi: 10.1002/eji.1830260915
- Brune, K. D., Leneghan, D. B., Brian, I. J., Ishizuka, A. S., Bachmann, M. F., Draper, S. J., et al. (2016). Plug-and-Display: decoration of virus-like particles via isopeptide bonds for modular immunization. *Sci. Rep.* 6, 19234. doi: 10.1038/srep19234
- Casella, C. R., and Mitchell, T. C. (2008). Putting endotoxin to work for us: monophosphoryl lipid a as a safe and effective vaccine adjuvant. *Cell Mol. Life Sci.* 65, 3231–3240. doi: 10.1007/s00108-008-8228-6
- Chackerman, B., Durfee, M. R., and Schiller, J. T. (2008). Virus-like display of a neo-self antigen reverses b cell anergy in a b cell receptor transgenic mouse model. *J. Immunol.* 180, 5816–5825. doi: 10.4049/jimmunol.180.9.5816
- Didierlaurent, A. M., Morel, S., Lockman, L., Giannini, S. L., Bisteau, M., Carlsen, H., et al. (2009). AS04, an aluminum salt- and TLR4 agonist-based adjuvant system, induces a transient localized innate immune response leading to enhanced adaptive immunity. *J. Immunol.* 183, 6186–6197. doi: 10.4049/jimmunol.0901474
- Ebrahimi, S. M., and Tebianian, M. (2011). Influenza A viruses: why focusing on M2e-based universal vaccines. *Virus Genes* 42, 1–8. doi: 10.1007/s11262-010-0547-7
- Fan, J., Liang, X., Horton, M. S., Perry, H. C., Citron, M. P., Heidecker, G. J., et al. (2004). Preclinical study of influenza virus A M2 peptide conjugate vaccines in mice, ferrets, and rhesus monkeys. *Vaccine* 22, 2993–3003. doi: 10.1016/j.vaccine.2004.02.021
- Frey, A., Di Canzio, J., and Zurakowski, D. (1998). A statistically defined endpoint titer determination method for immunoassays. *J. Immunol. Methods* 221, 35–41. doi: 10.1016/S0022-1759(98)00170-7
- González-Rodríguez, M. L., Nurminen, N., Kummola, L., Laitinen, O. H., Oikarinen, S., Parajuli, A., et al. (2022). Effect of inactivated nature-derived microbial composition on mouse immune system. *Immun. Inflammation Dis.* 10, e579. doi: 10.1002/iid3.579
- Hashemi, H., Pouyanfar, S., Bandehpour, M., Noroozbabaei, Z., Kazemi, B., Saelens, X., et al. (2012). Immunization with M2e-displaying T7 bacteriophage nanoparticles protects against influenza A virus challenge. *PLoS One* 7, e45765. doi: 10.1371/journal.pone.0045765
- Heer, A. K., Harris, N. L., Kopf, M., and Marsland, B. J. (2008). CD4+ and CD8+ T cells exhibit differential requirements for CCR7-mediated antigen transport during influenza infection. *J. Immunol.* 181, 6984–6994. doi: 10.4049/jimmunol.181.10.6984
- Heinimäki, S., Lampinen, V., Tamminen, K., Hankaniemi, M. M., Malm, M., Hytönen, V. P., et al. (2022). Antigenicity and immunogenicity of HA2 and M2e influenza virus antigens conjugated to norovirus-like, VP1 capsid-based particles by the SpyTag/SpyCatcher technology. *Virology* 566, 89–97. doi: 10.1016/j.virol.2021.12.001
- Jiang, X., Wang, M., Graham, D. Y., and Estes, M. K. (1992). Expression, self-assembly, and antigenicity of the Norwalk virus capsid protein. *J. Virol.* 66, 6527–6532. doi: 10.1128/jvi.66.11.6527-6532.1992
- Kaspersen, J. D., Sondergaard, A., Madsen, D. J., Otzen, D. E., and Pedersen, J. (2017). Refolding of SDS-unfolded proteins by nonionic surfactants. *Biophys. J.* 112, 1609–1620. doi: 10.1016/j.bpj.2017.03.013
- Kim, Y.-J., Kim, K.-H., Ko, E.-J., Kim, M.-C., Lee, Y.-N., Jung, Y.-J., et al. (2018). Complement C3 plays a key role in inducing humoral and cellular immune responses to influenza virus strain-specific hemagglutinin-based or cross-protective M2 extracellular domain-based vaccination. *J. Virol.* 92, e00969–e00918. doi: 10.1128/JVI.00969-18
- Kim, M.-C., Song, J.-M., Eunju, E., Kwon, Y.-M., Lee, Y.-J., Compans, R. W., et al. (2013). Virus-like particles containing multiple M2 extracellular domains confer improved cross-protection against various subtypes of influenza virus. *Mol. Ther.* 21, 485–492. doi: 10.1038/mt.2012.246
- Koho, T., Ihalainen, T. O., Stark, M., Uusi-Kerttula, H., Wieneke, R., Rahikainen, R., et al. (2015). His-tagged norovirus-like particles: a versatile platform for cellular delivery and surface display. *Eur. J. Pharmaceutics Biopharmaceutics* 96, 22–31. doi: 10.1016/j.ejpb.2015.07.002
- Lampinen, V., Heinimäki, S., Laitinen, O. H., Pesu, M., Hankaniemi, M. M., Blazevic, V., et al. (2021). Modular vaccine platform based on the norovirus-like particle. *J. Nanobiotechnology* 19, 25. doi: 10.1186/s12951-021-00772-0
- Lee, Y.-T., Kim, K.-H., Ko, E.-J., Kim, M.-C., Lee, Y.-N., Hwang, H.-S., et al. (2019). Enhancing the cross protective efficacy of live attenuated influenza virus vaccine by supplemented vaccination with M2 ectodomain virus-like particles. *Virology* 529, 111–121. doi: 10.1016/j.virol.2019.01.017
- Lee, Y. T., Ko, E. J., Lee, Y., Kim, K. H., Kim, M. C., Lee, Y. N., et al. (2018). Intranasal vaccination with M2e5x virus-like particles induces humoral and cellular immune responses conferring cross-protection against heterosubtypic influenza viruses. *PLoS One* 13, e0190868. doi: 10.1371/journal.pone.0190868
- Mosmann, T. R., and Coffman, R. L. (1989). "Heterogeneity of cytokine secretion patterns and functions of helper T cells," in *Advances in immunology*. Ed. F. J. Dixon (Elsevier, Amsterdam, Netherlands: Academic Press), 111–147. doi: 10.1016/S0065-2776(08)60652-5
- Neiryck, S., Deroo, T., Saelens, X., Vanlandschoot, P., Jou, W. M., and Fiers, W. (1999). A universal influenza A vaccine based on the extracellular domain of the M2 protein. *Nat. Med.* 5, 1157–1163. doi: 10.1038/13484
- Niesen, F. H., Berglund, H., and Vedadi, M. (2007). The use of differential scanning fluorimetry to detect ligand interactions that promote protein stability. *Nat. Protoc.* 2, 2212–2221. doi: 10.1038/nprot.2007.321
- Prasad, B. V., Hardy, M. E., Dokland, T., Bella, J., Rossmann, M. G., and Estes, M. K. (1999). X-Ray crystallographic structure of the Norwalk virus capsid. *Sci. (New York N.Y.)* 286, 287–290. doi: 10.1126/science.286.5438.287
- Prasad, B. V., Rothnagel, R., Jiang, X., and Estes, M. K. (1994). Three-dimensional structure of baculovirus-expressed Norwalk virus capsids. *J. Virol.* 68, 5117–5125. doi: 10.1128/jvi.68.8.5117-5125.1994
- Rahikainen, R., Rijal, P., Tan, T. K., Wu, H.-J., Andersson, A.-M. C., Barrett, J. R., et al. (2021). Overcoming symmetry mismatch in vaccine nanoassembly through spontaneous amidation. *Angewandte Chemie* 133, 325–334. doi: 10.1002/ange.202009663
- Tan, M., Zhong, W., Song, D., Thornton, S., and Jiang, X. (2004). E. coli-expressed recombinant norovirus capsid proteins maintain authentic antigenicity and receptor binding capability. *J. Med. Virol.* 74, 641–649. doi: 10.1002/jmv.20228
- Thrane, S., Janitzek, C. M., Matondo, S., Resende, M., Gustavsson, T., de Jongh, W. A., et al. (2016). Bacterial superglue enables easy development of efficient virus-like particle based vaccines. *J. Nanobiotechnology* 14, 30. doi: 10.1186/s12951-016-0181-1
- Tissot, A. C., Renhofs, R., Schmitz, N., Cielens, I., Meijerink, E., Ose, V., et al. (2010). Versatile virus-like particle carrier for epitope based vaccines. *PLoS One* 5, e9809. doi: 10.1371/journal.pone.0009809
- White, L. J., Hardy, M. E., and Estes, M. K. (1997). Biochemical characterization of a smaller form of recombinant Norwalk virus capsids assembled in insect cells. *J. Virol.* 71, 8066–8072. doi: 10.1128/JVI.71.10.8066-8072.1997
- Wolfe, N. D., Dunavan, C. P., and Diamond, J. (2007). Origins of major human infectious diseases. *Nature* 447, 279–283. doi: 10.1038/nature05775
- Xia, M., Tan, M., Wei, C., Zhong, W., Wang, L., McNeal, M., et al. (2011). A candidate dual vaccine against influenza and noroviruses. *Vaccine* 29, 7670–7677. doi: 10.1016/j.vaccine.2011.07.139
- Zakeri, B., Fierer, J. O., Celik, E., Chittock, E. C., Schwarz-Linek, U., Moy, V. T., et al. (2012). Peptide tag forming a rapid covalent bond to a protein, through engineering a bacterial adhesin. *Proc. Natl. Acad. Sci. United States America* 109, 690. doi: 10.1073/pnas.1115485109
- Zebedee, S. L., and Lamb, R. A. (1988). Influenza A virus M2 protein: monoclonal antibody restriction of virus growth and detection of M2 in virions. *J. Virol.* 62, 2762–2772. doi: 10.1128/JVI.62.8.2762-2772.1988

PUBLICATION IV

Experimental VLP vaccine displaying a furin antigen elicits autoantibodies and is well tolerated in mice

Lampinen V, Ojanen MJT, Muños Caro F, Gröhn S, Hankaniemi MM, Pesu M, Hytönen VP

Submitted manuscript

Publication reprinted with the permission of the copyright holders.

